

Natural Products from Marine Sponges

(Naturstoffe aus marinen Schwämmen)

Inaugural dissertation

for the attainment of the title of doctor

in the Faculty of Mathematics and Natural Sciences

at the Heinrich Heine University Düsseldorf

presented by

Amin Mokhlesi

from Iran

Düsseldorf, Feb. 2018

From the Institute for Pharmaceutical Biology and Biotechnology at the
Heinrich Heine University Düsseldorf

Published by permission of the Faculty of Mathematics and Natural Sciences at
Heinrich Heine University Düsseldorf

Supervisor: Prof. Dr. Dr. h.c. Peter Proksch

Co-supervisor: Prof. Dr. Rainer Kalscheuer

Date of the oral examination: 22.11.2017

Dedicated to my parents, my wife and my sweet daughter

Declaration of Academic Honesty/Erklärung

Hiermit erkläre ich ehrenwörtlich, dass ich die vorliegende Dissertation mit dem Titel “Antikrebs Natürliche Produkte von Marine Schwämmen “ selbst angefertigt habe. Außer den angegebenen Quellen und Hilfsmitteln wurden keine weiteren verwendet. Diese Dissertation wurde weder in gleicher noch in abgewandelter Form in einem anderen Prüfungsverfahren vorgelegt. Weiterhin erkläre ich, dass ich früher weder akademische Grade erworben habe, noch dies versucht habe.

Düsseldorf, den 20.02.2018

Amin Mokhlesi

Table of Contents

Abstract.....	7
Zusammenfassung	10
1 Significance of the study	13
2 Introduction	13
2.1 Marine sponges.....	14
2.1.1 Ecological functions of marine sponges	15
2.1.2 Symbiosis in marine sponges.....	15
2.2 Natural products from marine sponges.....	16
2.2.1 Alkaloids from marine sponges	16
2.2.2 Peptides from marine sponges	17
2.2.3 Fatty acids from marine sponges	18
2.3 Bioactivity of marine natural products	18
2.4 Marine anticancer natural products	19
2.4.1 Cell death mechanisms (apoptosis and necrosis).....	20
2.4.2 Cell autophagy	21
2.4.3 Biochemical pathways of apoptosis.....	21
2.4.4 Detection of apoptosis by western blot.....	22
2.5 Drug discovery using marine natural products.....	22
3 Aim of the study	24
4 Publication 1: Lissodendrins A and B, New 2-Aminoimidazole Alkaloids from the Marine Sponge <i>Lissodendoryx (Acanthodoryx) fibrosa</i>	26
4.1 Introduction	27
4.2 Results and Discussion	27
4.3 Conclusion.....	29
4.4 Experimental Section.....	29
4.5 Supporting Information	31
5 Publication 2: Cyclic Cystine-Bridged Peptides from the Marine Sponge <i>Clathria basilana</i> Induce Apoptosis in Tumor Cells and Depolarize the Bacterial Cytoplasmic Membrane	42
5.1 Results and Discussion	43
5.2 Experimental Section.....	62
5.3 Supporting Information	69
6 Publication 3: New 2-Methoxy Acetylenic Acids and Pyrazole Alkaloids from the Marine Sponge <i>Cinachyrella</i> sp.....	102
6.1 Introduction	103

6.2	Results	104
6.3	Discussion.....	110
6.4	Materials and Methods	110
6.5	Conclusions	111
6.6	Supplementary material	113
7	Discussion.....	130
7.1	Natural products from <i>Lissodendoryx (Acanthodoryx) fibrosa</i>	130
7.1.1	Lissodendrins A and B.....	130
7.1.2	2-(4-hydroxyphenyl)-3-hydroxypyridine.....	134
7.1.3	Known compounds	135
7.2	Natural products from <i>Clathria basilana</i>	136
7.2.1	Microcionamides and gombamides	137
7.2.2	(E)-2-amino-3-methyl-N-styrylbutanamide.....	144
7.2.3	Known compounds	145
7.3	Natural products from <i>Cinachyrella</i> sp.	146
7.3.1	Cinachylenic acids A, B, C, and D	147
7.3.2	Cinachyrazole A, B, and C	147
8	Abbreviations.....	149
9	Research contributions	152
10	Acknowledgements	153
11	References	155

Abstract

Discovering the mysteries of ocean has always been a matter of human interest. The first signs of drug potential from marine resources began with the discovery of the anti-cancer nucleoside compounds from marine sponges in the mid-nineteenth century. Indeed, the pharmaceutical research of various marine organisms to date has indicated the important role of marine sponges as a prolific source of novel bioactive compounds. Moreover, due to the accessibility of humans even to the depths of the oceans, the number of bioactive compounds from marine organisms has been significantly increased. Among marine organisms, the contribution of sponges is remarkable as highlighted by the anticancer Cytosar-U® (1969), the antiviral Vira-A® (1976), and the anticancer Halaven® (2010) sponge-derived drugs, which have already reached the market.

Based on the high pharmaceutical potential of marine sponges, this study was carried out to investigate the isolation and structure elucidation of bioactive secondary metabolites from three marine sponge specimens, *Lissodendoryx (Acanthodoryx) fibrosa*, *Clathria basilana*, and *Cinachyrella* sp., collected in Indonesia. After sampling and transfer of these sponge specimens to laboratory, the methanol crude extract from each sponge was submitted to liquid-liquid separation to obtain MeOH, EtOAc, *n*-Hexan, BuOH, and water subfractions. Afterwards, the pure compounds were isolated by using different chromatographic separation techniques, such as Sephadex column (LH-20), thin layer chromatography (TLC), vacuum liquid chromatography (VLC) (R18), reversed-phase vacuum liquid chromatography (RP-VLC), analytical high pressure liquid chromatography (HPLC), and semi-preparative high pressure liquid chromatography (HPLC). The structure elucidation of the secondary substances was performed by state of the art analytical methods, such as 1D (¹H, ¹³C) and 2D (COSY, TOCSY, ROESY, HSQC, HMBC) nuclear magnetic resonance spectroscopy (NMR), as well as by mass spectrometry (EI, ESI, MALDI-TOF). In addition, Marfey's analysis was used to determine the chirality of amino acids following peptide hydrolysis. *In vitro* cytotoxicity of the isolated compounds was measured against murine lymphoma (L5178Y), human lymphoma (Ramos), leukemia (HL-60, Nomo-1, Jurkat J16), and human ovarian carcinoma (A2780) cell lines. Moreover, the *in vitro* antibacterial activity of the isolated compounds was tested against different Gram-positive and Gram-negative bacteria. Finally, the cytotoxic and antibacterial mode of action for the active compounds was likewise evaluated.

Overall, in this research thirty-four compounds were isolated from three sponge species, which fourteen have been identified as new natural products. In the present thesis, the results of each sponge are individually printed in the form of already published or accepted manuscripts in scientific journals:

Lissodendoryx (Acanthodoryx) fibrosa

Two new 2-aminoimidazole alkaloid derivatives lissodendrins A and B, have been isolated from the marine sponge, *Lissodendoryx fibrosa* collected in Ambon, Indonesia. Lissodendrins A and B exhibited similar molecular formula with only one oxygen difference as C₁₇H₁₃N₃O₃

and C₁₇H₁₃N₃O₄ respectively. The unusual 2D spectrum of lissodendrins and significant number of quaternary carbons was challenging for the structure elucidation of these compounds. However, the structures were unequivocally elucidated by ¹H, ¹³C, ROESY and long-range HMBC correlations, as well by ESIMS/MS fragmentations. The skeletons of lissodendrins A and B include an unusual (p-hydroxyphenyl)glyoxal moiety, which is rarely reported in natural products. The biosynthetic pathway of lissodendrins A and B is proposed to originate from tyrosine and arginine.

Clathria basilana

In the second part of the thesis, the marine sponge *Clathria basilana* was investigated, which was collected in Indonesia. Chromatographic separation afforded six cyclic peptides, including five new compounds, microcionamides C and D, gombamides B, C, and D, along with a new derivative (*E*)-2-amino-3-methyl-N-styrylbutanamide. In addition, the known peptide microcionamide A, six known indole derivatives, 7-bromo-4(1H)-quinolinone, a δ -lactam derivative (3-(2-(4-hydroxyphenyl)-2-oxoethyl)-5,6-dihydropyridin-2(1H)-one), 2-deoxythymidine, and 4-hydroxybenzoic acid, were likewise isolated. The structures of the new compounds were unambiguously elucidated based on 1D and 2D NMR spectroscopy, mass spectrometry, as well as by comparison with the literature. Subsequent Marfey's analysis identified L-configurations for all amino acid residues of the isolated peptides (microcionamides A, C and D; gombamides B, C, and D). Moreover, HPLC resolution between L/D-Ile and L/D-*allo*-Ile residues was improved by using C₄ HPLC RP-column instead of C₁₈, to indicated presence of L-Ile in the isolated peptides.

Moreover, in an attempt to improve the HPLC resolution between L/D-Ile and L/D-*allo*-Ile residues, a C₄ HPLC RP-column was successfully employed, instead of the commonly used C₁₈ column, in analogy to the C₃ Marfey's method

All isolated compounds were evaluated in different bioassays. Among them, microcionamides exhibited promising anticancer and antibacterial activities. Cytotoxicity directed experiments showed IC₅₀ values in the range from 0.45 to 5.92 μ M for microcionamides A, C and D against lymphoma (Ramos), human ovarian carcinoma (A2780), and leukemia cell lines (HL-60, Nomo-1, Jurkat J16). The anticancer mechanism of microcionamides A, C, and D toward Jurkat J16 and Ramos cells indicated their ability to induce cell death via apoptosis. Microcionamides C and D were shown to block cell autophagy, which diminishes the survival of cancer cells. Moreover, microcionamides A and C inhibited Gram-positive bacteria (*Staphylococcus aureus* and *Enterococcus faecium*) with MICs from 6.25 to 12.5 μ M. Interestingly, antibacterial mode of action studies indicated that microcionamides A and C are able to destruct the bacterial membrane.

Cinachyrella sp.

The marine sponge *Cinachyrella* sp., collected in Indonesia, was investigated as the last sponge species in this study. Four 2-methoxy acetylenic acids consisting of three new

(cinachylenic acids B, C, and D) and the known derivative cinachylenic acid A, in addition to three new pyrazole alkaloids (cinachyrazoles A, B, and C) were isolated from the marine sponge *Cinachyrella* sp. One- and two-dimensional NMR spectroscopy, as well as mass spectrometry were used for the elucidation of the isolated compounds. Bioassay results showed strong cytotoxicity of all cinachylenic acids with IC₅₀ values of 0.3 μ M. Moreover, a plausible biosynthetic pathway for the cinachyrazole derivatives was proposed, originating from the linkage of an acetoacetic acid and an *N*-acetyl-*N*-methylhydrazine unit.

Zusammenfassung

Seit jeher steht die Erforschung der Geheimnisse des Ozeans im Interesse der Menschheit. Die ersten Anzeichen für das medizinische Potenzial von Naturstoffen aus marinen Quellen offenbarte sich in der Mitte des zwanzigsten Jahrhunderts durch die Entdeckung von antitumoralen Nucleosiden in Meeresschwämmen. Im Laufe der systematischen, pharmazeutischen Untersuchung verschiedener mariner Organismen konnte die Vorreiterrolle mariner Schwämme als Quelle für neuartige bioaktive Sekundärmetabolite bestätigt werden. Durch die Erschließung der Tiefen des Ozeans durch den Menschen konnte der Schatz an bioaktiven Stoffen aus Meeresorganismen beträchtlich erweitert werden. Der von den Schwämmen zu diesem Schatz geleistete Beitrag ist bemerkenswert hoch. Dies kann durch bereits in den Arzneimittelmarkt eingeführte Medikamente wie das Krebsmedikament Cytosar-U® (1969), das Virostatikum Vira-A® (1976), sowie das von Schwammmetaboliten abgeleitete Krebsmedikament Halaven® (2010), demonstriert werden.

Mit dem hohen pharmazeutischen Potenzial der Meeresschwämme als Ansporn, wurden in dieser Studie bioaktive Sekundärmetaboliten aus den, in Indonesien gesammelten Schwämmen *Lissodendoryx (Acanthodoryx) fibrosa*, *Clathria basilana* und *Cinachyrella sp.* isoliert und deren chemische Struktur aufgeklärt. Nach der Probenentnahme und dem Transfer in das Labor wurde jeweils ein methanolischer Extrakt hergestellt, welcher durch flüssig-flüssig Verteilungschromatographie in Unterfraktionen aus Hexan, Ethylacetat, n-Butanol, Methanol und Wasser aufgeteilt wurde. Aus diesen Unterfraktionen wurden im Anschluss Reinsubstanzen isoliert. Hierbei kamen unterschiedliche chromatographische Trennverfahren zum Einsatz wie Sephadex Säulenchromatographie (LH20), Dünnschichtchromatographie (TLC), Normal- und Umkehrphasen-Vakuumflüssigchromatographie (VLC/RP-VLC), sowie analytische und semipreparative Hochleistungsflüssigchromatographie (HPLC). Die Strukturaufklärung der isolierten Verbindungen erfolgte durch moderne eindimensionale (^1H , ^{13}C), sowie zweidimensionale (COSY, TOCSY, ROESY, HSQC und HMBC) Kernspinresonanzspektroskopie (NMR) in Kombination mit verschiedenen massenspektrometrischen Methoden (EI, ESI, MALDI-TOF). Zur Bestimmung der absoluten Konfiguration der isolierten Peptide, wurden diese hydrolysiert und die absolute Konfiguration der beteiligten Aminosäuren durch eine Marfey Analyse bestimmt. Die *in vitro* Zytotoxizität aller isolierten Substanzen wurde an einer Maus-Lymphomzelllinie (L5178Y), einer menschlichen Lymphomzelllinie (Ramos), drei Leukämiezelllinien (HL-60, Nomo-1 und Jurkat J16), sowie einer menschlichen Ovarialkarzinomzelllinie (A2780) bestimmt. Zusätzlich wurden antibakterielle Eigenschaften *in vitro* sowohl gegen grampositive, als auch gramnegative Bakterien untersucht. Abschließend wurden die Verbindungen, welche sich als bioaktiv herausstellten, auf ihren antibakteriellen und zytotoxischen Wirkmechanismus hin untersucht.

Zusammengefasst wurden während dieser Arbeit aus insgesamt drei Schwämmen vierunddreißig Verbindungen isoliert, von denen vierzehn als neue Naturstoffe identifiziert werden konnten. In der vorgelegten Dissertation sind die Ergebnisse zu jedem Schwamm einzeln in Form von Manuskripten abgedruckt, welche bereits in wissenschaftlichen Fachzeitschriften akzeptiert oder eingereicht worden sind.

Lissodendoryx (Acanthodoryx) fibrosa

Aus dem in Ambon (Indonesien) gesammelten Meeresschwamm *Lissodendoryx fibrosa* konnten die beiden neuen 2-Aminoimidazolalkaloide Lissodendrin A und B isoliert werden. Lissodendrin A und B unterscheiden sich nur durch ein einziges Sauerstoffatom und weisen die Molekularformeln $C_{17}H_{13}N_3O_3$ und $C_{17}H_{13}N_3O_4$ auf. Die Strukturaufklärung der Lissodendrine stellte sich aufgrund der hohen Anzahl quaternärer Kohlenstoffatome und einer ungewöhnlichen Beschaffenheit der zweidimensionalen Kernspinresonanzspektren als Herausforderung dar. Die eindeutige Bestimmung der Struktur gelang letztendlich durch den Einsatz von 1H , ^{13}C , ROESY und long-range HMBC, sowie die Auswertung des ESIMS/MS Fragmentierungsmusters. Das Kohlenstoffgerüst von Lissodendrin A und B enthält eine ungewöhnliche (p-Hydroxyphenyl)glyoxal Einheit, welche in Naturstoffen bisher nur äußerst selten beschrieben wurde. Als Biosyntheseweg für Lissodendrin A und B wird ein Weg ausgehend von Tyrosin und Arginin postuliert.

Clathria basilana

Der zweite Teil der Dissertation handelt von der Untersuchung des in Indonesien gesammelten Meeresschwamms *Clathria basilana*. Bei der chromatographischen Aufarbeitung konnte sechs zyklische Peptide zutage gefördert werden, von denen die fünf Verbindungen Microcionamid C und D, Gombamid B, C, und D zusammen mit dem Nichtpeptid (*E*)-2-Amino-3-methyl-N-styrylbutanamid als neue Naturstoffe identifiziert werden konnten. Außerdem konnten das bekannte Peptid Microcionamid A, sechs bekannte Indolderivate, 7-Bromo-4(1H)-quinolinon, das δ -lactam Derivat (3-(2-(4-Hydroxyphenyl)-2-oxoethyl)-5,6-dihydropyridin-2(1H)-on), 2-Deoxythymidin und 4-Hydroxybenzoesäure isoliert werden. Die Struktur der neuen Verbindungen wurde eindeutig durch den Einsatz von ein- und zweidimensionaler Kernspinresonanzspektroskopie, Massenspektrometrie, sowie durch Vergleich mit Literaturreferenzen bestimmt. Die absolute Konfiguration der an den Peptiden beteiligten Aminosäuren konnte durch Marfey Analyse als L-Konfiguration bestimmt werden (Microcionamid C und D, Gombamid B, C, und D). Durch den ergänzenden Einsatz einer C_4 Umkehrphasen HPLC konnte zudem die Auflösung zwischen L/D-Isoleucin und L/D-*allo*-Isoleucin im Vergleich zu einer C_{18} Umkehrphase verbessert werden, wodurch die Beteiligung von L-Isoleucin in allen Peptiden nachgewiesen werden konnte. Bei Versuchen zur Auflösungsverbesserung zwischen L/D-Isoleucin und L/D-*allo*-Isoleucin in der HPLC-Analytik konnte die weitverbreite C_{18} Umkehrphase durch eine C_4 Umkehrphase ersetzt werden, welche analog zur in der Marfey Analyse etablierten C_3 Umkehrphase aussagenkräftige Ergebnisse erzielen konnte. Alle isolierten Verbindungen wurden unterschiedlichen Bioassays unterzogen. Hierbei lieferten vor allem die Microcionamide vielversprechende antitumorale und antibakterielle Aktivitäten. Untersuchungen, die auf Zytotoxizität abzielten, lieferten für Microcionamid A, C und D zelllinienabhängige IC_{50} -Werte zwischen 0,45 und 5,95 μM , getestet wurde gegen eine menschliche Lymphomzelllinie (Ramos), eine menschliche Ovarialkarzinomzelllinie

(A2780) und Leukämiezelllinien (HL-60, Nomo-1 und Jurkat J16). Der antitumorale Mechanismus von Microcionamid A, C und D an Jurkat J16- und Ramoszellen beruht auf ihrer Fähigkeit an diesen Zellen Apoptose auszulösen. Für Microcionamid C und D konnte zudem gezeigt werden, dass diese in der Lage sind Autophagie zu inhibieren, was ein vermindertes Überleben der Krebszellen zur Folge hat. In Bezug auf die untersuchten antibakteriellen Eigenschaften zeigten Microcionamid A und C wachstumsinhibitorische Effekte auf grampositive Bakterien (*Staphylococcus aureus* und *Enterococcus faecium*) mit MIC Werten zwischen 6,25 und 12,5 μM . Interessanterweise weisen Untersuchungen am antibakteriellen Wirkmechanismus darauf hin, dass Microcionamid A und C in der Lage sind, die bakterielle Zellwand zu zerstören.

Cinachyrella sp.

Beim letzten in dieser Dissertation behandelten Organismus handelt es sich um den in Indonesien gesammelten Meereschwamm *Cinachyrella* sp.. Aus dem Schwamm konnten drei neue Pyrazolalkaloide (Cinachyrazol A, B, und C) und vier 2-Methoxy-Acetylsäuren isoliert werden. Unter den isolierten 2-Methoxy-Acetylsäuren befanden sich die bereits beschriebene Cinachylensäure A, sowie die drei neuen Naturstoffe Cinachylensäuren B, C und D. Die Strukturaufklärung erfolgte über ein- und zweidimensionale Kernspinresonanzspektroskopie, sowie den Einsatz von massenspektrometrischen Verfahren. Bioaktivitätsuntersuchungen zeigten starke zytotoxische Eigenschaften aller Cinachylensäuren mit IC_{50} -Werten von 0,3 μM . Zusätzlich wurde für die Cinachyrazolderivate ein Biosyntheseweg postuliert, welcher von der Verknüpfung von Acetoessigsäure und einer *N*-Acetyl-*N*-Methylhydrazineinheit ausgeht.

1 Significance of the study

Marine organisms represent a largely unexploited source of potential pharmaceuticals with a great diversity of novel and biologically active compounds.¹ In the past few years, investigation on marine natural products led to the discovery of several drug candidates. Considering the short duration of pharmaceutical research on marine sources, many of the obtained bioactive molecules are still under (pre-)clinical development or on the market, such as cytarabine (also known as cytosine arabinoside or ara-C) (Cytosar-U[®]) and trabectedin (also known as ecteinascidin 743 or ET-743) (Yondelis[™]).²

Marine sponges have been considered attractive among other marine organisms for drug discovery investigations. Sponges are reported as the source of nearly 30% of all marine natural products.³ Altogether, considering the global diversity of marine sponges, which includes more than 8.500 sponge species⁴, many of them have not yet been well investigated. Thus, marine sponges possess an amazing potential for the discovery of new natural products.

The respective metabolites are mostly reported from sponges of habitats with high fauna biodiversity, in which there is a strong competition between animals, and pressure from predators like the coral reef ecosystems.⁵ Indonesia is among the richest tropical ecosystems for marine sponges, and as far as up to 2007 about 77 new pharmacological compounds have been identified from only 14 Indonesian sponge species.⁶ Although more research is always needed to discover the hidden secrets of nature, marine sponges are still poorly represented in research and broader investigations are necessary to identify bioactive natural products produced by marine sponges.

2 Introduction

Nature is traditionally known as a big source of natural products with therapeutic potential. Natural products have been the most useful source for drug discovery, due to investigation of their pharmacological characteristics. Since around 70% of the earth's surface is covered by the oceans, it is expected that marine environments have a significant contribution among natural product sources. Marine organisms contain almost 50% of the total global biodiversity which accounts for a large number of natural bioactive molecule resources.⁷ In addition, wide ranges of thermal, pressure and nutrient condition, extensive photic and non-photoc zones in the marine environments,⁸ in addition to the diversity of macro- and microorganisms, which consist half of the total biodiversity on Earth provide a stressful condition for marine organisms. The biological diversity in some marine ecosystems like coral reefs and deep sea floors is even higher than in tropical rainforests.^{2, 9} This exhibits unique physiological exclusivity in marine animals to survive under the extremes of pressure, salinity, and temperature.¹⁰

In addition, the soft body structure and lack of a physical defence system, like protective shells or spines, is an additional reason for necessitating chemical defence mechanisms with the ability to synthesize toxic and/or deterrent compounds in sessile or slow moving marine invertebrates, such as sponges, soft corals, and molluscs.¹¹ In fact, development of the

chemical defence system of marine invertebrates to produce bioactive secondary metabolites has been the case of survival of these animals in the course of evolution.

Particularly, marine sponges, bryozoan, and molluscs have shown high application of their pharmaceutical potential, which makes them attractive in academic and industrial research.¹² In addition, sponges are known as the richest sources of interesting secondary metabolites among marine organisms.¹³

2.1 Marine sponges

The presence of marine sponges dates back to the Precambrian period.^{10b} Sponges belong to the Phylum Porifera as the most primitive multicellular animals with a benthic colonies system. These animals have no true tissues or organs, with an initial organization level of cellular functions such as feeding or protection.¹⁴ The main functional cell groups in sponges include choanocytes (interior cells with flagellum), porocytes (tubular cells to make ostium), amebocytes (mobile cells with function of distributing food, dispose of wastes, fighting infections, and change into other cell types), and pinacocytes (flat cells, capable of contracting with maintenance of the sponge shape and size). The body structure of sponges consists of three layers including an inner layer called the endoderm and an outer layer called the ectoderm, in addition to a jelly-like mesenchyme in the middle, which is protected by silica or calcium carbonate spicules as an initial endoskeleton system.

Three main classes of sponges have been recognized based on their spicules, as well as their different morphological and phylogenetic characteristics, including Calcarea, Hexactinellida (glass sponges), and Demospongiae (Table 2.1).¹⁵

Table 2.1. Characteristics of the main classes of sponges.¹⁶

	Habitat	Deep	Spicules	Massive exoskeleton	Body form
Calcarea	marine	<100m	calcium carbonate in the form of calcite or aragonite	common, from calcite	asconoid, syconoid, leuconoid
Hexactinellida	marine	>300m	four- and/or six-pointed siliceous	never	leuconoid
Demospongiae	marine, brackish, fresh waters	intertidal to abyssal	Silica or sponging or both	in some species. from aragonite	leuconoid

The body shape of sponges is like an empty bag with an interior water space, typically attached to the benthic stratum. Sponges are efficient filter feeder animals, which are able to strongly pump water for absorption of nutrients and food particles. They move water using the flagellums of choanocytes to the atrium (spongocoel or central body cavity) via entrances of hundreds of ostia (small entrance pores) and exit water from osculum (as a mouth). Three

types of the body structure in sponges have been clarified, including asconoid, syconoid, and leuconoid.¹⁵

Sponges are benthic sessile animals living in a diverse variety of areas, from marine to freshwater habitats. They can be found in almost every climate zones, commonly in tropical regions, from shallow intertidal areas to the deep oceans.^{4, 17} Recently, more than 8.500 sponge species have been established in WPD (World Porifera Database), of which almost 83% belong to the class of Demospongiae⁴ and about 1% inhabit the freshwater.¹⁸

2.1.1 Ecological functions of marine sponges

Sponges are epifaunal benthic animals that play important ecological functions in marine ecosystems ranging from tropical to polar habitats. Three main ecological roles have been described for marine sponges including:

- a) Effect on substrates, such as bioerosion for elimination of calcium carbonate substrates.
- b) Recycling of elements such as carbon, silicon, oxygen or nitrogen in benthopelagic areas.
- c) Associations with other organisms, mainly in the form of chemical interaction and symbiosis with microorganisms, such as cyanobacteria.

Marine sponges have successfully adapted to stressful marine environments. The lack of a physical defense system (e.g., hard outer shell), forced them to improve powerful chemical defense mechanisms by producing a variety of secondary metabolites toward predation, fouling organisms, or space competition with other marine organisms.

2.1.2 Symbiosis in marine sponges

Marine sponges are adapted to live peacefully together with diverse microbial communities of microorganisms through evolutionary and ecological long term changes. They have a broad number and types of symbionts, mostly including bacteria, archaea, microalgae, and fungi.¹⁹ The bacterial associated communities consist of more than 40% of the sponge biomass in many sponge species, whereas this value can even reach to almost 60% in certain cases.²⁰ Sponge symbionts play an important role in the nitrogen cycling and organic production in marine ecosystems, and more significantly in oligotrophic habitats.⁴

It has been estimated that up to 24.000 liters of water can be pumped through a 1 kg sponge per day.²¹ Hence, sponge tissue is a unique ecological niche for microorganisms, which can contribute significantly to sponge's metabolism via photosynthesis or nitrogen fixing.¹⁹ As a result of sponge-microorganism association, a great range of biologically active metabolites are produced, which makes them interesting targets for pharmaceutical investigations and discovery of several novel chemical compounds. Interestingly, in the past few years there is increasing evidence of the production of these metabolites by endosymbionts.²²

2.2 Natural products from marine sponges

Marine natural products are metabolites that are produced by marine organisms in nature. Although, the history of natural product isolation dates back to early 19th century, it is not more than half a century that human access to natural products from marine environments has been impressively increased by development of scuba diving techniques in the 1950s.²³ Insofar, more than 15.000 marine natural products, including alkaloids, terpenoids, steroids, polyketides, polysaccharides, peptides, and phenolic compounds have been reported from marine organisms such as sponges, cnidarians, microorganisms, molluscs, tunicates, echinodermata and algae.^{3, 24} Sponges are among the most prolific sources of marine secondary metabolites, with more than 2.000 new compounds reported only between 2001 to 2010.³

Sponges are attractive targets for natural product discovery from the marine environment. Investigations on marine sponges discovered a broad range of secondary metabolites, including nucleosides, terpenoids, sterols, peptides, alkaloids, fatty acids, and halogenated amino acid derivatives.²⁵ Most of these compounds exhibit potent bioactivities, such as antitumor, antibacterial, antifouling, antiviral, antimalarial, and anti-inflammatory activities, which make them potential leads in drug development.²⁴

For the first time in the early of 1950s, the structures of two unusual bioactive nucleoside derivatives spongothymidine and spongouridine have been identified from the sponge *Cryptotethya crypta* (Figure 2.2).²⁶ Interestingly, the first marine-derived anticancer agent cytarabine or cytosine arabinoside (ara-C), and the antiviral drug vidarabine or 9- β -D-arabinofuranosyladenine (ara-A), were synthesised based on those nucleosides.^{13b, 27} So far, more than 5.300 secondary metabolites have been isolated from marine sponges.²⁸

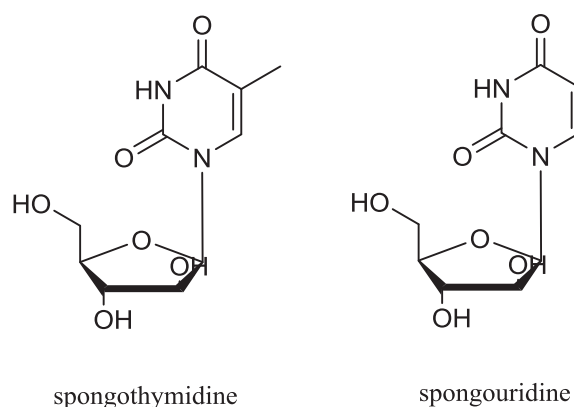


Figure 2.2. The structures of spongothymidine and spongouridine.

2.2.1 Alkaloids from marine sponges

Alkaloids are the most abundant group of marine natural products containing basic nitrogen atoms. Alkaloids are usually divided into five major groups, including true alkaloids, protoalkaloids, polyamine alkaloids, peptide alkaloids, and pseudoalkaloids. Interestingly,

alkaloids isolated from marine organisms have contributed to 20% of all of the isolated compounds from 2001 to 2010.³ Isolated alkaloids from marine sponges include a wide range of structures, from complex manzamine-type alkaloids to simple protoalkaloids, showing a high range of bioactivities (Table 2.2.1).

Table 2.2.1.Pharmaceutically active alkaloids derived from marine sponges²⁹

Class of alkaloids	Compound name	Sponge source	Biological activities
Alkyl piperidine	Arenosclerins A, B, and C ³⁰	<i>Arenosclera brasiliensis</i> / <i>Haplosclerida</i>	Antibacterial
Fused pyrrolophenanthroline	Discorhabdin D ³¹	<i>Latrunculia brevis</i> / <i>Prianos</i> sp.	Antitumor
Pyrrole guanidine	Keramadin ³²	<i>Agelas</i> sp.	Neurosuppressive
Pyrrole imidazole	Taurodispacamide A ³³	<i>Agelas oroides</i>	Immunosuppressive
Indole	Dragmacidin F ³⁴	<i>Halicortex</i> sp.	Antiviral
Bisindole	Bromotopsentin ³⁵	<i>Spongisorites</i> sp./ <i>Halichondria</i>	Neurosuppressive
Pyridoacridine	Neoamphimedine ³⁶	<i>Xestospongia</i> cf. <i>carbonaris</i>	Antitumor
Imidazole	Naamine D ³⁷	<i>Leucetta</i> cf. <i>chagosensis</i>	Antitumor
Bis-oxaquinolizidine	Xestospongins-C ³⁷⁻³⁸	<i>Xestospongia</i> sp.	Neurosuppressive
Pyridopyrrolo pyrimidine	Variolin B ³⁹	<i>Kirkpatrickia varialosa</i>	Antiviral
Manzamine	Manzamine A ⁴⁰	<i>Haliclona</i> sp.	Antimalarial
Imidazo-azoloimidazole	Axinellamines B–D ⁴¹	<i>Axinella</i> sp.	Antibacterial and antifungal

2.2.2 Peptides from marine sponges

Peptides are divided into different classes, mainly ribosomal and non-ribosomal peptides. Ribosomal peptides, such as hormones or signalling molecules in higher organisms are usually linear and are synthesised in ribosomes by translation of mRNA. On the other hand, non-ribosomal peptides are often present in both cyclic and linear forms and are biosynthetically assembled by specific enzymes. Marine peptides are a major group of natural products composed of linear and/or cyclic chains of amino acid monomers linked by peptide (amide) bonds. In the last decades, peptides from marine sponges have shown a wide range of pharmaceutical effects, such as anticancer, antibacterial, antifungal, and anti-HIV activities (Table 2.2.1). Sponges are well known as one of the main sources of peptides in the marine environment. In 1985 the first bioactive peptide, discodermin A was isolated from the marine sponge *Discodermia kiiensis*, which contains rare tertleucine and cysteine

acid, in addition to several D amino acids. Interestingly, discodermin A showed potent antimicrobial activity as well as inhibition of starfish embryo development.⁴² So far, a huge number of peptides have been reported from marine sponges, among them 155 new peptides from 2001 to 2010 that are represented by a wide range of bioactivities.³

Table 2.2.2. Examples of pharmaceutically active peptides derived from marine sponges⁴³

Peptide	Sponge source	Biological activities
Cyclic Mirabamides ⁴⁴	depsipeptides <i>Stelletta clavosa</i>	Anti-HIV and antibacterial
Papuamides A–F ⁴⁵	<i>Theonella mirabilis</i> / <i>Theonella swinhoei</i>	Anti-HIV and cytotoxic
Theopapuamides B–D ⁴⁶	<i>Siliquariaspongia mirabilis</i>	Anti-HIV, cytotoxic, and antifungal
Theonellamide A–E, G ⁴⁷	<i>Theonella</i> sp.	Cytotoxic and antifungal
Milnamide A ⁴⁸	<i>Pipestela candelabra</i>	Antiproliferative and antitumor

2.2.3 Fatty acids from marine sponges

Aliphatic marine natural compounds are fatty acids, including acetylenic (triple), double, and/or allenic bonds, as well as alcohols, aldehydes, and ketones. Fatty acids (FAs) comprise usually long chains of carbons, which are characterized by the presence of a carboxyl group (COOH) terminal at one side and a methyl terminal at the other side of the chain. They are usually referred to as short-chain, between 2 (or 4) and 6 carbons; medium-chain, between 8 (or 6) and 10; and long-chain fatty acids, between 12 and 24 carbons. In addition, depending on the presence and numbering of double bounds, fatty acids are divided into saturated or unsaturated ones. The fatty acids with only one double bond are called monounsaturated fatty acids (MUFAs), while polyunsaturated fatty acids (PUFAs or polyenoic) possess two or more double bonds that are commonly separated by methylene groups (methylene-interrupted unsaturation).⁴⁹

Marine sponges have been reported with the highest FAs diversity among aquatic animals. They exhibit a high content of long chain FAs, mostly with 22 carbon chains, which are phospholipids, the major component of biological membranes in sponges.⁵⁰ Many of them exhibit different bioactivities, such as cytotoxic,⁵¹ antimicrobial,⁵² and antifungal activities.⁵³

Moreover, fatty acids are used for sponge classification and chemotaxonomic purposes, such as demospongiac acids which are characteristic for Demospongia sponges.⁴⁹ The demospongiac acids content is almost 85% of the total fatty acids content in sponge phospholipids.⁵⁴

2.3 Bioactivity of marine natural products

The huge number of marine bioactive natural products indicates the unique and stressful marine environment conditions for organisms. Discovery of various compounds isolated from marine organisms led to an attempt for identification of the possible pharmaceutical properties of these compounds, such as anticancer, antibacterial, antifungal, and antiviral activities. Considering available reports in the literature, compounds with anticancer activities are proposed as the most abundant isolated metabolites reported from marine organisms (56%), following with the antibacterial compounds (13%). The antibacterial activity is the next most abundant among marine natural products. Moreover, it is reported that most of marine bioactive metabolites are belong to the chemical classes of alkaloids (23%) and terpenes (22%).⁵⁵

2.4 Marine anticancer natural products

Chemical compounds, capable of killing cancerous cells via different mechanisms, are referred to as anticancer drugs. Production of toxic compounds by organisms in nature has always been of interest for cancer research. It is estimated that about 60% of oncology drugs are derived from natural sources.⁵⁶ With the improvement of oncology studies and an increase in the availability and knowledge of marine resources, the anti-cancer research has expanded to marine organisms.

In anticancer research, the toxicity of compounds is evaluated based on *in vitro* assays for their inhibitory activity on different mammalian cancer cell lines. Usually, the toxicity result is measured based on cell resistance. The value of cell viability is determined via direct (determine cell culture parameters such as a number of living or dead cells) or via indirect (determine cell viability) experiments. In the direct assays by using the method like CVS (crystal violet staining), the DNA mass of living cells is measured, whereas indirect experiments are based on cell catalysis reactions by using methods such as MTT and CellTiter-Glo.⁵⁷

In the process of drug discovery, the success of toxic candidates is determined from their physiological effect mechanisms, structure synthesis, as well as various pre-clinical and clinical research phase studies. Currently, cytarabin, eribulin, trabectedin, and brentuximab vedotin are marine-derived natural products that are used as anticancer drugs on the market (Figure 2.4).

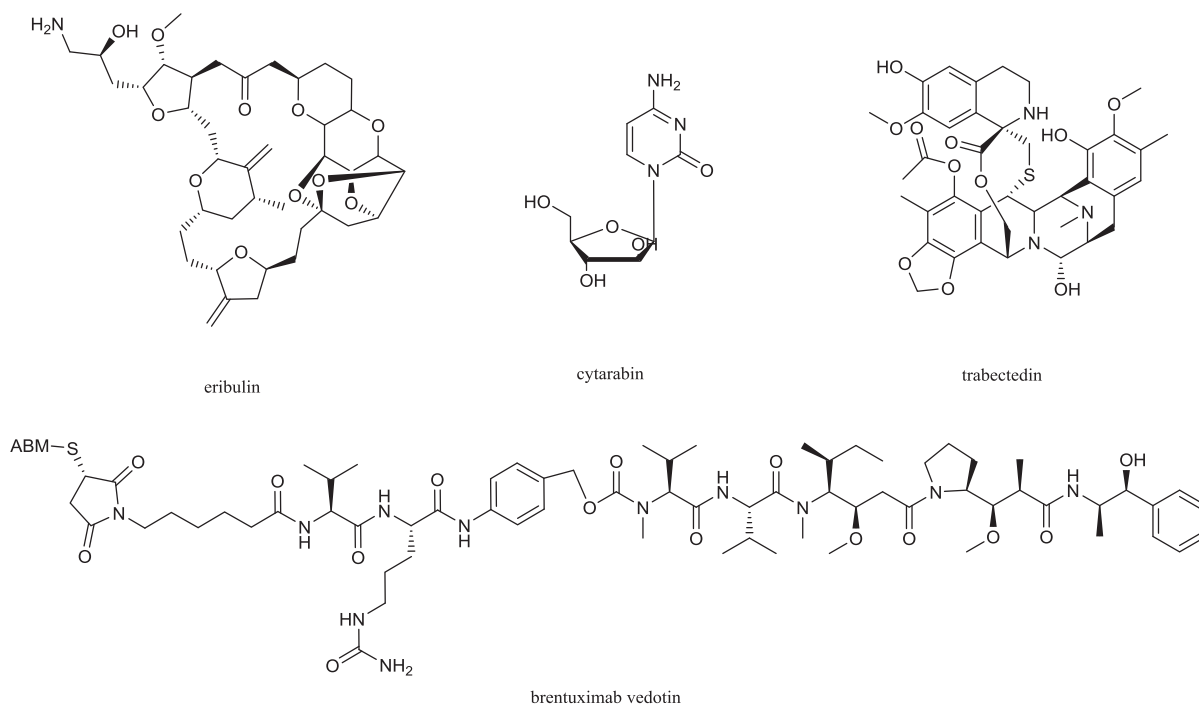


Figure 2.4. The structures of eribulin, cytarabine, trabectedin, and brentuximab vedotin.

2.4.1 Cell death mechanisms (apoptosis and necrosis)

Apoptosis and necrosis are two different types of cell death mechanisms in multicellular organisms, also known as uncontrollable or programmed cell death, respectively.

Apoptosis is a programmed physiological and energy dependence form of cell death. It is a normal biochemical process in multicellular organisms, in which unnecessary, old, or damaged cells are destroyed. Due to the process of apoptosis, morphological characteristic changes occur in the cell, including cell shrinkage, blebs of the cell membrane, nuclear and chromosomal DNA fragmentations, chromatin condensation, and decomposition of global mRNA. Apoptosis is important to a variety of normal cell physiological processes, such as fetal development, tissue homeostasis, immune response, aging, and others. Any problem in the process of apoptosis can lead to cases of cancer and autoimmune diseases or cases of neurodegenerative and AIDS diseases. Many cancer cells are resistant to apoptosis, which means that the apoptosis process can be disrupted allowing cells to continue to live and multiply.⁵⁸

In contrast to apoptosis, necrosis is a pathological, non-physiological, accidentally, uncontrolled, and energy independent form of cell death, which results to the unregulated digestion of cell components.⁵⁹ Hence, the cell membrane unity is disrupted and cells release uncontrolled cellular components to the extracellular space. That is the reason why inducing necrosis through natural compounds as potential therapeutic agents is absolutely undesired. Necrosis occurs due when the cell is damaged and lacks ATP (adenosine triphosphate).⁶⁰

2.4.2 *Cell autophagy*

Autophagy is an intracellular degradation pathway for the survival of cells. Due to the process of autophagy, the cell packs cytoplasmic components in a special double layer membrane (autophagosome) and set it with lysosomal enzymes in order to destroy the ingredients. For delivering components to the lysosome, the outer membrane layer of autophagosome fuses with the lysosome membrane to form an autolysosome. Thus, autophagy plays an important role in keeping cell homeostasis. Apart from the vital role of autophagy in surviving cells, since cancer cells have rapid growth rates under stress and nutrient competition, the progress of autophagy can support the survival of cancer cells.⁶¹ Since formation of autophagosome is under control of Atg gene and LC3 complexes, LC3 is usually used as a marker of autophagosomes in studies on drug mechanisms.⁶² Moreover, LC3 is commonly detected by using various fluorescent antibody labelling assays and flow cytometry techniques.⁶³

2.4.3 *Biochemical pathways of apoptosis*

Several signalling pathways have been described for apoptosis in mammalian cells, but the main consist of intrinsic (mitochondrial) and of extrinsic (death receptor) pathways. Both pathways are based on caspase activation. Caspases (cysteine-aspartic acid protease) are proteolytic enzymes which can cleave and degrade other proteins. They are known as death enzymes in the cell and are firstly synthesized as pro-caspases, which later are converted or cleaved into mature caspase enzymes by apoptotic signals. In healthy cells, caspases are present as inactive enzymes with less or no protease activity.⁶⁴

Caspases are divided into two different functional groups as initiator and effector (executioner) ones. Initiator caspases 8 and 9 in extrinsic and intrinsic pathways, respectively, cleave inactive pre-forms of effector caspases to the activated forms. The effector caspases activate other proteins (e.g. PARP) leading to apoptosis.

The extrinsic pathway is activated by death signals from out of the cell and is operated by binding of death ligands (e.g. TRAIL) to specific cell membrane death receptors (e.g. DR5). This process initiates recruitment of adapter specific proteins (e.g. FADD or TRADD) to the cytosolic death domain of the receptor. This, in turn, triggers recruitment of the caspase-8 initiator caspases that are activated and initiate cell death through the caspase cascade.⁶⁵

In contrast, the intrinsic pathway is operated by intracellular stress conditions (e.g. induction of DNA damage or oxidative stress).⁶⁶ This mechanism is regulated by balanced equilibria between pro-apoptotic (e.g. Bax) and anti-apoptotic (e.g. Bcl-2) proteins. This process results in translocation from the cytosol into the outer mitochondrial membrane, oligomerization, and formation of channels that mediate the release of cytotoxic protein factors (cytochrome C) and trigger caspase-dependent and independent cell deaths. The release of cytochrome C is operated by the formation of apoptosome, which is a large quaternary protein structure. Then, cytochrome C binds to the adapter protein APAF-1, which in turn binds to the initiator caspase-9.

In both apoptosis pathways, initiator caspase-8 (in extrinsic) or caspase-9 (in intrinsic) lead to activated effector caspases (caspase-3, caspase-6 and caspase-7), which are inducers of apoptosis. Natural products have the ability to induce apoptosis through both mitochondrial and death receptor pathways.⁶⁷

2.4.4 Detection of apoptosis by western blot

Toxic compounds with controlled and targeted stimulants of cell death via apoptosis are important in pharmaceutical studies and anticancer drug discovery. Hence, diagnosis of cell reactions and death mechanisms is important after vicinity with toxic natural compounds. There are different described techniques for apoptosis detection in the cell such as caspase activity assays, electron microscopy, proteomic and genomic methods, spectroscopic techniques, flow cytometry, microfluidic, and electrochemical applications.⁶⁸

Monitoring of the special proteins (e.g. cytochrome c and PARP-1) produced in the apoptosis process, can be an indicator for apoptosis. Western blot is a gel electrophoresis technique to separate and identify specific proteins from a complex mixture, based on the molecular weight. Accordingly, detection of cleaved PARP-1 (Poly (ADP-ribose) polymerase-1) is usually used as a marker for apoptosis. PARP-1 is a nuclear protein enzyme and one of the several known cellular substrates of caspases with a wide range of physiological and pathological functions. The cleavage of PARP-1 by caspases-3 and -7 leads to the formation of specific 89-kD C-terminal catalytic and 24-kD N-terminal DBD fragments.⁶⁹

2.5 Drug discovery using marine natural products

Marine natural products are known as prolific sources of drug molecules and have been used traditionally as medicines for treating diseases, in some countries like China and Japan. They have been recommended for pain, menstrual difficulties, abscesses, and cancer.⁷⁰ This has led to attempts to isolate and identify bioactive metabolites from marine organisms for drug discovery and pharmaceutical applications.⁷¹

In the middle of the last century, two arabinosyl glycosides derivatives were isolated from the marine sponge *Tectitethya crypta* that led to the first marine drug improvements by FDA (Food and Drug Administration of US), as cytarabine (anticancer) and vidarabine (antiviral) in 1969 and 1976, respectively.⁷²

Ziconotide is a ω -conotoxin synthetic peptide that was isolated from the tropical marine cone snail and approved by FDA, a few years later in 2004, as an analgesic drug. So far, more marine derived drugs have been approved by FDA, including omega-3-acid ethyl esters, eribulin mesylate or halichondrin B, brentuximab vedotin, and trabectedin. Currently, more than 25 marine natural compounds are known under clinical trials, based on the report of marine pharmaceuticals, the clinical pipeline of Midwestern University (Table 2.5). Furthermore, around 1,000 marine natural metabolites have been identified with promised bioactivities and are under pre-clinical trials.⁷³

Table 2.5. Current marine derived drugs, FDA approved, in pre-clinical and clinical trials (A.M.S. Mayer, Marine pharmaceuticals: the clinical pipeline, Midwestern University, Last Rev. 04/20/2017)

Clinical Status	Compound Name	Trademark isolated/ FDA Approved (Year)	Marine Organism	Chemical Class	Molecular Target	Disease Area
FDA-Approved	Trabectedin (ET-743)	Yondelis® (2015)	Tunicate	Alkaloid	Minor groove of DNA	Cancer
	Brentuximab vedotin (SGN-35)	Adcetris® (2011)	Mollusk/ cyanobacterium	ADC(MMAE)	CD30 & microtubules	Cancer
	Eribulin Mesylate (E7389)	Halaven® (2010)	Sponge	Macrolide	Microtubules	Cancer
	Omega-3-acid ethyl esters	Lovaza® (2004)	Fish	Omega-3 fatty acids	Trygliceride-synthesizing enzymes	Hypertriglyceridemia
	Ziconotide	Prialt® (2004)	Cone snail	Peptide	DNA polmerase	Chronic Pain
	Vidarabine (Ara-A)	Vira-A® (1976)	Sponge	Nucleoside	Viral DNA polymerase	Antiviral
	Cytarabine (Ara-C)	Cytosar-U® (1969)	Sponge	Nucleoside	DNA polymerase	Leukemia
Phase III	Plinabulin (NPI-2358)	NA	Fungus	Diketopiperazine	Microtubules	Cancer
	Plitidepsin	Aplidin®	Tunicate	Depsipeptide	Rac1 & JNK activation	Cancer
	Squalamine Lactate (OHR-102)	NA	Dogfish Shark	Aminosterol	Growth factors of neovascularization	Anti-angiogenic
	Tetrodotoxin	Tectin®	Pufferfish	Guanidinium alkaloid	Sodium Channel	Chronic Pain
Phase II	ABT-414 EGFRvIII - MMAF	NA	Mollusk/ cyanobacterium	ADC (MMAF)	EGFR & microtubules	Cancer
	Lurbinectedin (PM01183)	NA	Tunicate	Alkaloid	Minor groove of DNA	Cancer
	AGS-16C3F	NA	Mollusk/ cyanobacterium	ADC (MMAF)	ENPP3 & microtubules	Cancer

	Lifastuzumab vedotin (DNIB0600A)	NA	Mollusk/cyanobacterium	ADC (MMAE)	NaPi2b & microtubules	Cancer
	Polatuzumab vedotin (DCDS-4501A)	NA	Mollusk/cyanobacterium	ADC (MMAE)	CD79b & microtubules	Cancer
Phase I	GSK2857916	NA	Mollusk/cyanobacterium	ADC (MMAF)	BCMA	Cancer
	ASG-67E	NA	Mollusk/cyanobacterium	ADC (MMAE)	CD37 & microtubules	Cancer
	Enfortumab Vedotin ASG-22ME	NA	Mollusk/cyanobacterium	ADC (MMAE)	Nectin-4 & microtubules	Cancer
	Bryostatins	NA	Bryozoan	Macrolide lactone	Protein kinase C	Cancer
	Tisotumab Vedotin	HuMax®-TF-ADC	Mollusk/cyanobacterium	ADC (MMAE)	Tissue Factor & microtubules	Cancer
	Marizomib (Salinosporamide A; NPI-0052)	NA	Bacterium	Beta-lactone-gamma lactam	20S proteasome	Cancer
	MLN-0264	NA	Mollusk/cyanobacterium	ADC (MMAE)	GCC & microtubules	Cancer
	PM060184	NA	Sponge	Polyketide	Minor groove of DNA	Cancer
	SGN-LIV1A	NA	Mollusk/cyanobacterium	ADC (MMAE)	LIV-1 & microtubules	Cancer

3 Aim of the study

With regard to the discovery of bioactive properties of marine natural products, especially from marine sponges, further investigations are necessary to further identify novel and new bioactive metabolites from marine species in different areas. Thus, this study was carried out with the purpose of detecting the bioactive chemical structures from marine sponges. The study was focused on isolation and structure elucidation of the secondary metabolites from bioactive extracts obtained from three marine sponge specimens, *Lissodendoryx fibrosa*, *Clathria basilana*, and *Cinachyrella* sp., collected in Indonesia.

The pure isolated metabolites were evaluated in different bioassays, such as cytotoxicity assays against mouse lymphoma L5178Y, leukemia (HL-60, Nomo-1, Jurkat J16), and human ovarian carcinoma (A2780) cell lines, as well as antibacterial assays toward various Gram-positive and Gram-negative bacteria. Isolation of the secondary metabolites was performed based on chromatographic techniques, including TLC, VLC, column

chromatography, and HPLC. The structure elucidation of the isolated compounds was performed on the basis of modern spectroscopic methods, including MS, ESI-MS, EI-MS, HR-MS, and UV spectroscopy, as well as 1D and 2D NMR.

4 **Publication 1: Lissodendrins A and B, New 2-Aminoimidazole Alkaloids from the Marine Sponge *Lissodendoryx (Acanthodoryx) fibrosa***

Lissodendrins A and B, New 2-Aminoimidazole Alkaloids from the Marine Sponge *Lissodendoryx (Acanthodoryx) fibrosa*.

Amin Mokhlesi,^[a,b] Rudolf Hartmann,^[c] Elisabeth Achten,^[c] Chaidir,^[d] Thomas Hartmann,^[e] Wenhan Lin,^[f] Georgios Daletos,^{*[a]} Peter Proksch^{*[a]}

[a] Institute of Pharmaceutical Biology and Biotechnology, Heinrich-Heine-University, Universitaetsstrasse 1, 40225 Duesseldorf, Germany.
E-mail: proksch@uni-duesseldorf.de, georgios.daletos@uni-duesseldorf.de

[b] Department of Marine Biology, Faculty of Marine Sciences, Tarbiat Modares University, Noor, Iran.

[c] Institute of Complex Systems: Strukturbiochemie (ICS-6), Forschungszentrum Juelich, Wilhelm-Johnen-Straße, 52428 Juelich, Germany.

[d] Center for Pharmaceutical and Medical Technology, Agency for the Assessment and Application Technology, 10340 Jakarta, Indonesia.

[e] Institute of Pharmaceutical Biology, Technical University of Braunschweig, D-38106 Braunschweig, Germany.

[f] National Research Laboratories of Natural and Biomimetic Drugs, Peking University, Health Science Center, 100083 Beijing, People's Republic of China.

Supporting information for this article is given via a link at the end of the document

Chemical investigation of the Indonesian sponge *Lissodendoryx (Acanthodoryx) fibrosa* yielded the new 2-aminoimidazole alkaloids lissodendrins A (**1**) and B (**2**). Their structures were unambiguously determined by extensive NMR spectroscopic (^1H , ^{13}C , ROESY and long-range HMBC) studies and mass spectrometric (HRESIMS/MS) data. Lissodendrins A (**1**) and B (**2**) possess unprecedented skeletons with the latter compound bearing a *p*-hydroxyphenylglyoxylate moiety, which is rarely encountered in natural products. A plausible biosynthetic pathway for these new metabolites is proposed.

4.1 Introduction

Marine sponges are rich sources of alkaloids often exhibiting unprecedented structural frameworks and a wide range of biological activities.^[1] 2-Aminoimidazole alkaloids represent an important group of active secondary metabolites that are found primarily in calcareous sponges, especially in the genera *Leucetta* and *Clathrina*.^[2,3] The imidazole nucleus is a potentially important pharmacophore, as many of these compounds possess interesting biological activities. For example, naamine G, from the Indonesian sponge *Leucetta chagosensis*, showed strong antifungal activity against the phytopathogenic fungus *Cladosporium herbarum*, as well as mild cytotoxicity against mouse lymphoma (L5178Y) and human cervical carcinoma (HeLa) cell lines.^[4] Potent leukotriene B4 (LTB4) receptor binding affinity was reported for leucettamine A, obtained from the Palauan sponge *Leucetta microraphis*.^[5] The compound was found to specifically block the LTB4-induced Ca^{2+} transient associated with several inflammatory diseases.^[5] Furthermore, naamidine A, isolated from a Fijian *Leucetta* sp. sponge, selectively inhibited the epidermal growth factor (EGF) receptor and induced caspase-dependent apoptosis in tumor cells.^[6] The unique structures of 2-aminoimidazole alkaloids, along with the broad range of biological activities that they display, make them attractive targets for total synthesis and SAR studies.^[7,8]

Sponges from the genus *Lissodendoryx* (syn. *Acanthodoryx*) are well known for structurally complex polyether macrolides such as the halichondrins.^[9] Recently, the anti-tumor drug eribulin mesylate (Halaven) that was synthesized based on the lead structure halichondrin B was introduced into the drug market^[10]. In addition to halichondrins, several other secondary metabolites have been described from *Lissodendoryx* species, such as steroids,^[11] cembranes,^[12] and pyrrololactams.^[13]

In the course of our continued investigations of marine sponges,^[14] we investigated a specimen of *Lissodendoryx fibrosa* from Ambon, Indonesia. The MeOH extract was subjected to liquid-liquid fractionation to afford n-hexane, EtOAc, and n-BuOH fractions. Subsequent column chromatography of the EtOAc fraction followed by semi-preparative reversed-phase HPLC yielded two new 2-aminoimidazole alkaloids, lissodendrin A (**1**) (0.5 mg, 0.08% wet weight) and lissodendrin B (**2**) (4 mg, 0.62% wet weight). Herein, we describe the structure elucidation of these new unusual alkaloids and provide a rationale for their biosynthesis (Scheme 1).

4.2 Results and Discussion

Lissodendrin A (**1**) was isolated as a pale yellow, amorphous solid. The molecular formula $\text{C}_{17}\text{H}_{13}\text{N}_3\text{O}_3$ was established by a prominent ion peak at m/z 308.1030 $[\text{M} + \text{H}]^+$ in the HRESIMS, corresponding to 13 degrees of unsaturation. Inspection of the ^1H NMR spectrum of **1** indicated the presence of an aromatic proton at δ_{H} 8.38 and two para-substituted benzene rings as indicated by the characteristic AA'BB' patterns at δ_{H} 7.04 (H-8/12, $J = 8.6$ Hz) and 6.67 (H-9/11, $J = 8.6$ Hz) (ring B), as well as at δ_{H} 6.78 (H-16/18, $J = 8.8$ Hz) and 7.64 (H-15/19, $J = 8.8$ Hz) (ring C). Analysis of the ^{13}C and HC-HSQC spectra confirmed the corresponding carbon signals and revealed in addition four sp^2 quaternary carbons, including one carbonyl group at δ_{C} 194.3 (C-13) (Table 1).

HMBC correlations observed from H-8/12 to C-6 (δ_{C} 123.4) and C-10 (δ_{C} 158.4), and from H-9/11 to C-7 (126.9) confirmed the presence of a para-substituted phenol moiety and its connection to C-6. In addition, a para-hydroxybenzoyl moiety was assigned based on the HMBC correlations from H-16/18 to C-14 (δ_{C} 128.0), as well as from H-15/19 to C-17 (δ_{C} 164.9) and C-13. To further substantiate this conclusion, compound **1** was subjected to HRESIMS/MS analysis. A fragment ion observed at m/z 186.0660 corresponding to the loss of $[\text{M}-\text{C}_{10}\text{H}_8\text{N}_3\text{O}]^+$, confirmed the presence of this substructure. Finally, the remaining part of the molecule ($\text{C}_3\text{H}_3\text{N}_3$) and the missing four degrees of unsaturation were indicative of a monosubstituted 2-aminoimidazole moiety (ring A), as supported by the molecular formula and by HMBC correlations from H-4 to C-2 (δ_{C} 164.7) and C-6 (δ_{C} 123.4).

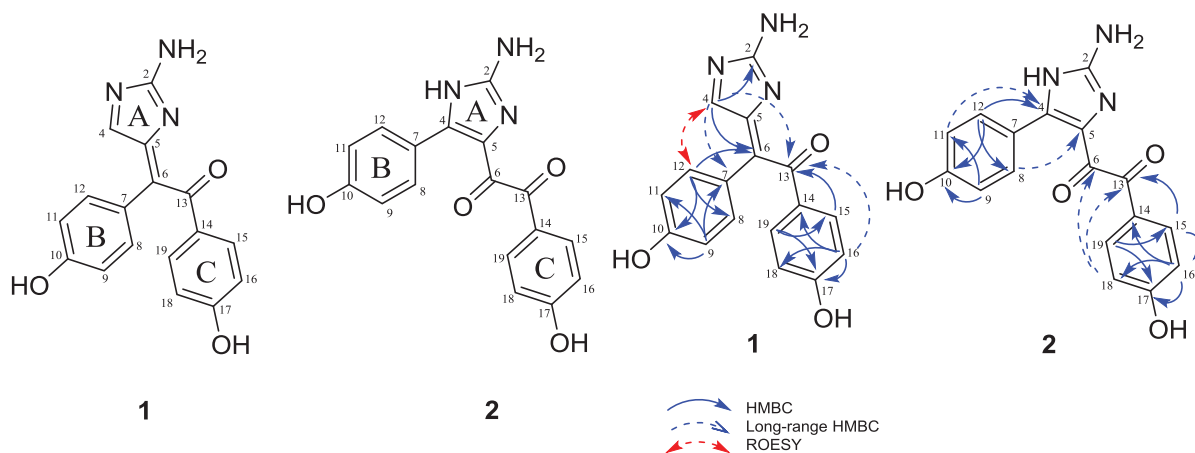
The assembly of these substructures was not a straightforward task and attempts to visualize the NH protons by changing the NMR solvent and/or the temperature parameters were unsuccessful. In order to overcome this obstacle, the HMBC experiment was optimized to detect correlations between protons and carbons separated by more than three bonds ($^nJ_{\text{H,C}}$ $n > 3$). Accordingly, in the HMBC spectrum of **1**, the 4J long-range correlations from H-4 to C-7 and C-13 offered additional evidence and established the attachment of the 2-aminoimidazole and *para*-hydroxybenzoyl moieties at C-6, as illustrated in Scheme 2. Moreover, the *Z* geometry of the C5/6 double bond was deduced on the basis of the observed ROESY correlation between H-4 and H-8/12 (Scheme 2). Thus, **1** was identified as a new natural product and was named lissodendrin A.

Table 4. ^1H (700 MHz) and ^{13}C (176 MHz) NMR data of **1** and **2** in MeOH-*d*₄.

position	1		2	
	δ_{C} (ppm)	δ_{H} (ppm) (mult., J in Hz)	δ_{C} (ppm)	δ_{H} (ppm) (mult., J in Hz)
1				
2	164.7, C		154.2, C	
3				
4	160.5, CH	8.38, s	151.6, C	
5	163.0, C		123.0, C	
6	123.4, C		184.2, C	
7	126.9, C		123.3, C	
8	130.8, CH	7.04, d (8.6)	132.1, CH	7.14, d (8.4)
9	116.4, CH	6.67, d (8.6)	115.7, CH	6.56, d (8.4)

10	158.4, C		160.1, C	184.2) respectively, thus indicating the presence of a <i>p</i> -hydroxyphenylglyoxylate moiety. ^[15,16] This was further corroborated by the HRESIMS/MS fragment ion peaks at <i>m/z</i> 121.0285 [C ₇ H ₅ O ₂] ⁺ and 202.0611 [M-C ₁₀ H ₈ N ₃ O ₂] ⁺ , originating from cleavage at C-6/C-13, as well as at <i>m/z</i> 176.0818 [M-C ₉ H ₁₀ N ₃ O] ⁺ , originating from cleavage at C-5/C-6. Moreover, the ⁴ <i>J</i> long-range HMBC correlations from H-9/11 to C-4 and from H-8/12 to C-5 (in H ₂ O, pH 3, + 50 μl DMSO- <i>d</i> ₆) confirmed the connectivity of ring B to C-4 (Scheme 2). Based on the molecular formula of 2 and its close biogenetic relationship with 1 , the remaining part of the molecule (CH ₃ N ₃) was attributed to a guanidine moiety fused to the rest of the molecule at C-4 and C-5 to form a 2-aminoimidazole ring (ring A), thus rationalizing the remaining elements of unsaturation. Further structural confirmation of ring A was evident from the chemical shifts of C-2 (δ _c 154.2), C-4 (δ _c 151.6), and C-5 (δ _c 123.0), which are consistent with 4,5-disubstituted 2-aminoimidazole moieties. ^[17] Finally, it should be noted that in contrast to 1 , where the two imidazole nitrogens are not protonated, the 2-aminoimidazole ring of 2 exists at neutral pH in two tautomeric forms with intermediate exchange rate that explains the broad lines in the ¹ H-NMR spectrum. However, at lower pH, both imidazole nitrogens are protonated and appear as sharp lines, due to the lack of tautomeric forms. Accordingly, the structure of 2 was assigned, and it was designated lissodendrin B.
11	116.4, CH	6.67, d (8.6)	115.7, CH	6.56, d (8.4)
12	130.8, CH	7.04, d (8.6)	132.1, CH	7.14, d (8.4)
13	194.3, C		193.7, C	
14	128.0, C		126.6, C	
15	133.9, CH	7.64, d (8.8)	133.4, CH	7.60, d (8.7)
16	116.5, CH	6.78, d (8.8)	116.5, CH	6.79, d (8.7)
17	164.9, C		165.0, C	
18	116.5, CH	6.78, d (8.8)	116.5, CH	6.79, d (8.7)
19	133.9, CH	7.64, d (8.8)	133.4, CH	7.60, d (8.7)

Compound **2** was isolated as a pale yellow, amorphous solid. The molecular formula was determined as C₁₇H₁₃N₃O₄, *m/z* 324.0979 [M + H]⁺ by HRESIMS measurement, indicating 13 degrees of unsaturation. The molecular formula of **2** differed from that of **1** only by one additional oxygen atom suggesting a close structural similarity between both compounds. The ¹H NMR spectrum of **2** revealed the presence of two pairs of doublets at δ_H 7.14 (H-8/12, *J* = 8.4 Hz), 6.56 (H-9/11, *J* = 8.4 Hz), 7.60 (H-15/19, *J* = 8.7 Hz) and 6.79 (H-16/18, *J* = 8.7 Hz), typical of two *para*-hydroxy-substituted phenyl rings (rings B and C, Scheme 1). ³*J* correlations observed for H-8/12 in the HMBC spectrum of **2** established the linkage of ring B to C-4 (δ_c 151.6), whereas ³*J* correlations of H-15/19 indicated the linkage of ring C to C-13 (δ_c 193.7) (Scheme 2).



Scheme 1. Structures of **1** and **2**.

In analogy to **1**, the significant number of quaternary carbons and the unusual arrangement of the oxygen functionalities within the molecule proved challenging and made the HMBC long-range correlation experiment an essential tool to connect the previously described moieties. Initial attempts to visualize the long-range ¹H-¹³C correlations were hindered due to the fact that the aromatic proton resonances in the ¹H-NMR spectrum of **2** appeared as broad signals in MeOH-*d*₄. However, changing of the NMR solvent and pH parameters resulted in sharper NMR resonances (in H₂O, pH 3, + 50 μl DMSO-*d*₆), thus improving the quality of the long-range HMBC NMR experiment. Accordingly, by an optimized HMBC delay for CH-coupling constants of <2 Hz ⁴*J* and ⁵*J* long-range HMBC correlations were observed from H-16/18 to C-13 (δ_c 193.7) and to C-6 (δ_c

Scheme 2. Key ROESY and HMBC correlations of **1** and **2**.

Compounds **1** and **2** belong to the rare class of 2-aminoimidazole alkaloids. Interestingly, the majority of these compounds has been isolated from *Calcarea* marine sponges, including the genera *Leucetta*,^[18] *Clathrina*^[18] and *Leucosolenia*,^[19] whereas they are less frequently encountered in marine sponges of the major class Demospongiae^[20] which includes sponges of the genus *Lissodendoryx* (*Acanthodoryx*). Published 2-aminoimidazole alkaloids are usually similar in that each analogue possesses a central 2-aminoimidazole ring that is often substituted at the C-4 and/or C-5 positions. The structures of naamines,^[21] dihydrosventrin,^[22] stylissazoles,^[23] hymenialdisine,^[24] and oroidin^[25] provide illustrations of these structural features.

Compounds **1** and **2** represent the first alkaloids incorporating a 2-aminoimidazole core structure from the genus *Lissodendoryx* (class Demospongiae). Structural analogues include phorbatopsins from the Mediterranean sponge *Phorbatopsenti*,^[26] as well as polyandrocarpamines from the Fijian ascidian *Polyandrocarpa sp.*^[27] (Scheme 3). However, the overall structures of **1** and **2** are unique featuring an unprecedented substitution pattern consisting of a 2-aminoimidazole ring and two para-substituted phenyl moieties (Scheme 1).

A literature survey revealed that no experimental confirmation of the biogenetic origin of 2-aminoimidazole alkaloids has hitherto been reported. The putative biosynthesis of **1** and **2** (Fig. 3) is suggested to start with a guanidine (probably originating from arginine) and a *p*-hydroxyphenylpyruvic acid moiety (probably originating from tyrosine) to generate intermediate A, which could then serve as the precursor of the phorbatopsins^[26] and polyandrocarpamines^[27] whereas addition of a *p*-hydroxybenzoic acid moiety (possibly catalyzed through a P450 dependent monooxygenase) at C-1 of intermediate A would yield lissodendrin A (**1**).

Lissodendrin B (**2**) is suggested to arise in a similar manner. In this case the guanidine moiety would be linked to *p*-hydroxyphenylpyruvic acid at the alpha and beta-carbons of the C₃ side chain of the latter. Formation of the unusual diketone could then take place by addition of the *p*-hydroxybenzoic acid precursor to the carboxyl (or aldehyde) group of the *p*-hydroxyphenylpyruvic acid moiety, possibly catalyzed by a P450 dependent monooxygenase.

Lissodendrins A (**1**) and B (**2**) were examined for their effects on the growth of the L5178Y mouse lymphoma cell line employing the MTT assay, however, both failed to exhibit significant activity when investigated at a dose of 10 µg/mL.

4.3 Conclusion

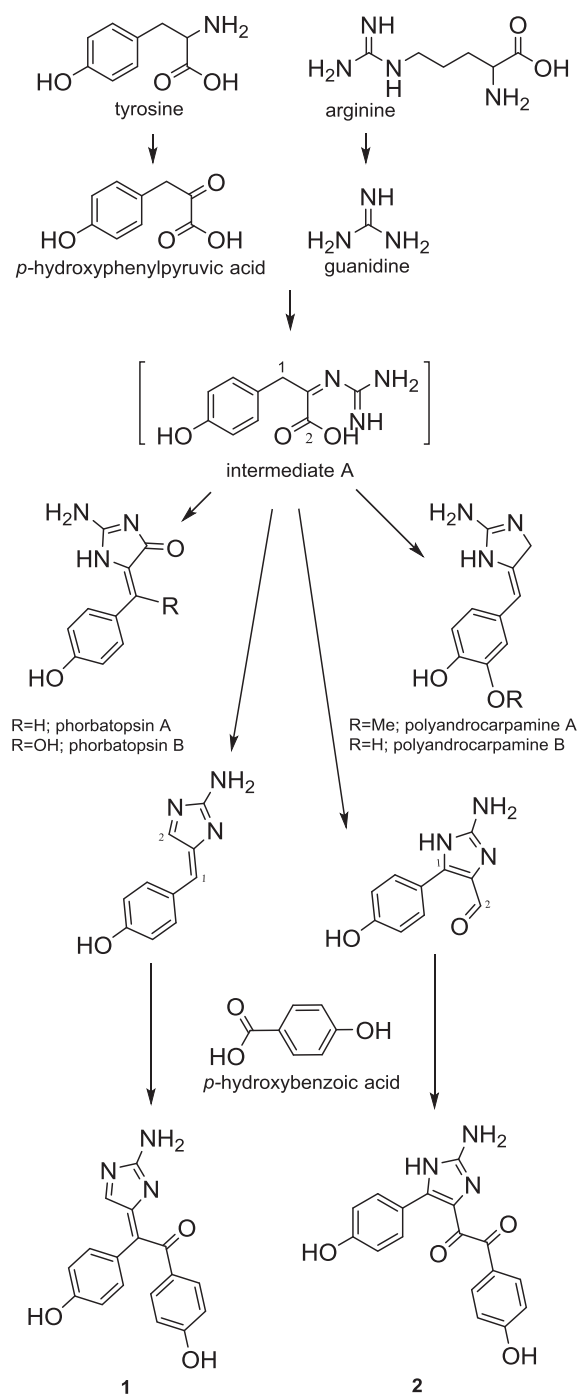
In summary, two new 2-aminoimidazole alkaloids, namely lissodendrins A (**1**) and B (**2**), have been isolated from the EtOAc fraction of the sponge *Lissodendoryx (Acanthodoryx) fibrosa*. Establishing the structures of these compounds was challenging due to their unusual substitution patterns, which are unprecedented among all 2-aminoimidazole alkaloids reported so far. In this context, our report highlights the value of the HMBC long-range correlation experiment as an effective tool for determining the structures of natural products with highly substituted heterocyclic cores.

4.4 Experimental Section

General Experimental Procedures

Optical rotations were determined with a Perkin-Elmer Lambda 25 UV/vis spectrometer. ¹H, ¹³C, and 2D NMR spectra (HH-ROESY, HC-HSQC and HC-HMBC) were recorded with standard pulse sequences on a Bruker AV III HD 700 spectrometer equipped with a TXI cryo-probe. The sweep width for the homonuclear experiments (HH-ROESY) was 7000 Hz in F2 and F1. Two thousand data points were collected in F2,

and 256 data points in F1 with quadrature detection in both dimensions. The mixing time for the HH-ROESY experiment was 450ms with a spin lock field of 5000 Hz. The HC-HSQC experiment was measured with a sweep width of 7000 Hz in F2 and 25500 Hz in F1. Two thousand data points were collected in F2, and 256 data points in F1 with quadrature detection in both dimensions. The sweep width for the HC-HMBC experiments was set to 7000 Hz in F2 and 17600 Hz in F1. Two thousand data points in F2 and 256 data points in F1 were collected with quadrature detection in F2.



Scheme 3. Proposed biosynthesis of **1** and **2**.

Three HC-HMBC experiments were measured with different delays for evolution of long range couplings [$1/(2 \times J_{\text{Long range}})$] set to $J_{\text{Long range}} = 8$ Hz, 5 Hz and 2 Hz. The chemical shifts (δ) are in ppm, referring to the solvent residual peaks at δ_{H} 3.31 (MeOH- d_4) and 2.50 (DMSO- d_6) for ^1H ; and at δ_{C} 49.0 (MeOH- d_4) and 39.5 (DMSO- d_6) for ^{13}C NMR. Low-resolution ESI mass spectra were recorded on a Thermoquest Finnigan LCQ Deca connected to an Agilent 1100 series LC. High-resolution mass measurements were obtained on a LTQ Orbitrap Velos Pro (Thermo Scientific). Solvents were distilled prior to use, and spectral grade solvents were used for spectroscopic measurements. HPLC analysis was performed using a Dionex UltiMate3400 SD coupled to a photodiode array detector (DAD3000RS) with detection wavelengths at 235, 254, 280, and 340 nm. The separation column (125 \times 4 mm, L X i.d) was prefilled with Eurospher 100-10, C18 (Knauer, Germany) and the following gradient was used (MeOH, 0.1% HCOOH in H₂O): 0 min (10% MeOH); 5 min (10% MeOH); 35 min (100% MeOH); 45 min (100% MeOH). Column chromatography was performed using Sephadex LH-20 or reversed-phase silica (RP C18) as stationary phase. Semipreparative purification was accomplished on a Merck Hitachi system (Pump L7100 and UV detector L7400; Eurospher 100 C18, 300 \times 8 mm, L X i.d; Knauer, Germany) with a flow rate of 5.0 mL/min. Thin-layer chromatography (TLC) was performed using precoated silica gel 60 F₂₅₄ plates (Merck) followed by detection under UV at 254 nm or after spraying the plates with anisaldehyde reagent.

Sponge material

The sponge was collected by SCUBA at Ambon, Indonesia, in October 1996. The sponge was identified as *Lissodendoryx* (*syn. Acanthodoryx*) *fibrosa* by Dr. Nicole de Voogd (Naturalis Biodiversity Center, Leiden, The Netherlands), and a voucher specimen was deposited at the Naturalis Biodiversity Center, Leiden, The Netherlands (reference number RMNH POR. 7739). The exterior color of the sponge was light brown to reddish. The sponge was preserved in a mixture of EtOH and H₂O (70:30) and stored in a -20°C freezer prior to extraction.

Extraction and isolation

The thawed sponge material (640 g) was cut into small pieces and exhaustively extracted with MeOH (3 \times 2L) at room temperature. The extracts were combined and concentrated under vacuum to yield 46.4 g of crude extract. Subsequent liquid-liquid partitioning afforded n-hexane, ethyl acetate and n-butanol fractions at amounts of 16.7 g, 0.76 g and 28.3 g, respectively. The ethyl acetate fraction was further purified by column chromatography on Sephadex LH-20 (MeOH as mobile phase), followed by semi-preparative HPLC in a gradient system of H₂O/MeOH to yield **1** (0.5 mg) and **2** (3.0 mg). The n-butanol fraction was subjected to reversed-phase vacuum liquid chromatography (RP-VLC), employing a step-gradient of H₂O/MeOH, to afford 10 fractions (L1 to L10). L6 (152 mg) was submitted to consecutive column chromatography on Sephadex LH-20 (MeOH as mobile phase), followed by semi-preparative HPLC to yield **2** (1mg).

Lissodendrin A (**1**):

Pale yellow, amorphous solid; UV (λ_{max} , MeOH) (log ϵ) 232 (3.13), 263 (3.12); ^1H NMR data (MeOH- d_4 , 700 MHz) see Table S1; ^{13}C NMR data (MeOH- d_4 , 176 MHz) see Table S1; ESIMS m/z 308.1 [M + H]⁺, 614.6 [2M + H]⁺; HRESIMS m/z 308.1028 [M + H]⁺ (calcd for C₁₇H₁₄N₃O₃ 308.1030); HRESIMS/MS m/z 186.066 [C₁₀H₈N₃O]⁺ [calcd for C₁₀H₈N₃O 186.0662]⁺.

Lissodendrin B (**2**):

Pale yellow, amorphous solid; UV (λ_{max} , MeOH) (log ϵ) 223 (3.32), 301 (3.29); ^1H NMR data (MeOH- d_4 , 700 MHz) see Table S1; ^{13}C NMR data (MeOH- d_4 , 176 MHz) see Table S1; ESIMS m/z 324.1 [M + H]⁺, 646.6 [2M + H]⁺; HRESIMS m/z 324.0979 [M + H]⁺ (calcd for C₁₇H₁₄N₃O₄ 324.0979); HRESIMS/MS m/z 121.0285 [C₇H₅O₂]⁺ [calcd for C₇H₅O₂ 121.0284]⁺, 176.0818 [C₉H₁₀N₃O]⁺ [calcd for C₉H₁₀N₃O 176.0818]⁺ and 202.0611 [C₁₀H₈N₃O₂]⁺ [calcd for C₁₀H₈N₃O₂ 202.0611]⁺.

Acknowledgements

We wish to acknowledge the help and support of Dr. Elizabeth Ferdinandus (University of Ambon, Indonesia) during sponge collection and of Dr. Nicole de Voogd (Leiden, Naturalis Biodiversity Center, Leiden, Netherlands) for identification of the sponge. We are indebted to Prof. W. E. G. Müller (Johannes Gutenberg University, Mainz, Germany) for cytotoxicity assays with L5178Y mouse lymphoma cells. A. M. gratefully thanks the Ministry of Science, Research and Technology (MSRT) of Iran for awarding him a scholarship. P. P. wishes to thank the Federal Ministry of Education and Research (16GW0107K) for support.

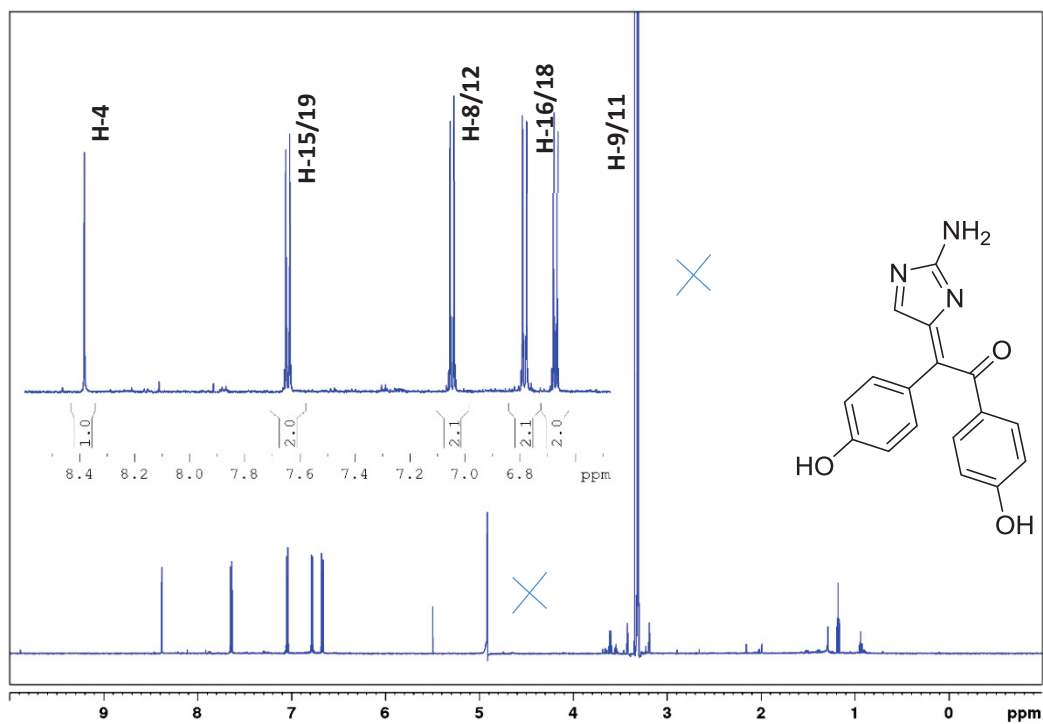
The authors acknowledge access to the Jülich-Düsseldorf Biomolecular NMR Center.

Keywords: Marine Sponge • *Lissodendoryx* • 2-Aminoimidazole • Alkaloid • Natural Product

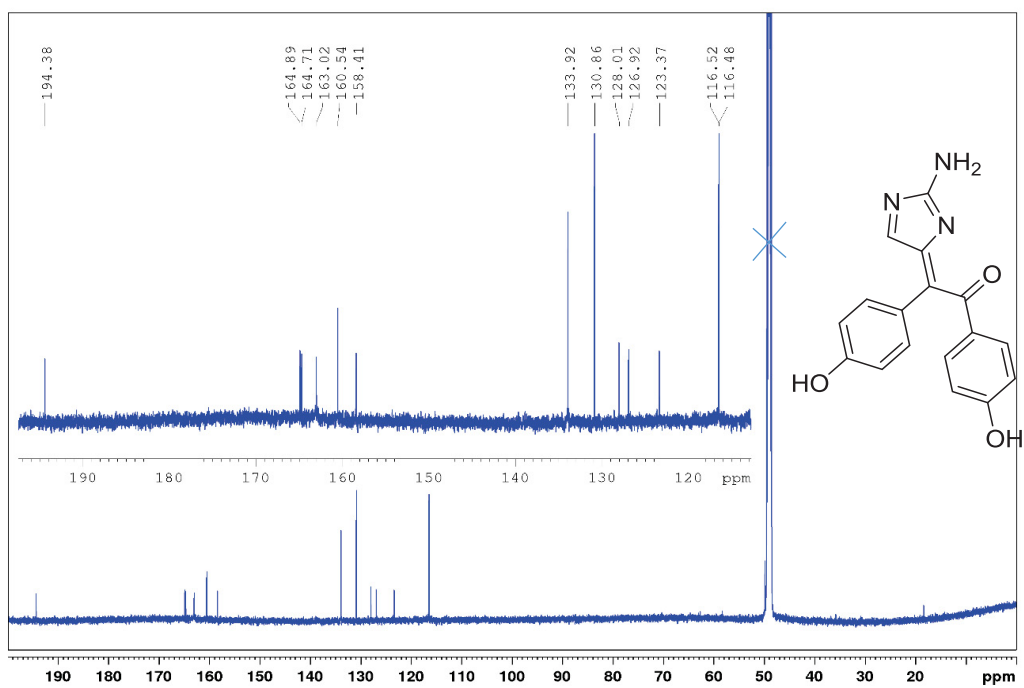
4.5 Supporting Information

S1.1. ¹H (700 MHz), ¹³C (176 MHz), HMBC, and ROESY NMR data of 1 (MeOH-d₄).

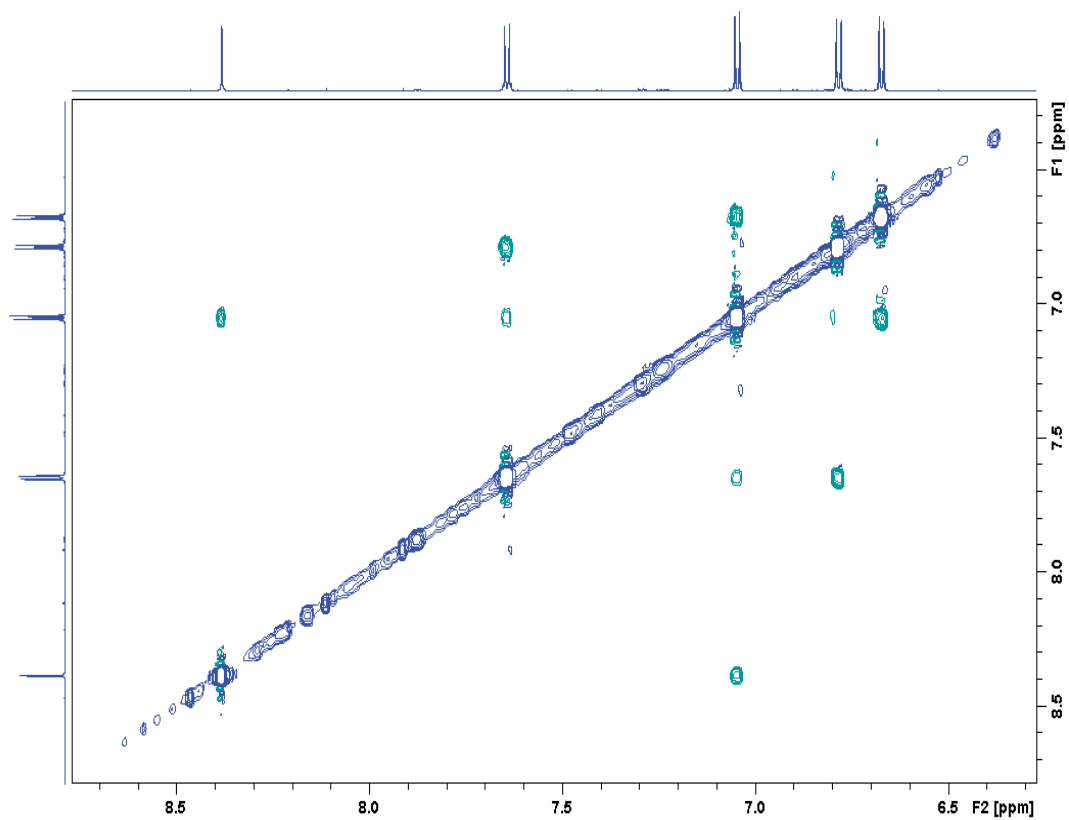
No.	δ_c (ppm)	δ_H (ppm) (mult., <i>J</i> in Hz)	HMBC (H→C)	Long-range HMBC (H→C)	ROESY
1					
2	164.7, C				
3					
4	160.5, CH	8.38, s	C-2, 6	C-7, 13	H-8, 12
5	163.0, C				
6	123.4, C				
7	126.9, C				
8	130.8, CH	7.04, d (8.6)	C-10, 12		H-15, 19
9	116.4, CH	6.67, d (8.6)	C-10, 11		
10	158.4, C				
11	116.4, CH	6.67, d (8.6)	C-9, 10		
12	130.8, CH	7.04, d (8.6)	C-6, 8, 10		H-4, 15, 19
13	194.3, C				
14	128.0, C				
15	133.9, CH	7.64, d (8.8)	C-13, 17, 19		H-8, 12
16	116.5, CH	6.78, d (8.8)	C-14, 17, 18		
17	164.9, C				
18	116.5, CH	6.78, d (8.8)	C-14, 16, 17		
19	133.9, CH	7.64, d (8.8)	C-15, 17		H-8, 12



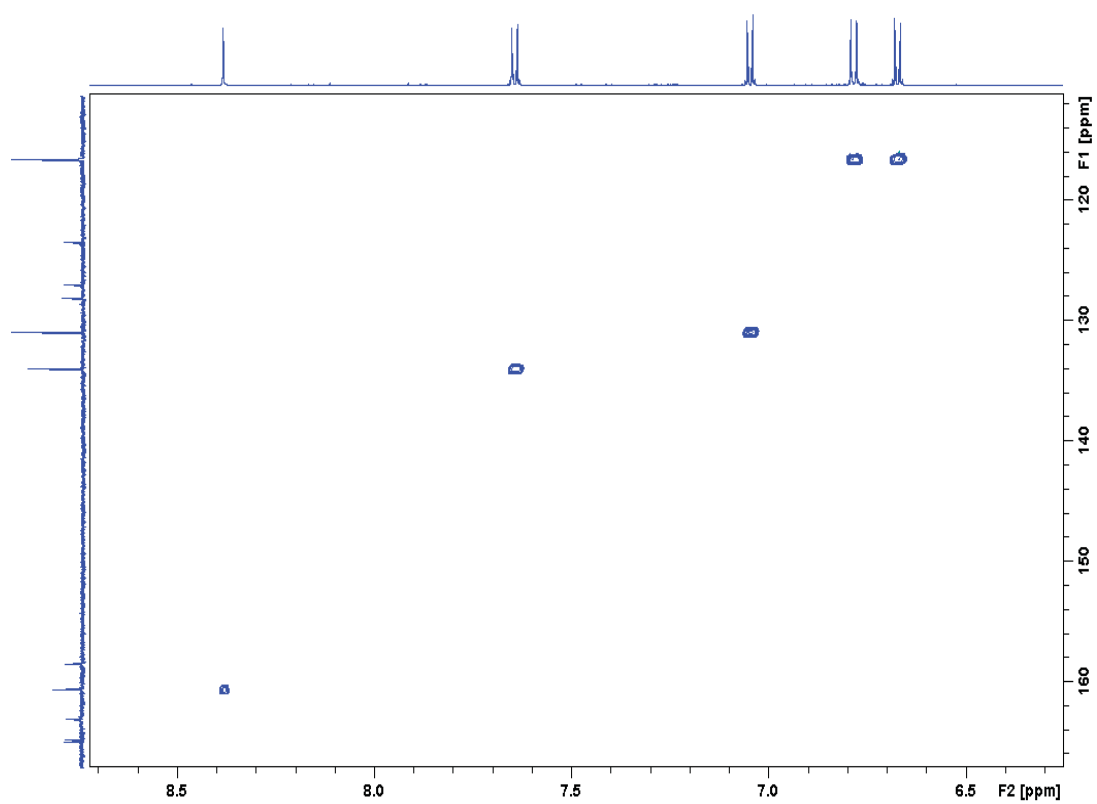
S1.2. ¹H-NMR spectrum of 1 (MeOH-d₄, 700MHz).



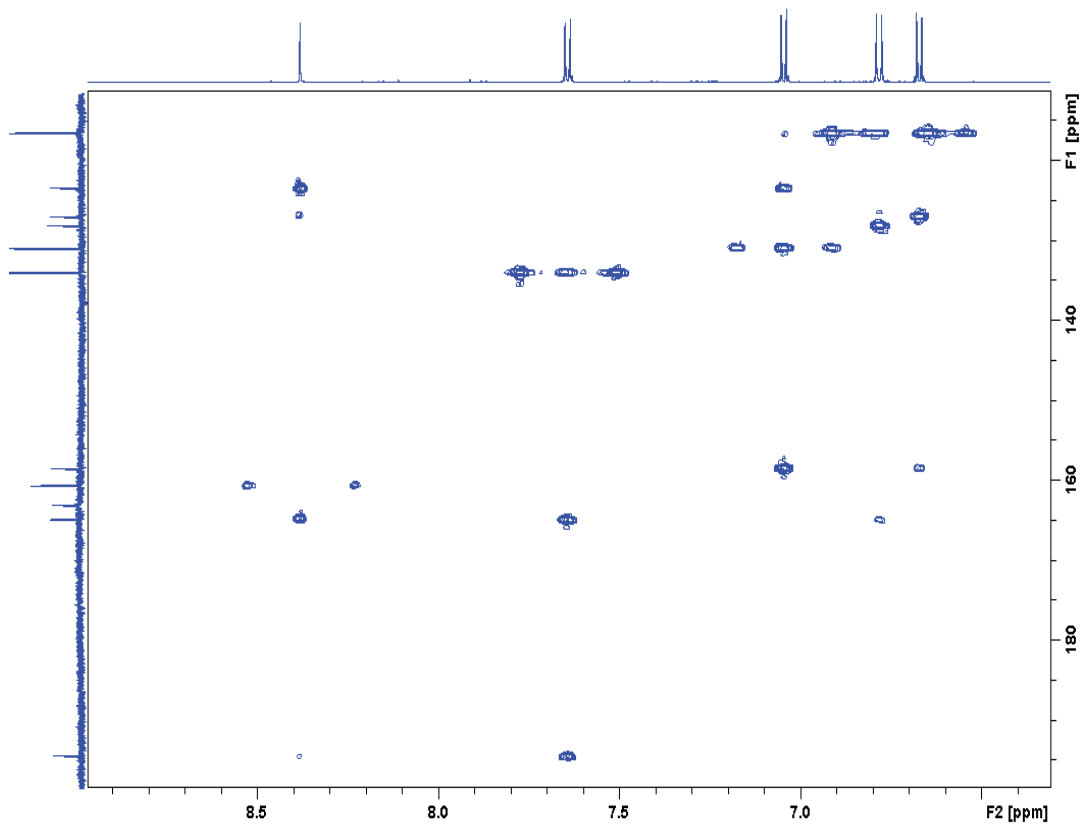
S1.3. ¹³C-NMR spectrum of 1 (MeOH-d₄, 176 MHz).



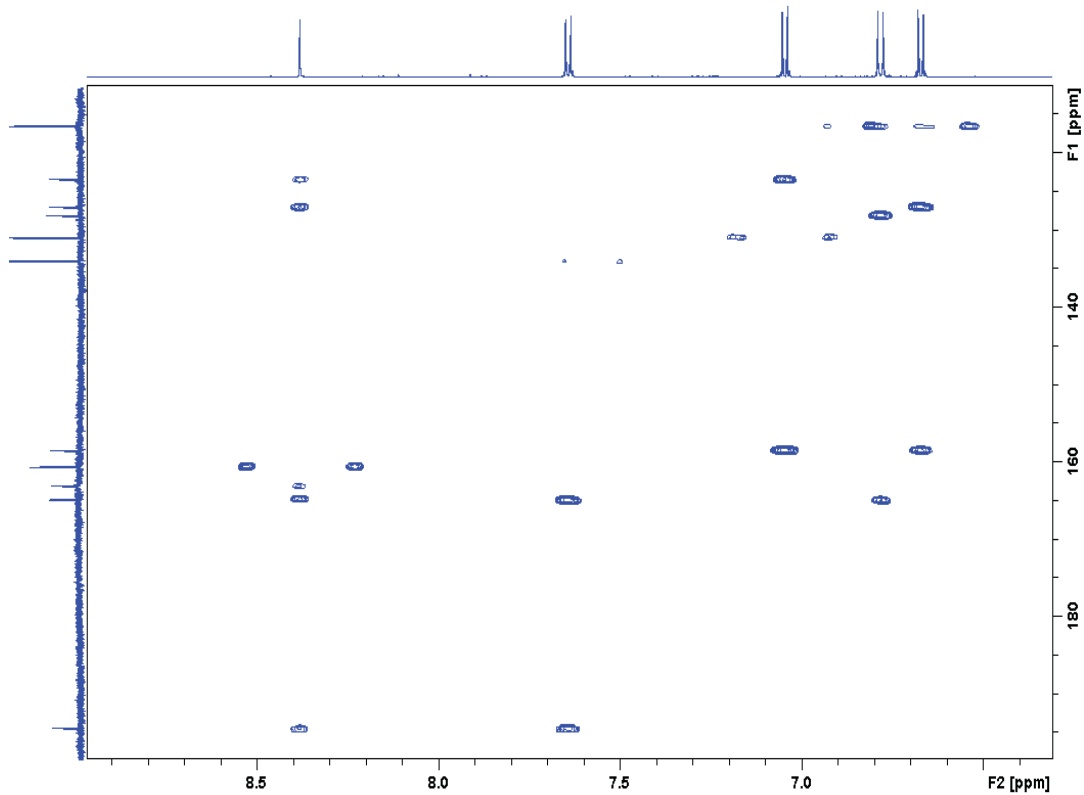
S1.4. ROESY spectrum of **1** (MeOH-d₄, 700 MHz).



S1.5. HSQC spectrum of **1** (MeOH-d₄, 700 MHz).



S1.6. HMBC spectrum of **1** (MeOH- d_4 , 700 MHz).



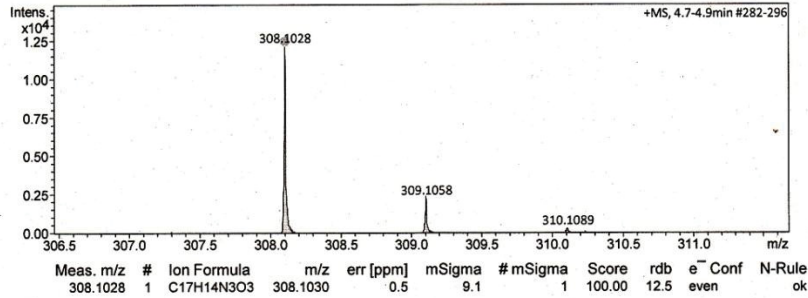
S1.7. Long-range HMBC spectrum of **1** (MeOH- d_4 , 700 MHz).

Mass Spectrum SmartFormula Report

Analysis Info Acquisition Date 9/17/2014 1:15:59 PM
Analysis Name D:\Data\Spektren2014\Proksch14000128.d
Method tune_low.m **Operator** Peter Tommes
Sample Name Mokhlesi TF9 E(2) 54-61 P.10 in CH3OH (CH3CN/H2O) **Instrument** maXis 288882.20213
Comment

Acquisition Parameter

Source Type	ESI	Ion Polarity	Positive	Set Nebulizer	0.3 Bar
Focus	Not active	Set Capillary	4000 V	Set Dry Heater	180 °C
Scan Begin	50 m/z	Set End Plate Offset	-500 V	Set Dry Gas	4.0 l/min
Scan End	1500 m/z	Set Collision Cell RF	600.0 Vpp	Set Divert Valve	Source



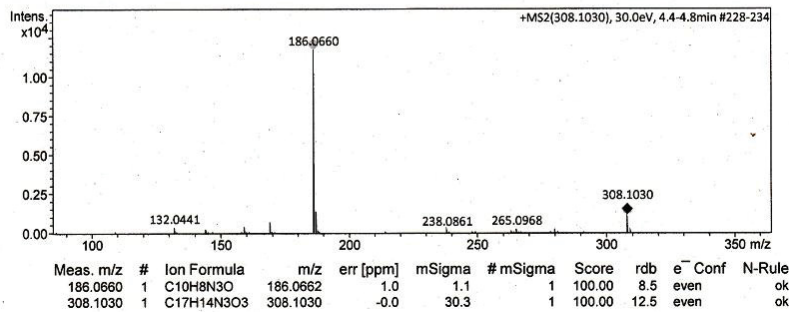
S1.8. HRESIMS spectrum of **1**.

Mass Spectrum SmartFormula Report

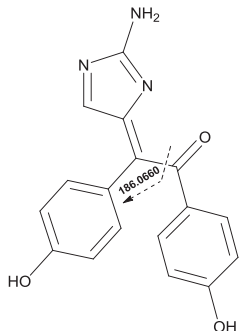
Analysis Info Acquisition Date 11/28/2014 12:48:37 PM
Analysis Name D:\Data\Spektren2014\Proksch14000206.d
Method tune_low.m **Operator** Peter Tommes
Sample Name Amin TF9 54-61 P.10 in CH3OH (CH3CN/H2O) **Instrument** maXis 288882.20213
Comment

Acquisition Parameter

Source Type	ESI	Ion Polarity	Positive	Set Nebulizer	0.3 Bar
Focus	Not active	Set Capillary	4000 V	Set Dry Heater	180 °C
Scan Begin	50 m/z	Set End Plate Offset	-500 V	Set Dry Gas	4.0 l/min
Scan End	1500 m/z	Set Collision Cell RF	600.0 Vpp	Set Divert Valve	Source



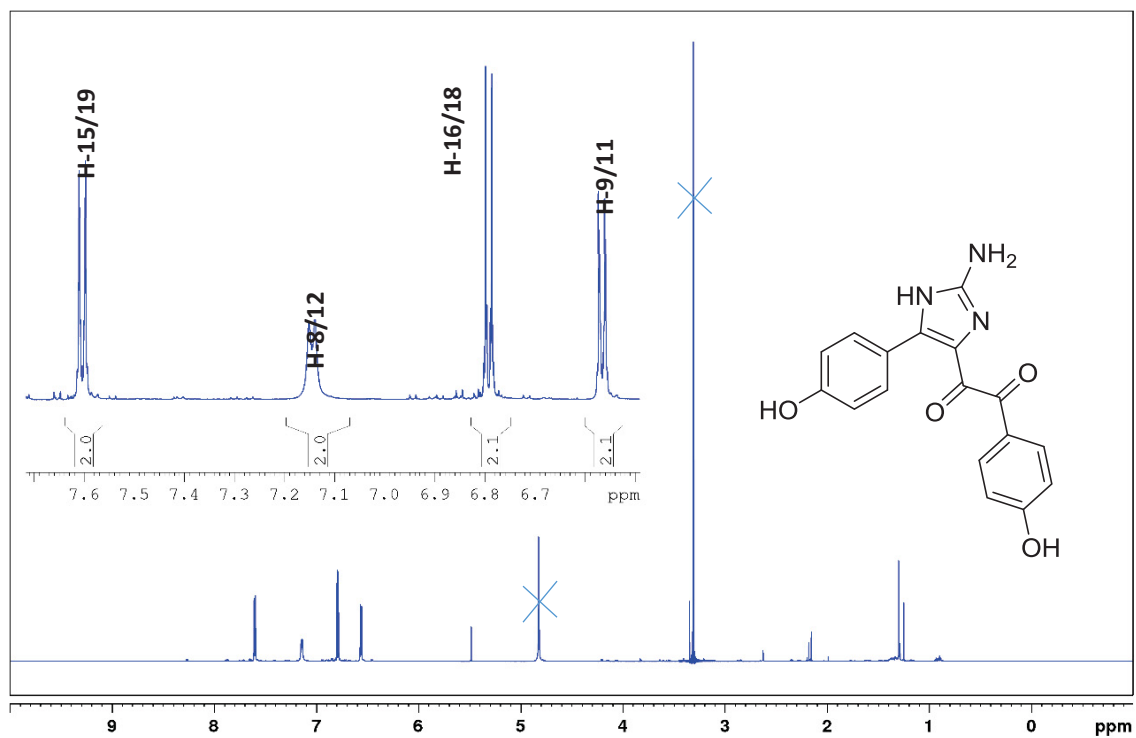
S1.9. HRESIMS/MS spectrum of **1**.



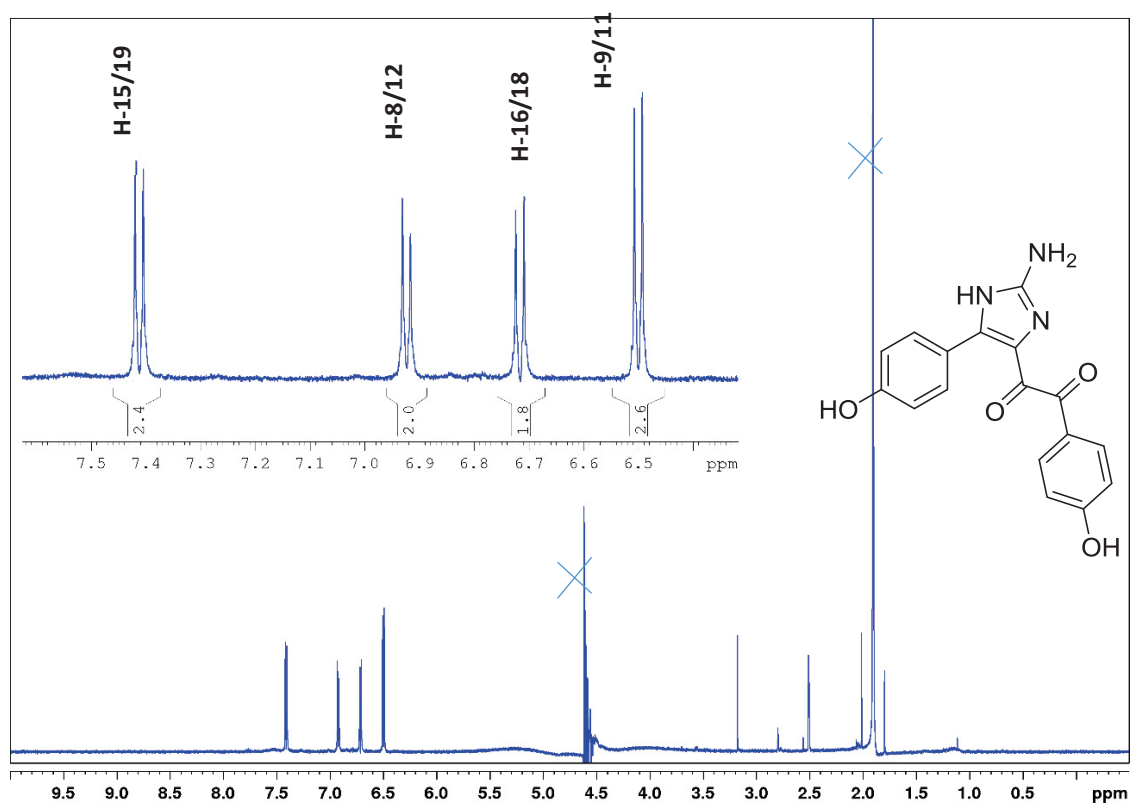
S1.10. HRESIMS/MS fragmentation of **1**.

S2.1. ^1H (700 MHz), ^{13}C (176 MHz), and HMBC NMR, and ROESY NMR data of 2 (MeOH- d_4).

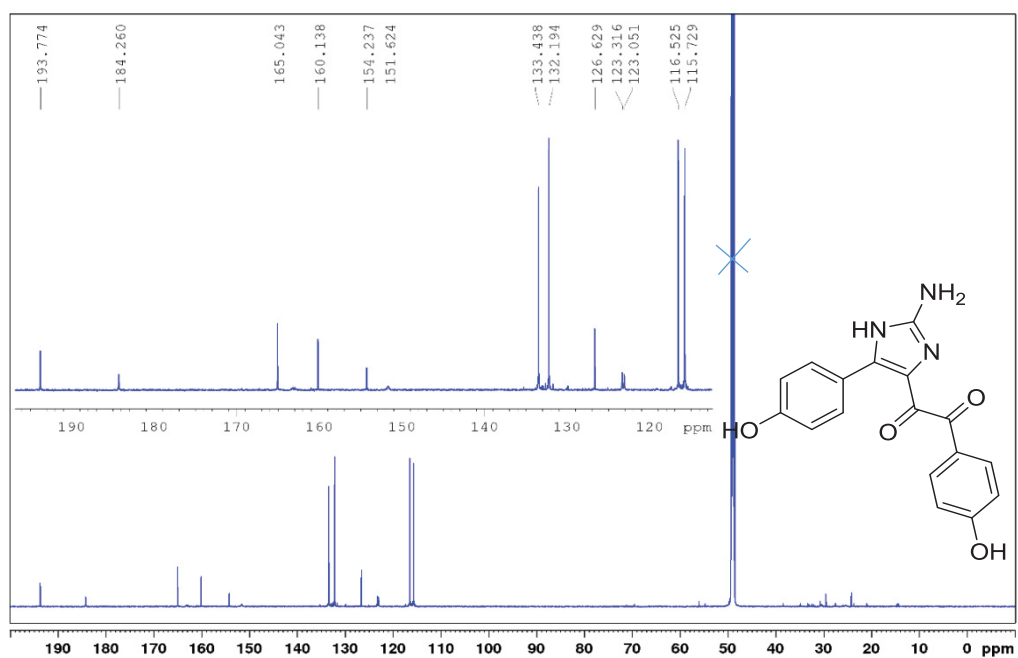
No.	δ_c (ppm)	δ_H (ppm) (mult., J in Hz)	COSY	HMBC (H \rightarrow C)	Long-range HMBC (H \rightarrow C)	ROESY
1						
2	154.2, C					
3						
4	151.6, C					
5	123.0, C					
6	184.2, C					
7	123.3, C					
8	132.1, CH	7.14, d (8.4)	H-9	C-4, 10, 12	C-5	H-15, 19
9	115.7, CH	6.56, d (8.4)	H-8	C-10, 11	C-4	
10	160.1, C					
11	115.7, CH	6.56, d (8.4)	H-12	C-9, 10	C-4	
12	132.1, CH	7.14, d (8.4)	H-11	C-4, 8, 10	C-5	H-15, 19
13	193.7, C					
14	126.6, C					
15	133.4, CH	7.60, d (8.7)	H-19	C-13, 16, 19		H-8, 12
16	116.5, CH	6.79, d (8.7)	H-18	C-14, 16, 18	C-6, 13	
17	165.0, C					
18	116.5, CH	6.79, d (8.7)	H-16	C-14, 16, 17	C-6, 13	
19	133.4, CH	7.60, d (8.7)	H-15	C-13, 15, 16, 17		H-8, 12



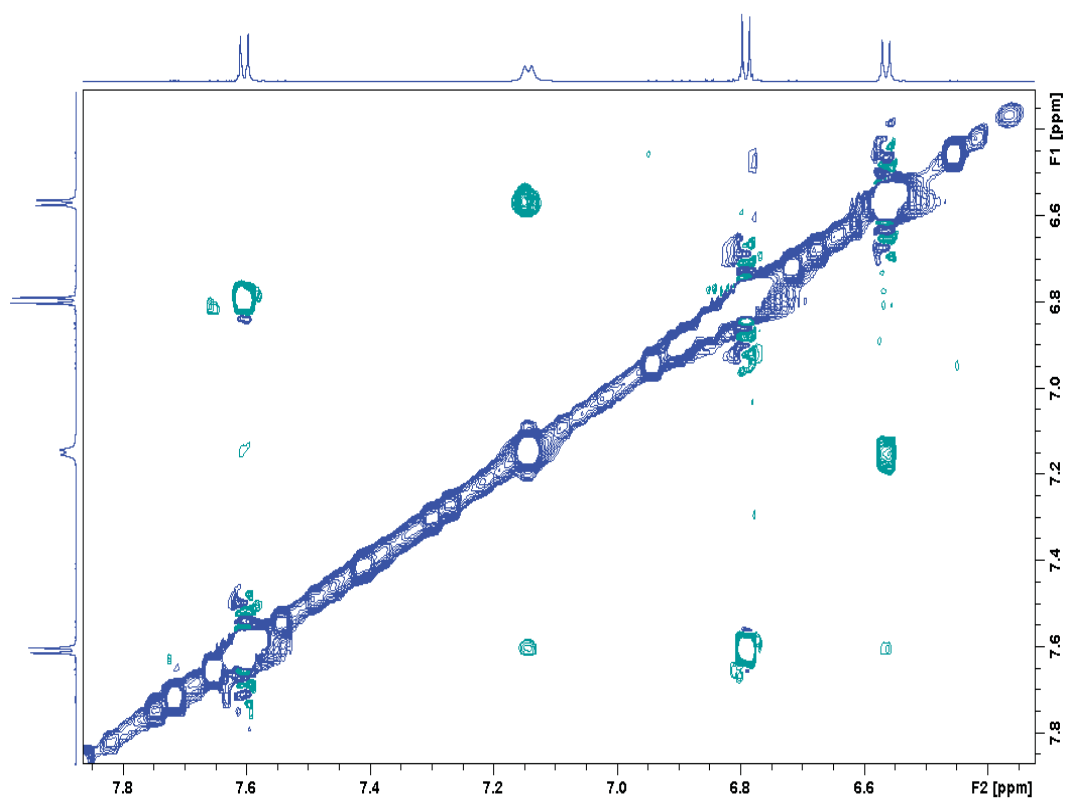
S2.2. $^1\text{H-NMR}$ spectrum of **2** (MeOH- d_4 , 700 MHz).



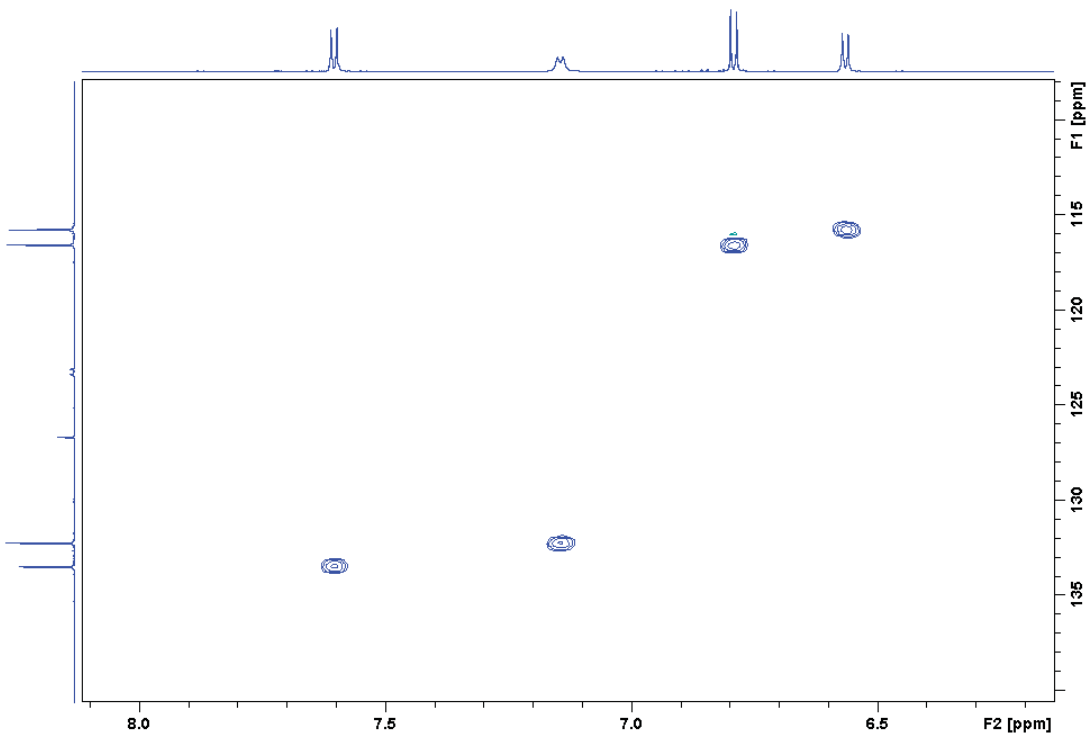
S2.3. $^1\text{H-NMR}$ spectrum of **2** (H_2O , pH 5, + 50 μM DMSO- d_6 , 700 MHz).



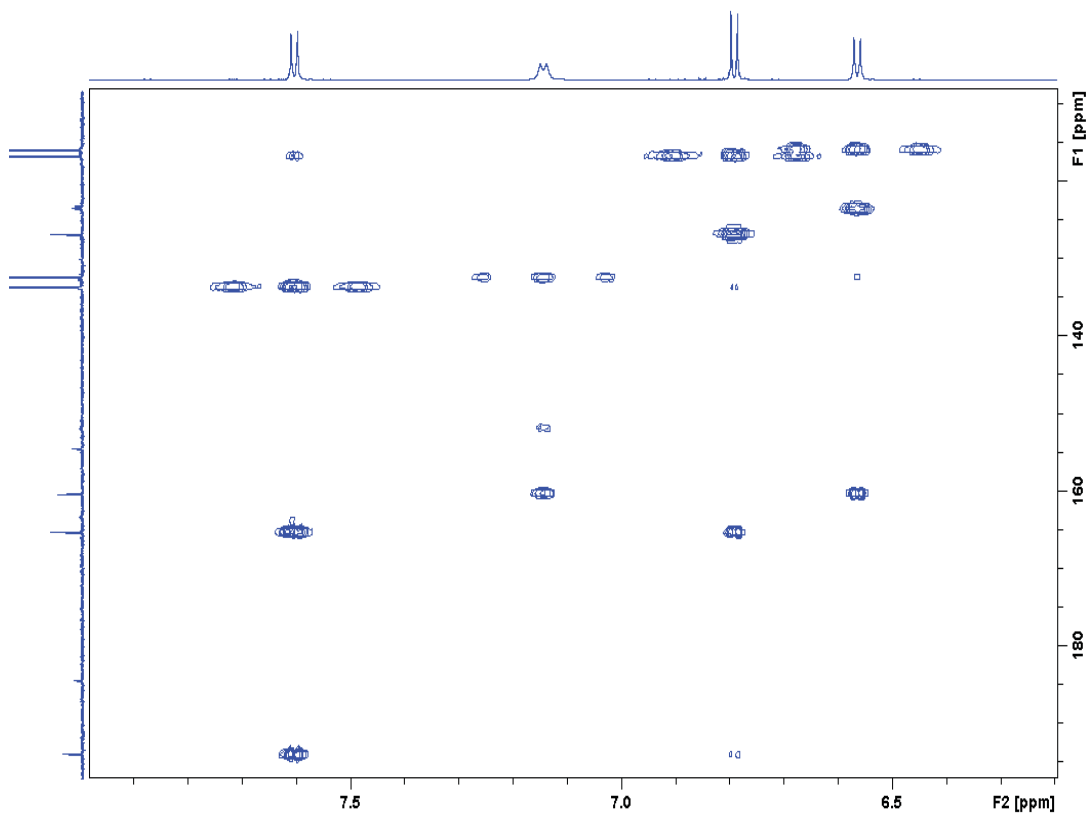
S2.4. ¹³C-NMR spectrum of **2** (MeOH-d₄, 176 MHz).



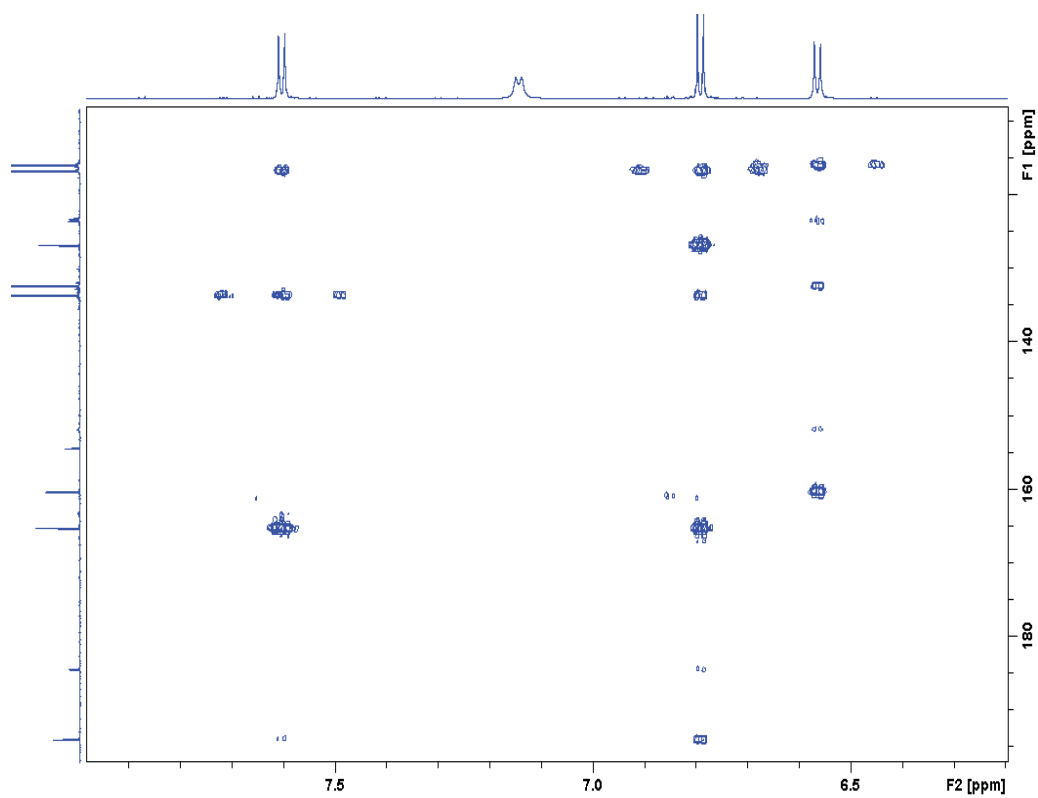
S2.5. ROESY spectrum of **2** (MeOH-d₄, 700 MHz).



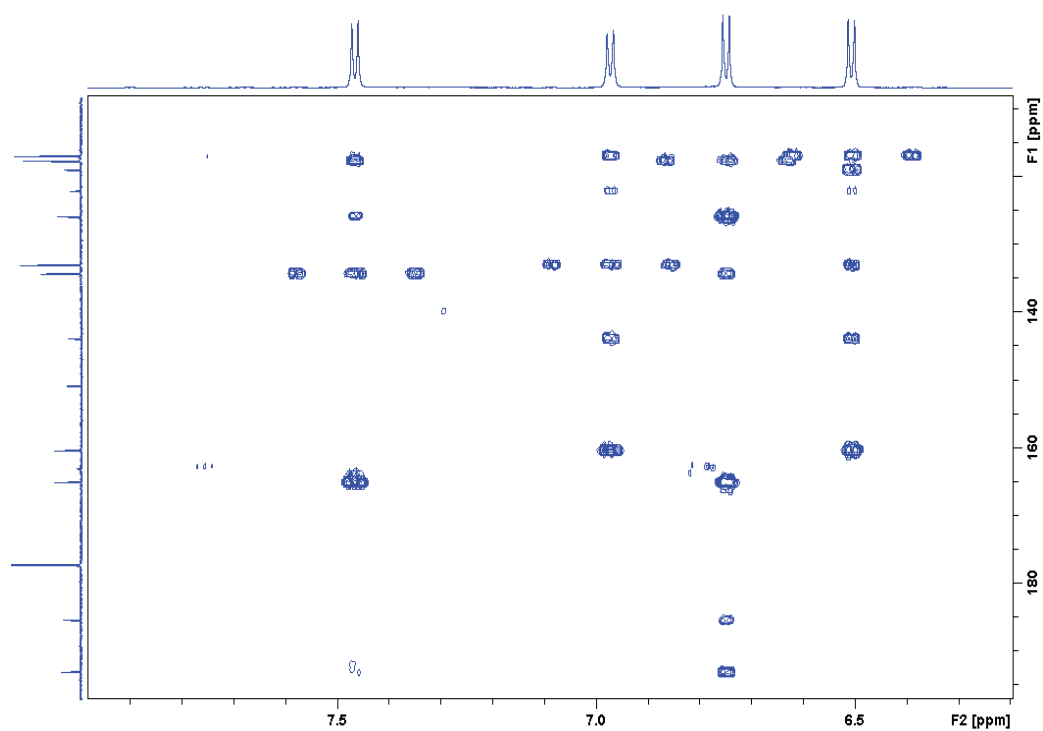
S2.6. HSQC spectrum of **2** (MeOH- d_4 , 700 MHz)



S2.7. HMBC spectrum of **2** (MeOH- d_4 , 700 MHz).



S2.8. Long-range HMBC spectrum (optimized for $J_{CH} = 2$ Hz) of **2** (MeOH- d_4 , 700 MHz).

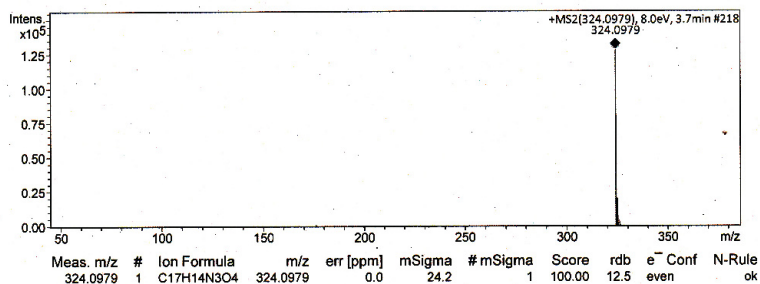


S2.9. Long-range HMBC spectrum (optimized for $J_{CH} = 2$ Hz) of **2** (H_2O , pH 3, + 50 μ l DMSO- d_6 , 700 MHz).

Mass Spectrum SmartFormula Report

Analysis Info Acquisition Date 11/25/2014 9:34:55 AM
 Analysis Name D:\Data\Spektren 2014\Proksch14000189.d
 Method tune_low.m Operator Peter Tommes
 Sample Name Amin Mokhlesi TF9 P.9 (CH3OH) Instrument maXis 288882.20213
 Comment 2 ug/ml

Acquisition Parameter
 Source Type ESI Ion Polarity Positive Set Nebulizer 0.3 Bar
 Focus Not active Set Capillary 4000 V Set Dry Heater 180 °C
 Scan Begin 50 m/z Set End Plate Offset -500 V Set Dry Gas 4.0 l/min
 Scan End 1500 m/z Set Collision Cell RF 600.0 Vpp Set Divert Valve Source

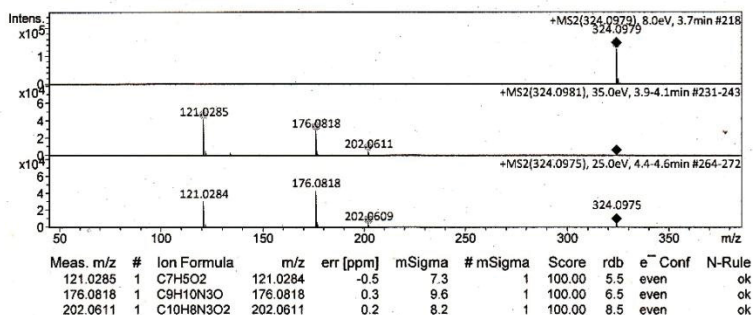


S2.10. HRESIMS spectra of 2.

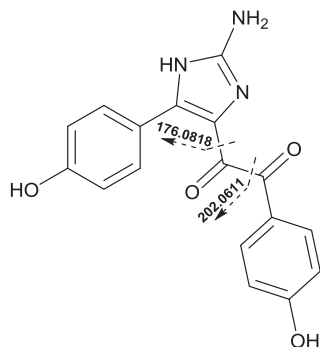
Mass Spectrum SmartFormula Report

Analysis Info Acquisition Date 11/25/2014 9:34:55 AM
 Analysis Name D:\Data\Spektren 2014\Proksch14000189.d
 Method tune_low.m Operator Peter Tommes
 Sample Name Amin Mokhlesi TF9 P.9 (CH3OH) Instrument maXis 288882.20213
 Comment 2 ug/ml

Acquisition Parameter
 Source Type ESI Ion Polarity Positive Set Nebulizer 0.3 Bar
 Focus Not active Set Capillary 4000 V Set Dry Heater 180 °C
 Scan Begin 50 m/z Set End Plate Offset -500 V Set Dry Gas 4.0 l/min
 Scan End 1500 m/z Set Collision Cell RF 600.0 Vpp Set Divert Valve Source



S2.11. HRESIMS/MS spectra of 2.



S2.12. HRESIMS/MS fragmentation of 2.

5 Publication 2: Cyclic Cystine-Bridged Peptides from the Marine Sponge *Clathria basilana* Induce Apoptosis in Tumor Cells and Depolarize the Bacterial Cytoplasmic Membrane

Cyclic Cystine-Bridged Peptides from the Marine Sponge *Clathria basilana* Induce Apoptosis in Tumor Cells and Depolarize the Bacterial Cytoplasmic Membrane

Amin Mokhlesi,^{†,‡} Fabian Stuhldreier,[§] Katharina W. Wex,[⊥] Anne Berscheid,[⊥] Rudolf Hartmann,^{||} Nidja Rehberg[†], Parichat Sureechatchaiyan,[∇] Chaidir Chaidir,[○] Matthias U. Kassack,[∇] Rainer Kalscheuer,[†] Heike Brötz-Oesterhelt,[⊥] Sebastian Wesselborg,[§] Björn Stork,[§] Georgios Daletos,^{†,*} Peter Proksch^{†,*}

[†]Institute of Pharmaceutical Biology and Biotechnology, Heinrich Heine University, Universitätsstraße 1, 40225 Düsseldorf, Germany.

[‡]Department of Marine Biology, Faculty of Marine Sciences, Tarbiat Modares University, Noor, Iran.

[§]Institute of Molecular Medicine I, Medical Faculty, Heinrich Heine University, Universitätsstraße 1, D-40225 Düsseldorf, Germany.

[⊥]Department of Microbial Bioactive Compounds, Interfaculty Institute of Microbiology and Infection Medicine, University of Tübingen, Auf der Morgenstelle 28/E8, 72076 Tübingen, Germany.

^{||} Institute of Complex Systems: Strukturbiochemie, Forschungszentrum Jülich, Wilhelm-Johnenstrasse, 52428 Jülich, Germany.

[∇]Institute of Pharmaceutical and Medicinal Chemistry, Heinrich Heine University, Universitätsstraße 1, D-40225 Düsseldorf, Germany.

[○]Center for Pharmaceutical and Medical Technology, Agency for the Assessment and Application Technology, 10340 Jakarta, Indonesia.

ABSTRACT: Investigation of the sponge *Clathria basilana* collected in Indonesia afforded six new peptides, including microcionamides C (**1**) and D (**2**), gombamides B (**4**), C (**5**), and D (**6**), and an unusual amide, (*E*)-2-amino-3-methyl-*N*-styrylbutanamide (**7**), along with 11 known compounds, among them microcionamide A (**3**). The structures of the new compounds were elucidated by one- and two-dimensional NMR spectroscopy as well as by high-resolution mass spectrometry. The absolute configurations of the constituent amino acid residues in **1–7** were determined by Marfey's analysis. Microcionamides A, C, and D (**1–3**) showed strong *in vitro* cytotoxicity against lymphoma (Ramos) and leukemia cell lines (HL-60, Nomo-1, Jurkat J16), as well as against a human ovarian carcinoma cell line (A2780) with IC₅₀ values ranging from 0.45 to 28 μ M. Mechanistic studies showed that compounds **1–3** rapidly induce apoptotic cell death in Jurkat J16 and Ramos cells, and that **1** and **2** potently block autophagy upon starvation conditions, thereby impairing pro-survival signaling of cancer cells. In addition, microcionamides C and A (**1** and **3**) inhibited bacterial growth of *Staphylococcus aureus* and *Enterococcus faecium* with minimal inhibitory concentrations between 6.2 and 12 μ M. Mechanistic studies indicate dissipation of the bacterial membrane potential.

Marine sponges represent a prolific source of structurally unique peptides possessing diverse bioactivities, primarily as antibiotics, anticancer, and neuroprotective agents, thus suggesting their potential value for the development of leads in drug discovery.⁷⁴ Prominent examples of bioactive sponge-derived peptides include koshikamide A₁ and calyxamide A reported from *Theonella* sp. and *Discodermia calyx*, respectively, both showing strong cytotoxicity toward P388 murine leukemia cells,^{75,76} as well as the diaminoacrylic acid-containing cyclic peptides callaerins A and B possessing inhibitory activity against *Mycobacterium tuberculosis*.⁷⁷

The genus *Clathria* (order Poecilosclerida, family Microcionidae)⁷⁸ includes more than 800 species that are widely distributed in the shallow waters of tropical and temperate regions. Chemical investigation of sponges belonging to this genus has provided a diverse array of secondary metabolites, such as alkaloids,⁷⁹ carotenoids,⁸⁰ steroids,⁸¹ and peptides.⁸² The latter class of compounds includes microcionamides A and B as well as gombamide A from *Clathria abietina* and *Clathria gombawuiensis*, respectively, all featuring a disulfide linkage that is rarely found in sponge-derived metabolites.^{82a,82b}

During our ongoing research for bioactive metabolites from marine sponges, we investigated a specimen of the marine sponge *Clathria basilana*, which was collected at Ambon Island, Indonesia. Notably, the MeOH extract completely inhibited the growth of the murine lymphoma L5178Y cell line at a concentration of 10 μ g/mL. Bioactivity-guided isolation afforded six new peptides (**1**, **2**, **4–7**) and 11 known metabolites (**3**, **8–17**). In this study, the structure elucidation of the new compounds as well as results of cytotoxicity and antibacterial assays, followed by mechanistic studies, are reported.

5.1 Results and Discussion

The MeOH extract of *C. basilana* was subjected to liquid-liquid fractionation to yield *n*-hexane, EtOAc, and *n*-BuOH fractions. Subsequent column chromatography of the EtOAc or *n*-BuOH fraction followed by semipreparative reversed-phase HPLC afforded five new peptides (**1**, **2**, **4–6**) and a new amide derivative **7**.

Compound **1** was obtained as a white, amorphous solid. Its molecular formula was determined to be C₄₄H₇₂N₈O₇S₂ on the basis of the prominent ion peak at *m/z* 889.5033 [M + H]⁺ in the HRESIMS spectrum, accounting for 13 degrees of unsaturation. In the ¹H NMR spectrum, measured in DMSO-*d*₆, the peptidic nature of **1** was evident from the presence of NH signals in the amide region (δ_{H} 7.34–10.02) and characteristic signals of α -amino protons (δ_{H} 3.66–4.62), as well as from a cluster of primary and secondary methyl groups in the aliphatic region (δ_{H} 0.81–2.00). Detailed analysis of the 2D NMR (HSQC, TOCSY, ROESY, and HMBC) spectra of **1** allowed the assignment of seven spin systems, including those of five isoleucine (Ile) and two cysteine (Cys) residues (Table 1). The remaining signals included those of a monosubstituted phenyl ring [δ_{H} 7.32 (2H, dd, *J* = 7.4, 1.4 Hz), 7.28 (2H, dd, *J* = 7.4, 7.1 Hz), and 7.16 (1H, tt, *J* = 7.1, 1.4 Hz)], and two olefinic protons at δ_{H} 6.26 (PEA-H β) and 7.35 (PEA-H α) suggesting the presence of a 2-phenylethen-1-amine (PEA) unit, as supported by the HMBC correlations from PEA-H α to PEA-C1 (δ_{C} 136.0) and from PEA-H β to PEA-C2/6 (δ_{C} 124.9), as well as by the TOCSY correlations of both PEA-H α and PEA-H β with PEA-NH. The configuration of the double bond of PEA was deduced as *E* on the basis of the large coupling constant (³*J* = 14.8 Hz) measured for the respective protons.

The connectivity of the amino acid residues and of *E*-PEA was established by key HMBC and ROESY correlations (Figure 1). Accordingly, the HMBC correlations from *E*-PEA-H α to Cys₁-CO (δ_{C} 167.2), from Cys₁-NH to Ile₂-CO (δ_{C} 170.3) and from Ile₁-H α to Ile₃-CO (δ_{C} 171.2), along with the ROESY correlations between Cys₁-H α and *E*-PEA-NH and between Ile₂-H α and Cys₁-NH suggested the peptide substructure *E*-PEA-Cys₁-Ile₂-Ile₃. Moreover, the sequence Ile₄-Ile₅-Cys₆ was supported by the HMBC correlations from Ile₅-NH and Ile₅-H α to Cys₆-CO, as well as by the ROESY correlations between Ile₄-H α and Ile₅-H β and between Ile₅-NH and Cys₆-H α (Figure 1). The latter cysteine moiety (Cys₆) was linked to Ile₇ based on the HMBC cross-peak from Cys₆-H α to Ile₇-CO (δ_{C} 167.8) and the ROESY correlation between Cys₆-NH and Ile₇-H α , thus leading to the overall peptide structure *E*-PEA-Cys₁-Ile₂-Ile₃-Ile₄-Ile₅-Cys₆-Ile₇. Additionally, the cyclic nature of **1** was evident from the disulfide linkage of the two cysteine residues that formed a cystine moiety, thus accounting for the last degree of unsaturation based on the molecular formula (C₄₄H₇₂N₈O₇S₂). The assignment was further supported by HRESIMS/MS, which showed the fragmentation ions at *m/z* 770.4297 for [M - *E*-PEA]⁺ and at *m/z* 657.3454 for [M - (*E*-PEA+Ile₇)]⁺, originating from subsequent cleavage of the *E*-PEA and Ile₇ units, both located at the linear parts of the peptide (Figure S1-7). Hence, compound **1** was identified as a new natural product and the name microcionamide C was proposed given the structural relationship between this compound and the known compounds microcionamides A and B.¹¹

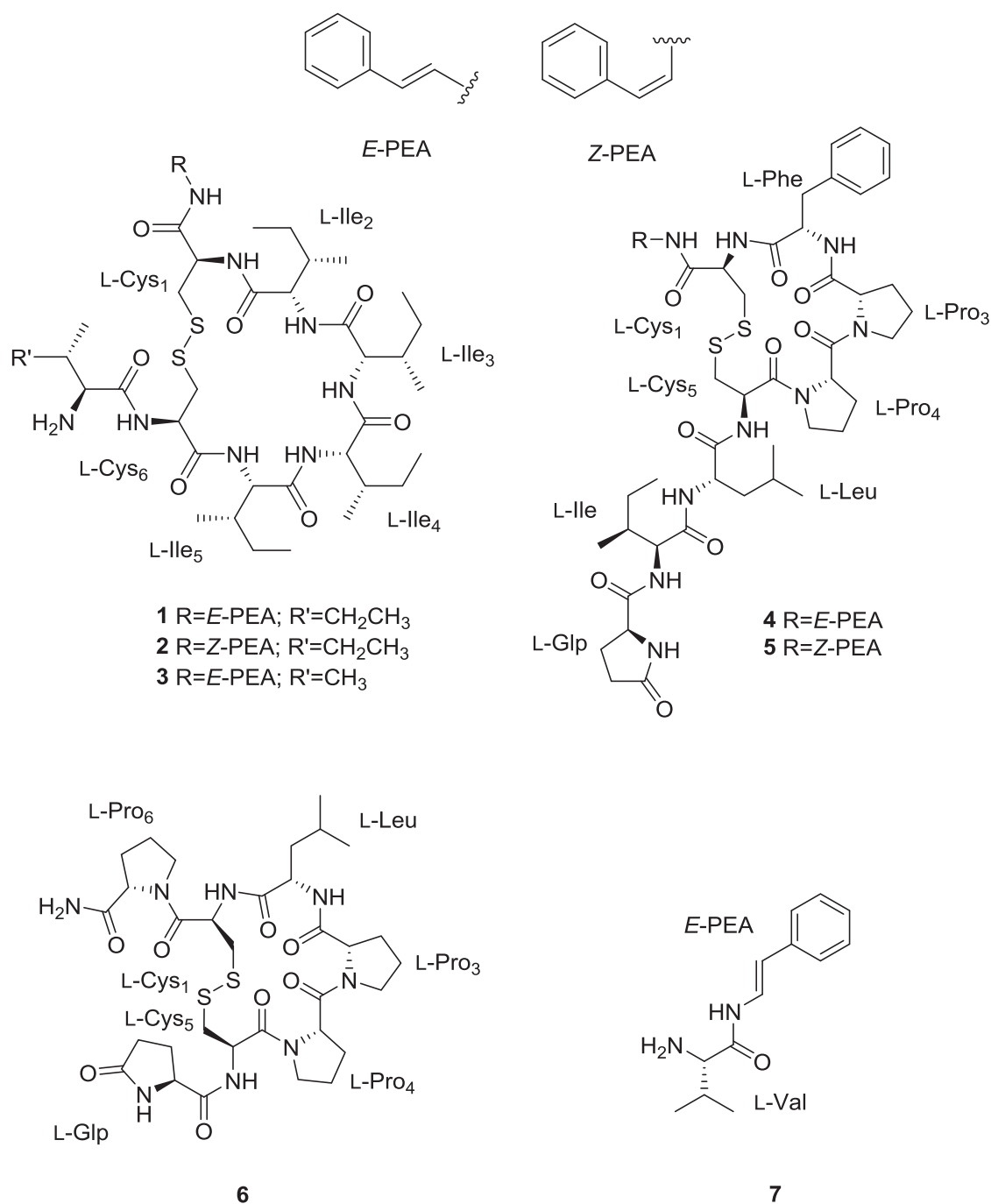


Table 1. ¹H (600 MHz), ¹³C (150 MHz), HMBC, and ROESY NMR Data (DMSO-*d*₆, δ in ppm) of Microcionamide C (1)

Unit	Position	δ _c , ^a type	δ _H (J in Hz)	HMBC	ROESY ^b
<i>E</i> -PEA	NH		10.02, d (10.0)		Cys ₁ -α, <i>E</i> -PEA-β
	α	122.8, CH	7.35, dd (10.0,	Cys ₁ -CO, <i>E</i> -PEA-β, <i>E</i> -	

	β	112.5, CH	14.8) 6.26, d (14.8)	PEA-1 <i>E</i> -PEA- α , <i>E</i> -PEA-1, <i>E</i> -PEA-2/6	Ile ₂ - γ'
	aromatic	1: 136.0, C			
		2: 124.9, CH	7.32, br dd (7.4, 1.4)	<i>E</i> -PEA- β , <i>E</i> -PEA-1, <i>E</i> -PEA-6, <i>E</i> -PEA-4	
		3: 128.5, CH	7.28, br dd (7.4, 7.1)	<i>E</i> -PEA-1, <i>E</i> -PEA-5, <i>E</i> -PEA-4	
		4: 126.1, CH	7.16, tt (7.1, 1.4)	<i>E</i> -PEA-2/6, <i>E</i> -PEA-3/5	
		5: 128.5, CH	7.28, br dd (7.4, 7.1)	<i>E</i> -PEA-1, <i>E</i> -PEA-3, <i>E</i> -PEA-4	
		6: 124.9, CH	7.32, br dd (7.4, 1.4)	<i>E</i> -PEA- β , <i>E</i> -PEA-1, <i>E</i> -PEA-2, <i>E</i> -PEA-4	
Cys ₁	NH		8.15, d (7.8)	Ile ₂ -CO	Ile ₂ - α
	CO	167.2, C			
	α	52.6, CH	4.34 ^c	Cys ₁ -CO, Cys ₁ - β , Ile ₂ -CO	<i>E</i> -PEA- α , <i>E</i> -PEA-NH
	β	40.7, CH ₂	3.19, br t (13.2); 3.30, dd (13.2, 4.7) 7.99, br s	Cys ₁ -CO, Cys ₁ - α	
Ile ₂	NH				
	CO	170.3, C			
	α	57.7, CH	3.96, t (7.6)	Ile ₂ -CO, Ile ₃ -CO, Ile ₂ - β , Ile ₂ - γ , Ile ₂ - γ'	Cys ₁ -NH
	β	34.6, CH	1.88, m	Ile ₂ - α	
	γ	24.5, CH ₂	1.51, m; 1.06, m	Ile ₂ - α	Ile ₃ - α
	γ'	15.4, CH ₃	0.86, d (6.9)	Ile ₂ - α	
	δ	11.0, CH ₃	0.81 ^c		
Ile ₃	NH		7.75, br s		
	CO	171.2, C			
	α	57.6, CH	4.04, br s	Ile ₃ - γ , Ile ₃ - γ'	Ile ₂ - γ
	β	36.2, CH	1.82, m	Ile ₃ - γ , Ile ₃ - γ' , Ile ₃ - δ , Ile ₃ -CO	
	γ	24.5, CH ₂	1.20, m; 1.54, m	Ile ₃ - α	
	γ'	15.1, CH ₃	0.93, d (6.8)	Ile ₃ - α	
	δ	11.2, CH ₃	0.87 ^c		
Ile ₄	NH		7.34 ^c		
	CO	n.d. ^d			
	α	56.7, CH	4.33 ^c	Ile ₄ - γ , Ile ₄ - γ'	Ile ₅ - β
	β	35.9, CH	2.00, br s		
	γ	23.5, CH ₂	1.16, m; 1.35, m	Ile ₄ - α , Ile ₄ - γ' , Ile ₄ - δ	

Ile ₅	γ'	15.6, CH ₃	0.89 ^c	Ile ₄ - α , Ile ₄ - γ	
	δ	11.1, CH ₃	0.82 ^c	Ile ₄ - β	
	NH		8.53, d (9.8)	Cys ₆ -CO	Cys ₆ - α
	CO	170.4, C			
	α	57.8, CH	4.19, dd (9.8, 6.9)	Ile ₅ -CO, Cys ₆ -CO, Ile ₅ - β , Ile ₅ - γ , Ile ₅ - γ'	
	β	36.2, CH	1.84, m	Ile ₅ - α , Ile ₅ - γ'	Ile ₄ - α
	γ	23.9, CH ₂	1.40, m; 1.10, m	Ile ₅ - α	
	γ'	15.2, CH ₃	0.84 ^c	Ile ₅ - α , Ile ₅ - β	
Cys ₆	δ	10.7, CH ₃	0.80 ^c		
	NH		8.83, d (8.1)	Cys ₆ - β	Ile ₇ - α , Ile ₇ - β , Ile ₇ - γ
Ile ₇	CO	168.9, C			
	α	52.3, CH	4.62, br ddd (10.3, 8.1, 4.6)	Cys ₆ -CO, Ile ₇ -CO, Cys ₆ - β	Ile ₅ -NH
	β	40.1, CH ₂	3.11, br dd (12.8, 10.3); 3.39, dd (12.8, 4.6)	Cys ₆ -CO, Cys ₆ - α	
	NH ₂		8.1, br d (5.6)	Ile ₇ -CO, Ile ₇ - α , Ile ₇ - β	Ile ₇ - α , Ile ₇ - β , Ile ₇ - γ'
	CO	167.8, C			
	α	56.0, CH	3.66, br t (5.4)	Ile ₇ -CO, Ile ₇ - γ , Ile ₇ - γ'	Cys ₆ -NH
	β	36.2, CH	1.79, m	Ile ₇ -CO, Ile ₇ - δ	Cys ₆ -NH
γ	23.4, CH ₂	1.10, m; 1.47, m	Ile ₇ - α	Cys ₆ -NH	
	γ'	14.1, CH ₃	0.89 ^c	Ile ₇ - α	
	δ	10.8, CH ₃	0.83 ^c		

^aData extracted from HSQC and HMBC spectra. ^bSequential NOEs. ^cSignal overlap prevents determination of couplings. ^dn.d. : not detected.

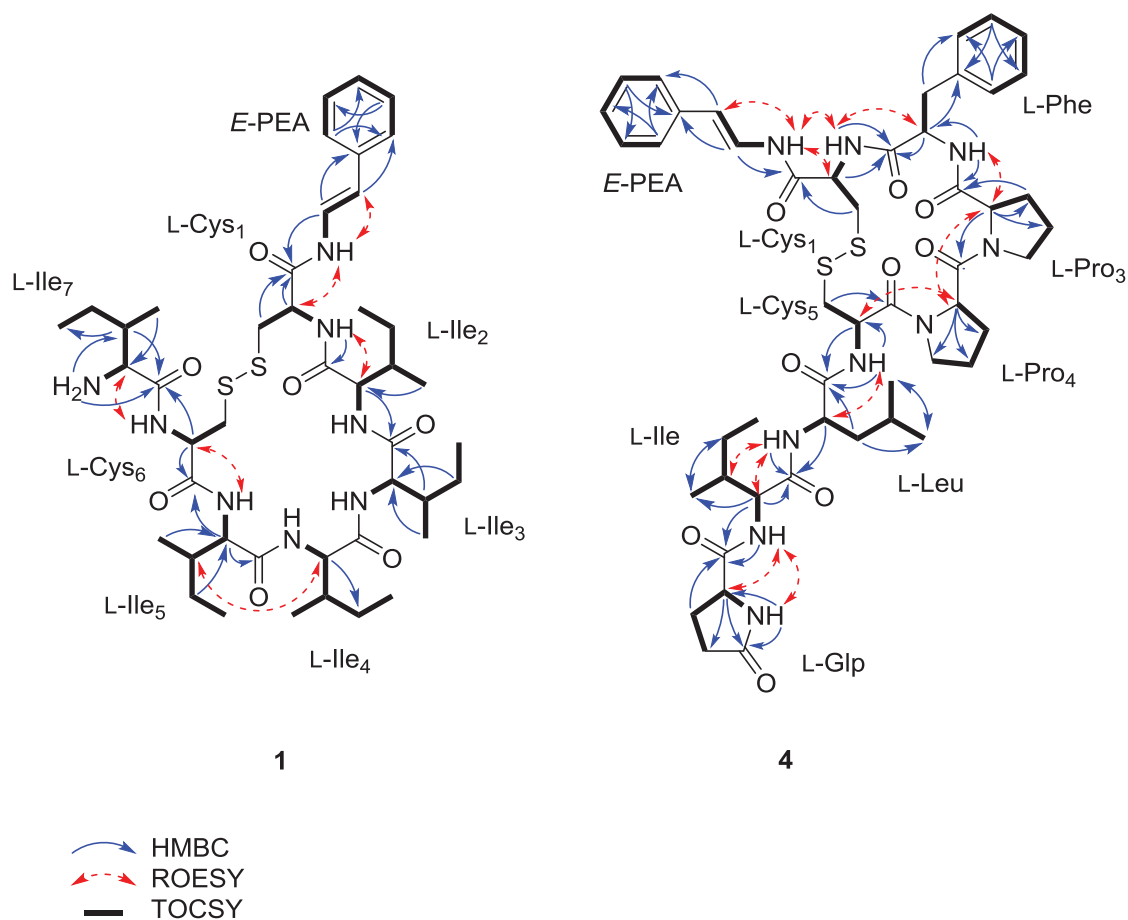


Figure 1. Key HMBC, ROESY and TOCSY correlations of **1** and **4**

Compound **2** was isolated as a white, amorphous solid. The molecular formula of **2** was established as $C_{44}H_{72}N_8O_7S_2$ by HRESIMS, identical to that found in **1**. Moreover, the 1H NMR data of **2** were almost superimposable to those of **1**, the only notable difference being the resonances and coupling constants of the olefinic protons at δ_H 5.74 (1H, d, $J = 10.0$ Hz) and 6.72 (1H, t, $J = 10.0$ Hz), suggesting a (*Z*)-2-phenylethen-1-amine (*Z*-PEA) unit in **2** instead of a *E*-PEA unit, as in the case of **1** (Table S2-1). Likewise, HRESIMS/MS of **2** showed fragmentation ions originating from cleavage of the *Z*-PEA and Ile₇ units (Figure S2-9). Hence, the structure of **2** was assigned as the *Z* isomer of **1** and was named microcionamide D.

Compound **4** was obtained as a white, amorphous solid. The molecular formula of **4** was deduced to be $C_{50}H_{67}N_9O_9S_2$ based on the prominent ion peak at m/z 1002.4572 $[M + H]^+$ in the HRESIMS spectrum, accounting for 22 degrees of unsaturation. The planar peptidic structure of **4** was distinguished by the abundance of the amide (NH) (δ_H 7.72–10.32) and α -amino (δ_H 4.10–4.84) protons, as well as by the cluster of primary and secondary methyl groups in the aliphatic region of the 1H NMR spectrum (Table 2). Analysis of the COSY and TOCSY NMR spectra revealed the spin systems of seven amino acid residues, including Pro (2 eq.), Cys (2 eq.), Phe, Leu, and Ile, together with the *E*-PEA unit and the unusual amino

acid residue pyroglutamic acid (Glp). The presence of the latter was confirmed by key HMBC correlations from Glp-H α to Glp-CO' (δ_c 177.4) and Glp-C γ (δ_c 29.0), from Glp-NH to Glp-CO' and Glp-C α (δ_c 55.1), and from Glp-H β to Glp-CO (δ_c 172.4). In analogy to **1** and **2**, the linkages and assignments of the amino acid residues in **4** were established by HMBC and ROESY NMR data (Table 2). Accordingly, the connection between *E*-PEA and Cys₁ was deduced by the HMBC correlation from *E*-PEA-H α to Cys₁-CO (δ_c 167.8) as well as the ROESY cross-peak between *E*-PEA-NH and Cys₁-H α . Moreover, the HMBC correlations from Cys₁-H α and Cys₁-NH to Phe-CO (δ_c 170.8), from Phe-H α and Phe-NH to Pro₃-CO (δ_c 171.4), as well as from Pro₃-H α to Pro₄-CO (δ_c 169.3) disclosed the peptide fragment *E*-PEA-Cys₁-Phe-Pro₃-Pro₄ (Figure 1). This was further corroborated by the ROESY cross-peaks between Cys₁-NH/Phe-H α , Phe-NH/Pro₃-H α , and Pro₃-H α /Pro₄-H α . Likewise, the HMBC correlations from Cys₅-H α to Leu-CO (δ_c 170.5), from Leu-H α to Ile-CO (δ_c 170.7), as well as from Ile-H α to Glp-CO (δ_c 172.4), in addition to the ROESY correlations between Pro₄-H α /Cys₅-H α , Cys₅-NH/Leu-H α , Leu-NH/Ile-H α , and Ile-NH/Glp-H α extended this fragment leading to the overall peptide sequence *E*-PEA-Cys₁-Phe-Pro₃-Pro₄-Cys₅-Leu-Ile-Glp. Finally, a disulfide bond between the two Cys residues was evident, consistent with the 22 elements of unsaturation required by the molecular formula. The structure of **4** was further corroborated by the fragment ions at m/z 665.2566 [M - Leu-Ile-Glp]⁺ and 883.3826 [M - *E*-PEA]⁺ in the HRESIMS/MS spectrum, originating from cleavage of the linear peptide sequence Leu-Ile-Glp and the PEA unit, respectively (Figure S4-9). Hence, compound **4** was identified as a new natural product and was named gombamide B, based on the structural relationship with the known compound gombamide A.¹²

Table 2. ¹H (600 MHz), ¹³C (150 MHz), HMBC, and ROESY NMR Data (DMSO-*d*₆, δ in ppm) of Gombamide B (**4**)

Unit	Position	δ_c , type	δ_H (<i>J</i> in Hz)	HMBC	ROESY ^a	
<i>E</i> -PEA	NH		10.32, d (10.0)		Cys ₁ -NH, Cys ₁ - α	
	α	123.0, CH	7.36, dd (14.7, 10.0)	Cys ₁ -CO, <i>E</i> -PEA-1		
	β	113.2, CH	6.33, d (14.7)	<i>E</i> -PEA-NH, <i>E</i> -PEA- α , <i>E</i> -PEA-2/6, <i>E</i> -PEA-1	<i>E</i> -PEA-NH	
	aromatic	1: 136.2, C				
		2: 125.3, CH		7.37, br d (7.7)	<i>E</i> -PEA- β , <i>E</i> -PEA-1, <i>E</i> -PEA-6, <i>E</i> -PEA-4	
		3: 128.6, CH		7.30, br t (7.7)	<i>E</i> -PEA-1, <i>E</i> -PEA-5	
4: 126.4, CH			7.17, br t (7.7)	<i>E</i> -PEA-2/6		
	5: 128.6, CH		7.30, br t (7.7)	<i>E</i> -PEA-1, <i>E</i> -PEA-3		

		CH				
		6: 125.3,	7.37, br d (7.7)	<i>E</i> -PEA- β , <i>E</i> -PEA-1, <i>E</i> -PEA-2		
		CH				
Cys ₁	NH		7.72, d (8.6)	Phe-CO, Cys ₁ - α , Cys ₁ - β	<i>E</i> -PEA-NH, Phe- α	
	CO	167.8, C				
	α	51.6, CH	4.64, ddd (12.0, 8.6, 3.5)	Cys ₁ -CO, Cys ₁ - β , Phe-CO	<i>E</i> -PEA-NH	
	β	42.1, CH ₂	2.93, dd (14.4, 12.0); 3.15, dd (14.4, 3.5)	Cys ₁ -CO, Cys ₁ - α		
Phe	NH		8.97, d (8.8)	Phe- α , Phe- β , Pro ₃ -CO	Pro ₃ - α	
	CO	170.8, C				
	α	53.5, CH	4.81, m	Phe-CO, Phe- β , Phe-1, Pro ₃ -CO	Cys ₁ -NH	
	β	34.0, CH ₂	2.99, m; 3.02, m	Phe-CO, Phe- α , Phe-1, Phe-2/6		
	aromat ic	1: 138.3, C				
		2: 129.3,	7.43, br d (7.5)	Phe- β , Phe-6, Phe-4		
		CH				
		3: 128.1,	7.29, br t (7.5)	Phe-1, Phe-5		
		CH				
		4: 126.2,	7.20, br t (7.5)	Phe-2/6		
		CH				
		5: 128.1,	7.29, br t (7.5)	Phe-1, Phe-3		
		CH				
		6: 129.3,	7.43, br d (7.5)	Phe- β , Phe-2, Phe-4		
		CH				
Pro ₃	CO	171.4, C				
	α	60.3, CH	4.36, d (7.8)	Pro ₃ -CO, Pro ₄ -CO, Pro ₃ - β , Pro ₃ - γ , Pro ₃ - δ	Pro ₄ - α , Pro ₄ - β , Phe-NH	
	β	31.2, CH ₂	1.73, m; 1.88, m	Pro ₃ -CO, Pro ₃ - α , Pro ₃ - γ		
	γ	20.1, CH ₂	1.42, m; 0.55, m	Pro ₃ - α		
	δ	45.9, CH ₂	3.29, m; 3.26, m	Pro ₃ - α , Pro ₃ - β		
Pro ₄	CO	169.3, C				
	α	59.2, CH	4.84, dd (9.5, 2.0)	Pro ₄ - β , Pro ₄ - γ , Pro ₄ - δ	Pro ₃ - α , Cys ₅ - α	
	β	30.2, CH ₂	1.87, m; 2.22, m	Pro ₄ -CO, Pro ₄ - α , Pro ₄ - δ	Pro ₃ - α	
	γ	21.9, CH ₂	1.76, m	Pro ₄ - α		
	δ	46.3, CH ₂	3.34, m; 3.48, m	Pro ₄ - β , Pro ₄ - γ		
Cys ₅	NH		8.01, d (10.0)	Leu-CO, Cys ₅ - α , Cys ₅ - β	Leu- α	
	CO	167.9, C				

	α	48.4, CH	4.56, td (10.0, 5.2)	Leu-CO, Cys ₅ -CO, Cys ₅ - β	Pro ₄ - α
	β	38.0, CH ₂	2.61, br dd (12.0, 10.0); 3.22, br dd (12.0, 5.2)	Cys ₅ - α , Cys ₅ -CO	
Leu	NH		8.05, d (9.2)	Leu- α , Leu- β , Ile-CO	Ile- α , Ile- β
	CO	170.5, C			
	α	50.5, CH	4.49, ddd (9.2, 8.0, 7.7)	Leu-CO, Leu- β , Leu- γ , Ile-CO	Cys ₅ -NH
	β	41.2, CH ₂	1.58, m	Leu-CO, Leu- α , Leu- γ , Leu- δ , Leu- δ'	
	γ	24.0, CH	1.63, m	Leu- δ , Leu- δ'	
	δ	21.3, CH ₃	0.86, d (6.3)	Leu- β , Leu- γ , Leu- δ'	
	δ'	23.3, CH ₃	0.89, d (6.4)	Leu- β , Leu- γ , Leu- δ	
Ile	NH		8.07, d (8.8)	Glp-CO, Ile- α , Ile- β	Glp- α , Glp- NH
	CO	170.7, C			
	α	57.0, CH	4.16, t (8.8)	Ile-CO, Ile- β , Ile- γ , Ile- γ' , Glp-CO,	Leu-NH
	β	35.5, CH	1.73, m	Ile-CO, Ile- α , Ile- γ	
	γ	24.2, CH ₂	1.02, m; 1.42, m	Ile- α , Ile- β , Ile- δ , Ile- γ'	
	γ'	15.4, CH ₃	0.75, d (6.7)	Ile- α , Ile- β , Ile- γ	
	δ	10.4, CH ₃	0.72, t (7.4)	Ile- β , Ile- γ	
Glp	NH		7.80, s	Glp-CO', Glp- α , Glp- β , Glp- γ	Ile-NH
	CO	172.4, C			
	CO'	177.4, C			
	α	55.1, CH	4.10, dd (8.7, 4.0)	Glp-CO, Glp-CO', Glp- β , Glp- γ	Ile-NH
	β	25.3, CH ₂	1.78, m; 2.21, m	Glp-CO, Glp-CO'	
	γ	29.0, CH ₂	2.09, m; 2.07, m	Glp-CO', Glp- α , Glp- β	

^aSequential NOEs.

Compound **5** was isolated as a white, amorphous solid. The molecular formula of **5** was deduced to be C₅₀H₆₇N₉O₉S₂ by HRESIMS analysis, as in the case of **4**. In analogy to **1** and **2**, the ¹H NMR spectrum of **5** was similar to that of **4**, the only difference being the *Z*-configuration of the ethylene protons in the PEA moiety instead of the *E*-configuration, as deduced by their vicinal coupling constant (³J_{H α ,H β = 9.7 Hz; Table S5-1). In a similar manner to **4**, HRESIMS/MS of **5** showed MS fragment ions of [M - *Z*-PEA]⁺ and [M - Leu-Ile-Glp]⁺ (Figure S5-7). Thus, compound **5** was characterized as a new natural product and was named gombamide C.}

Compound **6** was isolated as a white, amorphous solid. The molecular formula of **6** was determined as C₃₂H₄₈N₈O₈S₂ by HRESIMS, consistent with 13 degrees of unsaturation. Detailed interpretation of the COSY and HMBC NMR spectra of **6** established the presence of six amino acid residues, including Pro (3 eq.), Cys (2 eq.), Leu, along with a Glp unit. As described for peptides **1**, **2**, **4**, and **5**, key HMBC correlations from Pro₆-H α to Cys₁-CO (δ_C 168.1), from Cys₁-NH to Leu-CO (δ_C 170.9), from Leu-NH to Pro₃-CO (δ_C 171.0), from Pro₃-H α to Pro₄-CO (δ_C 169.6), and from Cys₅-NH to Glp-CO (δ_C 171.5) established the overall amino acid sequence of **6** as Pro₆-Cys₁-Leu-Pro₃-Pro₄-Cys₅-Glp. This assignment was also evident by the ROESY cross-peaks between Cys₁-NH/Leu-NH, Leu-NH/Pro₃-H α , and Cys₅-NH/Glp-H α . The remaining two NH protons at δ_H 6.90 (1H, s) and 7.27 (1H, s) were attributed to a terminal carboxamide group, as supported by their HMBC correlations to Pro₆-CO and Pro₆-C α (Figure 2, Table 3). Finally, cyclization via a disulfide bond between the two Cys residues was suggested to satisfy the remaining element of unsaturation in the structure of **6**. This assignment was further corroborated by the fragment ions at m/z 623.2317 [M - Pro₆-NH₂]⁺ and 595.2367 [M - (Pro₆-NH₂ + CO)]⁺, which were observed in the HRESIMS/MS data of **6** (Figure S6-8). Accordingly, compound **6** was identified as a new natural product and was given the name gombamide D.

Table 3. ¹H (600 MHz), ¹³C (150 MHz), HMBC, and ROESY NMR Data (DMSO-*d*₆, δ in ppm) of Gombamide D (**6**)

Unit	Position	δ_C , ^a type	δ_H (<i>J</i> in Hz)	HMBC	ROESY ^b
Pro ₆	CONH ₂		6.90, s; 7.27, s	Pro ₆ -CO, Pro ₆ - α	Pro ₆ - α , Cys ₁ - β
	CO	173.4, C			
	α	59.9, CH	4.16, dd (8.8, 3.5)	Pro ₆ -CO, Cys ₁ -CO, Pro ₆ - β , Pro ₆ - γ , Pro ₆ - δ	
	β	29.3, CH ₂	1.80, m; 2.02, m	Pro ₆ -CO, Pro ₆ - α , Pro ₆ - γ , Pro ₆ - δ	
	γ	24.3, CH ₂	1.87, m	Pro ₆ - α , Pro ₆ - β , Pro ₆ - δ	
	δ	46.6, CH ₂	3.52 ^c ; 3.63, ddd (9.7, 7.4, 4.5)	Pro ₆ - α , Pro ₆ - β	Cys ₁ - α
Cys ₁	NH		7.87, d (8.3)	Leu-CO, Cys ₁ - β , Cys ₁ - α	Leu- α , Leu-NH
	CO	168.1, C			
	α	49.2, CH	4.75, ddd (11.6, 8.3, 3.2)	Cys ₁ -CO, Cys ₁ - β	Pro ₆ - δ
	β	41.3, CH ₂	2.78, dd (14.6, 11.6); 3.12, dd (14.6, 3.2)	Cys ₁ -CO, Cys ₁ - α	
Leu	NH		9.17, d (9.0)	Leu- α , Pro ₃ -CO	Cys ₁ -NH, Pro ₃ - α , Pro ₃ - δ
	CO	170.9, C			

	α	50.1, CH	4.53 ^c	Leu-CO, Leu- β , Leu- γ	Cys ₁ -NH
	β	37.7, CH ₂	1.37, m; 1.71, m	Leu-CO, Leu- α , Leu- γ , Leu- δ , Leu- δ'	
	γ	24.2, CH	1.42, m	Leu- α , Leu- δ , Leu- δ'	
	δ	21.4, CH ₃	0.79, d (6.4)	Leu- β , Leu- γ , Leu- δ'	
	δ'	23.1, CH ₃	0.88, d (6.4)	Leu- β , Leu- γ , Leu- δ	
Pro ₃	CO	171.0, C			
	α	60.6, CH	4.52 ^c	Pro ₃ -CO, Pro ₄ -CO, Pro ₃ - β , Pro ₃ - γ , Pro ₃ - δ	Leu-NH, Pro ₄ - α
	β	31.2, CH ₂	2.08, m; 2.21, m	Pro ₃ -CO, Pro ₃ - α , Pro ₃ - γ , Pro ₃ - δ	
	γ	21.2, CH ₂	1.56, m; 1.91, m	Pro ₃ - α	
	δ	45.9, CH ₂	3.27, br t (10.4); 3.43 ^c	Pro ₃ - β , Pro ₃ - γ	Leu-NH
Pro ₄	CO	169.6, C			
	α	59.4, CH	4.91, dd (8.7, 2.5)	Pro ₄ - β , Pro ₄ - γ , Pro ₄ - δ	Pro ₃ - α , Cys ₅ - α
	β	30.4, CH ₂	2.30, m; 1.94, m	Pro ₄ -CO, Pro ₄ - α , Pro ₄ - δ	
	γ	21.8, CH ₂	1.73, m; 1.79, m		
	δ	46.5, CH ₂	3.50 ^c ; 3.35, dt (11.7, 7.7)	Pro ₄ - β	
Cys ₅	NH		8.54, d (9.7)	Glp-CO, Cys ₅ - α	Glp- α , Glp-NH
	CO	168.2, C			
	α	48.4, CH	4.58, ddd (11.1, 9.7, 5.2)	Cys ₅ -CO, Glp-CO, Cys ₅ - β	Pro ₄ - α
	β	37.5, CH ₂	2.62, dd (12.4, 11.1); 3.23, dd (12.4, 5.2)	Cys ₅ - α , Cys ₅ -CO	
Glp	NH		7.67, s	Glp-CO', Glp- α , Glp- β , Glp- γ	Cys ₅ -NH
	CO	171.5, C			
	CO'	177.6, C			
	α	54.9, CH	4.02, dd (8.9, 2.6)	Glp-CO', Glp- β	Cys ₅ -NH
	β	25.1, CH ₂	2.07, m; 2.15, td (9.2, 3.4)	Glp-CO, Glp-CO', Glp- γ	
	γ	28.9, CH ₂	2.00, m; 2.24, m	Glp-CO', Glp- α	

^aData extracted from HSQC and HMBC spectra. ^bSequential NOEs. ^cSignal overlap prevents determination of couplings.

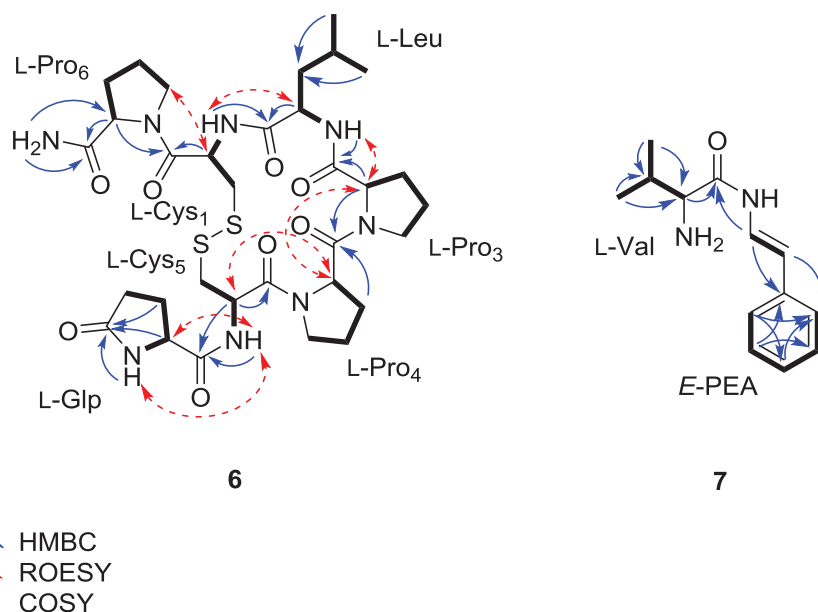


Figure 2. Key HMBC, ROESY and COSY correlations of **6** and **7**

Compound **7** was isolated as a white, amorphous solid. The molecular formula of **7** was determined as $C_{13}H_{18}N_2O$ based on HRESIMS analysis, consistent with six degrees of unsaturation. Detailed analysis of the 2D NMR (COSY, HSQC, and HMBC) spectra of **7** allowed the assignment of an unusual amide consisting of Val and *E*-PEA residues, connected through an amide linkage, as supported by the HMBC correlation from *E*-PEA- H_α to Val-CO (δ_C 167.2) (Figure 2, Table 4). Thus, compound **7** was assigned as (*E*)-2-amino-3-methyl-*N*-styrylbutanamide, which is a new natural product.

Table 4. 1H (600 MHz), ^{13}C (150 MHz), and HMBC NMR Data (MeOH- d_4 , δ in ppm) of (*E*)-2-amino-3-methyl-*N*-styrylbutanamide (**7**)

Unit	Positio n	δ_c , type	δ_H (<i>J</i> in Hz)	HMBC	
<i>E</i> - PEA	α	122.8, CH	7.46, d (14.7)	Val-CO, <i>E</i> -PEA-1	
	β	116.4, CH	6.32, d (14.7)	<i>E</i> -PEA-2/6	
	aromat ic	1: 137.2, C			
		2: 126.6, CH	7.35, dt (8.3, 1.5)	<i>E</i> -PEA- β , <i>E</i> -PEA-6, <i>E</i> - PEA-4	
	3: 129.8,	7.29, br dd (8.3,	<i>E</i> -PEA-1, <i>E</i> -PEA-5		

	CH	4: 128.1,	7.3) 7.19, tt (7.3, 1.5)	<i>E</i> -PEA-2/6
	CH	5: 129.8,	7.29, br dd (8.3,	<i>E</i> -PEA-1, <i>E</i> -PEA-3
	CH	6: 126.6,	7.35, dt (8.3, 1.5)	<i>E</i> -PEA- β , <i>E</i> -PEA-2, <i>E</i> -PEA-4
Val	CO	167.2, C		
	α	59.9, CH	3.69, d (5.8)	Val-CO, Val- γ , Val- γ'
	β	31.6, CH	2.24, m	Val- γ , Val- γ'
	γ	17.8, CH ₃	1.07, d (6.9)	Val- β , Val- α
	γ'	18.9, CH ₃	1.10, d (6.9)	Val- β , Val- α

The remaining compounds were identified based on NMR, HRESIMS, and specific rotation data analysis, as well as by comparison with published data as microcionamide A (**3**)^{82a} and six indole derivatives (8–13): [*1H*-indole-3-carbaldehyde (8), *1H*-indole-3-carboxylic acid (9), 6-bromo-*1H*-indole-3-carbaldehyde (10), 6-bromo-*1H*-indole-3-carboxylic acid (11), methyl 6-bromo-*1H*-indole-3-carboxylate (12), ethyl 6-bromo-*1H*-indole-3-carboxylate (13)],⁸³ along with 7-bromo- 4(*1H*)-quinolinone (14),⁸⁴ a δ -lactam derivative (3-(2-(4-hydroxyphenyl)-2-oxoethyl)-5,6-dihydropyridin-2(*1H*)-one) (15),⁸⁵ 2-deoxythymidine (16),⁸⁶ and 4-hydroxybenzoic acid (17) (Figure S9-1).

The absolute configuration of each amino acid residue was determined by Marfey's method following acid hydrolysis (6 N HCl) of the isolated peptides **1–7** (0.5 mg each).⁸⁷ Comparison of the resulting derivatives with those of standard amino acids by HPLC led to the assignment of the L-configuration for all amino acid residues (Table S8-1). Moreover, in an attempt to improve the HPLC resolution between L/D-Ile and L/D-*allo*-Ile residues, a C₄ HPLC RP-column was successfully employed, instead of the commonly used C₁₈ column, in analogy to the C₃ Marfey's method,⁸⁸ revealing the presence of only L-Ile residues as constituents of the respective peptides (**1–5**) (Table S8-2). Moreover, the ROESY correlations between Pro₃-H α /Pro₄-H α and Pro₄-H α /Cys₅-H α (Figure 1) in **4** and **5** suggested a *cis* configuration for the amide peptide bonds, which was further corroborated by the large Pro-C β and Pro-C γ shift difference values ($\Delta\delta_{C\beta-C\gamma} \sim 8\text{--}11$ ppm). Similarly, in the case of **6** a *cis* peptide bond was deduced between Pro₃-Pro₄ and Pro₄-Cys₅, whereas the ROESY correlation between Cys₁-H α and Pro₆-H δ in addition to the carbon resonances of C β and C γ in Pro₆ (29.4 and 24.2 ppm, respectively) suggested a *trans* peptide bond between Pro₆-Cys₁.^{77, 89}

Microcionamides C (**1**) and D (**2**) are stereoisomers differing in the *E/Z* double bond configuration of the PEA moiety, as previously observed for the known analogs microcionamides A (**3**) and B.^{82a} The only difference between the structures of **1** and **2** compared to **3** and microcionamide B is the replacement of the terminal Val residue in the latter compounds by Ile. In analogy to **1** and **2**, compounds **4** and **5** were found to be *E/Z*

stereoisomers. It should be noted, however, that the *Z*-PEA derivatives **2** and **5** were detected as the minor components in the crude extract, and thus these compounds may be artefacts arising from the respective *E*-PEA analogs **1** and **4** during extraction and/or isolation (e.g., upon exposure to natural light), as previously suggested for **3** and microcionamide B.^{82a} Compounds **4** and **5** are structurally related to the known peptide gombamide A from the sponge *Clathria gombawuiensis*, the latter compound bearing pyroglutamic acid (Glp) and *para*-hydroxystyrylamide units instead of the linear peptide chain Leu-Ile-Glp and PEA, respectively.^{82b} Interestingly, Glp is rarely reported from marine invertebrates. In addition to the aforementioned gombamide A, other examples of peptides bearing this unit include didemnins from the tunicate *Trididemnum solidum*,⁹⁰ as well as asteropsin A and two pyroglutamyl dipeptides from *Asteropus* sp. sponges.^{91,92} The intramolecular cyclization of *N*-terminal glutamine residues into Glp is of special interest, as it protects peptides from degradation by the action of exopeptidase enzymes or even enables them to adopt the right conformation for binding to their receptors.⁹³ Gombamide D (**6**) possesses a similar cyclic part as **4** and **5**, the only difference being that the Phe residue is substituted by Leu, as in the case of the cyclic thiopeptides eudistomides A and B, reported from a Fijian ascidian of the genus *Eudistoma*.⁹⁴ The promiscuous occurrence of these peptide analogs in different phyla of marine invertebrates argues for symbiont microorganisms as true producers.

Cytotoxicity of the isolated metabolites (**1–7** and known compounds **8 – 17**) was investigated using different tumor cell lines. Microcionamides A, C, and D (**1–3**) showed strong *in vitro* cytotoxicity against lymphoma (Ramos) and leukemia cell lines (HL-60, Nomo-1, Jurkat J16), as well as against a human ovarian carcinoma cell line (A2780) with IC₅₀ values ranging from 0.45 to 28 μ M. (Figures S10-1 and 3, Table 5). The remaining isolated compounds proved to be inactive in concentrations up to 10 μ M.

Table 5. Cytotoxicity of Compounds 1–3 after Incubation for 24 h Reported as IC₅₀ (μ M)

Com p.	A 2780	Ramos	Jurkat J16	Nomo-1	HL-60
1	0.45	1.4	0.81	1.4	1.9
2	0.53	1.9	1.3	2.4	2.5
3	2.6	5.9	4.6	10	28

Due to their strong cytotoxic activity we next addressed the question whether **1–3** cause apoptotic cell death. Activation of caspase-3 was measured employing two different methods – firstly by immunoblotting for the cleavage of the caspase-3 substrate poly(ADP-ribose) polymerase-1 (PARP-1) and secondly by measuring the fluorescence of the profluorescent caspase-3 substrate Ac-DEVD-AMC. Activated caspase-3 cleaves the latter substrate

between aspartate (D) and 7-amino-4-methylcoumarin (AMC), hence releasing the fluorogenic AMC, which can be subsequently detected with a spectrofluorometer. Because cysteine-dependent aspartate-directed proteases (caspases) in general and caspase-3 as an effector caspase in particular are central players of apoptotic processes, activation of caspase-3 indicates induction of apoptosis. As shown in Figure 3A, compounds **1–3** induced the activation of caspases in Jurkat and Ramos cells with rapid kinetics within 4 h and a reached maximum after 6 to 7 h, indicating a fast induction of apoptotic processes. However, compound **3** induced caspase activation only at 10 μM whereas in contrast to **1** and **2** it displayed no effect at 1 μM (data not shown), which is in accordance with the higher IC_{50} . To confirm activation of caspase-3 via a further endpoint, we detected cleavage of the caspase-3 substrate PARP after treatment with **1**, **2** and **3** (same concentrations as in 3A). In line with the results of the caspase-3 activity assay, all compounds induced cleavage of PARP within 4 to 8 h, indicating again activation of caspase-3 and thus execution of apoptosis. To prove caspase dependency of the observed PARP cleavage, we additionally performed co-incubation with the pan-caspase inhibitor QVD (Figure 3B). QVD completely blocked cleavage of PARP after treatment with **1**, **2** and **3**, demonstrating a causative role of caspases and thereby occurrence of apoptosis.

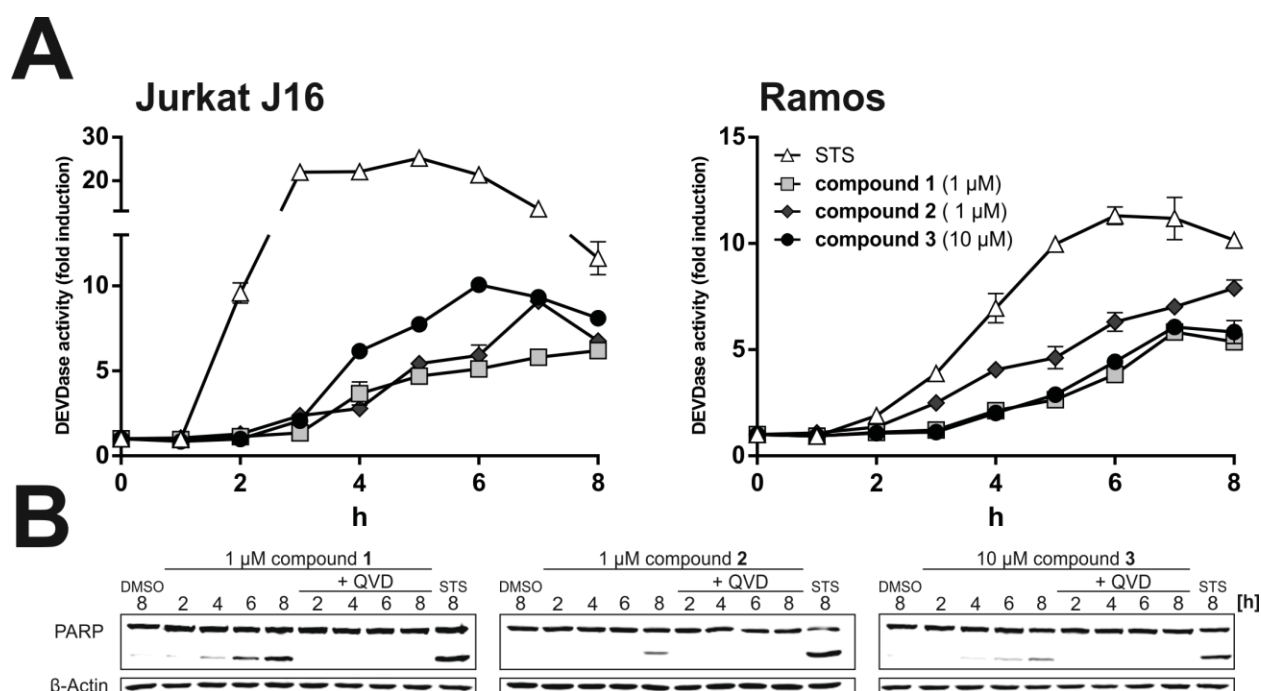


Figure 3. Compounds **1–3** rapidly induce apoptosis in human lymphoma and leukemia cell lines. (A) The kinetics of caspase-3 activation in Jurkat J16 (acute T cell leukemia; left panel) and Ramos (Burkitt’s lymphoma; right panel) cells after treatment with indicated concentrations of compounds **1–3** were compared to those of staurosporine (STS, 2.5 μM), a well-established inducer of apoptosis. Caspase-3 activity was measured by the rate of

cleavage of the profluorescent caspase-3 substrate Ac-DEVD-AMC. Relative caspase-3 activity in DMSO (0.1% v/v) treated control cells was set to 1. Data shown are the mean \pm SD from a representative experiment performed in triplicate. (B) Ramos cells were treated with compounds **1** (1 μ M), **2** (1 μ M) or **3** (10 μ M) in the absence or presence of the caspase inhibitor Q-VD-OPh (QVD, 10 μ M) for the indicated duration between 2 and 8 h. After the incubation period cleavage of PARP was determined by Western blot analysis. The expression of β -actin was determined as a protein loading control. Shown is the result of a representative blot. STS (2.5 μ M) served as the positive control for caspase-dependent cleavage of PARP.

Autophagy is a major intracellular degradation route responsible for the lysosome-mediated breakdown of soluble cytosolic components and therefore plays a crucial role in maintaining cellular homeostasis.⁶¹ Cancer cells in particular suffer from metabolic stress and nutrient deprivation due to fast proliferation. Thus, autophagy can support cancer cells to overcome microenvironmental stress by allowing them to recycle dysfunctional or unessential components. Autophagy thereby acts as a mechanism of cell survival. Accordingly, inhibition of autophagy is a promising therapeutic target for anticancer chemotherapy.⁹⁵ In order to investigate potential inhibitory or stimulating effects of **1–3** with regard to autophagy, we used murine embryonic fibroblast (MEF) cells stably expressing mCitrine-hLC3B and measured lysosomal degradation of mCitrine-hLC3B under starvation conditions and after treatment with compounds **1–3** or alternatively with the known autophagy inhibitor bafilomycin A1 via flow cytometry.⁹⁶ LC3 is an essential component of autophagosomes (double membraned key structures of autophagy), which deliver engulfed cytoplasmic components to lysosomes and get degraded by the lysosomal system during autophagy. Thus, breakdown of LC3 is a suitable indicator of autophagic processes. Incubation with 10 μ M compound **1** or **2** distinctly blocked starvation-induced degradation of LC3, indicating inhibition of autophagy by these compounds (Figure 4). Compound **3** on the other hand was inactive in this experiment, indicating the relevance of the terminal Ile for the autophagy-inhibitory effect. In order to determine whether the observed inhibition of autophagy by compounds **1** and **2** is caspase-dependent, we additionally performed experiments with co-treatment of QVD. Because QVD counteracted compound **1**-related inhibition of autophagy, this inhibitory effect was at least partially due to apoptotic processes. In contrast, the inhibitory effect mediated by compound **2** was completely unaffected by co-treatment with QVD, indicating independence of apoptosis.

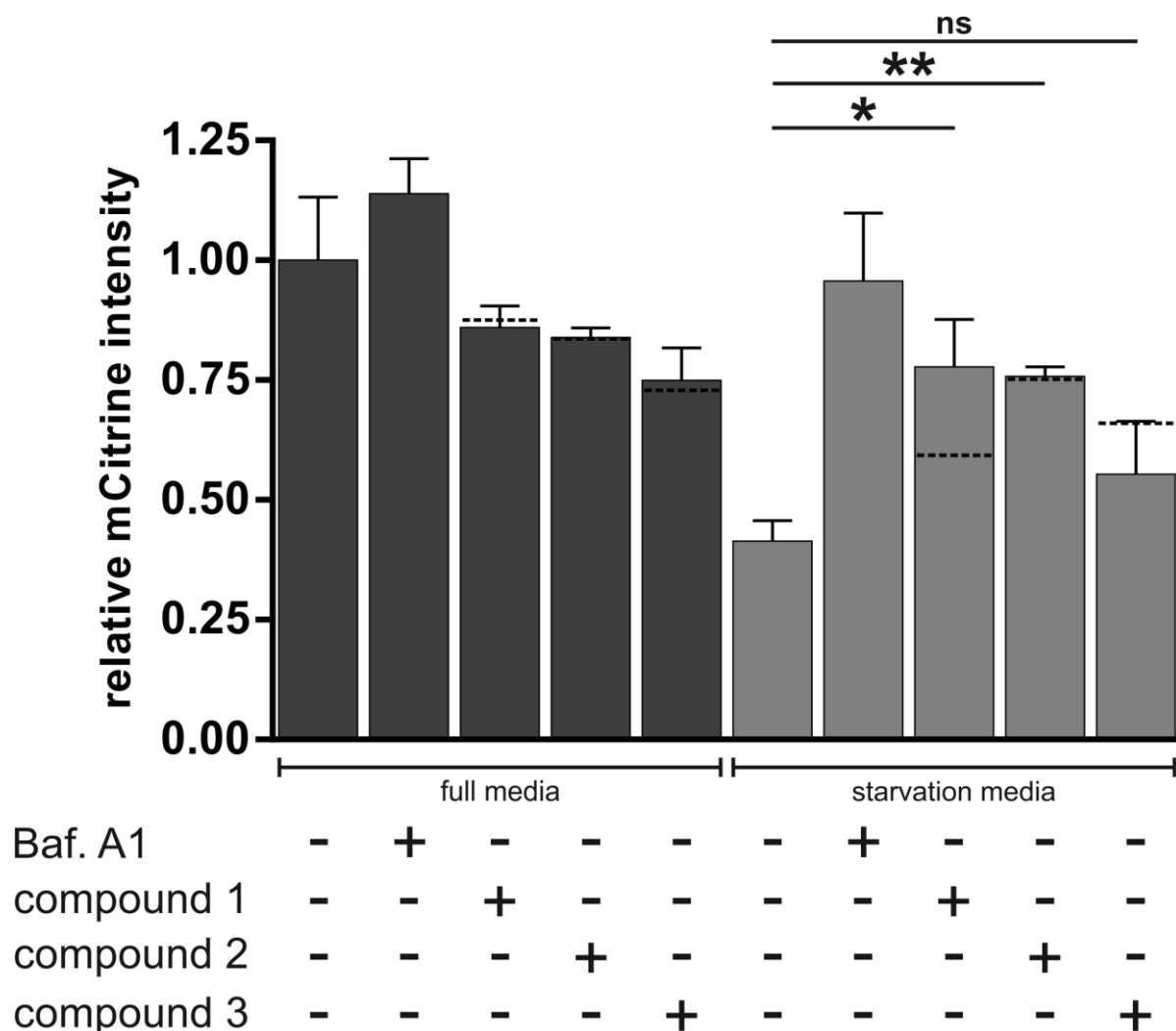


Figure 4. Compounds **1** and **2** impair amino acid starvation-induced autophagy. MEFs stably expressing mCitrine-hLC3B were cultivated in full medium or starvation medium (EBSS) with 10 μ M compounds **1**, **2** or **3** for 4 h. 10 nM bafilomycin A₁ (Baf. A1) served as the positive control for inhibition of autophagy. Total cellular mCitrine-hLC3B signals were analyzed by flow cytometry. The median of fluorescence intensity was plotted in a bar diagram. Values are normalized to DMSO (0.1% v/v) treated cells cultivated in full medium (1.0) and represent mean \pm SD of 3 independent analyses. * = $p \leq 0.05$, ** = $p \leq 0.01$ (Student's t-test, two-sample assuming unequal variances). Dashed lines represent median mCitrine fluorescence intensity of cells co-treated with caspase inhibitor Q-VD-OPh (10 μ M) performed in triplicate.

Finding new antibacterial agents unaffected by available resistance determinants is of paramount importance in the light of increasing bacterial resistance development. Thus, we were also interested in the antibacterial potential of the compounds (Table S10-2). Compounds **1** and **3** showed antibacterial activity against the Gram-positive bacterial species *Enterococcus faecium* and *Staphylococcus aureus* in the low μ M range. For both compounds, the minimal inhibitory concentrations (defined as the lowest concentrations completely preventing visible bacterial growth) were 6.2 μ M for *S. aureus* and 12 μ M for *E. faecium*,

respectively (Table S10-2). *Mycobacterium tuberculosis* as well as the Gram-negative species *Klebsiella pneumoniae*, *Enterobacter aerogenes*, *Escherichia coli*, *Pseudomonas aeruginosa*, and *Acinetobacter baumannii* were not inhibited up to 100 μ M. Compounds **2** and **5** were not investigated due to compound limitation. The remaining compounds showed no antibacterial activity.

In order to investigate the mechanism of bacterial growth inhibition, we employed as a first step a panel of bacterial reporter strains that we constructed in the background of the Gram-positive model organism *Bacillus subtilis*. These strains express the reporter gene β -galactosidase from five selected promoters that were previously found and validated to react specifically to disturbances of certain metabolic pathways or cell structures.⁹⁷ Previous whole genome mRNA profiling of *B. subtilis* after treatment with a broad range of antibiotic classes had identified these promoters as particularly responsive to DNA-, RNA-, protein- or cell envelope damage. Compounds **1** and **3** showed a specific induction of the cell envelope stress sensing promoters *liaI* and *ypuA* (Figure 5). While *ypuA* is known to respond broadly to disturbances at the bacterial cell envelope, *liaI* showed in previous studies a particularly strong reaction to compounds that interfere with cycling of undecaprenyl precursors in cell wall synthesis.⁹⁸

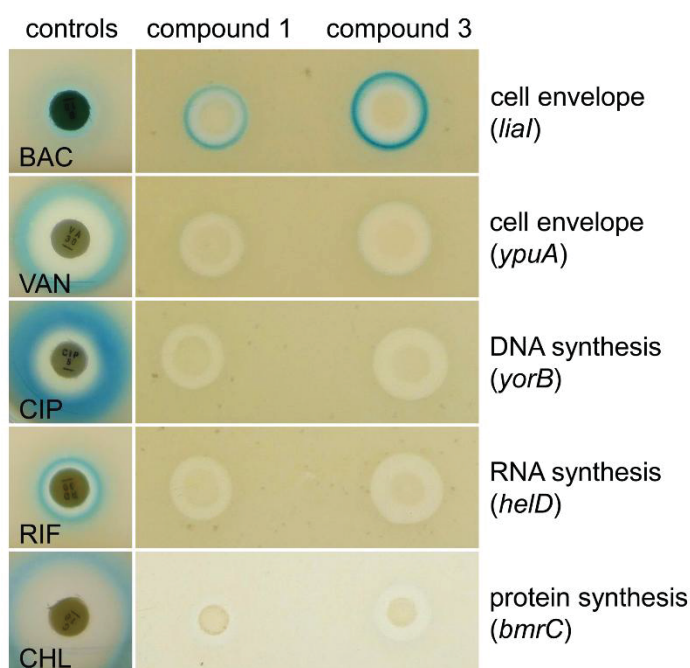


Figure 5. Reporter gene assay with compounds **1** and **3** for orienting mode of action studies. Compounds **1** and **3** strongly induced the *liaI* promoter and a weak induction was detected for the *ypuA* promoter, indicating that these compounds cause cell envelope stress. The other three promoters indicating DNA damage (*yorB*), RNA damage (*helD*) or translation arrest (*bmrC*) were not induced. The five different promoters showed a strong induction when treated with the respective positive controls: bacitracin (BAC), vancomycin (VAN), ciprofloxacin (CIP), rifampicin (RIF) and chloramphenicol (CHL).

With the aim to further explore the effects of the microcionamides on the bacterial cell envelope, we determined effects of compounds **1** and **3** on the membrane potential of *S. aureus*. The membrane potential is an electrical gradient across the bacterial cytoplasmic membrane, with a surplus of positive charge outside, that bacteria establish in the course of respiration. The membrane potential is essential for ATP-generation by the F₀F₁-ATPase and for active transport processes across the cytoplasmic membrane. For measurement of the membrane potential the fluorescent dye DiOC₂(3) was used, which enters bacterial cells to some extent and emits green fluorescence. The higher the membrane potential the more dye molecules accumulate in the cells and aggregation triggers a red-shift of fluorescence emission. Addition of compound **1** and **3** efficiently dissipated the membrane potential of *S. aureus* as indicated by the strong loss of red fluorescence (Figure 6). The effect occurred already at sub-micromolar concentrations of **1** and **3**, the latter compound being slightly more potent. Consequently, microcionamides A (**3**) and C (**1**) seem to kill bacteria by energy depletion.

Notably, while some energy depleting agents induce the *liaI* promoter, e.g. the lantibiotic nisin, which uses the undecaprenyl precursor lipid II as a docking molecule to form pores within the bacterial cytoplasmic membrane,⁹⁹ many energy-depleting agents, such as ionophores, do not effectively induce *liaI*. Whether or not the strong *liaI* signal triggered by the microcionamides indicates that bacterial cells sense an interference with their undecaprenyl precursor cycle, will require further studies.

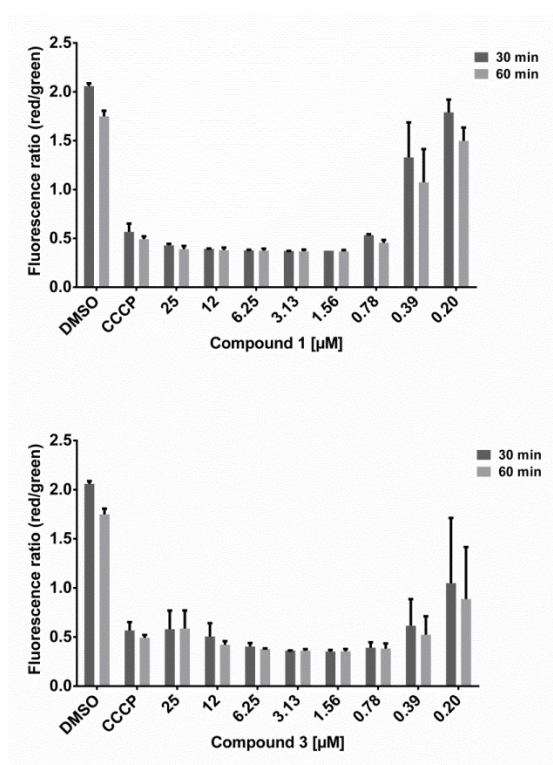


Figure 6. Effect of microcionamides A (**3**) and C (**1**) on the membrane potential of *Staphylococcus aureus* NCTC 8325. A prominent loss of red fluorescence indicative of

strong membrane potential dissipation occurs already at 0.8 μM of **1** or 0.2 μM of **3**. The protonophor carbonyl cyanide *m*-chlorophenyl hydrazone (CCCP) at 5 μM served as a positive control and DMSO was the negative control. Samples were analysed after 30 and 60 min of exposure to compounds. The experiment was performed two times on two different days with independent bacterial cultures. Results for both biological replicates are shown in the graphs. Error bars indicate the standard error of the mean.

In summary, microcionamides A, B, and C (**1–3**) exhibited cytotoxicity on different human cancer cell lines via both induction of apoptosis and inhibition of starvation-induced autophagy. Furthermore, microcionamides A (**3**) and C (**1**) showed a significant inhibitory effect on Gram-positive bacteria, which is probably correlated with their abilities to depolarize bacterial cytoplasmic membranes. It is noteworthy that microcionamide C (**1**) showed increased cytotoxic activity over microcionamide A (**3**) by a factor of five or more on different eukaryotic cell lines, while **3** was more potent against Gram-positive bacteria compared to **1**. Even though the difference in the MIC between **1** and **3** against *S. aureus* was smaller than a whole titration step in the MIC assay, a larger zone of inhibition of **3** was detected on agar (Figure 5) and lower concentrations of **3** were able to cause a disruption of the membrane potential in comparison to **1** (Figure 6). Conversely, gombamides B (**4**) and D (**6**) proved to be inactive against both human and bacterial cells.

5.2 Experimental Section

General Experimental Procedures. Optical rotations were measured with a JASCO P-2000 polarimeter. UV data were recorded on a Perkin-Elmer Lambda 25 UV/vis spectrometer. ^1H , ^{13}C , and 2D NMR spectra (HH-ROESY, HH-TOCSY, HC-HSQC and HC-HMBC) were recorded with standard pulse sequences on a Bruker AVIII HD 600 spectrometer equipped with a QXI/QCI cryo-probe. The sweep width for the homonuclear experiments (HH-ROESY) was 7000 Hz in F2 and F1. Two thousand data points were collected in F2, and 256 data points in F1 with quadrature detection in both dimensions. The mixing time for the HH-ROESY experiment was 450ms with a spin lock field of 5000 Hz. The HC-HSQC experiment was measured with a sweep width of 7000 Hz in F2 and 25500 Hz in F1. Two thousand data points were collected in F2, and 256 data points in F1 with quadrature detection in both dimensions. The sweep width for the HC-HMBC experiments was set to 7000 Hz in F2 and 17600 Hz in F1. Two thousand data points in F2 and 256 data points in F1 were collected with quadrature detection in F2. The chemical shifts were referenced to the residual solvent peaks at δ_{H} 3.31 (MeOH-*d*₄) and 2.50 (DMSO-*d*₆) for ^1H ; and at δ_{C} 49.0 (MeOH-*d*₄) and 39.5 (DMSO-*d*₆) for ^{13}C NMR. Low-resolution ESI mass spectra were recorded on a Thermoquest Finnigan LCQ Deca connected to an Agilent 1100 series LC. High-resolution mass measurements were obtained on a LTQ Orbitrap Velos Pro (Thermo Scientific). Solvents were distilled prior to use, and spectral grade solvents were used for spectroscopic measurements. HPLC analysis was performed using a Dionex UltiMate3400 SD coupled to a photodiode array detector (DAD3000RS) with detection wavelengths at 235, 254, 280, and 340 nm. The separation column (125 \times 4 mm, L X i.d) was prefilled with Eurospher 100-10,

C18 (Knauer, Germany). HPLC analysis of L/D-Ile and L/D-*allo*-Ile following Marfey's derivatization was carried out on the EC 250/4.6 Nucleosil 120-5, C₄ (Macherey-Nagel) separation column. Column chromatography was performed using Sephadex LH-20 or reversed-phase silica (RP C₁₈) as stationary phase. Semipreparative purification was accomplished on a Merck Hitachi system (Pump L7100 and UV detector L7400; Eurospher 100 C₁₈, 300 x 8 mm, L X i.d; Knauer) with a flow rate of 5.0 mL/min. Thin-layer chromatography (TLC) was performed using precoated silica gel 60 F₂₅₄ plates (Merck) followed by detection under UV at 254 nm or after spraying the plates with anisaldehyde reagent.

Sponge Material. The sponge was collected by SCUBA at Ambon, Indonesia. The sponge was identified as *Clathria basilana* by Dr. Nicole de Voogd (Naturalis Biodiversity Center, Leiden, The Netherlands), and a voucher specimen was deposited at the Naturalis Biodiversity Center, Leiden, The Netherlands (reference number RMNH POR 8636). The sponge was preserved in a mixture of EtOH and H₂O (70:30) and stored in a -20 °C freezer prior to extraction.

Extraction and Isolation. The thawed sponge material (820 g wet) was cut into small pieces and exhaustively extracted with MeOH (3 x 2L) at room temperature (rt). The extracts were combined and concentrated under vacuum to yield 6.5 g of crude extract. Subsequent liquid-liquid partitioning afforded *n*-hexane, EtOAc, *n*-BuOH, and aqueous fractions at amounts of 420 mg, 700 mg, 540 mg, and 4.9 g, respectively. The EtOAc fraction was further purified by column chromatography on Sephadex LH-20 (MeOH as mobile phase), followed by reversed-phase vacuum liquid chromatography (RP-VLC) and semipreparative HPLC in a gradient system of H₂O/MeOH, respectively, to yield **1** (7.7 mg), **2** (2 mg), **3** (1 mg), **4** (4.5 mg), **5** (1 mg), **7** (0.8 mg), **8** (0.6 mg), **9** (0.5 mg), **10** (1.2 mg), **11** (1 mg), **12** (1 mg), **13** (1.7 mg), **14** (1 mg), **15** (2.2 mg), **16** (2.5 mg), and **17** (4 mg). The *n*-BuOH fraction was subjected to column chromatography on Sephadex LH-20 (MeOH as mobile phase), followed by reversed-phase vacuum liquid chromatography (RP-VLC) and semipreparative HPLC to yield **6** (5.6 mg).

Microcionamide C (1): White, amorphous solid; $[\alpha]_D^{20}$ -56 (*c* 1.0, MeOH); UV (λ_{\max} , MeOH) (log ϵ) 201 (3.72), 287 (3.09); ¹H (600 MHz) and ¹³C (150 MHz) NMR data (DMSO-*d*₆), Table 1; HRESIMS *m/z* 889.5033 [M + H]⁺ (calcd for C₄₄H₇₃N₈O₇S₂, 889.5038); HRESIMS/MS *m/z* 770.4297 [M- *E*-PEA]⁺ (calcd for C₃₆H₆₄N₇O₇S₂, 770.4303); 657.3454 [M- (*E*-PEA+Ile₇)]⁺ (calcd for C₃₀H₅₂N₆O₆S₂, 657.3463).

Microcionamide D (2): White, amorphous solid; $[\alpha]_D^{20}$ -40 (*c* 1.0, MeOH); UV (λ_{\max} , MeOH) (log ϵ) 210 (3.8), 271 (4.01); ¹H (600 MHz) and ¹³C (150 MHz) NMR data (DMSO-*d*₆), Table S2-1; HRESIMS *m/z* 889.5034 [M + H]⁺ (calcd for C₄₄H₇₃N₈O₇S₂, 889.5038); HRESIMS/MS *m/z* 770.4294 [M- *Z*-PEA]⁺ (calcd for C₃₆H₆₄N₇O₇S₂, 770.4294); 657.3451 [M- (*Z*-PEA+Ile₇)]⁺ (calcd for C₃₀H₅₂N₆O₆S₂, 657.3451); 776.4184 [M- Ile₇]⁺ (calcd for C₃₈H₆₀N₇O₆S₂, 776.4184).

Gombamide B (4): White, amorphous solid; $[\alpha]_D^{20} +28$ (*c* 1.0, MeOH); UV (λ_{\max} , MeOH) (log ϵ) 212 (4.1), 290 (4.56); ^1H (600 MHz) and ^{13}C (150 MHz) NMR data (DMSO-*d*₆), Table 2; HRESIMS *m/z* 1002.4572 $[\text{M} + \text{H}]^+$ (calcd for C₅₀H₆₈N₉O₉S₂, 1002.4576);); HRESIMS/MS *m/z* 883.3826 $[\text{M} - \text{E-PEA}]^+$ (calcd for C₄₂H₅₉N₈O₉S₂, 883.3826); 665.2566 $[\text{M} - \text{Leu-Ile-Glp}]^+$ (calcd for C₃₃H₄₁N₆O₅S₂, 665.2566); 546.1833 $[\text{M} - (\text{E-PEA} + \text{Leu-Ile-Glp})]^+$ (calcd for C₂₅H₃₂N₅O₅S₂, 546.1833).

Gombamide C (5): White, amorphous solid; $[\alpha]_D^{20} +16$ (*c* 1.0, MeOH); UV (λ_{\max} , MeOH) (log ϵ) 214 (4.01), 288 (4.4); ^1H (600 MHz) and ^{13}C (150 MHz) NMR data (DMSO-*d*₆), Table S5-1; HRESIMS *m/z* 1002.4576 $[\text{M} + \text{H}]^+$ (calcd for C₅₀H₆₈N₉O₉S₂, 1002.4576);); HRESIMS/MS *m/z* 883.3826 $[\text{M} - \text{Z-PEA}]^+$ (calcd for C₄₂H₅₉N₈O₉S₂, 883.3841); 665.2566 $[\text{M} - \text{Leu-Ile-Glp}]^+$ (calcd for C₃₃H₄₁N₆O₅S₂, 665.2566); 546.1833 $[\text{M} - (\text{Z-PEA} + \text{Leu-Ile-Glp})]^+$ (calcd for C₂₅H₃₂N₅O₅S₂, 546.1839).

Gombamide D (6): White, amorphous solid; $[\alpha]_D^{20} -6$ (*c* 1.0, MeOH); UV (λ_{\max} , MeOH) (log ϵ) 210 (3.8), 271 (4.01); ^1H (600 MHz) and ^{13}C (150 MHz) NMR data (DMSO-*d*₆), Table 3; HRESIMS *m/z* 737.3107 $[\text{M} + \text{H}]^+$ (calcd for C₃₂H₄₉N₈O₈S₂, 737.3109);); HRESIMS/MS *m/z* 623.2317 $[\text{M} - \text{Pro}_6\text{-NH}_2]^+$ (calcd for C₂₇H₃₉N₆O₇S₂, 623.2317); 595.2367 $[\text{M} - (\text{Pro}_6\text{-NH}_2 + \text{CO})]^+$ (calcd for C₂₆H₃₉N₆O₆S₂, 595.2367).

(E)-2-amino-3-methyl-N-styrylbutanamide (7): White, amorphous solid; $[\alpha]_D^{20} -38$ (*c* 1.0, MeOH); UV (λ_{\max} , MeOH) (log ϵ) 220 (3.07), 285 (3.22); ^1H (600 MHz) and ^{13}C (150 MHz) NMR data (DMSO-*d*₆), Table 4; HRESIMS *m/z* 219.1490 $[\text{M} + \text{H}]^+$ (calcd for C₁₃H₁₉N₂O, 219.1492).

Marfey's Analysis. For acid hydrolysis of the isolated peptides (1–7), 0.5 mg of each was treated separately with 2 mL 6 N HCl and heated at 110 °C for 24 h. The resulting solutions were concentrated, with consecutive addition of H₂O (5 mL each) to ensure complete elimination of HCl. Accordingly, the mixture of 50 μL of each acid hydrolysate, 100 μL FDNPL (1% *N*-(5-fluoro-2,4-dinitrophenyl)-L-leucinamide in acetone) and 20 μL 1 M NaHCO₃ were heated at 40 °C for 1 h with frequent mixing. After cooling, 10 μL of 2 N HCl was added into the reaction solution. Subsequently, the derivatized product was concentrated to dryness and prepared for HPLC analysis by dissolving in 1000 μL MeOH. The same procedure was followed for L- and D-amino acid standards. HPLC (C₁₈) analysis of the derivatized amino acids was performed by comparing their retention times with those of standards [gradient (MeOH, 0.1% HCOOH in H₂O): 0 min (10% MeOH); 5 min (10% MeOH); 35 min (100% MeOH); 45 min (100% MeOH); 25 °C, 1 mL/min] (Table S8-1). For improved resolution, HPLC analysis of the derivatized L/D-Ile and L/D-*allo*-Ile residues was performed on a C₄ analytical column [gradient (MeOH, 0.1% HCOOH in H₂O): 0% to 60% (MeOH) for 160 min; 25 °C, 1 mL/min] (Table S8-2).^{87, 100}

Eukaryotic Cell Lines and Reagents. Acute T cell leukemia cells (Jurkat J16, no. ACC-282), Burkitt's lymphoma B lymphocytes (Ramos, no. ACC-603), acute promyelocytic leukemia cells (HL-60, no. ACC-3) and acute myeloid leukemia cells (Nomo-1, no. ACC-

542) were obtained from the German Collection of Microorganisms and Cell Cultures (DSMZ). Wild-type murine embryonic fibroblasts (MEFs, kindly provided by Xiaodong Wang)_ENREF_33¹⁰¹ expressing mCitrine-hLC3B were generated by retroviral gene transfer using pMSCVpuro/mCitrine-hLC3B. To generate pMSCVpuro/mCitrine-hLC3B, full-length human *MAP1LC3B* cDNA was cloned into pMSCVpuro/mCitrine vector (kindly provided by Michael Engelke, University of Göttingen). All cell lines were grown at 37 °C under humidified air supplemented with 5% CO₂ in RPMI 1640 (HL-60, Jurkat J16, Nomo-1, Ramos) or DMEM (mCitrine-hLC3B-MEF) containing 10% fetal calf serum, 1% HEPES, 120 IU/mL penicillin, and 120 µg/mL streptomycin. The broad-range caspase inhibitor N-(2-Quinoly)-L-valyl-L-aspartyl-(2,6-difluorophenoxy) methylketone [(QVD), #SML0063], the autophagy inhibitor bafilomycin A1 [(Baf. A1), #B1793] and the kinase inhibitor staurosporine [(STS), #S5921], used as positive control for induction of apoptosis, were obtained from Sigma-Aldrich. The profluorescent caspase-3 substrate Ac-DEVD-AMC was purchased from Biomol (# ABD-13402). Human ovarian carcinoma (A2780) cells were obtained from ECACC (Salisbury, Wiltshire/UK) and cultivated in RPMI-1640 medium supplemented with 10% FBS, 120 µg/mL streptomycin and 120 U/mL penicillin. Cells were grown at 37 °C in a humidified atmosphere containing 5% CO₂.

Determination of Eukaryotic Cell Viability. HL-60, Jurkat J16, Nomo-1, and Ramos cells were seeded at a density of 5×10^5 cells/mL and incubated with different concentrations of compound **1**, **2**, and **3** for 24 h. Cells treated with DMSO (0.1% v/v) for 24 h were used as the negative control. After the incubation period MTT (3-(4,5-Dimethyl-2-thiazolyl)-2,5-diphenyl-2H-tetrazolium bromide; Calbiochem #475989) was added to the cells to a final concentration of 1 mg/mL, the cells were incubated further for 60 min and then centrifuged at 600 rcf for 5 min. The medium was aspirated and 100 µL DMSO were added to each well to extract the formazan product from the cells. After 25 min of incubation on a shaker at rt, the absorbances at 650 nm (reference wavelength) and 570 nm (test wavelength) were measured using a multiplate reader (Synergy Mx, BioTek). Viability and IC₅₀ values (IC₅₀ = half maximal inhibitory concentration) were calculated using Prism 6 (GraphPad Software). Relative viability in DMSO (0.1% v/v) treated control cells was set to 100%. A2780 cells were plated into 96-well microtiter plates (approximately 9,000 cells/well) (Sarstedt) and pre-incubated with growth medium overnight. Then, cells were incubated with increasing concentrations of test compounds for 72 h. After 72 h, 25 µL of a solution of MTT were added to each well. After approximately 10 min, formazan crystals occurred, and medium was removed. Formazan crystals were then dissolved in 75 µL DMSO. Absorptions were measured at 544 nm (test wavelength) and 690 nm (reference wavelength) using the BMG FLUOstar (BMG Labtechnologies, Offenburg, Germany). Absorption of the reference wavelength was subtracted from the absorption of the test wavelength.

Determination of Antibacterial Activity. MIC values for bacterial strains were determined in cation-adjusted Mueller-Hinton broth by the broth microdilution method according to the recommendations of the Clinical and Laboratory Standards Institute (CLSI).¹⁰² For preparation of the inoculum the direct colony suspension method was used. Briefly, serial twofold dilutions of test compounds were prepared in microtiter plates and seeded with a

final bacterial inoculum of 5×10^5 colony forming units per mL (CFU/mL). After 16 to 20 h at 37 °C and ambient air, the minimal inhibitory concentration was read as the lowest compound concentration preventing visible bacterial growth. The strain panel included antibiotic-susceptible CLSI quality control strains obtained from the American Type Culture Collection as indicated by the ATCC strain label. *E. faecium* BM 4147-1 is a clinical isolate cured of its vancomycin resistance plasmid¹⁰³ and *A. baumannii* 09987 is a clinical isolate from the University of Bonn, Germany.

Cells of *M. tuberculosis* H37Rv were grown aerobically in Middlebrook 7H9 medium supplemented with 10% (v/v) ADS enrichment (5%, w/v, bovine serum albumin fraction V; 2%, w/v, glucose; 0.85%, w/v, sodium chloride), 0.5% (v/v) glycerol, and 0.05% (v/v) tyloxapol at 37 °C. For the determination of MIC against *M. tuberculosis*, bacteria were precultured until log-phase ($OD_{600\text{ nm}} = 0.5-1$) and then seeded at 1×10^5 cells per well in a total volume of 100 μL in 96-well round bottom microtiter plates containing twofold serially diluted compounds at a concentration range of 100-0.78 μM . Microplates were incubated at 37 °C for five days. Afterwards, 10 μL /well of a 100 $\mu\text{g}/\text{mL}$ resazurin solution were added and incubated at ambient temperature for further 16 h. Then cells were fixed for 30 min after formalin addition (5%, v/v, final concentration). For viability determination, fluorescence was quantified using a microplate reader (excitation 540 nm, emission 590 nm). Percentage of growth was calculated relative to rifampicin treated (0% growth) and DMSO treated (100% growth) controls.

Western Blot Analysis. Ramos cells were treated for the indicated durations with 1 μM of **1**, 1 μM of **2** or 10 μM of **3**, respectively. Coincubation with the caspase inhibitor QVD at a concentration of 10 μM was used as proof of caspase-dependency of the observed effects. Subsequently, cells were pelleted at 600 rcf at 4 °C for 5 min, washed with PBS and frozen in liquid nitrogen. The cells were lysed in ice-cold lysis buffer [20 mM Tris-HCl, pH 7.5, 150 mM NaCl, 0.5 mM EDTA, 1% Triton X-100, 10 mM NaF, 2.5 mM $\text{Na}_4\text{P}_2\text{O}_7$, 10 μM Na_2MoO_4 , 1 mM Na_3VO_4 , protease inhibitor cocktail (Sigma #P2714)]. The lysates were cleared from cell debris by centrifugation at 11,000 rcf at 4 °C for 15 min and the total protein concentration was measured by Bradford assay and adjusted to equal concentrations. After loading with Laemmli buffer and heating to 95 °C for 5 min, 25 μg of the protein extract was separated by SDS-PAGE [10% tris-glycine polyacrylamide gel (v/v)] and transferred to a PVDF membrane by Western blotting according to the standard protocol. Analysis of proteins of interest was performed using primary mouse antibodies to Poly (ADP-ribose) polymerase-1 (Enzo Life Sciences #BML- SA250) or β -actin (Sigma-Aldrich #A5316) and IRDye800- conjugated secondary antibodies (LI-COR Biosciences #926-32210/11). Signals were detected with an infrared imaging system.

Caspase-3 Activity Assay. Caspase activity was analyzed as previously described.¹⁰⁴ Briefly, Jurkat J16 cells and Ramos cells were seeded at a density of 1×10^6 cells/mL in 96-well microtiter plates and incubated with different concentrations of **1**, **2** and **3** for the indicated times. Cells treated with DMSO (0.1% v/v) were used as negative control. After incubation period, cells were harvested by centrifugation at 600 rcf at 4 °C and lysed by incubation with ice-cold lysis buffer (20 mM HEPES, 84 mM KCl, 10 mM MgCl_2 , 200 μM

EDTA, 200 μ M EGTA, 0.5% NP-40, 1 μ g/mL Leupeptin, 1 μ g/mL Pepstatin, 5 μ g/mL Aprotinin) for 10 min. After addition of 150 μ L reaction buffer (50 mM HEPES, 100 mM NaCl, 10% Sucrose, 0.1% CHAPS, 2 mM CaCl₂, 13.35 mM DTT, 70 μ M DEVD-AMC) per well, fluorescence (Ex 360 nm, Em 450 nm) was measured at 37 °C over a time course of 150 min using a multiplate reader (Synergy Mx, BioTek). Caspase activity was determined as the slope of the resulting linear regressions. Data points shown are the mean of triplicates, error bars = SD. Values are normalized to DMSO (0.1% v/v) treated cells (fold change = 1.00).

FACS-based Analysis of Autophagy. The FACS-based analysis of autophagy was adapted from a protocol previously described by Shvets et al.¹⁰⁵ MEF cells stably expressing mCitrine-hLC3B were cultured in the indicated medium for 4 h with bafilomycin A1 (Baf. A1, 10 nM), compound **1**, **2** or **3** (10 μ M), harvested with 0.05% trypsin-EDTA, and washed once with phosphate-buffered saline. Subsequently, the intensity of mCitrine fluorescence was analyzed by flow cytometry using FACSDiva software. Reduction of mCitrine-hLC3B compared to medium control indicates autophagy induction. Baf. A1 served as positive control for inhibition of autophagy. Co-treatment with QVD was performed to exclude caspase-dependent processes.

Bacterial Reporter Gene Assay. For mode of action studies, five bacterial reporter strains were constructed in the genetic background of *B. subtilis* 1S34, each carrying one of the following promoters fused to the β -galactosidase reporter gene and inserted into the chromosomal *amyE* locus. Induction of the *yorB* promoter indicates DNA damage, the *hcd* promoter (synonym *yvgS*) senses RNA damage, and the *bmrC* promoter senses translation arrest. Induction of the *ypuA* or *lial* (synonym *yvqI*) promoters indicate cell envelope stress. Promoter regions were chosen according to a previous publication by Urban et al.⁹⁷ For the agar-based reporter gene assay 20 mL lysogeny broth (LB) containing spectinomycin (50 μ g/mL) were inoculated with 500 μ L of an overnight culture of *B. subtilis* 1S34 and grown to the stationary phase. Cells were adjusted to a total cell number of 3×10^7 CFU/mL in 50 ml LB softagar (0.7 % agar) containing 150 μ g/mL of 5-bromo-4-chloro-3-indolyl- β -D-galactopyranoside (X-Gal) and poured into a square petri dish. After solidification, test compounds (20 nmol) were spotted onto the agar plates. Paper discs (Oxoid) containing the following reference antibiotics were used as positive controls: bacitracin (10 μ g), chloramphenicol (10 μ g), ciprofloxacin (5 μ g), rifampicin (30 μ g), and vancomycin (30 μ g). Plates were analyzed for promoter induction after incubation at 30 °C for 14 to 18 h. In the case of the *bmrC* promoter, soft agar was prepared from Belitzky minimal medium and the plates were incubated at 37 °C.¹⁰⁶

Measurement of Bacterial Membrane Potential. Determination of membrane potential changes upon antibiotic treatment was performed using the membrane potential-sensitive fluorescent dye 3,3'-diethyloxacarbocyanine iodide (DiOC₂(3), Molecular Probes). *S. aureus* NCTC 8325 was grown to the exponential phase in LB medium, harvested and resuspended to an optical density at 600 nm (OD₆₀₀) of 0.5 in phosphate buffered saline (PBS). Cells were incubated with 30 μ M DiOC₂(3) for 15 min and subsequently treated with compounds **1** and **3** at different concentrations for 30 min. The protonophor carbonyl cyanide m-chlorophenyl

hydrazone (CCCP, Sigma Aldrich) at a concentration of 5 μ M, was used as a positive control and DMSO as a negative control. Fluorescence was measured 30 and 60 min after addition of the respective compound at an excitation wavelength of 485 nm and two emission wavelengths, 530 nm (green) as well as 630 nm (red), using a microplate reader (TECAN Infinite M200). Increased membrane potential promotes intracellular dye accumulation, self-association of which causes a redshift of the fluorescence emission signal.

ASSOCIATED CONTENT

Supporting Information

¹H NMR spectra of **1–7**; ¹³C NMR spectra of **4**, **6**, and **7**; 2D NMR and HRESIMS spectra of the new compounds **1**, **2**, **4–7**; HRESIMS/MS spectra of **1**, **2**, **4–6**; Tables of ¹H, ¹³C, and 2D NMR data for **2** and **5**; HPLC analysis of the acid hydrolysates of **1–7** using Marfey's method; Structures of the known compounds **8–17**; **Cytotoxicity effects of 1–3 on human lymphoma and leukemia cell lines**, measured by MTT assay; **Table of antibacterial activity of compounds 1–17 reported as minimal inhibitory concentration (MIC)** The supporting information is available free of charge on the ACS Publications website as DOI:

AUTHOR INFORMATION

Corresponding Author

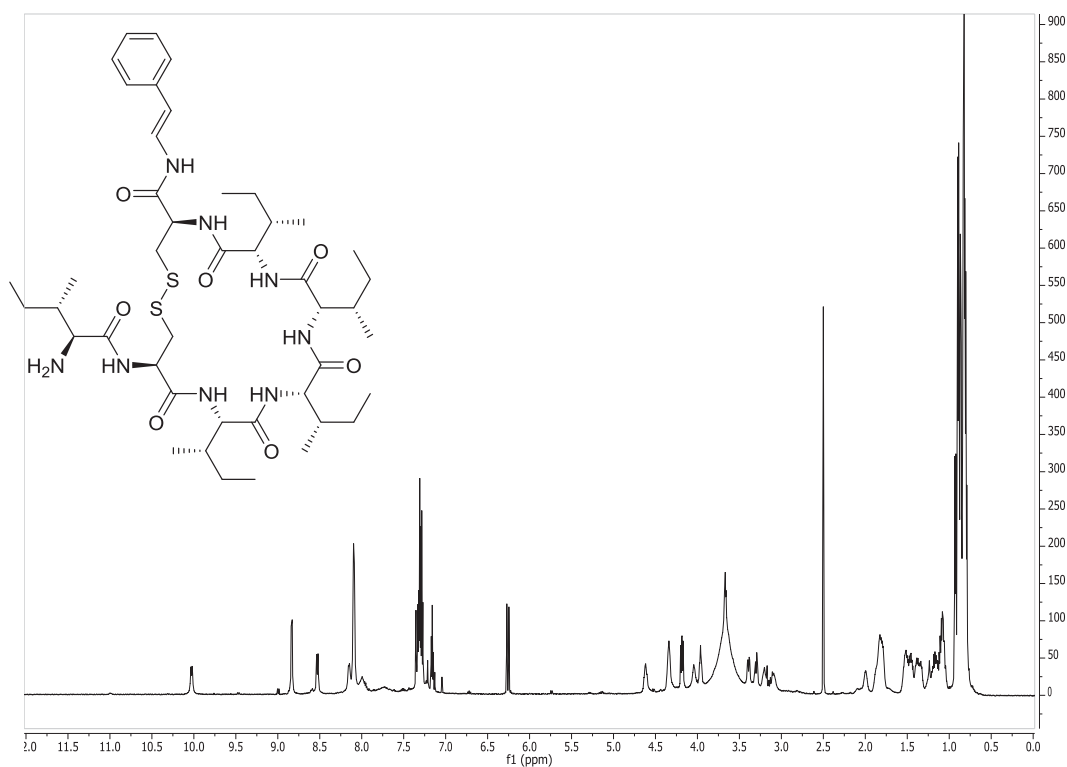
* Corresponding authors. Tel: ++492118114163. E-mail: georgios.daletos@uni-duesseldorf.de; proksch@uni-duesseldorf.de.

ACKNOWLEDGMENTS

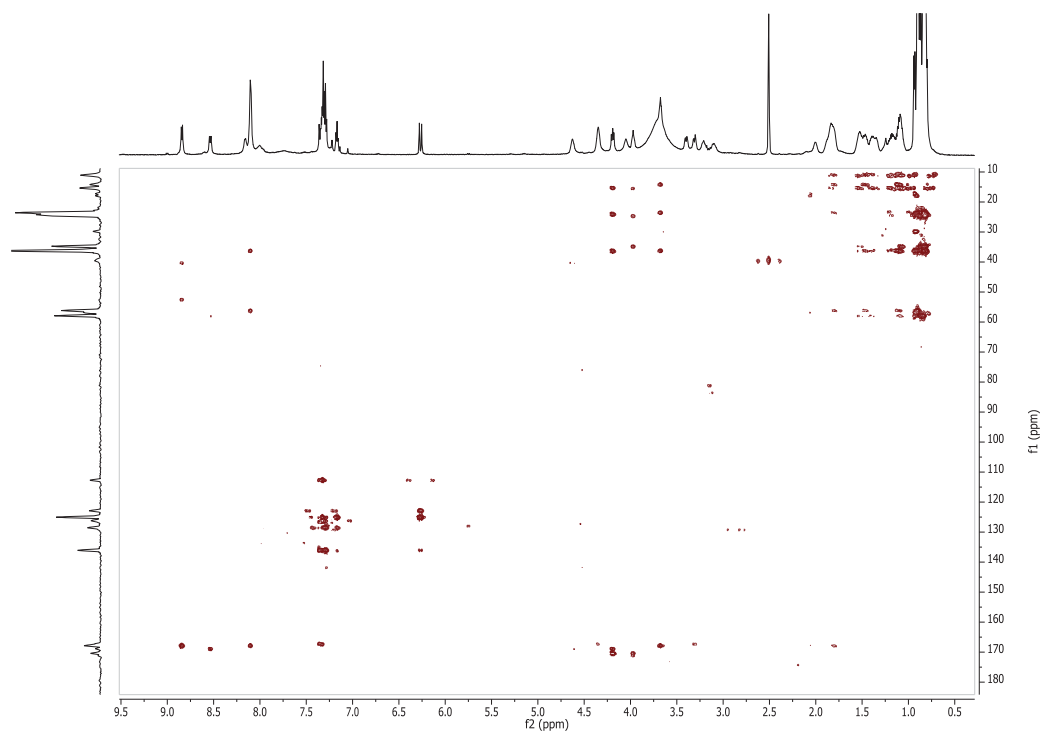
Support of this project to P.P., H.B.-O., M.K., R. K. and A.B. by the BMBF (project BALIPEND) and to K.W.W by the German Center for Infection Control is gratefully acknowledged. We thank Dr. N. de Voogd (Leiden, Naturalis Biodiversity Center, Leiden, Netherlands) for identification of the sponge. We appreciate the help of Prof. W. E. G. Müller (Johannes Gutenberg University, Mainz, Germany) for cytotoxicity assays with the L5178Y mouse lymphoma cell line. A. M. gratefully acknowledges the Ministry of Science, Research and Technology (MSRT) of Iran for awarding him a scholarship. We furthermore wish to acknowledge Ms. Okoniewski and Mr. Straetener for expert technical assistance. Support of this project to P.P., H.B.-O., M.K., R. K. and A. B. by the BMBF (project BALIPEND) and to K.W.W by the German Center for Infection Research is gratefully acknowledged. The authors wish to thank Dr. E. Ferdinandus (University Pattimura, Ambon, Indonesia) and Prof. Dr. S. Wiryowidagdo (University Hassanudin, Makassar, Indonesia) for their support and help during sponge collection.

5.3 Supporting Information

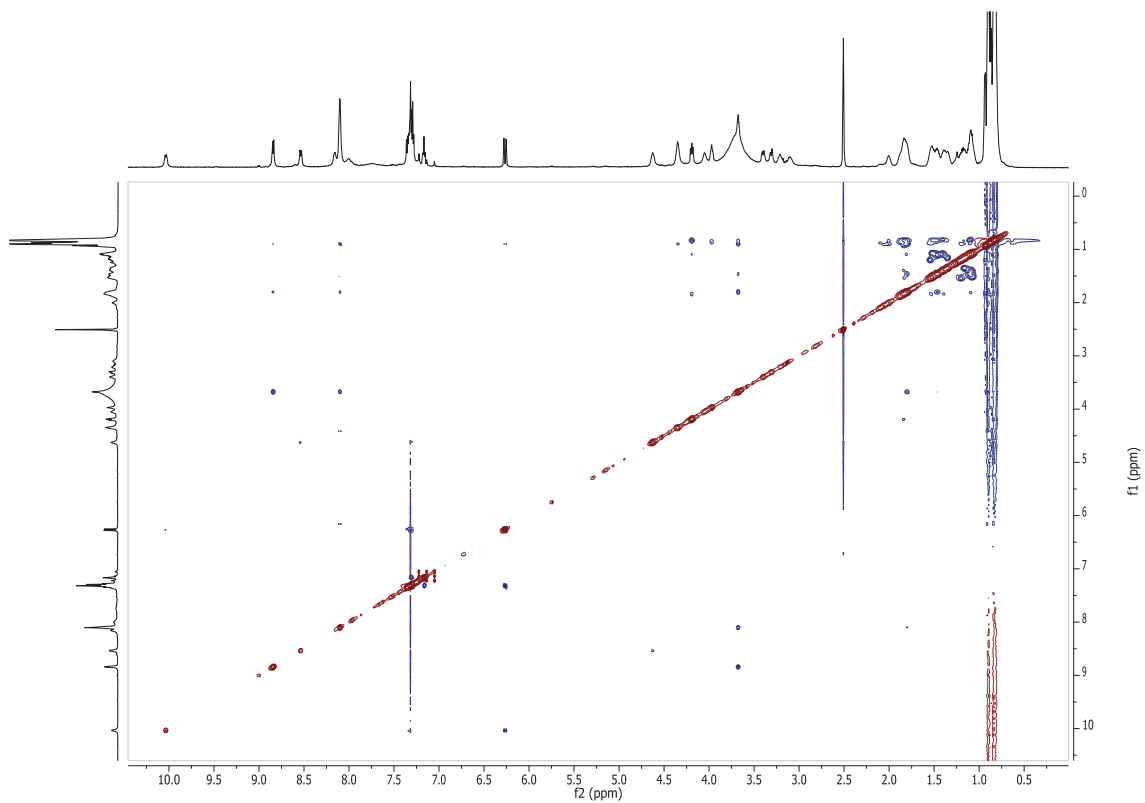
S1. Microcionamide C (1)



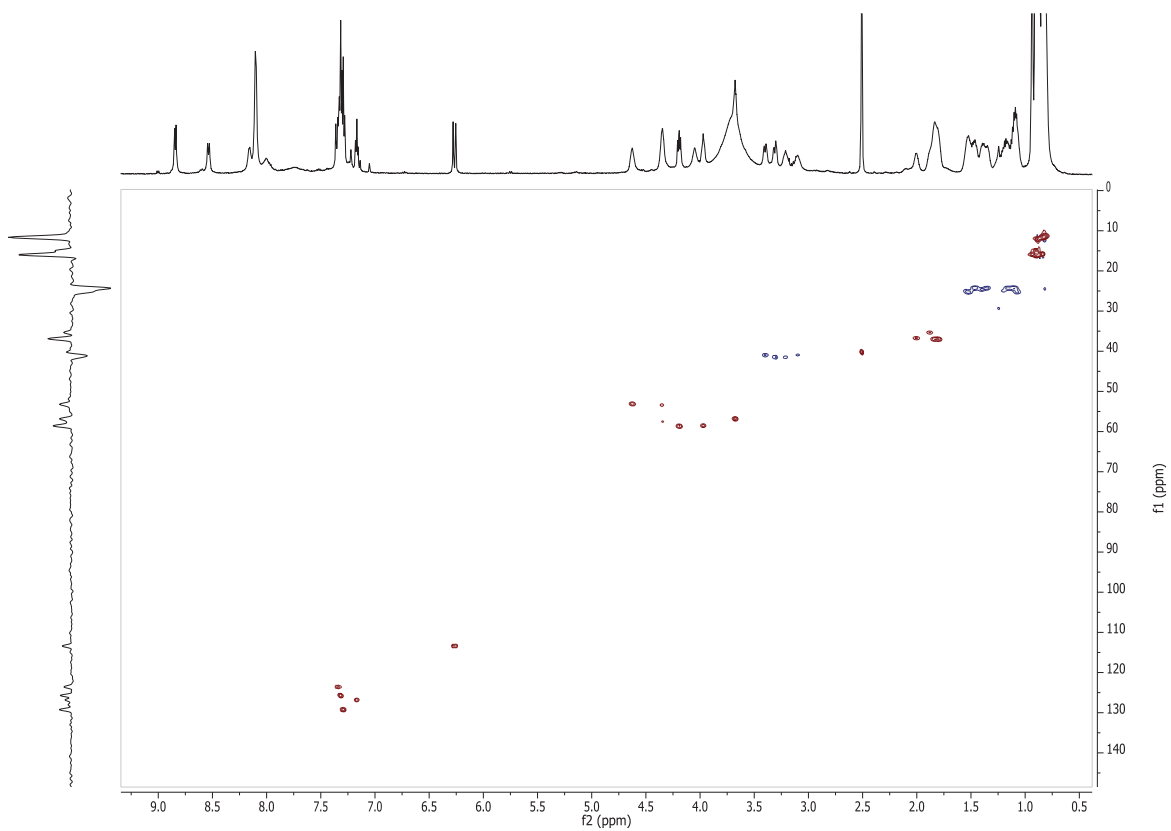
S1-1. ¹H NMR (DMSO-*d*₆, 600 MHz) spectrum of **1**



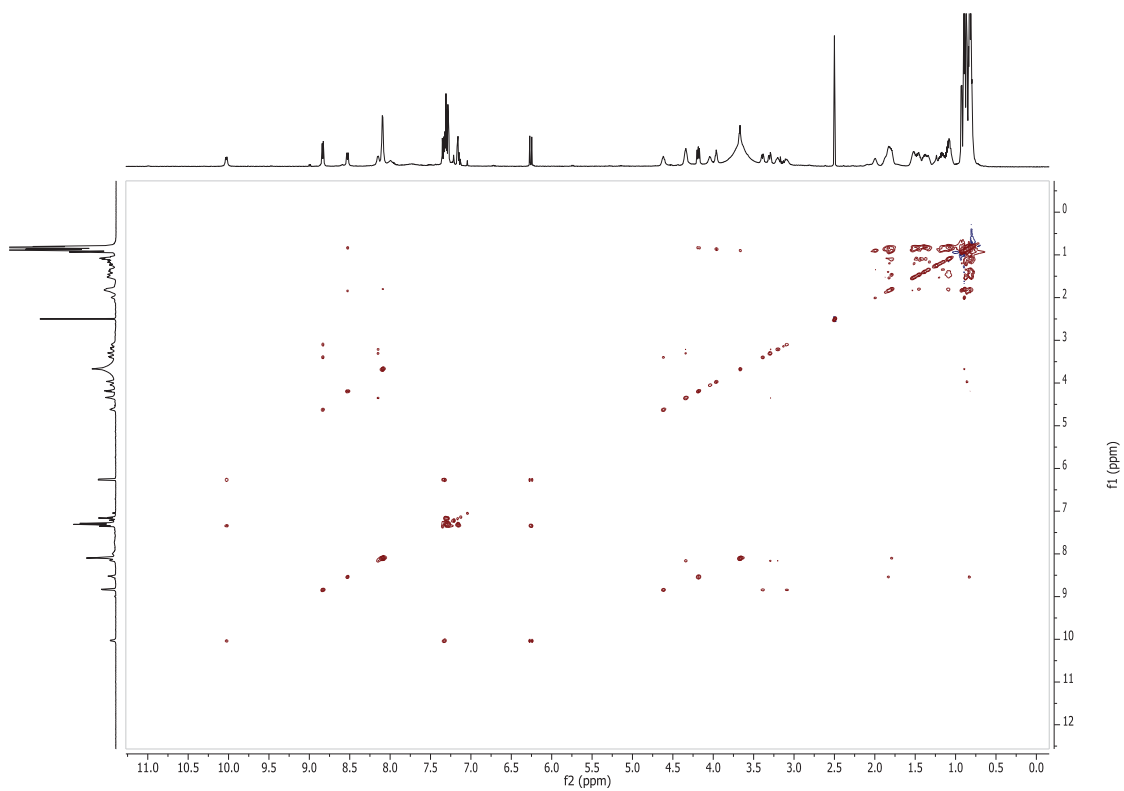
S1-2. HMBC NMR (DMSO-*d*₆, 600 MHz) spectrum of **1**



S1-3. ROESY NMR (DMSO- d_6 , 600 MHz) spectrum of **1**



S1-4. HSQC NMR (DMSO- d_6 , 600 MHz) spectrum of **1**



S1-5. TOCSY NMR (DMSO- d_6 , 600 MHz) spectrum of **1**

Mass Spectrum SmartFormula Report

Analysis Info

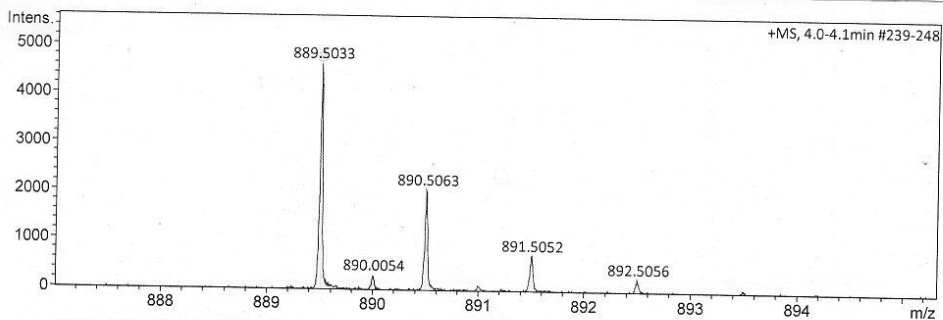
Analysis Name D:\Data\spektren2016\Proksch16HR000001.d
 Method tune_low_new.m
 Sample Name Amin Mokhesi CE1SiA1P2 (CH3OH)
 Comment 2 ug/ml

Acquisition Date 1/5/2016 2:58:54 PM

Operator Peter Tommes
 Instrument maXis 288882.20213

Acquisition Parameter

Source Type	ESI	Ion Polarity	Positive	Set Nebulizer	0.3 Bar
Focus	Not active	Set Capillary	4000 V	Set Dry Heater	180 °C
Scan Begin	50 m/z	Set End Plate Offset	-500 V	Set Dry Gas	4.0 l/min
Scan End	1500 m/z	Set Collision Cell RF	600.0 Vpp	Set Divert Valve	Source



Meas. m/z	#	Ion Formula	m/z	err [ppm]	mSigma	# mSigma	Score	rdb	e ⁻ Conf	N-Rule
889.5033	1	C43H77N4O11S2	889.5025	-1.0	49.2	1	100.00	7.5	even	ok
	2	C41H65N18OS2	889.5025	-1.0	53.6	2	86.79	18.5	even	ok
	3	C44H73N8O7S2	889.5038	0.5	57.3	3	95.07	12.5	even	ok
	4	C45H69N12O3S2	889.5052	2.0	66.4	4	31.39	17.5	even	ok
	5	C56H69N6S2	889.5020	-1.6	115.5	5	4.74	25.5	even	ok
	6	C60H73O2S2	889.5047	1.5	129.2	6	2.33	24.5	even	ok

S1-6. HRESIMS spectrum of 1

Mass Spectrum SmartFormula Report

Analysis Info

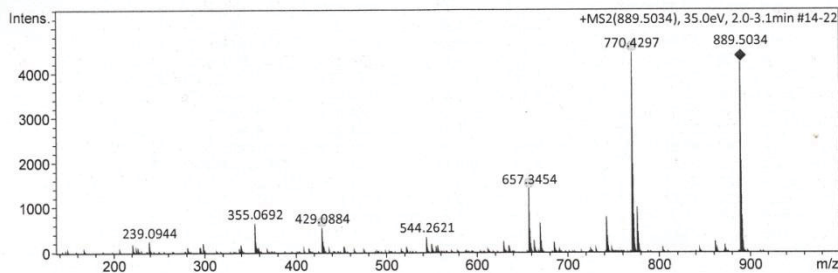
Analysis Name D:\Data\spektren2016\Proksch16HR000002.d
 Method tune_low_new.m
 Sample Name Amin Mokhesi CE1SiA1P2 (CH3OH)
 Comment 2 ug/ml

Acquisition Date 1/5/2016 3:04:23 PM

Operator Peter Tommes
 Instrument maXis 288882.20213

Acquisition Parameter

Source Type	ESI	Ion Polarity	Positive	Set Nebulizer	0.3 Bar
Focus	Not active	Set Capillary	4000 V	Set Dry Heater	180 °C
Scan Begin	50 m/z	Set End Plate Offset	-500 V	Set Dry Gas	4.0 l/min
Scan End	1500 m/z	Set Collision Cell RF	600.0 Vpp	Set Divert Valve	Source



Meas. m/z	#	Ion Formula	m/z	err [ppm]	mSigma	# mSigma	Score	rdb	e ⁻ Conf	N-Rule
657.3454	2	C30H52N6O6S2	657.3463	1.3	22.1	4	75.45	7.5	even	ok
770.4297	3	C36H64N7O7S2	770.4303	0.8	9.8	3	99.80	8.5	even	ok

S1-7. HRESIMS/MS spectrum of 1

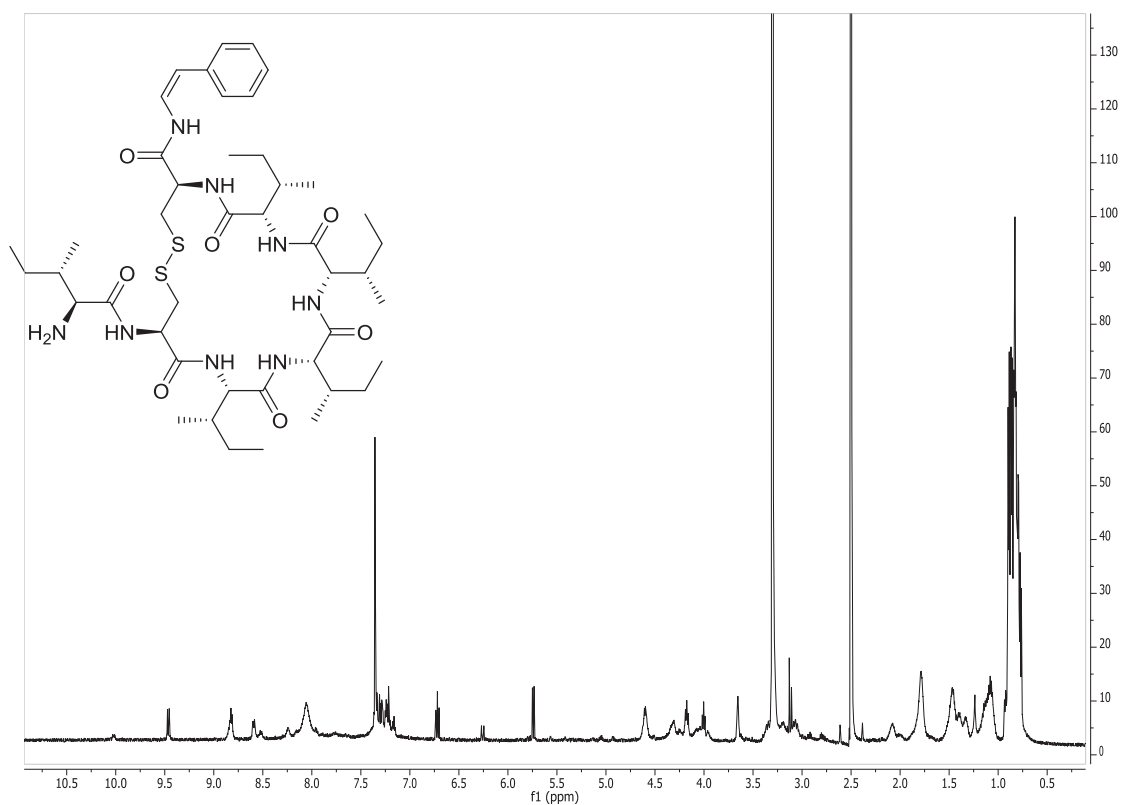
S2. Microcionamide D (2)

S2-1. Table of ^1H (600 MHz), ^{13}C (150 MHz), HMBC, and ROESY NMR Data (DMSO- d_6 , δ in ppm) of Microcionamide D (2)

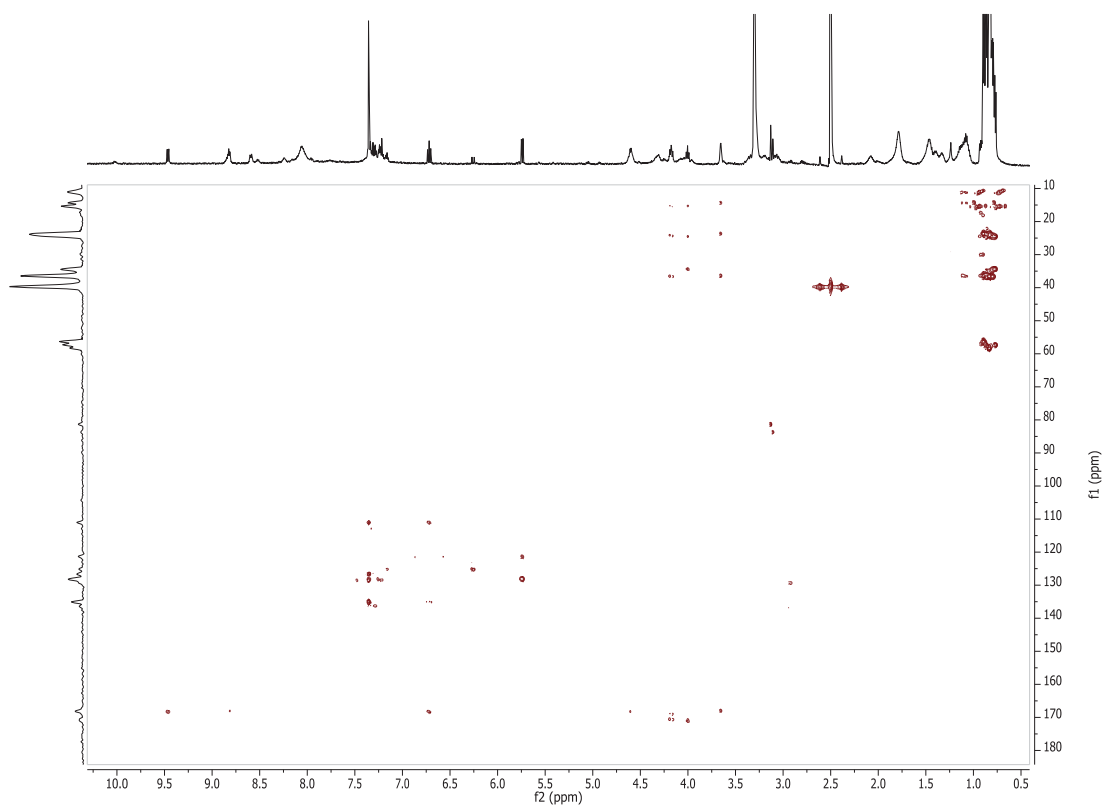
Unit	Position	δ_c , ^a type	δ_H (J in Hz)	HMBC	ROESY ^b
Z-PEA	NH		9.46, d (10.5)	Cys ₁ -CO	Cys ₁ - α , Cys ₁ -NH
	α	121.1, CH	6.72, d (10.0)	Cys ₁ -CO, Z-PEA- β , PEA-1	Z-PEA-1, Z-PEA-2/6
	β	110.8, CH	5.74, d (10.0)	Z-PEA- α , Z-PEA-1, PEA-2/6	
	aromatic	1: 134.7, C			
		2: 127.9, CH	7.35 ^c	Z-PEA- β , Z-PEA-1, PEA-6, Z-PEA-4	Z-PEA-1, Z-PEA-5, Z-PEA-4
		3: 128.3, CH	7.35 ^c	Z-PEA-1, Z-PEA-5, PEA-4	
		4: 126.4, CH	7.24, m	Z-PEA-2/6	
		5: 128.3, CH	7.35 ^c	Z-PEA-1, Z-PEA-3, PEA-4	
		6: 127.9, CH	7.35 ^c	Z-PEA- β , Z-PEA-1, PEA-2, Z-PEA-4	
Cys ₁	NH		8.24, br s		Z-PEA-NH, Ile ₂ - α
	CO	168.0, C			
	α	51.7, CH	4.62 ^c	Cys ₁ -CO, Ile ₂ -CO, Cys ₁ - β	Z-PEA-NH
	β	40.9, CH ₂	3.07, br t (11.0); 3.28 ^c	Cys ₁ - α , Cys ₁ -CO	
Ile ₂	NH		7.77, br s		
	CO	170.5, C			
	α	57.2, CH	4.01, br t (8.5)	Ile ₁ -CO, Ile ₃ -CO, Ile ₂ - β , Ile ₂ - γ , Ile ₂ - γ'	Cys ₁ -NH
	β	34.3, CH	1.77, m	Ile ₂ - α	
	γ	24.3, CH ₂	1.07, m; 1.48, m	Ile ₂ - α	
	γ'	15.1, CH ₃	0.78 ^c	Ile ₂ - α	
	δ	11.0, CH ₃	0.81 ^{c,d}		
Ile ₃	NH		n.d. ^e		
	CO	170.9			
	α	n.d. ^e	4.08 ^c		
	β	36.4, CH	1.79, m		
	γ	24.4, CH ₂	1.07, m; 1.51, m		
	γ'	15.2, CH ₃	0.89 ^c		
	δ	11.0, CH ₃	0.83 ^{c,d}		

Ile ₄	NH		7.39 ^c		
	CO	n.d. ^e			
	α	57.0, CH	4.31, br s		Ile ₅ - β
	β	35.9, CH	2.08, br s		
	γ	23.5, CH ₂	1.16, m; 1.33, m		
	γ'	15.6, CH ₃	0.87 ^c		
	δ	11.1, CH ₃	0.86 ^{c,d}		
Ile ₅	NH		8.59, d (9.3)	Cys ₆ -CO	Cys ₆ - α
	CO	170.4, C			
	α	58.0, CH	4.17 ^c	Ile ₅ -CO, Cys ₆ -CO, Ile ₅ - β , Ile ₅ - γ , Ile ₅ - γ'	Cys ₆ - α
	β	36.4, CH	1.80, m	Ile ₅ - α	Ile ₄ - α , Cys ₆ -NH, Cys ₆ - α
	γ	24.3, CH ₂	1.08, m; 1.41, m	Ile ₅ - α	
	γ'	15.2, CH ₃	0.84 ^c	Ile ₅ - α	
	δ	10.9, CH ₃	0.80 ^{c,d}		
Cys ₆	NH		8.82, br d (7.0)	Ile ₇ -CO	Ile ₇ - α , Ile ₇ - β , Ile ₇ - γ , Ile ₅ - β
	CO	168.6, C			
	α	52.5, CH	4.61 ^c	Ile ₅ -CO	Ile ₅ -NH, Ile ₇ - α , Ile ₅ - α
	β	40.2, CH ₂	3.19, m; 3.35, m		
Ile ₇	NH ₂		8.06, br s		
	CO	167.8, C			
	α	56.1, CH	3.66, br t (5.0)	Ile ₇ -CO, Ile ₇ - β , Ile ₇ - γ , Ile ₇ - γ'	Cys ₆ - α , Cys ₆ -NH
	β	36.2, CH	1.79, m	Ile ₇ - α	Cys ₆ -NH
	γ	23.4, CH ₂	1.10, m; 1.46, m	Ile ₇ - α	Cys ₆ -NH
	γ'	14.2, CH ₃	0.89 ^c	Ile ₇ - α	
	δ	10.8, CH ₃	0.83 ^{c,d}		

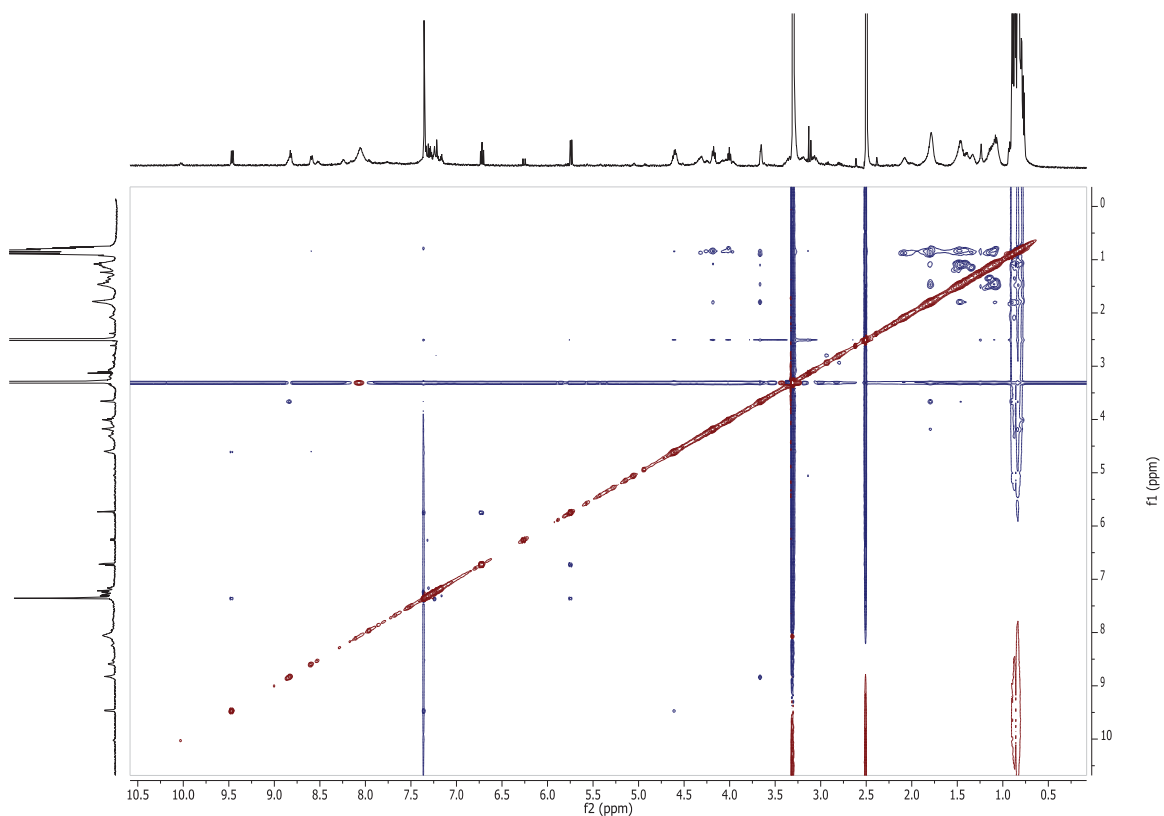
^aData extracted from HSQC and HMBC spectra. ^bSequential NOEs. ^cSignal overlap prevents determination of couplings. ^dAssignments within the same column may be interchanged. ^en.d. : not detected



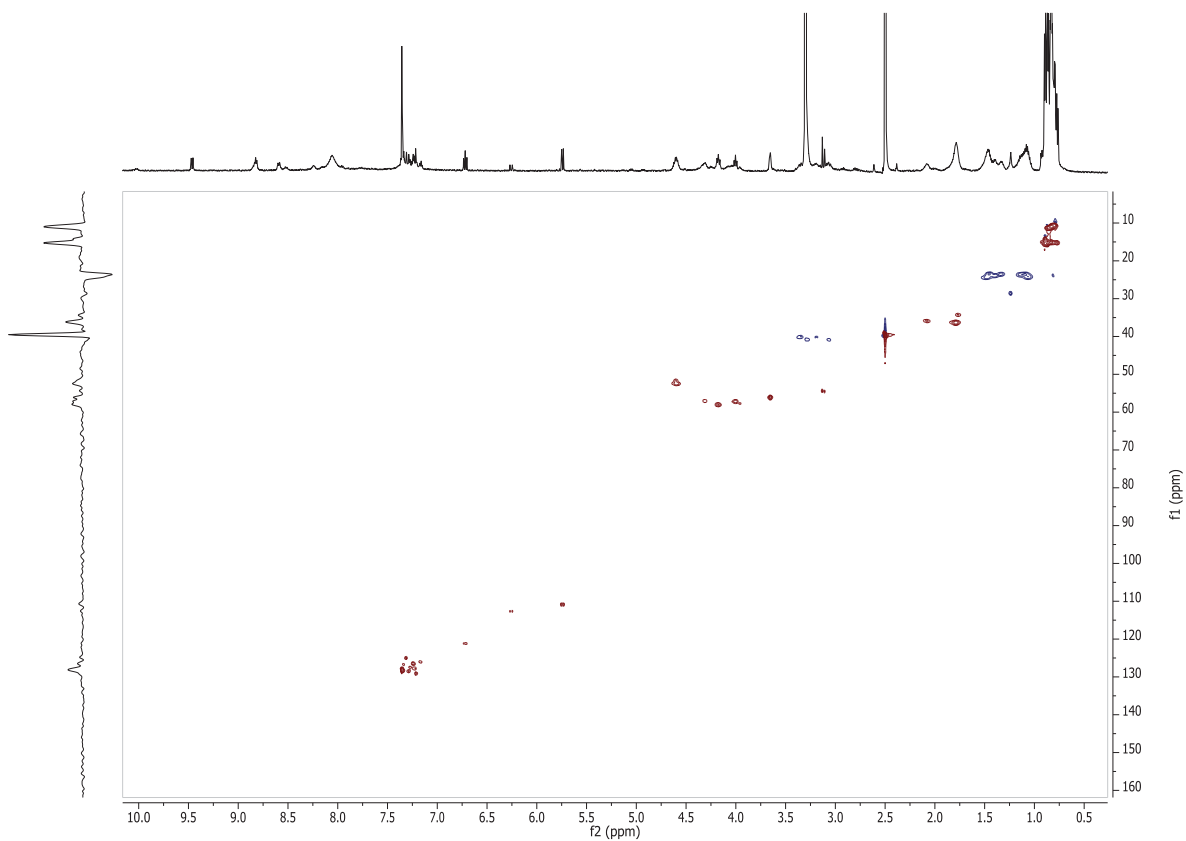
S2-2. ^1H NMR (DMSO- d_6 , 600 MHz) spectrum of **2**



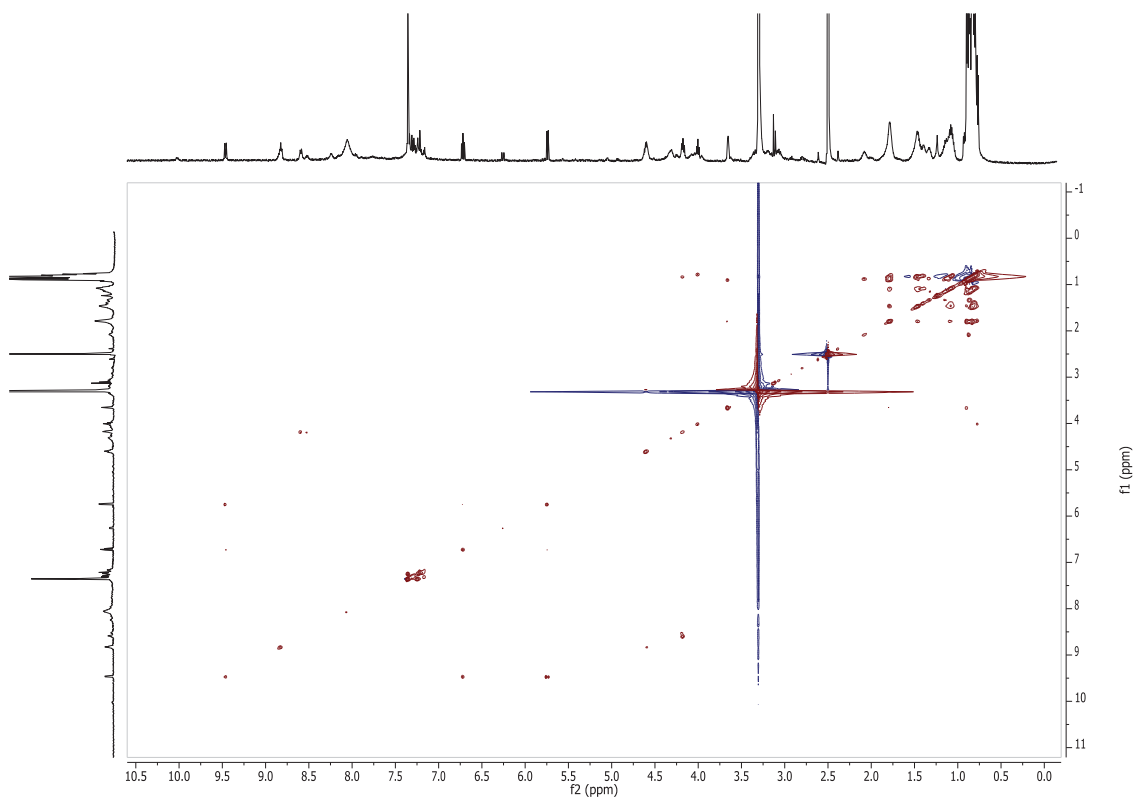
S2-3. HMBC NMR (DMSO- d_6 , 600 MHz) spectrum of **2**



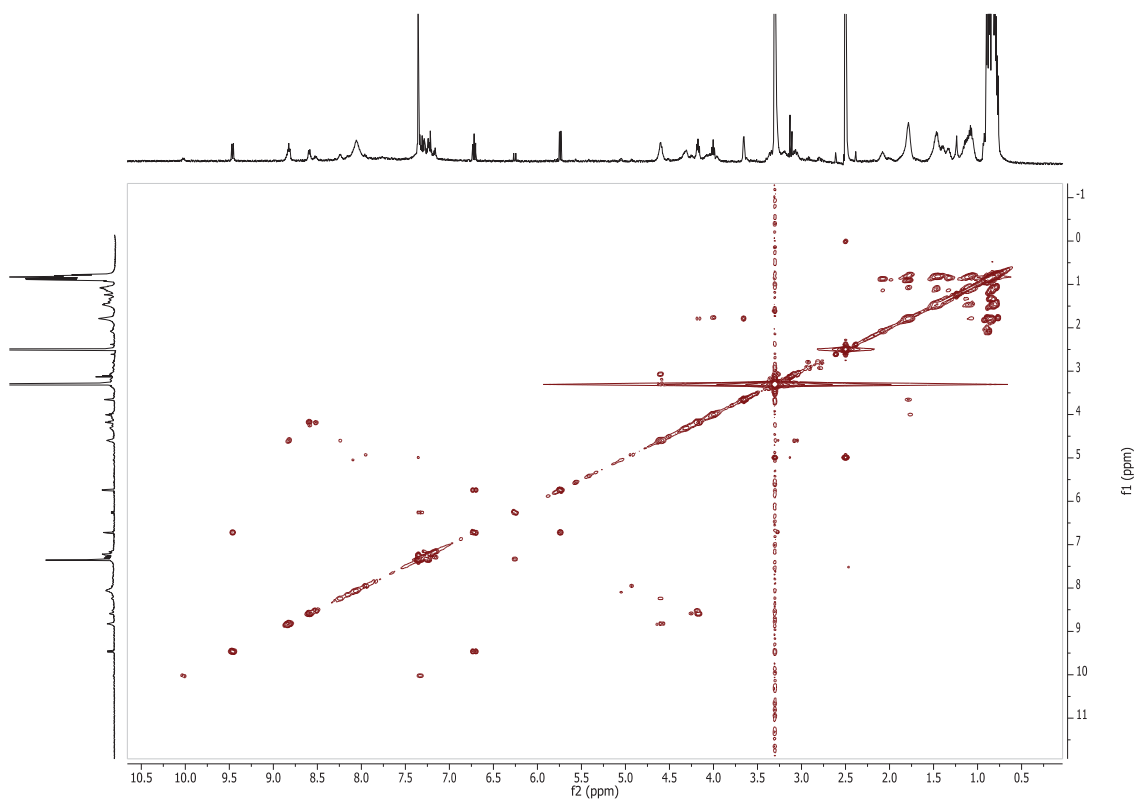
S2-4. ROESY NMR (DMSO-d₆, 600 MHz) spectrum of 2



S2-5. HSQC NMR (DMSO-d₆, 600 MHz) spectrum of 2



S2-6. TOCSY NMR (DMSO-d₆, 600 MHz) spectrum of 2



S2-7. COSY NMR (DMSO-d₆, 600 MHz) spectrum of 2

Mass Spectrum SmartFormula Report

Analysis Info

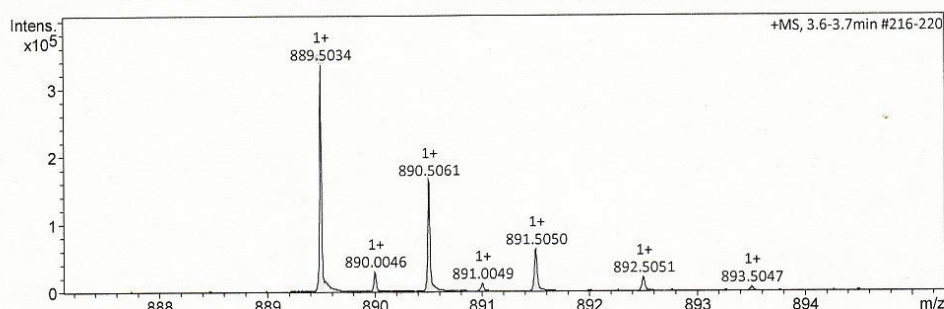
Analysis Name D:\Data\spektren2016\Proksch16HR000193.d
 Method tune_low_new.m
 Sample Name Amin Mokhlesi CE1 RP100b P6 (CH3OH)
 Comment

Acquisition Date 7/21/2016 9:27:49 AM

Operator Peter Tommes
 Instrument maXis 288882.20213

Acquisition Parameter

Source Type	ESI	Ion Polarity	Positive	Set Nebulizer	0.3 Bar
Focus	Not active	Set Capillary	4000 V	Set Dry Heater	180 °C
Scan Begin	50 m/z	Set End Plate Offset	-500 V	Set Dry Gas	4.0 l/min
Scan End	1500 m/z	Set Collision Cell RF	600.0 Vpp	Set Divert Valve	Source



Meas. m/z	#	Ion Formula	m/z	err [ppm]	mSigma	# mSigma	Score	rdb	e ⁻ Conf	N-Rule
889.5034	1	C43H77N4O11S2	889.5025	-1.0	25.9	1	89.32	7.5	even	ok
	2	C41H65N18O8S2	889.5025	-1.1	28.2	2	84.28	18.5	even	ok
	3	C44H73N8O7S2	889.5038	0.5	32.5	3	100.00	12.5	even	ok
	4	C45H69N12O3S2	889.5052	2.0	40.9	4	36.59	17.5	even	ok
	5	C56H69N6S2	889.5020	-1.6	89.9	5	7.83	25.5	even	ok
	6	C60H73O2S2	889.5047	1.4	103.7	6	4.71	24.5	even	ok

S2-8. HRESIMS spectrum of 2

Mass Spectrum SmartFormula Report

Analysis Info

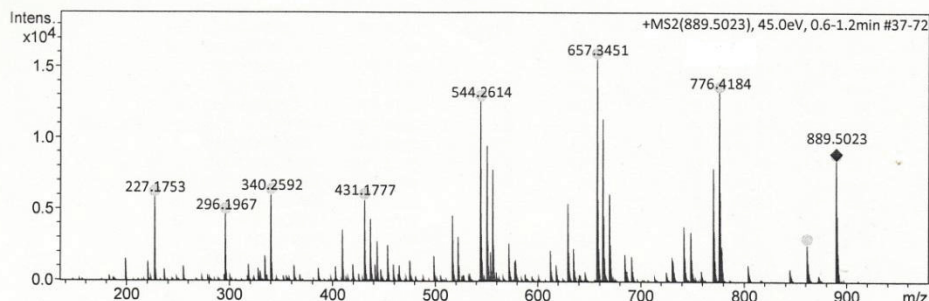
Analysis Name D:\Data\spektren2016\Proksch16HR000194.d
 Method tune_low_new.m
 Sample Name Amin Mokhlesi CE1 RP100b P6 (CH3OH)
 Comment

Acquisition Date 7/21/2016 9:31:55 AM

Operator Peter Tommes
 Instrument maXis 288882.20213

Acquisition Parameter

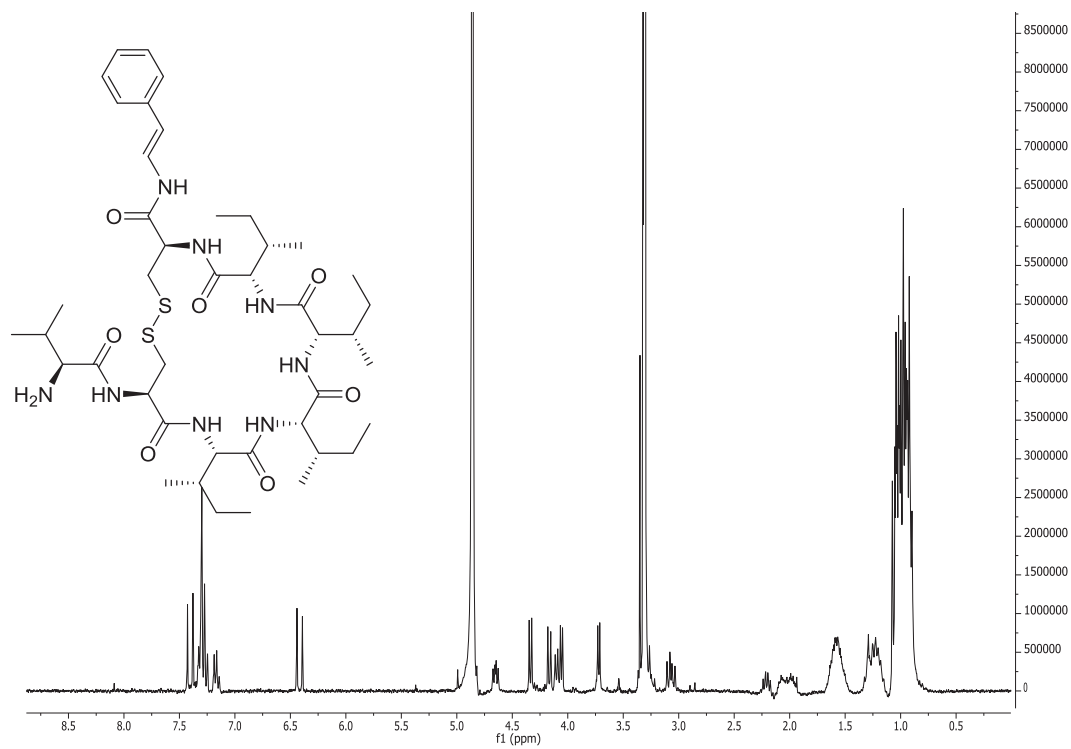
Source Type	ESI	Ion Polarity	Positive	Set Nebulizer	0.3 Bar
Focus	Not active	Set Capillary	4000 V	Set Dry Heater	180 °C
Scan Begin	50 m/z	Set End Plate Offset	-500 V	Set Dry Gas	4.0 l/min
Scan End	1500 m/z	Set Collision Cell RF	600.0 Vpp	Set Divert Valve	Source



Meas. m/z	#	Ion Formula	m/z	err [ppm]	mSigma	# mSigma	Score	rdb	e ⁻ Conf	N-Rule
657.3451	2	C30H52N6O6S2	657.3451	1.8	9.3	4	54.33	7.5	even	ok
770.4294	3	C36H64N7O7S2	770.4294	0.8	9.8	3	99.80	8.5	even	ok
776.4184	4	C38H60N7O6S2	776.4184	1.7	12.5	4	55.23	11.5	even	ok

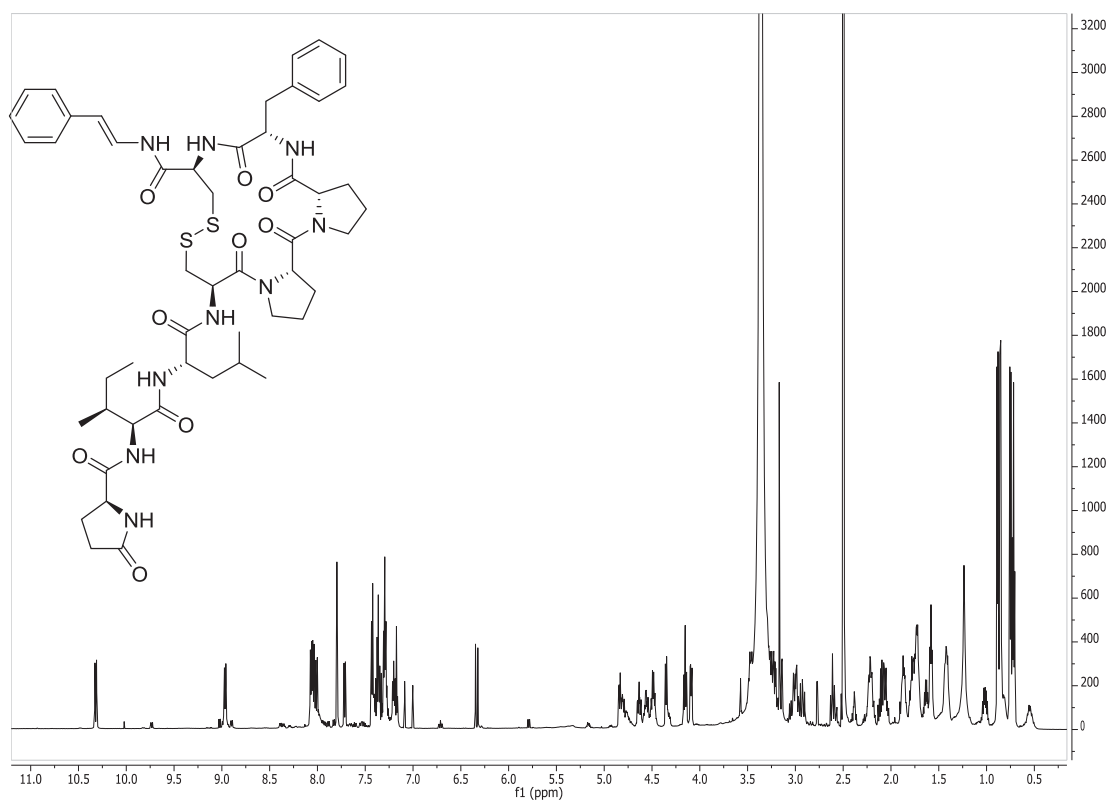
S2-9. HRESIMS/MS spectrum of 2

S3. Microcionamide A (3)

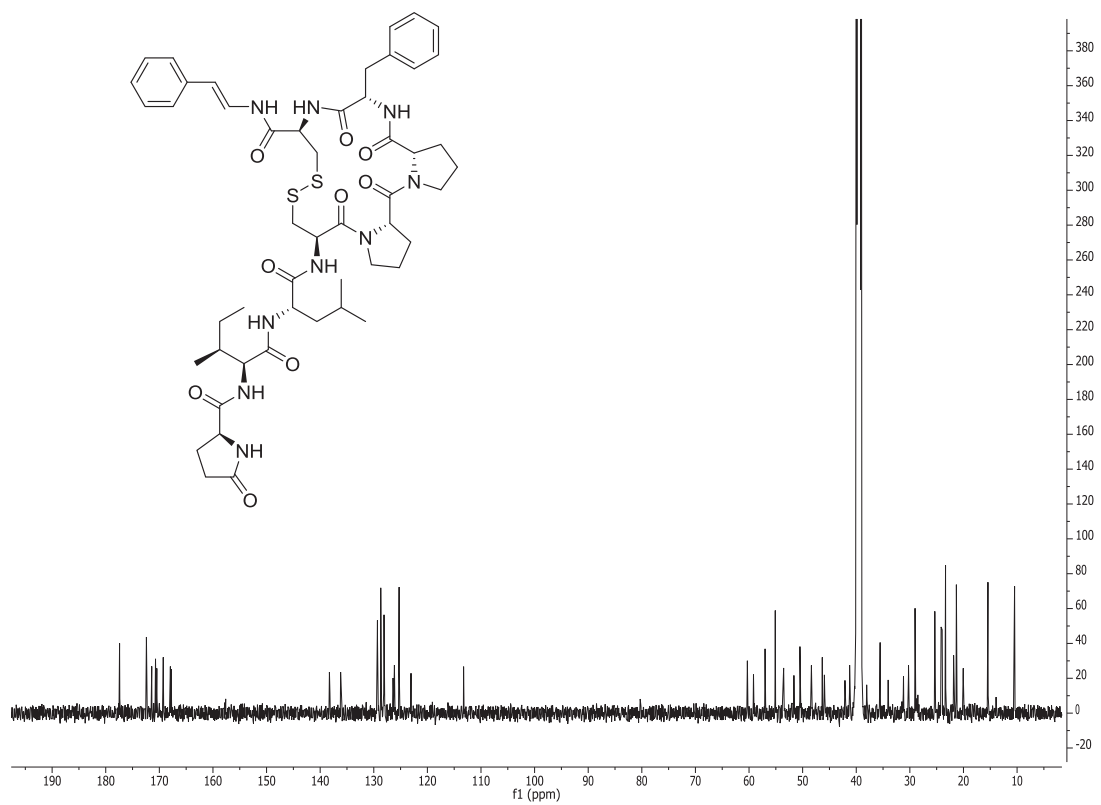


S3-1. ¹H NMR (MeOH-d₄, 600 MHz) spectrum of 3

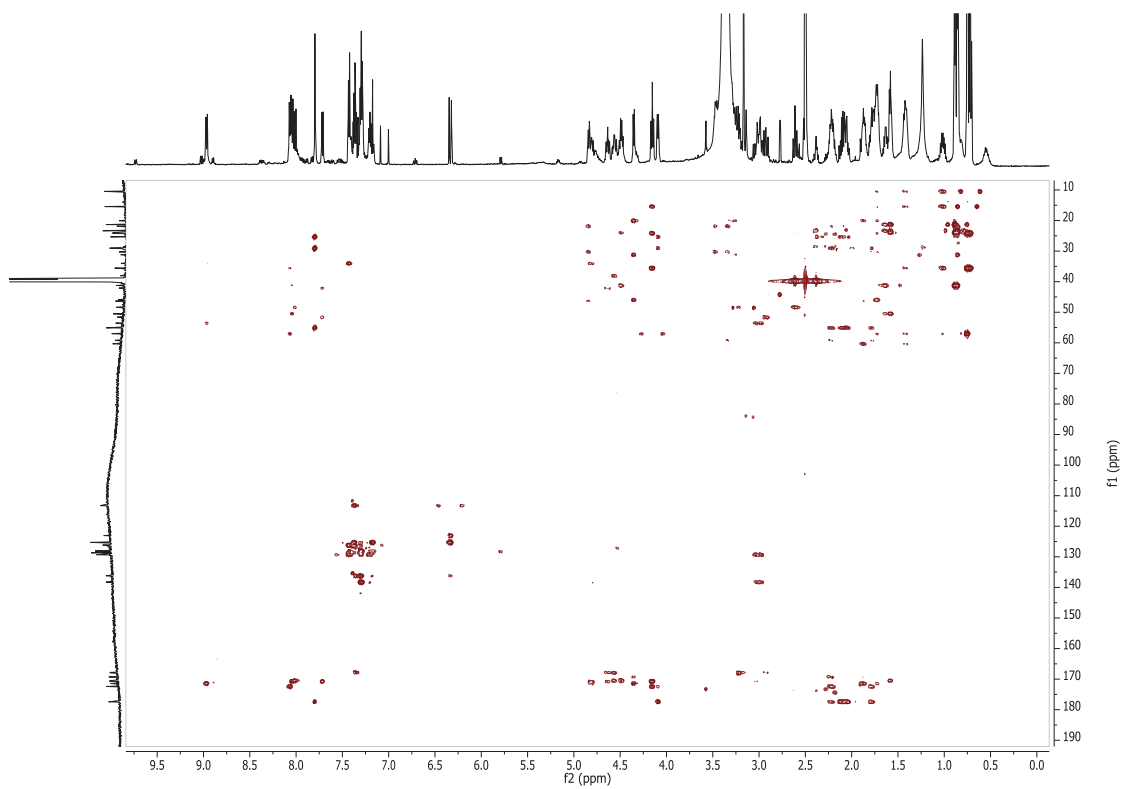
S4. Gombamide B (4)



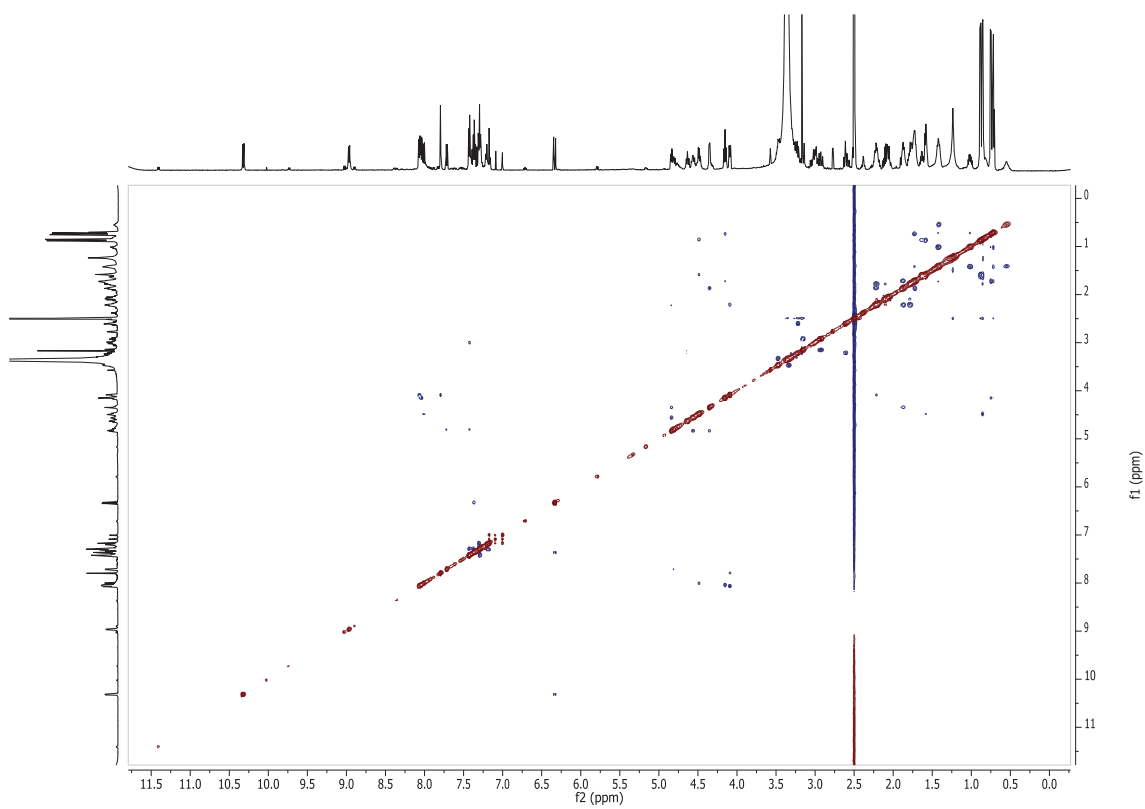
S4-1. ¹H NMR (DMSO-d₆, 600 MHz) spectrum of 4



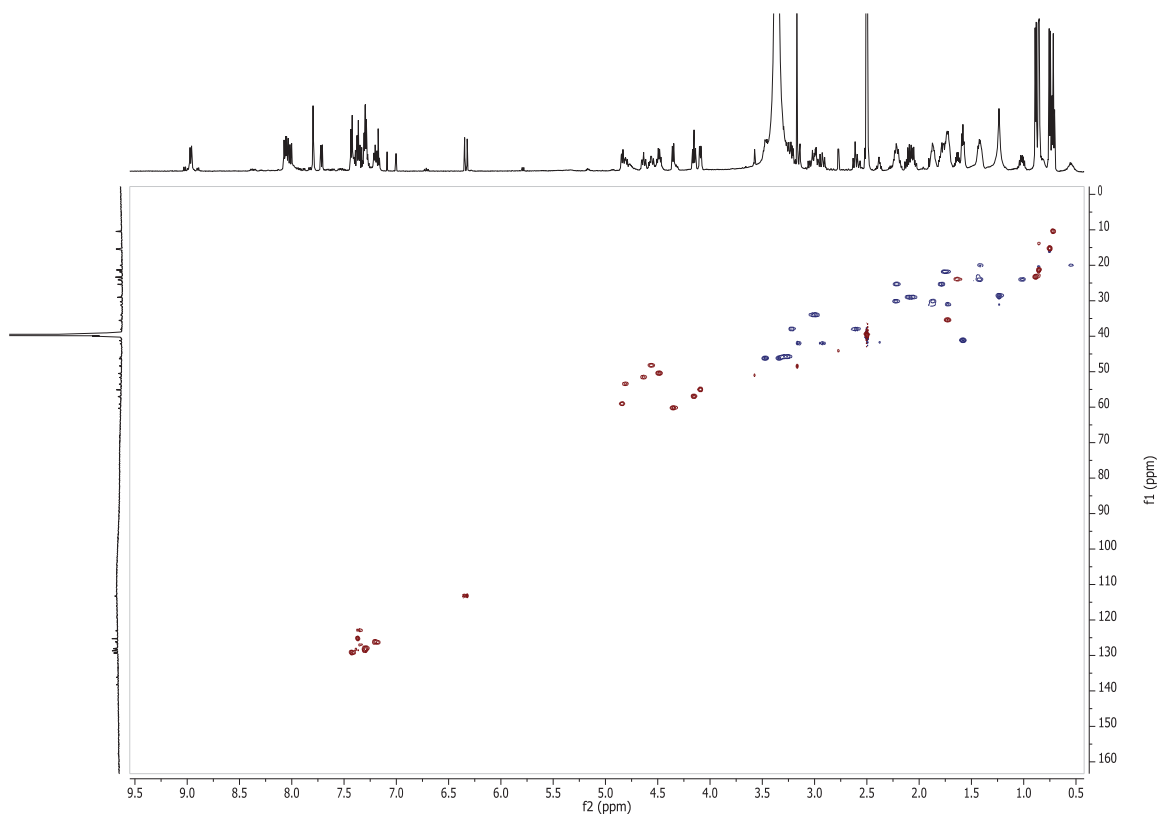
S4-2. ¹³C NMR (DMSO-d₆, 600 MHz) spectrum of 4



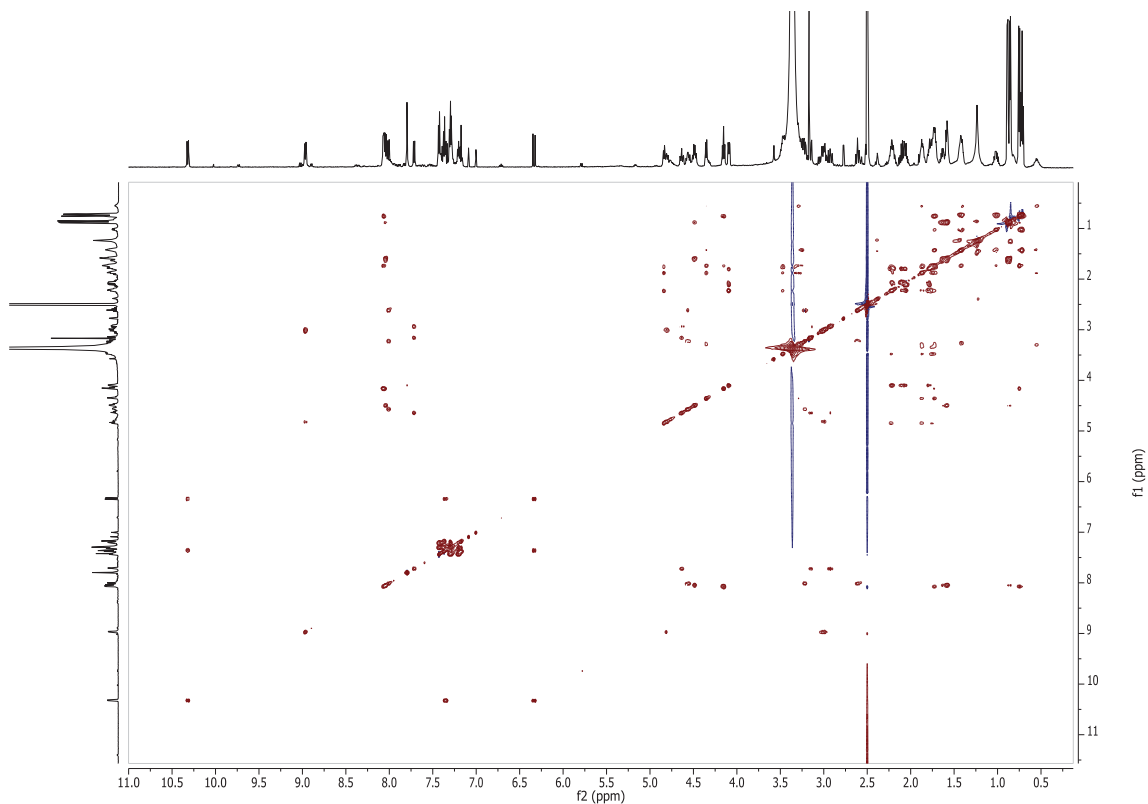
S4-3. HMBC NMR (DMSO-d₆, 600 MHz) spectrum of 4



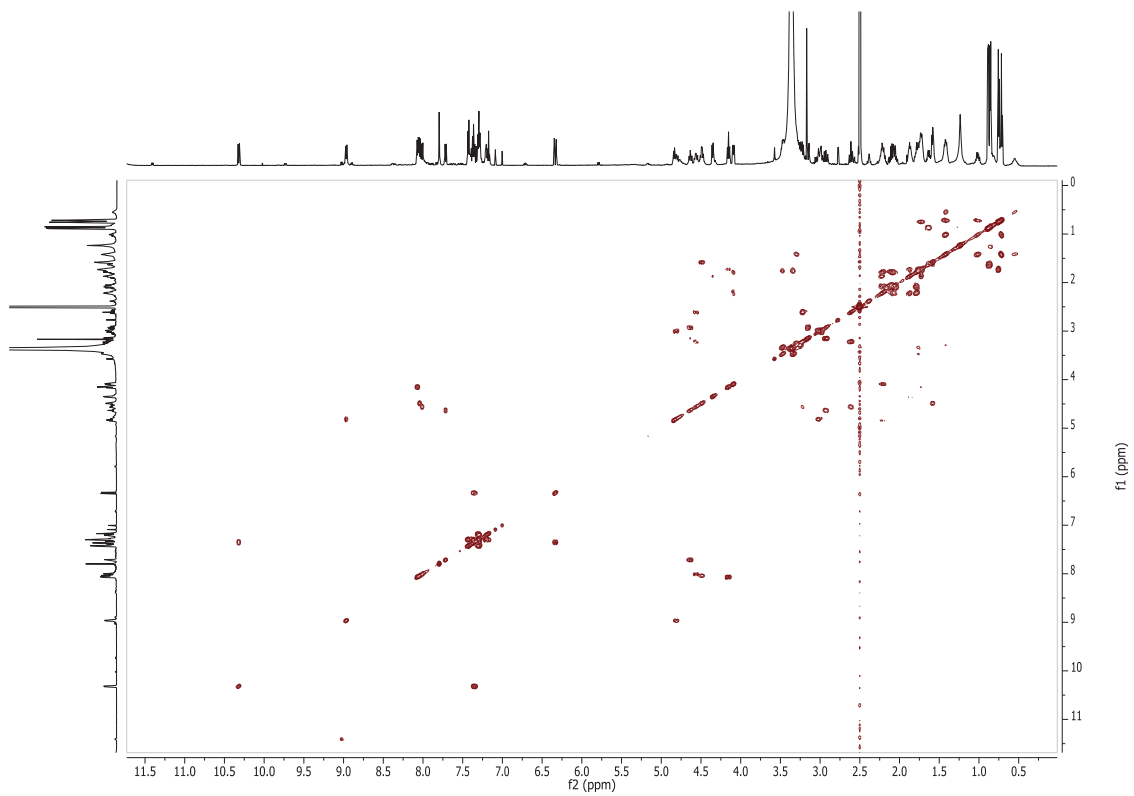
S4-4. ROESY NMR (DMSO-d₆, 600 MHz) spectrum of 4



S4-5. HSQC NMR (DMSO-d₆, 600 MHz) spectrum of 4



S4-6. TOCSY NMR (DMSO-d₆, 600 MHz) spectrum of 4

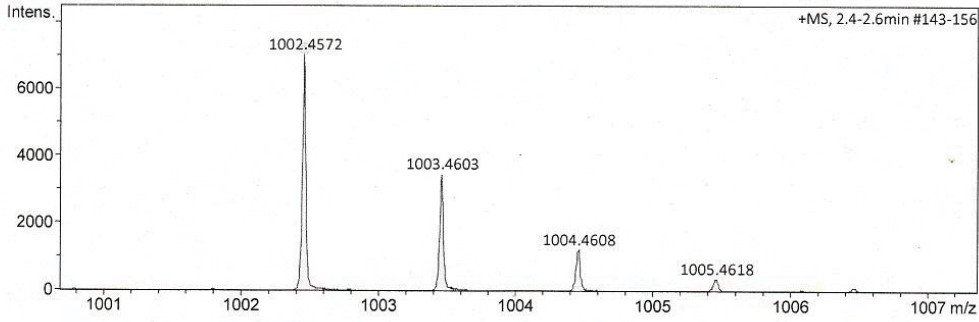


S4-7. COSY NMR (DMSO-d₆, 600 MHz) spectrum of 4

Mass Spectrum SmartFormula Report

Analysis Info		Acquisition Date	1/8/2016 9:34:08 AM	
Analysis Name	D:\Data\spektren2016\Proksch16HR000010.d	Operator	Peter Tommes	
Method	tune_low_new.m	Instrument	maXis	288882.20213
Sample Name	Amin Mokhlesi CE2RP70P1 (CH3OH)	Comment		
Comment	2 ug/ml			

Acquisition Parameter					
Source Type	ESI	Ion Polarity	Positive	Set Nebulizer	0.3 Bar
Focus	Not active	Set Capillary	4000 V	Set Dry Heater	180 °C
Scan Begin	50 m/z	Set End Plate Offset	-500 V	Set Dry Gas	4.0 l/min
Scan End	1500 m/z	Set Collision Cell RF	600.0 Vpp	Set Divert Valve	Source



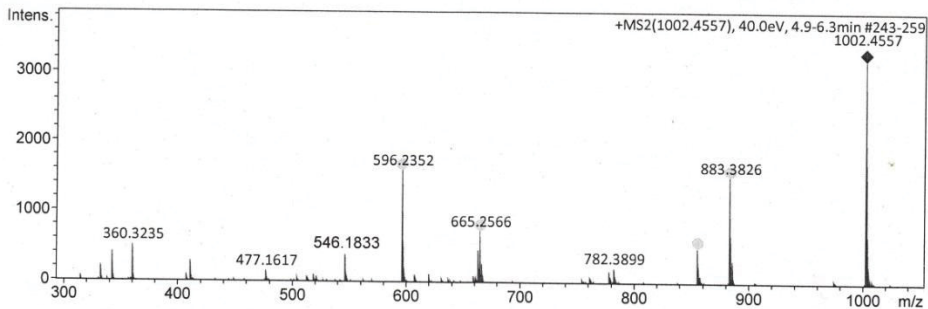
Meas. m/z	#	Ion Formula	m/z	err [ppm]	mSigma	# mSigma	Score	rdB	e ⁻ Conf	N-Rule
1002.4572	1	C49H72N5O13S2	1002.4563	-0.9	65.7	1	100.00	16.5	even	ok
	2	C47H60N19O3S2	1002.4562	-0.9	69.7	2	85.93	27.5	even	ok
	3	C50H68N9O9S2	1002.4576	0.4	74.1	3	95.65	21.5	even	ok
	4	C51H64N13O5S2	1002.4589	1.7	83.1	4	30.36	26.5	even	ok
	5	C62H64N7O2S2	1002.4557	-1.4	134.0	5	2.86	34.5	even	ok
	6	C66H68NO4S2	1002.4584	1.2	135.6	6	3.52	33.5	even	ok

S4-8. HRESIMS spectrum of 4

Mass Spectrum SmartFormula Report

Analysis Info		Acquisition Date	1/19/2016 2:17:52 PM	
Analysis Name	D:\Data\spektren2016\Proksch16HR000029.d	Operator	Peter Tommes	
Method	tune_low_new.m	Instrument	maXis	288882.20213
Sample Name	Amin Mokhlesi CE2RP75P2 (CH3OH)	Comment		
Comment	2 ug/ml			

Acquisition Parameter					
Source Type	ESI	Ion Polarity	Positive	Set Nebulizer	0.3 Bar
Focus	Not active	Set Capillary	4000 V	Set Dry Heater	180 °C
Scan Begin	50 m/z	Set End Plate Offset	-500 V	Set Dry Gas	4.0 l/min
Scan End	1500 m/z	Set Collision Cell RF	600.0 Vpp	Set Divert Valve	Source



Meas. m/z	#	Ion Formula	m/z	err [ppm]	mSigma	# mSigma	Score	rdB	e ⁻ Conf	N-Rule
546.1833	2	C25H32N5O5S2	546.1833	1.2	68.7	10	30.45	12.5	even	ok
665.2566	3	C33H41N6O5S2	665.2566	1.2	85.3	15	21.60	16.5	even	ok
883.3826	4	C42H59N8O9S2	883.3826	1.7	47.2	25	28.11	17.5	even	ok

S4-9. HRESIMS/MS spectrum of 4

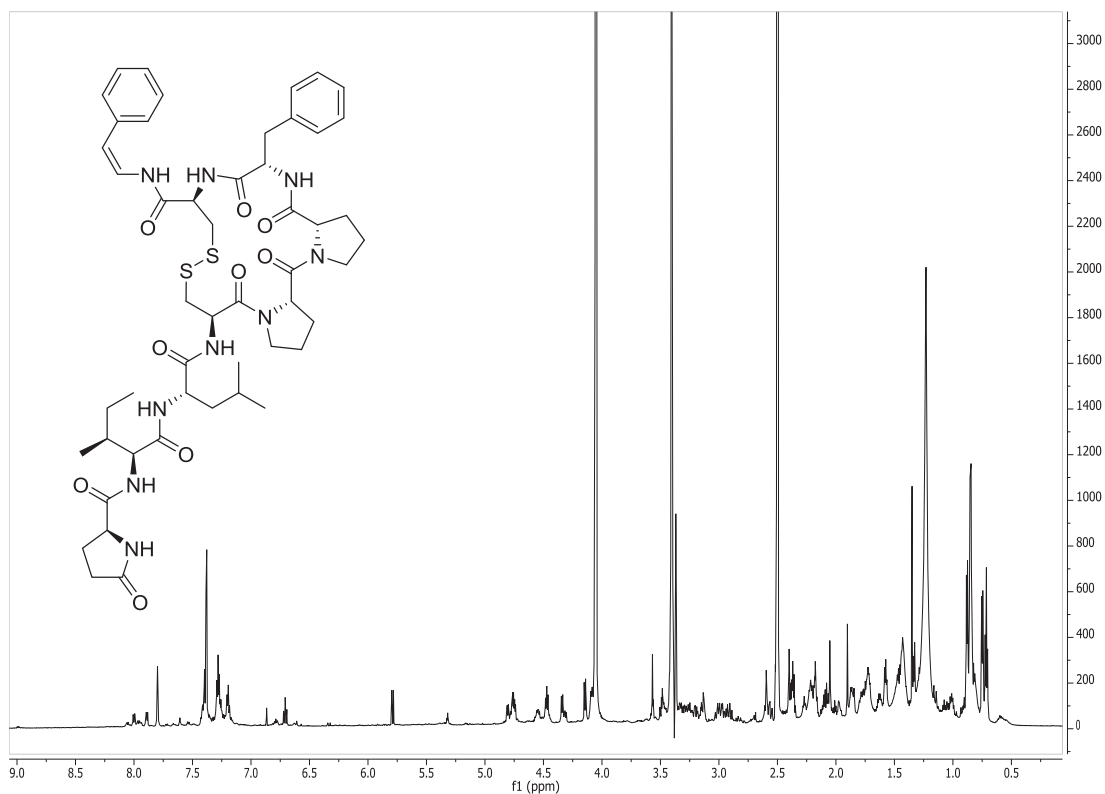
S5. Gombamide C (5)

S5-1. Table of ¹H (600 MHz), ¹³C (150 MHz), and HMBC NMR Data (DMSO-d₆, δ in ppm) of Gombamide C (5)

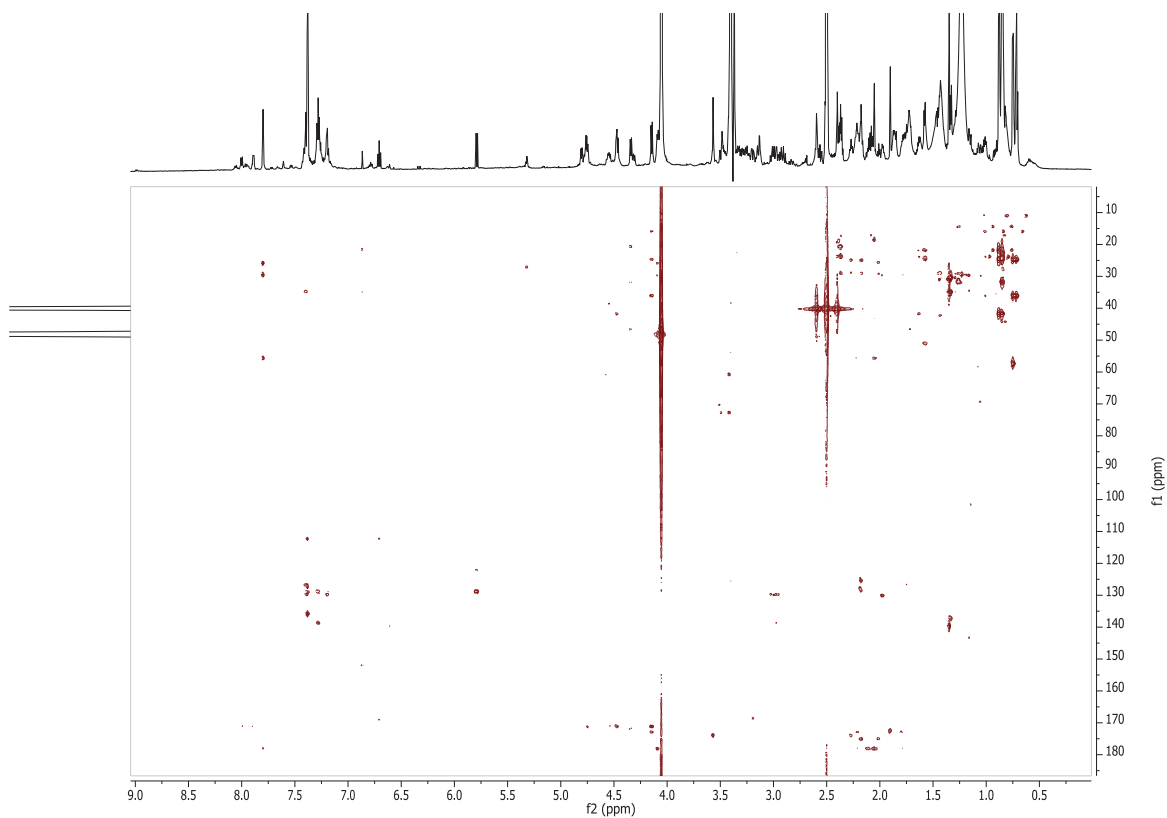
Unit	Position	δ _c , a type	δ _H (J in Hz)	HMBC
Cys1	NH		7.89, br d (8.6)	Phe-CO
	CO	168.4, C		
	α	51.5, CH	4.76b	
Z- PEA	β	41.7, CH ₂	2.91, dd (14.4, 12.4); 3.14, dd (14.4, 3.4)	Cys1-CO Cys1-CO, Z-PEA-β Z-PEA-α, Z-PEA-2/6, Z- PEA-1
	NH		9.72, br d (10.1)	
	α	121.3, CH	6.71, dd (10.1, 9.7)	
	β	111.6, CH	5.79, d (9.7)	
	aromatic	1: 135.2, C		
		2: 128.1, CH	7.38b	
		3: 128.4, CH	7.38b	
	4: 126.6, CH	7.38b		
	5: 128.4, CH	7.38b		
	6: 128.1, CH	7.38b		
Phe	NH		9.00, br d (8.8)	Phe-CO, Phe-β, Pro3-CO Phe-α, Phe-1, Phe-2/6 Phe-β, Phe-6, Phe-4 Phe-1, Phe-5 Phe-2/6 Phe-1, Phe-3 Phe-β, Phe-6, Phe-4
	CO	170.5, C		
	α	53.4, CH	4.75b	
	β	34.1, CH ₂	2.98, m	
	aromatic	1: 138.0, C		
		2: 129.1, CH	7.40, br d (7.5)	
		3: 128.0, CH	7.28, br t (7.5)	
		4: 126.1, CH	7.19, br t (7.5)	
	5: 128.0, CH	7.28, br t (7.5)		
	6: 129.1, CH	7.40, br d (7.5)		
Pro3	CO	171.2, C		Pro3-CO, Pro4-CO, Pro3-β, Pro3-γ, Pro3-δ
	α	60.7, CH	4.34, d (8.0)	
	β	31.1, CH ₂	1.72, m; 1.87, m	
	γ	20.0, CH ₂	1.42, m; 0.58, m	
	δ	45.9, CH ₂	3.28, m	
Pro4	CO	169.2, C		Pro4-γ
	α	59.0, CH	4.80, dd (8.8, 3.0)	
	β	30.1, CH ₂	1.86, m; 2.22, m	

Cys5	γ	21.6, CH2	1.74, m	Leu-CO
	δ	46.7, CH2	3.34, m; 3.47, m	
	NH		8.00, br d (10.0)	
	CO	167.9, C		
	α	48.1, CH	4.55, td (10.0, 5.1)	
β	37.9, CH2	2.58, dd (13.0, 10.0); 3.20, dd (13.0, 5.1)		
Leu	NH		8.04, br d (9.9)	Leu-CO, Leu- β , Ile-CO Leu- α , Leu- δ , Leu- δ' , Leu- CO
	CO	170.3, C		
	α	50.3, CH	4.47, ddd (9.9, 8.6, 6.1)	
	β	41.0, CH2	1.58, m	
Ile	γ	23.8, CH	1.62, m	Leu- β , Leu- δ' Leu- β , Leu- δ
	δ	21.2, CH3	0.85, d (6.5)	
	δ'	23.2, CH3	0.88, d (6.6)	
	NH		8.06, br d (8.7)	
	CO	170.5, C		Glp-CO, Ile-CO, Ile- β , Ile- γ , Ile- γ' Ile- α , Ile- δ Ile- α Ile- β , Ile- γ
	α	56.8, CH	4.15, t (8.5)	
	β	35.4, CH	1.72, m	
	γ	24.0, CH2	1.01, m; 1.42, m	
γ'	15.2, CH3	0.75, d (6.8)		
δ	10.2, CH3	0.71, t (7.4)		
Glp	NH		7.80, s	Glp-CO', Glp- α , Glp- β , Glp- γ
	CO	172.2, C		
	CO'	177.4, C		
	α	55.0, CH	4.09, dd (8.7, 3.6)	Glp-CO', Glp- β , Glp- γ
	β	25.2, CH2	1.79, m; 2.22, m	Glp-CO, Glp- α
	γ	28.8, CH2	2.05, m; 2.09, m	Glp- α

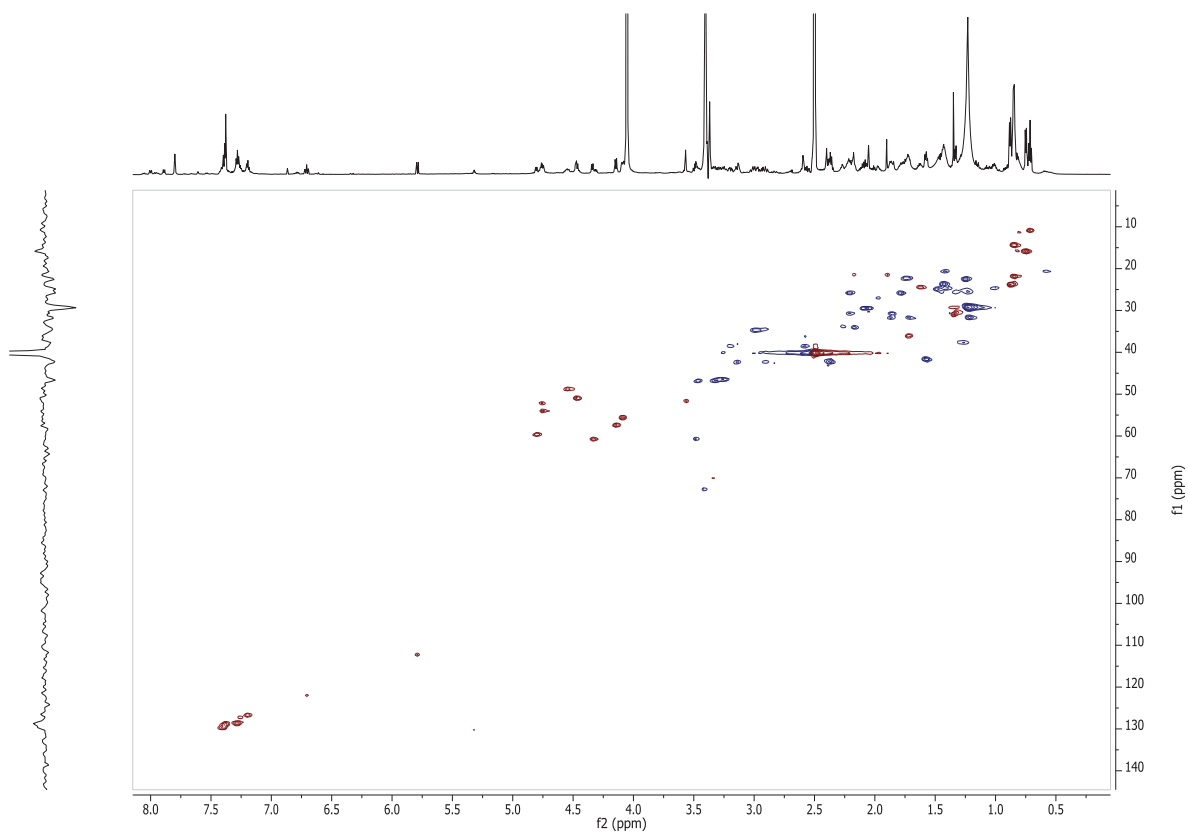
aData extracted from HSQC and HMBC spectra. bSignal overlap prevents determination of couplings.



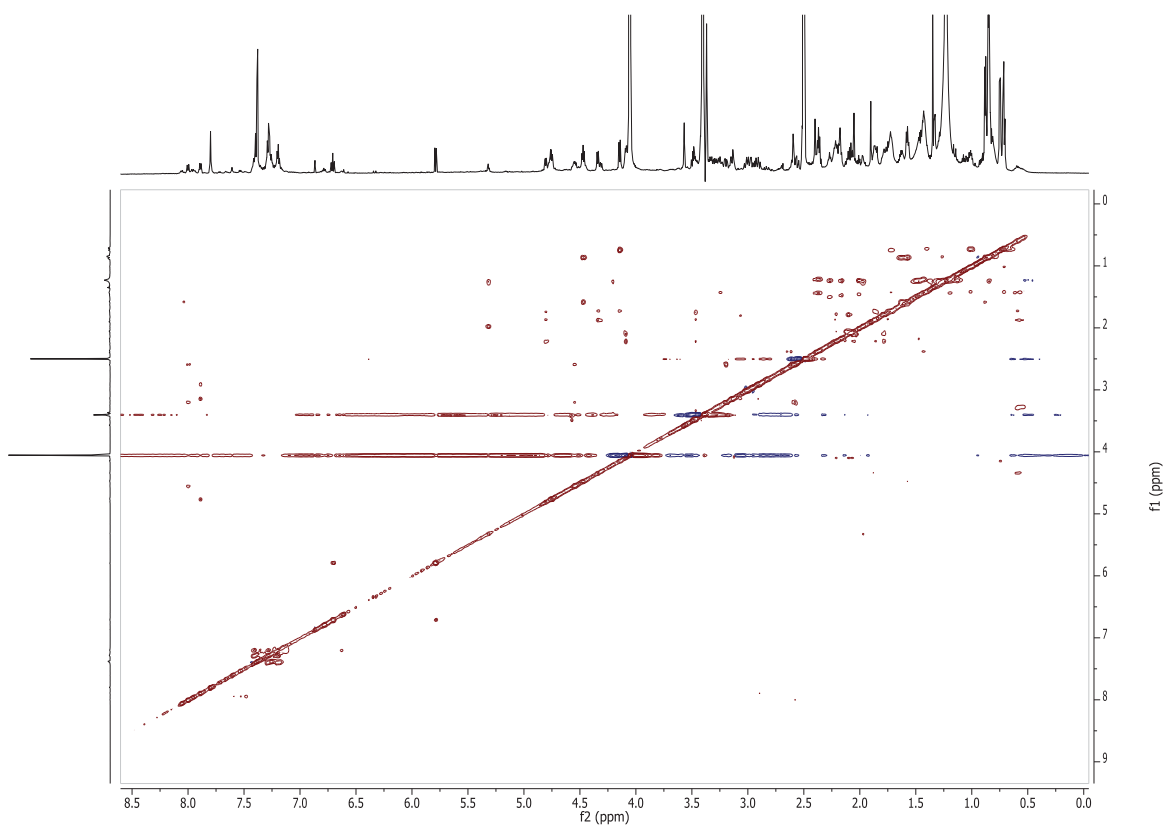
S5-2. ^1H NMR (DMSO- d_6 , 600 MHz) spectrum of 5



S5-3. HMBC NMR (DMSO- d_6 , 600 MHz) spectrum of 5



S5-4. HSQC NMR (DMSO-d₆, 600 MHz) spectrum of 5

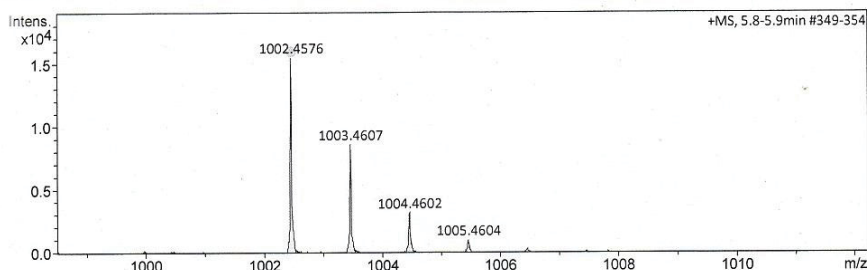


S5-5. TOCSY NMR (DMSO-d₆, 600 MHz) spectrum of 5

Mass Spectrum SmartFormula Report

Analysis Info		Acquisition Date	3/27/2015 1:47:25 PM
Analysis Name	D:\Data\Spektrn2015\Proksch15HR000119.d	Operator	Peter Tommes
Method	tune_midneu.m	Instrument	maXis 288882.20213
Sample Name	Amin CE2RP70P3 in CH3OH (ACN/H2O)		
Comment			

Acquisition Parameter					
Source Type	ESI	Ion Polarity	Positive	Set Nebulizer	0.3 Bar
Focus	Active	Set Capillary	4000 V	Set Dry Heater	180 °C
Scan Begin	300 m/z	Set End Plate Offset	-500 V	Set Dry Gas	4.0 l/min
Scan End	2800 m/z	Set Collision Cell RF	2500.0 Vpp	Set Divert Valve	Source



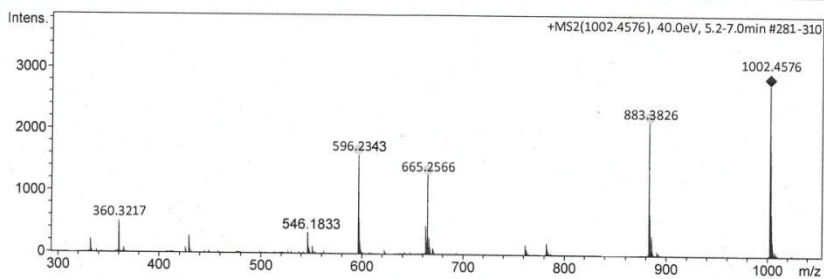
Meas. m/z	#	Ion Formula	m/z	err [ppm]	mSigma	# mSigma	Score	rdb	e ⁻ Conf	N-Rule
1002.4576	1	C43H60N19O8S	1002.4587	1.2	5.6	1	65.86	23.5	even	ok
	2	C42H64N15O12S	1002.4574	-0.1	12.1	2	100.00	18.5	even	ok
	3	C45H72N5O18S	1002.4588	1.2	14.0	3	56.06	12.5	even	ok
	4	C49H64N9O14	1002.4567	-0.8	14.2	4	68.98	22.5	even	ok
	5	C53H68N3O16	1002.4594	1.8	20.9	5	31.37	21.5	even	ok
	6	C50H60N13O10	1002.4581	0.5	22.4	6	68.71	27.5	even	ok
	7	C44H76NO22S	1002.4574	-0.1	22.9	7	80.22	7.5	even	ok
	8	C47H52N23O4	1002.4567	-0.8	27.3	8	41.36	33.5	even	ok
	9	C51H56N17O6	1002.4594	1.8	35.3	9	17.97	32.5	even	ok
	10	C48H48N27	1002.4581	0.5	37.2	10	38.54	38.5	even	ok
	11	C49H72N5O13S2	1002.4563	-1.3	39.3	11	29.25	16.5	even	ok
	12	C47H60N19O3S2	1002.4562	-1.3	40.4	12	28.20	27.5	even	ok
	13	C50H68N9O9S2	1002.4576	0.0	45.5	13	46.91	21.5	even	ok
	14	C54H60N13O5S	1002.4556	-2.0	50.3	14	13.12	31.5	even	ok

S5-6. HRESIMS spectrum of 5

Mass Spectrum SmartFormula Report

Analysis Info		Acquisition Date	1/19/2016 3:13:09 PM
Analysis Name	D:\Data\spektrn2016\Proksch16HR000030.d	Operator	Peter Tommes
Method	tune_low_new.m	Instrument	maXis 288882.20213
Sample Name	Amin Mokhlesi CE2RP75P3 (CH3OH)		
Comment	2 ug/ml		

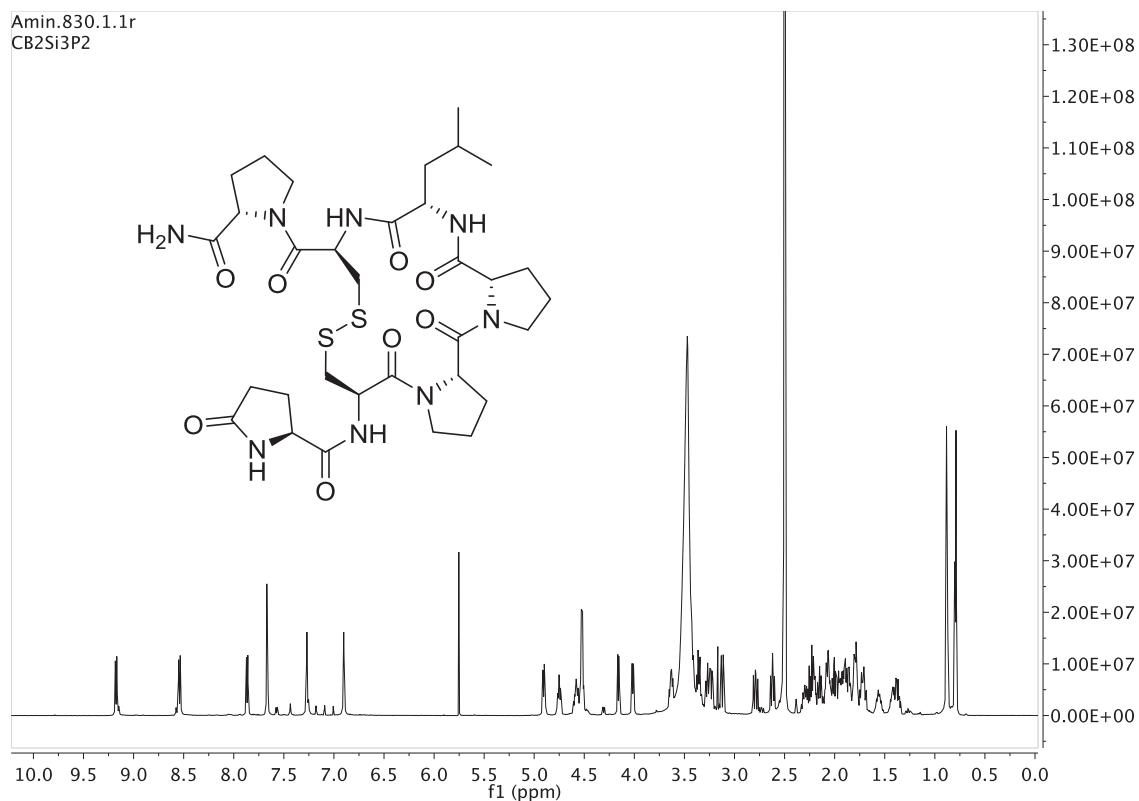
Acquisition Parameter					
Source Type	ESI	Ion Polarity	Positive	Set Nebulizer	0.3 Bar
Focus	Not active	Set Capillary	4000 V	Set Dry Heater	180 °C
Scan Begin	50 m/z	Set End Plate Offset	-500 V	Set Dry Gas	4.0 l/min
Scan End	1500 m/z	Set Collision Cell RF	600.0 Vpp	Set Divert Valve	Source



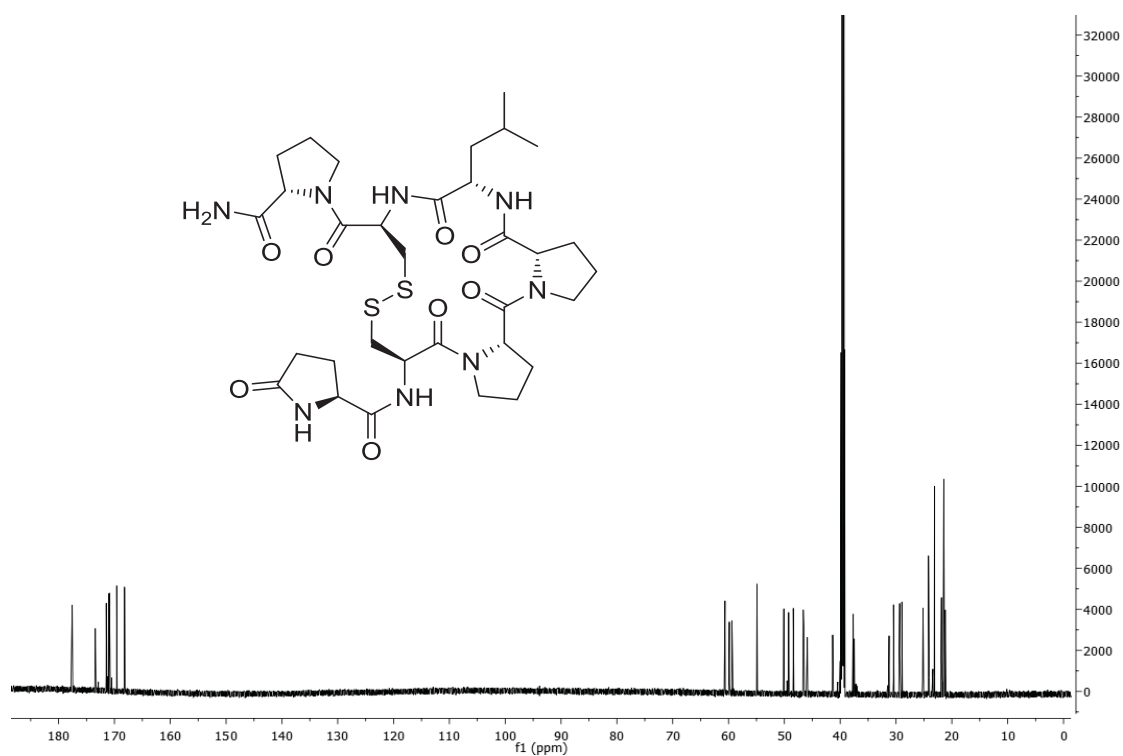
Meas. m/z	#	Ion Formula	m/z	err [ppm]	mSigma	# mSigma	Score	rdb	e ⁻ Conf	N-Rule
546.1833	2	C25H32N5O5S2	546.1839	0.2	15.6	8.5	100.00	2.5	even	ok
665.2566	3	C33H41N6O5S2	665.2566	1.4	32.1	10	98.38	13.5	even	ok
883.3826	4	C42H59N8O9S2	883.3841	1.3	18.5	19	66.25	8.5	even	ok

S5-7. HRESIMS/MS spectrum of 5

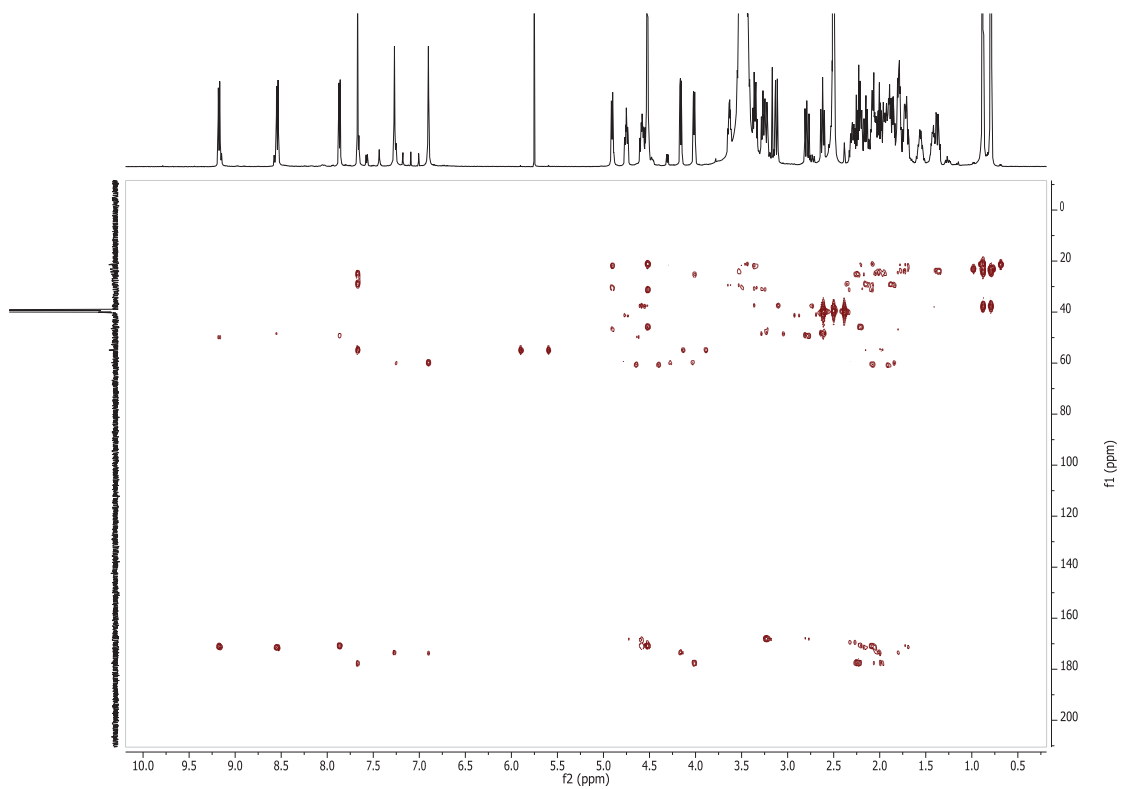
S6. Gombamide D (6)



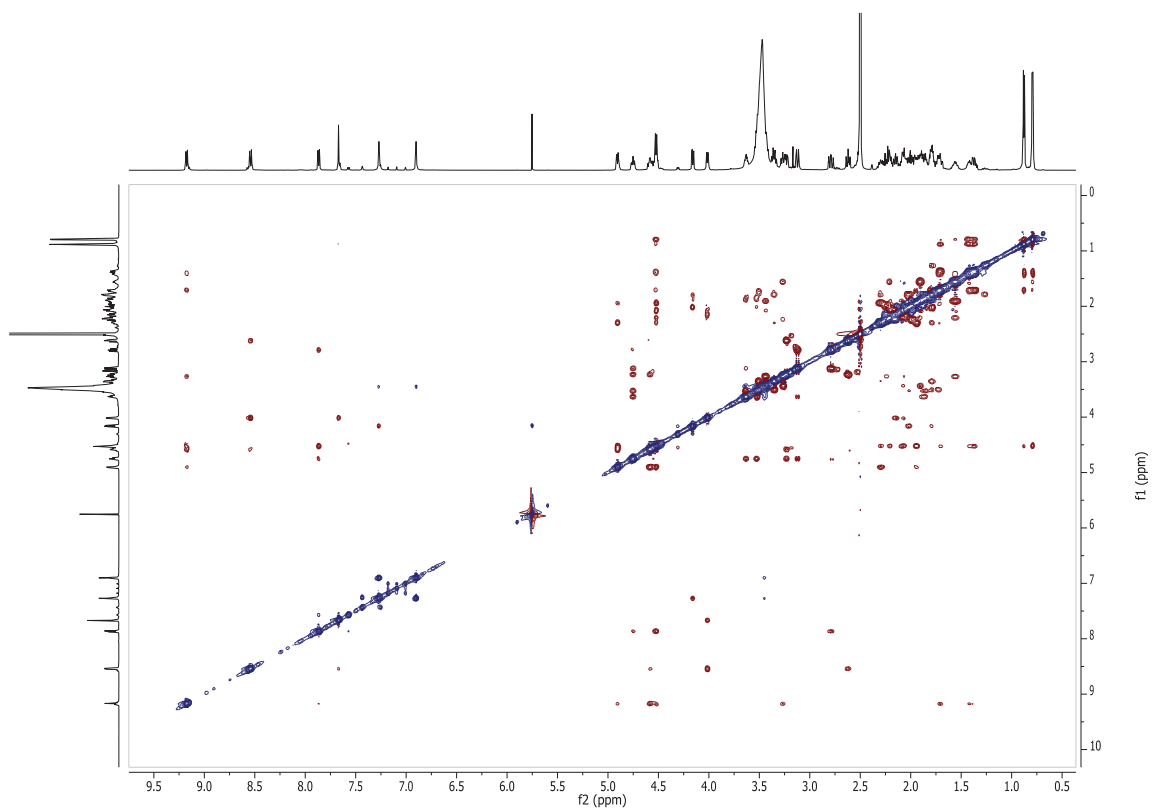
S6-1. ¹H NMR (DMSO-d₆, 600 MHz) spectrum of 6



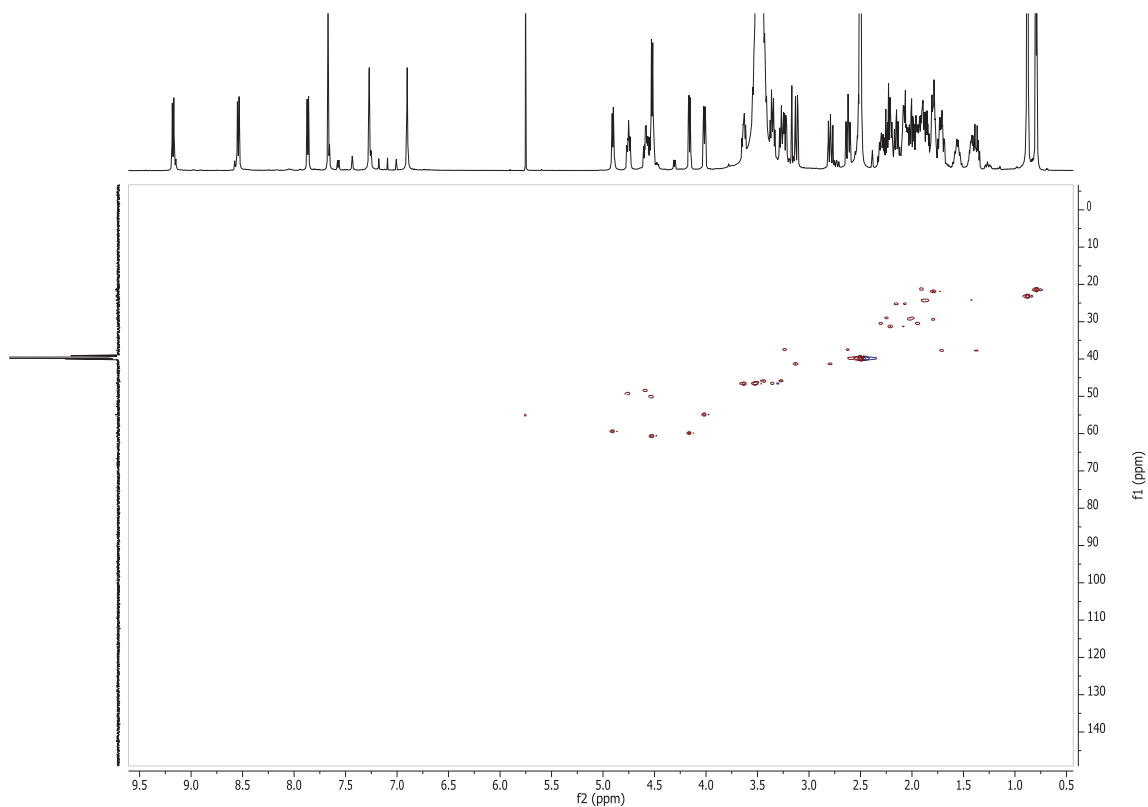
S6-2. ¹³C NMR (DMSO-d₆, 150 MHz) spectrum of 6



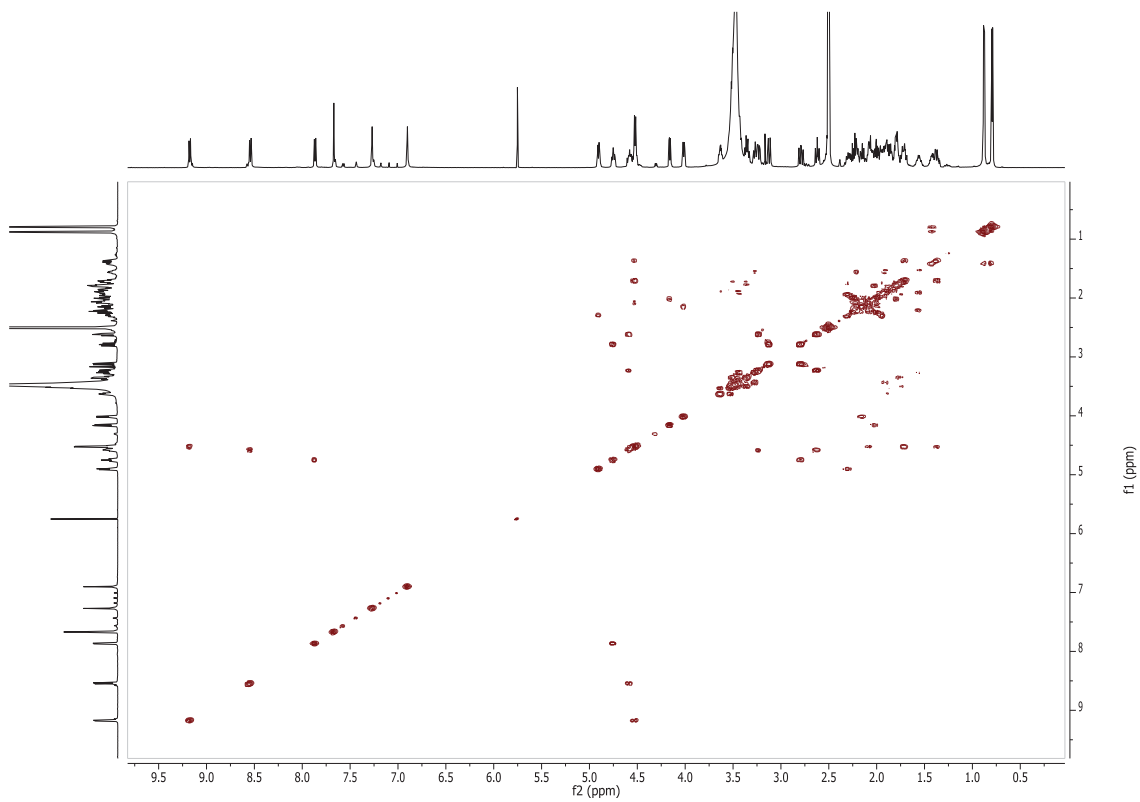
S6-3. HMBC NMR (DMSO-d₆, 600 MHz) spectrum of 6



S6-4. ROESY NMR (DMSO-d₆, 600 MHz) spectrum of 6



S6-5. HSQC NMR (DMSO-d₆, 600 MHz) spectrum of 6

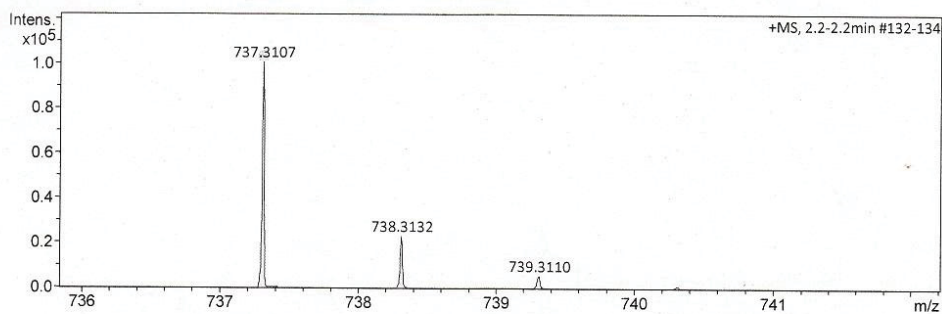


S6-6. COSY NMR (DMSO-d₆, 600 MHz) spectrum of 6

Mass Spectrum SmartFormula Report

Analysis Info		Acquisition Date	1/18/2016 1:16:26 PM
Analysis Name	D:\Data\spektren2016\Proksch16HR000026.d	Operator	Peter Tommes
Method	tune_low_new.m	Instrument	maXis 288882.20213
Sample Name	Amin Mokhlesi CB2Si3P2 (CH3OH)		
Comment	2,0 ug/ml		

Acquisition Parameter					
Source Type	ESI	Ion Polarity	Positive	Set Nebulizer	0.3 Bar
Focus	Not active	Set Capillary	4000 V	Set Dry Heater	180 °C
Scan Begin	50 m/z	Set End Plate Offset	-500 V	Set Dry Gas	4.0 l/min
Scan End	1500 m/z	Set Collision Cell RF	600.0 Vpp	Set Divert Valve	Source



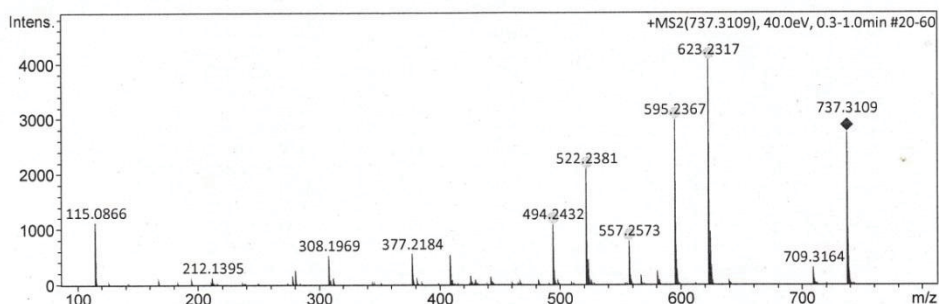
Meas. m/z	#	Ion Formula	m/z	err [ppm]	mSigma	# mSigma	Score	rdb	e ⁻ Conf	N-Rule
737.3107	1	C31H53N4O12S2	737.3096	-1.5	89.6	1	92.52	7.5	even	ok
	2	C29H41N18O2S2	737.3096	-1.5	94.6	2	73.52	18.5	even	ok
	3	C32H49N8O8S2	737.3109	0.3	97.8	3	100.00	12.5	even	ok
	4	C48H49O3S2	737.3118	1.4	165.3	4	1.22	24.5	even	ok

S6-7. HRESIMS spectrum of 6

Mass Spectrum SmartFormula Report

Analysis Info		Acquisition Date	1/18/2016 1:19:01 PM
Analysis Name	D:\Data\spektren2016\Proksch16HR000027.d	Operator	Peter Tommes
Method	tune_low_new.m	Instrument	maXis 288882.20213
Sample Name	Amin Mokhlesi CB2Si3P2 (CH3OH)		
Comment	2,0 ug/ml		

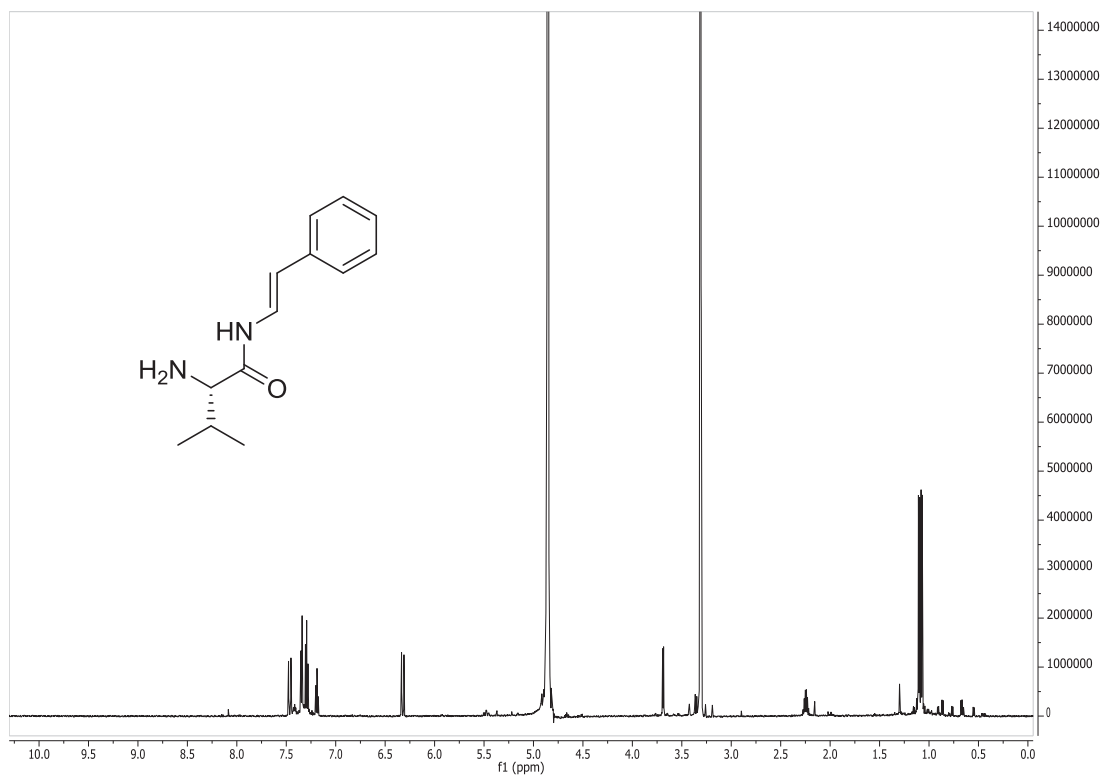
Acquisition Parameter					
Source Type	ESI	Ion Polarity	Positive	Set Nebulizer	0.3 Bar
Focus	Not active	Set Capillary	4000 V	Set Dry Heater	180 °C
Scan Begin	50 m/z	Set End Plate Offset	-500 V	Set Dry Gas	4.0 l/min
Scan End	1500 m/z	Set Collision Cell RF	600.0 Vpp	Set Divert Valve	Source



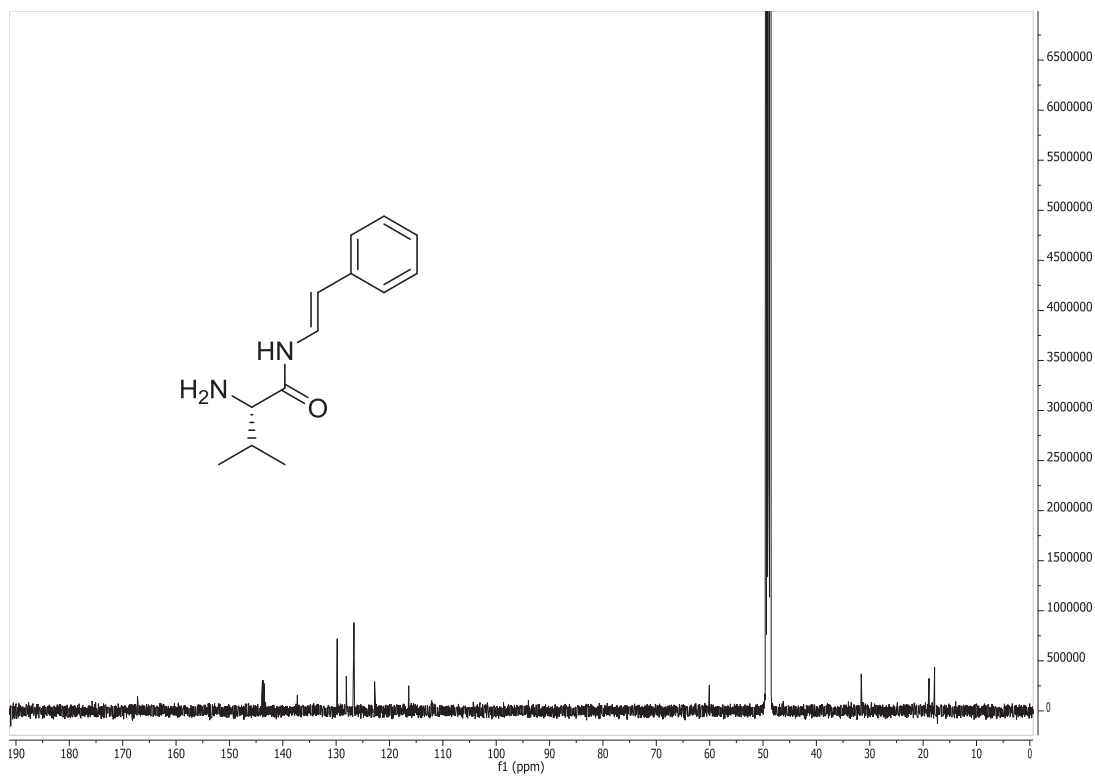
Meas. m/z	#	Ion Formula	m/z	err [ppm]	mSigma	# mSigma	Score	rdb	e ⁻ Conf	N-Rule
595.2367	2	C26H39N6O6S2	595.2367	-0.1	49.1	12	52.82	10.5	even	ok
623.2317	3	C27H39N6O7S2	623.2317	-0.1	57.8	15	44.61	11.5	even	ok

S6-8. HRESIMS/MS spectrum of 6

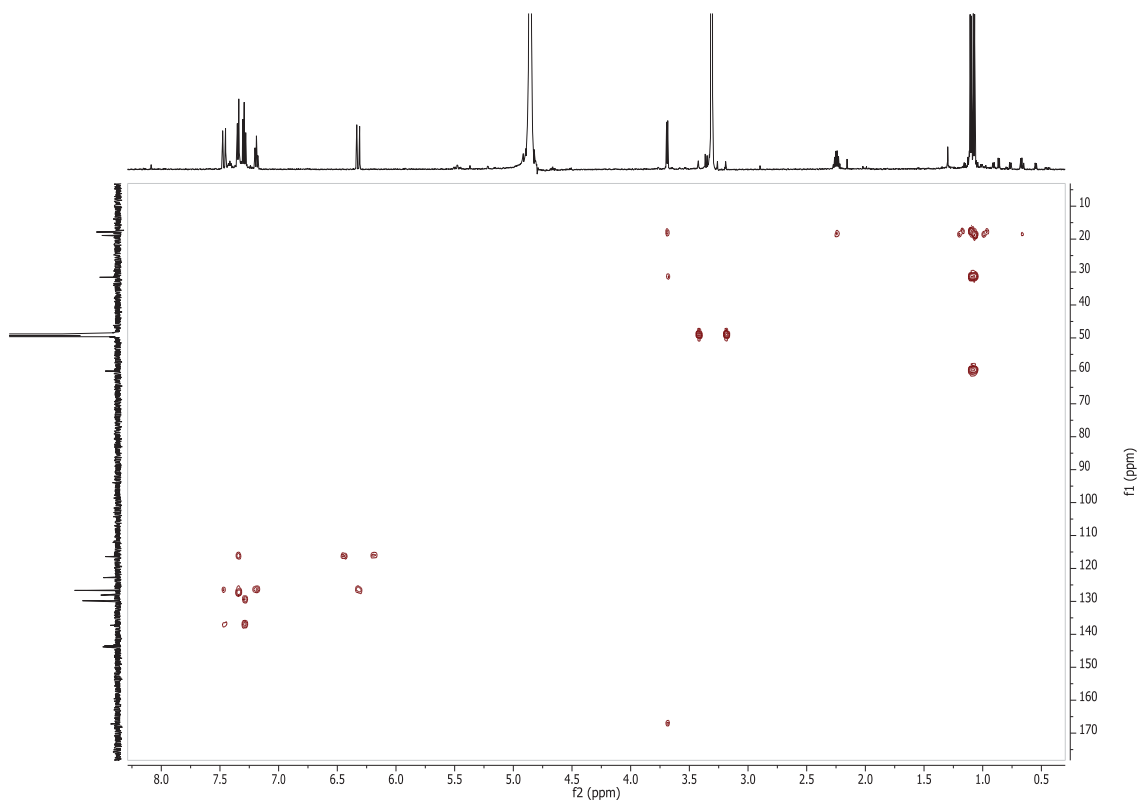
S7. (E)-2-amino-3-methyl-N-styrylbutanamide (7)



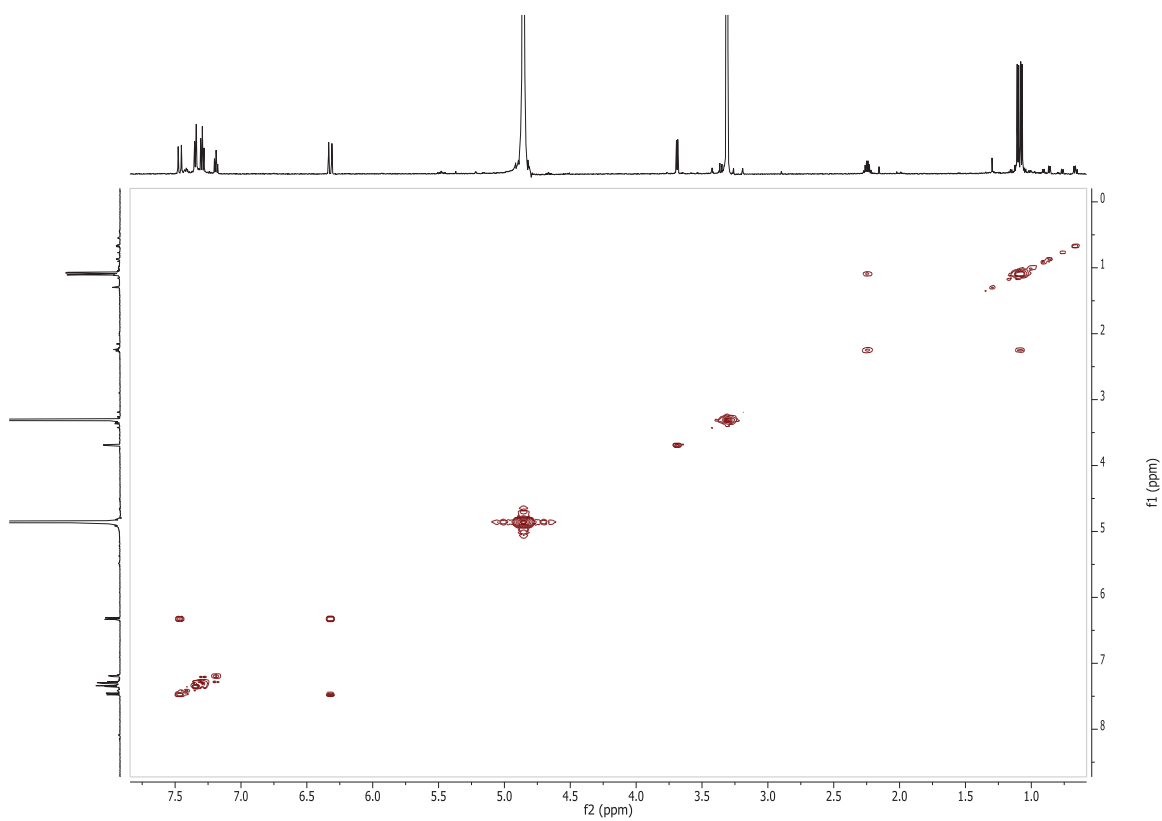
S7-1. 1H NMR (MeOH-d4, 600 MHz) spectrum of 7



S7-2. 13C NMR (MeOH-d4, 600 MHz) spectrum of 7



S7-3. HMBC NMR (MeOH-d₄, 600 MHz) spectrum of 7



S7-4. COSY NMR (MeOH-d₄, 600 MHz) spectrum of 7

Mass Spectrum SmartFormula Report

Analysis Info

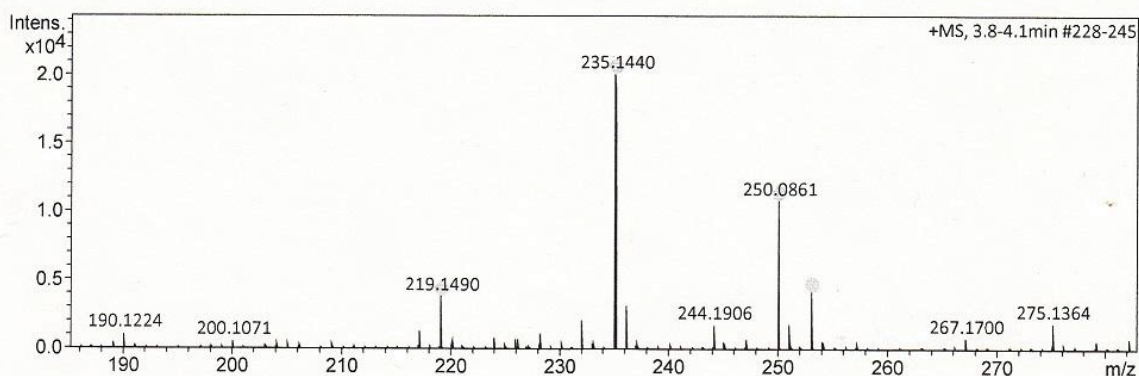
Analysis Name D:\Data\spektren 2016\Proksch16HR000195.d
 Method tune_low_new.m
 Sample Name Amin Mokhlesi CE3 Si4 P3 (CH3OH)
 Comment

Acquisition Date 7/21/2016 10:03:47 AM

Operator Peter Tommes
 Instrument maXis 288882.20213

Acquisition Parameter

Source Type	ESI	Ion Polarity	Positive	Set Nebulizer	0.3 Bar
Focus	Not active	Set Capillary	4000 V	Set Dry Heater	180 °C
Scan Begin	50 m/z	Set End Plate Offset	-500 V	Set Dry Gas	4.0 l/min
Scan End	1500 m/z	Set Collision Cell RF	600.0 Vpp	Set Divert Valve	Source



Meas. m/z	#	Ion Formula	m/z	err [ppm]	mSigma	# mSigma	Score	rdb	e ⁻ Conf	N-Rule
219.1490	1	C13H19N2O	219.1492	0.9	10.8	1	100.00	5.5	even	ok
235.1440	1	C13H19N2O2	235.1441	0.5	2.6	1	100.00	5.5	even	ok
250.0861	1	C16H12NO2	250.0863	0.5	3.7	1	100.00	11.5	even	ok
253.1545	1	C13H21N2O3	253.1547	0.7	13.1	1	100.00	4.5	even	ok

S7-5. HRESIMS spectrum of 7

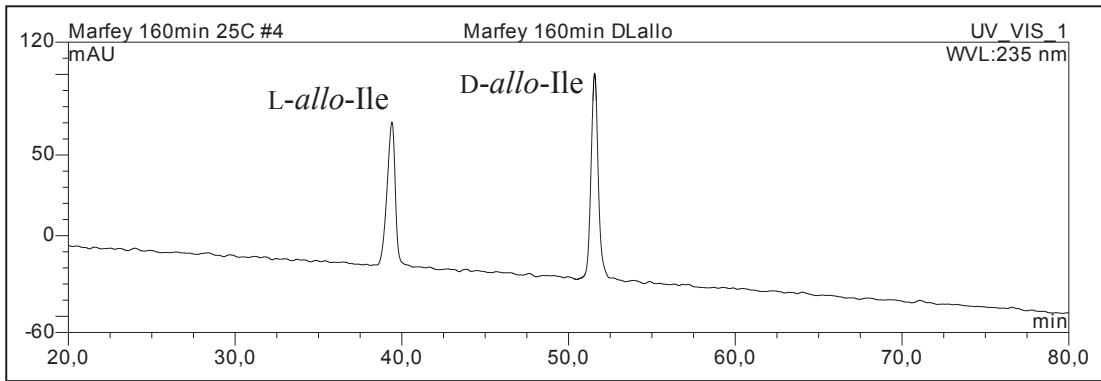
S8. Marfey's analysis

S8-1. Table of HPLC (C18) retention times of acid hydrolysates of 1–7 using Marfey's method

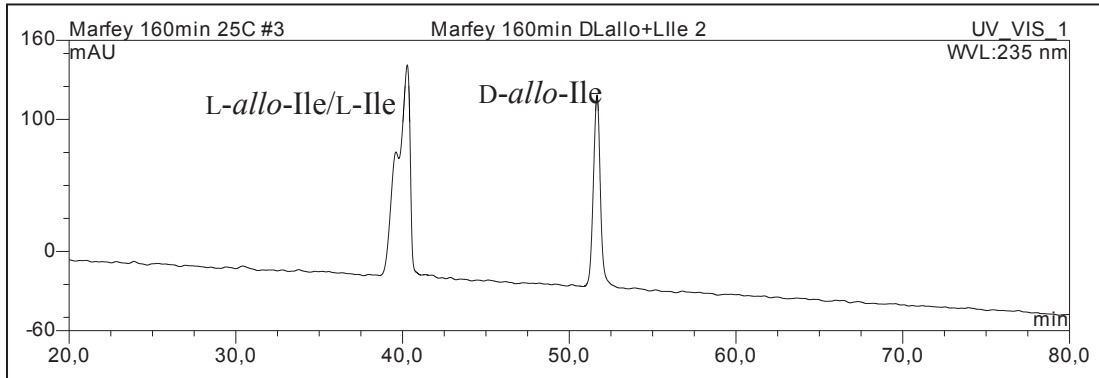
Amino acid	Standard	1	2	3	4	5	6	7
L-Cys	20.0	19.9	19.8	20.4	19.9	20.0	20.0	
D-Cys	21.2							
L-Ile	21.4	21.4	21.3	21.9	20.8	21.0		
D-Ile	24.2							
L-Leu	21.7				21.3	21.5	21.5	
D-Leu	24.3							
L-Val	14.5							
D-Val	19.4			19.9				19.4
L-Pro	8.8				8.5	8.5	8.8	
D-Pro	11.4							
L-Glu	12.4	12.3			12.4	12.3		
D-Glu	14.2							
L-Phe	20.9				20.8	21.0		
D-Phe	23.3							

S8-2. Table of HPLC (C4) retention times for L-Ile and L-allo-Ile of 1–5 using Marfey's method

Amino acid	Standard	1	2	3	4	5
L-Ile	40.6	40.4	40.6	40.2	40.5	40.5
L-allo-Ile	39.5					

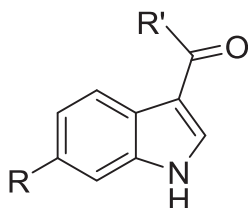


S8-2-1. HPLC chromatogram of derivatized L- and D-allo-Ile standards

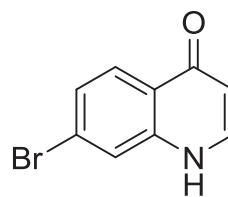


S8-2-2. HPLC chromatogram of derivatized D-allo-Ile, L-allo-Ile, and L-Ile standards

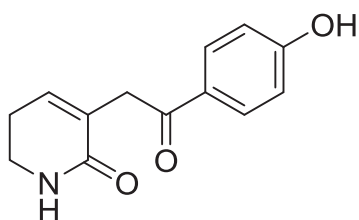
S9. Known compounds



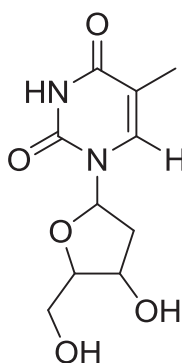
- 8 R=H; R'=H
- 9 R=H; R'=OH
- 10 R=Br; R'=H
- 11 R=Br; R'=OH
- 12 R=Br; R'=OCH₃
- 13 R=Br; R'=OCH₂CH₃



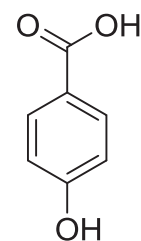
14



15

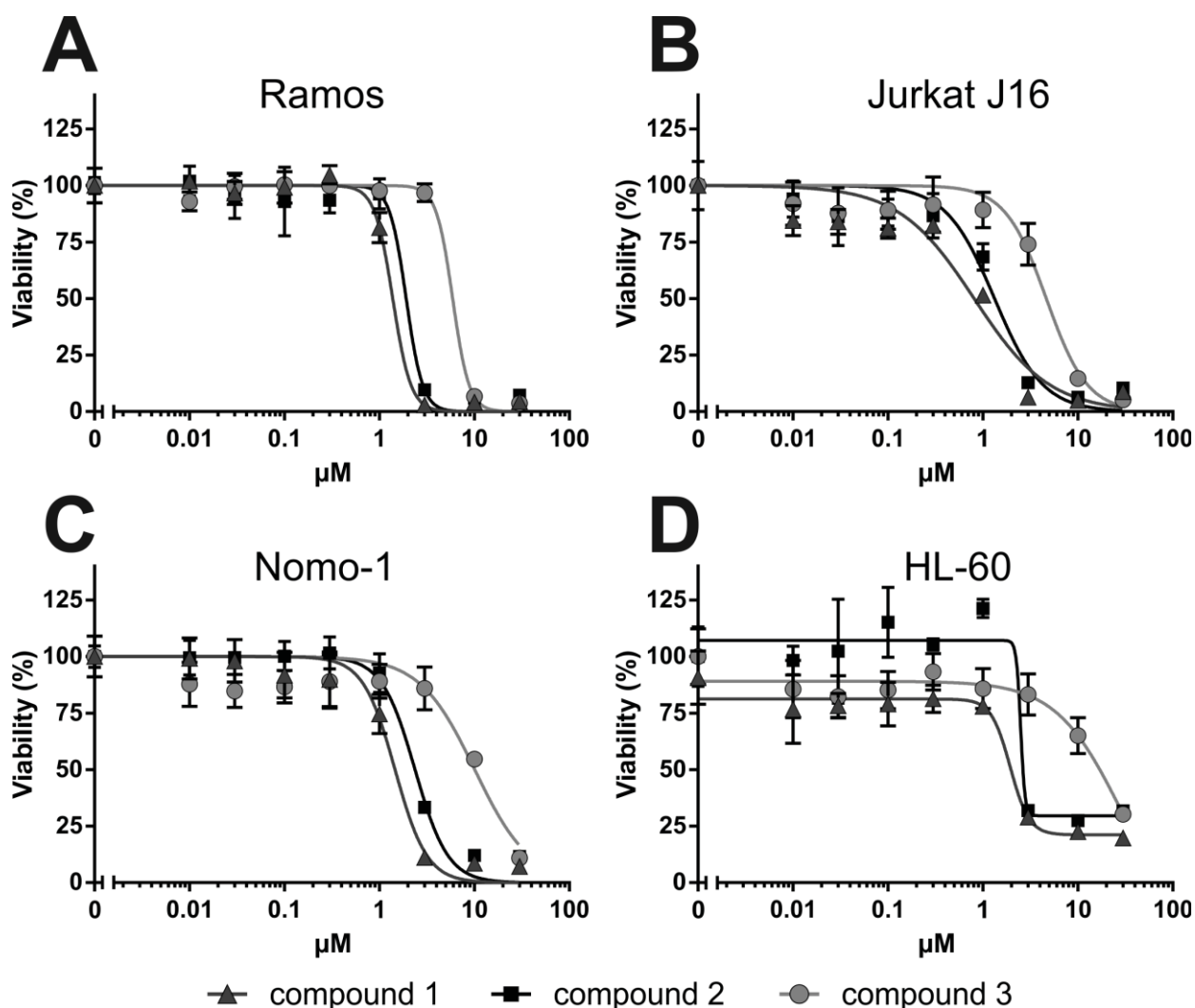


16



17

S9-1. Structures of the known compounds, including 1*H*-indole-3-carbaldehyde (8), 1*H*-indole-3-carboxylic acid (9), 6-bromo-1*H*-indole-3-carbaldehyde (10), 6-bromo-1*H*-indole-3-carboxylic acid (11), methyl 6-bromo-1*H*-indole-3-carboxylate (12), ethyl 6-bromo-1*H*-indole-3-carboxylate (13), 7-bromo-4(1*H*)-quinolinone (14), (3-(2-(4-hydroxyphenyl)-2-oxoethyl)-5,6-dihydropyridin-2(1*H*)-one) (15), 2-deoxythymidine (16), and 4-hydroxybenzoic acid (17).



S10-1. Cytotoxicity effects of 1–3 on human lymphoma and leukemia cell lines, measured by MTT assay. (A) Ramos (Burkitt’s lymphoma), (B) Jurkat J16 (acute T cell leukemia), (C) Nomo-1 (acute myeloid leukemia) and (D) HL-60 (acute promyelocytic leukemia) cells were seeded at a density of 5×10^5 cells/mL and incubated with increasing concentrations of 1, 2 and 3, respectively. Cells treated with DMSO (0.1% v/v) for 24 h were used as the negative control. After an incubation period of 24 h cell viability was monitored using the MTT assay as described in methods. Relative viability in DMSO-treated control cells was set to 100%. Data points shown are the mean of triplicates, error bars = SD. Viability and IC₅₀ values (IC₅₀ = half maximal inhibitory concentration) were calculated using Prism 6 (GraphPad Software).

S10-2. Table of antibacterial activity of compounds 1–17 reported as minimal inhibitory concentration (MIC)^a

Compound	Staphylococcus aureus ATCC 29213	Enterococcus faecium BM 4147-1	Escherichia coli ATCC 25922	Klebsiella pneumoniae ATCC 12657	Enterobacter aerogenes ATCC 13048	Pseudomonas aeruginosa ATCC 27853	Acinetobacter baumannii 09987	Mycobacterium tuberculosis H37Rv
1	6.2	12	> 100	> 100	> 100	> 100	> 100	= 100
2	n.i.b	n.i.	n.i.	n.i.	n.i.	n.i.	n.i.	n.i.
3	6.2c	12	> 100	> 100	> 100	> 100	> 100	= 100
4	> 50	> 50	> 100	> 100	> 100	> 100	> 100	> 100
5	n.i.	n.i.	n.i.	n.i.	n.i.	n.i.	n.i.	n.i.
6–17	> 50	> 50	> 100	> 100	> 100	> 100	> 100	n.i.
ciprofloxacin	0.12	2	0.01	≤ 0.25	≤ 0.01	0.25	0.03	n.i.
doxycycline	0.5	4.0	2.0	2.0	4.0	n.i.	n.i.	n.i.
vancomycin	1.0	4.0	> 64	> 64	> 64	> 64	> 64	n.i.

^aMIC values are reported for test compounds in μM and for reference antibiotics in $\mu\text{g/ml}$ and indicate the lowest concentration fully inhibiting visible bacterial growth. bn.i. : not investigated. cGrowth reduction was already observed at 3.1 μM

6 Publication 3: New 2-Methoxy Acetylenic Acids and Pyrazole Alkaloids from the Marine Sponge *Cinachyrella* sp.

Article

New 2-Methoxy Acetylenic Acids and Pyrazole Alkaloids from the Marine Sponge *Cinachyrella* sp.

Amin Mokhlesi ^{1,2}, Rudolf Hartmann ³, Tibor Kurtán ⁴, Horst Weber ⁵, Wenhan Lin ⁶, Chaidir Chaidir ⁷, Werner E. G. Müller ⁸, Georgios Daletos ^{1,*}, and Peter Proksch ^{1,*}

¹ Institute of Pharmaceutical Biology and Biotechnology, Heinrich Heine University, Universitätsstrasse 1, 40225 Düsseldorf, Germany; amin.mokhlesi@uni-duesseldorf.de (A.M.); Georgios.Daletos@uni-duesseldorf.de (G.D.); proksch@uni-duesseldorf.de (P.P.)

² Department of Marine Biology, Faculty of Marine Sciences, Tarbiat Modares University, Noor, Iran; amin.mokhlesi@uni-duesseldorf.de

³ Institute of Complex Systems: Strukturbiochemie, Forschungszentrum Jülich GmbH, ICS-6, 52425 Jülich, Germany; r.hartmann@fz-juelich.de

⁴ Department of Organic Chemistry, University of Debrecen, P. O. B. 20, 400, 4002, Debrecen, Hungary; kurtan.tibor@science.unideb.hu

⁵ Institute of Pharmaceutical and Medicinal Chemistry, Heinrich Heine University, Universitätsstrasse 1, D-40225 Duesseldorf, Germany; Horst.Weber@uni-duesseldorf.de

⁶ State Key Laboratory of Natural and Biomimetic Drugs, Peking University, Health Science Center, 100191 Beijing, People's Republic of China; whlin@bjmu.edu.cn

⁷ Center for Pharmaceutical and Medical Technology, Agency for the Assessment and Application Technology, 10340 Jakarta, Indonesia; chaidir@bppt.go.id

⁸ Institute of Physiological Chemistry, University Medical Center of the Johannes Gutenberg University Mainz, Mainz, Germany; wmueller@uni-mainz.de

* Correspondence: Georgios.Daletos@uni-duesseldorf.de (G.D.); proksch@uni-duesseldorf.de (P.P.); Tel.: +49-211-81-14173 (G.D.); +49-211-81-14163 (P.P.)

Academic Editor: name

Received: date; Accepted: date; Published: date

Abstract: Three new 2-methoxy acetylenic acids (**1** – **3**) and a known derivative (**4**), in addition to three new natural pyrazole alkaloids (**5** – **7**) were isolated from an Indonesian marine sponge of the genus *Cinachyrella*. Compounds **5** and **6** have previously been reported as synthetic compounds. The structures of the new compounds were established on the basis of one- and two-dimensional NMR spectroscopy as well as by mass spectrometric data. The absolute configuration of the new acetylenic acid derivatives (**1** – **3**) was established by ECD spectroscopy. All isolated compounds were evaluated for their cytotoxicity against L5178Y mouse lymphoma cells. Compounds **1** – **4** exhibited strong activity with IC₅₀ values of 0.3 μM. A plausible biosynthetic pathway for the pyrazole metabolites **5** – **7** is proposed.

Keywords: Natural products; marine sponge; *Cinachyrella* sp.; 2-methoxy acetylenic acid; pyrazole alkaloid

6.1 Introduction

Marine sponges (phylum Porifera) are sessile filter feeder animals with the ability to produce bioactive secondary metabolites as an efficient defence mechanism against predators, fouling organisms or pathogenic microorganisms.³ Several of these metabolites possess pronounced biological activities in disease relevant screens and have proven to be a valuable source of novel lead compounds in drug discovery. Prominent examples of drug leads based on marine natural products include halichondrin B (macrocyclic polyether; lead structure of anticancer drug Halaven®), dictyodendrins (pyrrolo-carbazole derivatives; lead structures of a preclinical telomerase inhibitor), and sarcodictyin (diterpene; lead structure of a preclinical tubulin inhibitor) from the sponges *Halichondria okadaei*, *Dictyodendrilla verongiformis*, and *Sarcodictyon roseum*, respectively.¹⁰⁷

Sponges of the genus *Cinachyrella* sp. are mostly known for the production of steroids¹⁰⁸ and fatty acid metabolites, such as the 2-methoxy acetylenic acid cinachylenic acid A from *C. australiensis*,¹⁰⁹ or long-chain isoprenoid fatty acids from *C. schulzei*.¹¹⁰ In addition, sterols have been used in chemotaxonomic studies of *C. cavernosa*.¹¹¹ Notably, enigmazole A, an unprecedented phosphate-containing macrolide from the Papua New Guinea marine sponge *C. enigmatica*, has been reported to exhibit pronounced cytotoxicity against the NCI60 human tumour cell line and to interfere with c-Kit receptor signaling, a transmembrane glycoprotein with tyrosine kinase activity, which is involved in the growth and development of various cancers.¹¹²

As part of our ongoing search on bioactive secondary metabolites from marine sponges, we investigated a specimen of *Cinachyrella* sp. collected at Ambon Island in Indonesia. The MeOH extract exhibited significant activity against the murine lymphoma L5178Y cell line at a concentration of 10 $\mu\text{g/mL}$. Chromatographic separation of the extract afforded three new (**1** – **3**) acetylenic acid derivatives and one known (**4**) congener, in addition to three new pyrazole alkaloids (**5** – **7**) (Figure 1). Herein, we report the structure elucidation and cytotoxic activity of the isolated compounds and provide a rationale for the biosynthesis of the new pyrazole derivatives.

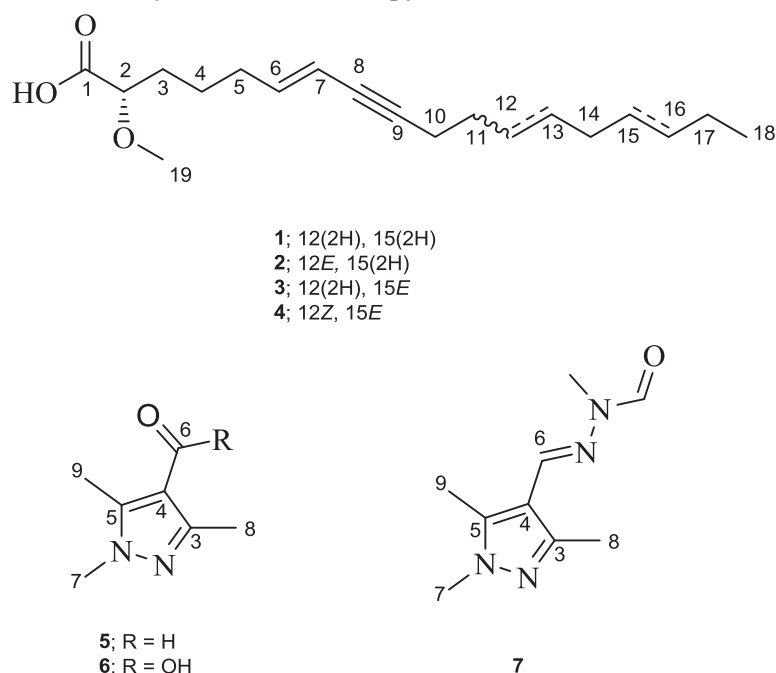


Figure 1. Structures of **1** - **7**.

6.2 Results

2.1. Cinachylenic acid B (**1**)

Cinachylenic acid B (**1**) was obtained as yellow oil. The molecular formula was determined as C₁₉H₃₁O₃ on the basis of the pseudomolecular ion peak at *m/z* 309.2420 [M + H]⁺ in the HRESIMS indicating 4 degrees of unsaturation. In the ¹H NMR spectrum, the fatty acid nature of **1** was apparent from the presence of a cluster of eleven methylene groups (δ_{H} 1.30-2.26) as well as a terminal methyl group at δ_{H} 0.90 (H₃-18). Moreover, the ¹H NMR spectrum revealed signals at δ_{H} 5.46 and 5.95 corresponding to an *E*-configured disubstituted double bond on the basis of the large coupling constant (³*J* = 15.8 Hz), as well as a methoxy group and an oxygenated methine proton based on their integration and low field resonances at δ_{H} 3.36 and 3.76, respectively. The COSY spectrum of **1** showed two continuous spin systems corresponding to the fragments extending from H-2 to H-7 and from H₂-10 to H₃-18 (Figure 2). The HMBC spectrum confirmed the identified substructures and established their connection through key ³*J*-correlations from H-6 and H₂-10 to C-8 (δ_{C} 78.8) and from H₂-11 to C-9 (δ_{C} 88.2), denoting the presence of an alkyne group (C-8/9) in the structure of **1** (Figure 2). In addition, the correlation from H-2 and H₂-3 to the ester carbonyl at δ_{C} 174.5 (C-1), suggested a terminal carboxylic acid group being located at C-2. Likewise, the remaining methoxy group (2-OCH₃) was assigned at C-2, as confirmed by inspection of the respective HMBC correlation. Thus, the planar structure of **1** was established as shown in Figure 1. This assignment was further supported by EIMS, which showed fragmentation ions at *m/z* 178 and 263 originating from cleavage at C-5/6 and C-1/2, respectively (Figure 3). Hence, compound **1** was identified as a new natural product and was named cinachylenic acid B.

Table 1. ¹H (600 MHz), ¹³C (150 MHz), COSY, and HMBC data of cinachylenic acid B (**1**) in MeOH-*d*₄, δ in ppm.

Position	¹³ C, type ¹	¹ H (J in Hz)	COSY	HMBC
1	174.5, C			
2	79.9, CH	3.76, dd (7.6, 4.6)	3-H	C-1/4/19
3	31.7, CH ₂	1.74, dtd (13.0, 8.1, 4.6)	2/4-H	C-1
4	24.5, CH ₂	1.49 ² ;1.66, m	3/5-H	C-5/6
5	32.2, CH ₂	2.10, qt (7.2, 1.9)	4/6-H	C-3/6/7
6	141.8, CH	5.95, dt (15.8, 7.1)	5/7-H	C-8
7	110.3, CH	5.46, dt (15.8, 1.9)	6-H	
8	78.8, C			
9	88.2, C			
10	18.5, CH ₂	2.26, td (7.0, 2.1)	11-H	C-8/9/11
11	28.6, CH ₂	1.49 ²	10-H	C-9/10/12/13
12	28.6, CH ₂	1.39, m	13-H	C-14
13	31.8, CH ₂ ³	1.30 ²	12/14-H	C-14/15
14	29.1, CH ₂ ³	1.30 ²	13/15-H	C-15
15	29.1, CH ₂ ³	1.30 ²	14/16-H	C-14
16	31.8, CH ₂ ³	1.30 ²	15/17-H	C-14/15
17	22.3, CH ₂	1.30 ²	16/18-H	C-15
18	13.0, CH ₃	0.9, t (7.5)	17-H	C-16/17
19	56.9, CH ₃	3.36, s		C-2

¹Data extracted from HMBC spectra, ²Overlapped signals ²Assignments may be interchangeable within the same column.

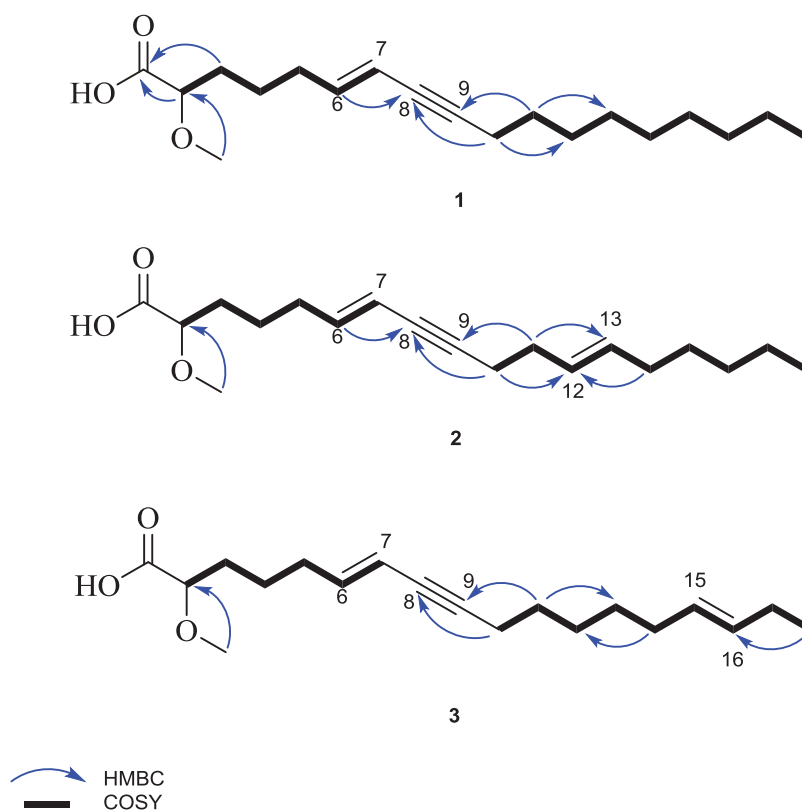


Figure 2. HMBC and COSY correlations of 1 – 3

2.2. Cinachylenic acid C (2)

Compound **2** was isolated as yellow oil. The HRESIMS exhibited the pseudomolecular ion peak at m/z 307.2263 $[M + H]^+$, consistent with the molecular formula $C_{19}H_{29}O_3$, thus revealing 5 degrees of unsaturation. The 1H NMR spectrum of **2** was similar to that of **1**, apart from the replacement of the methylene groups H₂-12 and H₂-13 in **1** by two olefinic protons resonating at δ_H 5.45 and 5.48, respectively. The aforementioned spectroscopic differences, suggested that **2** features the same molecular framework as **1**, bearing an additional double bond (C-12/13), which is in agreement with the 2 amu molecular weight difference observed between both compounds. This assumption was supported by the HMBC correlations from H₂-10 and H₂-14 to C-12 (δ_C 128.6) and from H₂-11 to C-13 (δ_C 131.3), as well as by the COSY cross-peaks between H₂-11 (δ_H 2.16) and H-12, and between H₂-14 (δ_H 2.00) and H-13 (Figure 2). In analogy to **1**, the structure of **2** was further corroborated by the EIMS fragment ion peaks at m/z 175 and 131, originating from cleavage at C-5/6, as well as at m/z 209 and 97, originating from cleavage at C-11/12 (Figure 3). In addition, the geometry of the double bond C-12/13 was established as *E* based on the large coupling constant between H-12 and H-13 (3J = 15.3 Hz). Accordingly, compound **2** was identified as a new natural product and the name cinachylenic acid C is proposed.

Table 2. 1H (600 MHz), ^{13}C (150 MHz), COSY, and HMBC data of cinachylenic acid C (**2**) in MeOH-*d*₄, δ in ppm.

Position	^{13}C , type ¹	1H (J in Hz)	COSY	HMBC
----------	------------------------------	--------------------	------	------

1	– ²			
2	79.9, CH	3.76, dd (7.5, 4.6)	3-H	C-4
3	31.7, CH ₂	1.74, dtd (13.6, 8.0, 4.6)	2/4-H	
4	24.5, CH ₂	1.49, m; 1.68, m	3/5-H	C-3/6
5	31.7, CH ₂	2.10, qt (7.3, 2.0)	4/6-H	C-3/4/6
6	141.8, CH	5.95, dt (15.7, 7.1)	5/7-H	C-8
7	110.4, CH	5.45, d (15.7)	6-H	
8	79.0, C			
9	87.6, C			
10	19.6, CH ₂	2.28, td (7.1, 2.1)	11-H	C-8/9/11/12
11	31.6, CH ₂	2.16, br q (6.5)	10-H	C-9/12/13
12	128.6, CH	5.45 dt (15.3, 6.5)	11/13-H	
13	131.3, CH	5.48 dt (15.3, 6.0)	12/14-H	
14	31.4, CH ₂	2.00, br q (6.0)	13/15-H	C-12/13/15/16
15	29.1, CH ₂	1.36, m	14/16-H	
16	30.9, CH ₂	1.32, m	15/17-H	C-14
17	22.2, CH ₂	1.30, m	16/18-H	C-15
18	12.9, CH ₃	0.90, t (7.5)	17-H	C-16/17
19	57.1, CH ₃	3.36, s		C-2

¹Data extracted from HMBC spectra, ² Not observed

2.3. Cinachylenic acid D (**3**)

Compound **3** was isolated as yellow oil and shared the same molecular formula with **2** (C₁₉H₂₉O₃), as indicated by the pseudomolecular ion peak at *m/z* 307.2264 [M + H]⁺ in the HRESIMS. In a similar manner to **2**, the ¹H NMR data of **3** showed close similarity to those of **1** apart from the presence of an additional *E*-configured double-bond at C-15/16, as supported by the HMBC correlation from H₃-18 to C-16 (δ_c 131.7) and by the large coupling constant between H-15 and H-16 (³*J* = 15.3 Hz). Similarly, the structure of **3** was further corroborated by the EIMS fragment ion peaks at *m/z* 175 and 278 originating from cleavage at C-5/6 and C-16/17, respectively (Figure 3). Thus, **3** was characterized as the double-bond positional isomer of **2** and was named cinachylenic acid D.

Table 3. ¹H (600 MHz), ¹³C (150 MHz), COSY, and HMBC data of cinachylenic acid D (**3**) in MeOH-*d*₄, δ in ppm.

Position	¹³ C, type ¹	¹ H (<i>J</i> in Hz)	COSY	HMBC
1	– ²			
2	80.1, CH	3.74, dd (8.1, 4.7)	3-H	
3	31.5, CH ₂	1.74, dtd (13.6, 8.1, 4.6)	2/4-H	C-2
4	24.2, CH ₂	1.49 ³ ; 1.66, m	3/5-H	C-2/5/6
5	32.1, CH ₂	2.10, qt (7.2, 1.9)	4/6-H	C-3/6/7
6	141.8, CH	5.95, dt (15.9, 7.1)	5/7-H	C-8
7	110.4, CH	5.46, d (15.9)	6-H	
8	78.6, C			
9	87.8, C			

10	18.4, CH ₂	2.25, td (7.0, 2.2)	11-H	C-8/9/12
11	29.1, CH ₂	1.49 ³	10/12-H	C-9/13
12	28.1, CH ₂	1.30, m	11-H	
13	28.6, CH ₂	1.38, m	14-H	C-12
14	31.8, CH ₂	1.99 ³	13/15-H	C-12
15	129.2, CH	5.43 ³	14/16-H	
16	131.7, CH	5.38, dt (15.3, 6.3)	15/17-H	
17	25.2, CH ₂	1.99 ³	16/18-H	C-18
18	13.2, CH ₃	0.96, t (7.5)	17-H	C-16/17
19	57.0, CH ₃	3.36, s		C-2

¹Data extracted from HMBC spectra, ²Not observed, ³Overlapped signals

2.4. Cinachylenic acid A (**4**)

Compound **4** was identified as 2-methoxy-6,12,15-trien-8-yne-octadecanoic acid, originally reported from the marine sponge *C. australiensis*, based on its NMR and HRESIMS data and by comparison with the literature.¹⁰⁹ The trivial name cinachylenic acid A is proposed.

2.5. Absolute configuration of cinachylenic acids A – D (**1** – **4**)

The experimental ECD spectra of **1** – **3** were rather weak suggesting that these compounds were obtained as enantiomeric mixtures. Nevertheless, their ECD spectra showed a positive Cotton effect at around 210 nm (Figures S1-6, S2-6, and S3-6), which could be attributed to the low enantiomeric excess of the (*S*) enantiomer as previously established for 2-methoxy acetylenes and fatty acids.¹¹³ It should be noted that the ECD spectrum of **4** was not obtained due to its rapid decomposition during storage. However, the stereocenter C-2 in **4** was assumed to be (*S*) based on its specific rotation value, which has a negative sign similarly to those of **1** – **3**, as well as its close biogenetic relationship with the latter metabolites.

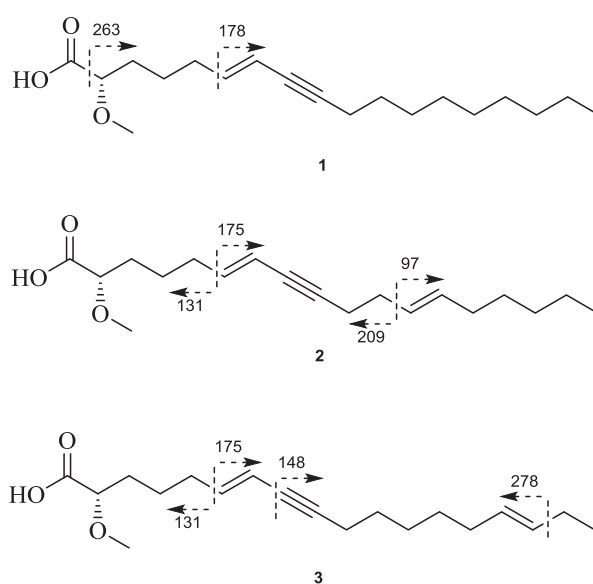


Figure 3. Key EIMS fragmentations of **1** – **3**.

2.5. Cinachyrazole A (**5**)

Compound **5** was isolated as a white, amorphous solid. Its molecular formula was established as $C_7H_9N_2O$ based on the pseudomolecular ion peak observed at m/z 139.0865 $[M + H]^+$ in HRESIMS, corresponding to 5 degrees of unsaturation. Inspection of the 1H NMR spectrum indicated the presence of three methyl groups at δ_H 3.74 (H₃-7), 2.38 (H₃-8), and 2.51 (H₃-9), in addition to a singlet proton at δ_H 9.85 (6-H) characteristic of an aldehyde group. Analysis of the HMBC spectrum confirmed the corresponding carbon signals and revealed in addition three sp^2 quaternary carbon atoms at δ_C 151.2 (C-3), 118.6 (C-4), and 146.8 (C-5) (Table 4). HMBC correlations from H₃-8 to C-3 and C-4, from H₃-9 to C-5 and C-4, and from H₃-7 to C-5 were indicative of a 1,2,4-trimethylpyrazole ring. The remaining aldehyde group was attached to C-4 based on the observed HMBC correlations from H-6 to C-5 and C-3 (Figure 4). This structural assignment was further supported by the ROESY cross-peaks between H₃-7 and H₃-9 as well as between H-6 and both H₃-8 and H₃-9. Hence, compound **5** was identified as a new natural product and was named cinachyrazole A.

Table 4. 1H NMR (600 MHz) and ^{13}C NMR (150 MHz) data of **5**, **6**, and **7** in MeOH- d_4 , δ in ppm.

Position	Com. 5		Com. 6		Com. 7	
	1H (J in Hz)	^{13}C , type ¹	1H (J in Hz)	^{13}C , type ¹	1H (J in Hz)	^{13}C , type ¹
3		151.2, C		151.4, C		147.0, C
4		118.6, C		110.5, C		112.0, C
5		146.8, C		145.8, C		140.2, C
6	9.85, s	186.5, CHO		– ²	7.95, d (0.8)	136.8, CH
7	3.74, s	35.3, CH ₃	3.72, s	35.8, CH ₃	3.73, s	34.5, CH ₃
8	2.38, s	12.0, CH ₃	2.35, s	– ²	2.35, s	11.6, CH ₃
9	2.51, s	9.3, CH ₃	2.50, s	11.3, CH ₃	2.45, s	8.8, CH ₃
N'CHO					8.69, s	165.0, CH
N'CH ₃					3.29, s	25.3, CH ₃

¹Data extracted from HMBC spectra, ² Not observed

2.6. Cinachyrazole B (**6**)

Compound **6** was isolated as a white, amorphous solid. Its molecular formula was determined as $C_7H_9N_2O_2$, in accordance with the pseudomolecular ion peak observed at m/z 155.0814 $[M + H]^+$ in HRESIMS. The 1H NMR data of **6** were almost superimposable to those of **5**, except for the absence of the aldehyde group signal at δ_H 9.85 (H-6 in **5**). This spectral difference suggested that **6** features the same pyrazole core structure as **5**, the only difference being the replacement of the aldehyde group by a carboxylic acid group, which is in accordance with the 16 amu increase in the molecular weight compared to **5** (Table 4). Accordingly, the structure of **6** was assigned and the compound was named cinachyrazole B.

2.7. Cinachyrazole C (**7**)

Compound **7** was isolated as a white, amorphous solid. The HRESIMS of **7** exhibited the pseudomolecular ion peak at m/z 195.1241 $[M + H]^+$, consistent with the molecular formula $C_9H_{13}N_4O$. The 1H and ^{13}C NMR data of **7** denoted the same pyrazole basic unit as in **5** and **6** (Table 4). The remaining resonances included an olefinic signal at δ_H 7.95 (CH-6, δ_C 136.8), an *N*-methyl group at δ_H 3.29 (*N'*-CH₃, δ_C 25.3), and an aldehyde group at δ_H 8.69 (*N'*-CHO, δ_C 165.0). These signals were indicative for the presence of an *N*-methyl-*N'*-methyleneformohydrazide moiety at C-4, as supported

by the HMBC correlations from H-6 to C-5 and C-3 and from H₃-N'-CH₃ to N'-CHO. In addition, the *E* geometry of the double bond (C-6/N) was established based on the observed ROESY cross-peak between H-6 and H₃-N'-CH₃ (Figure 4). For compound 7 the name cinachyrazole C is suggested.

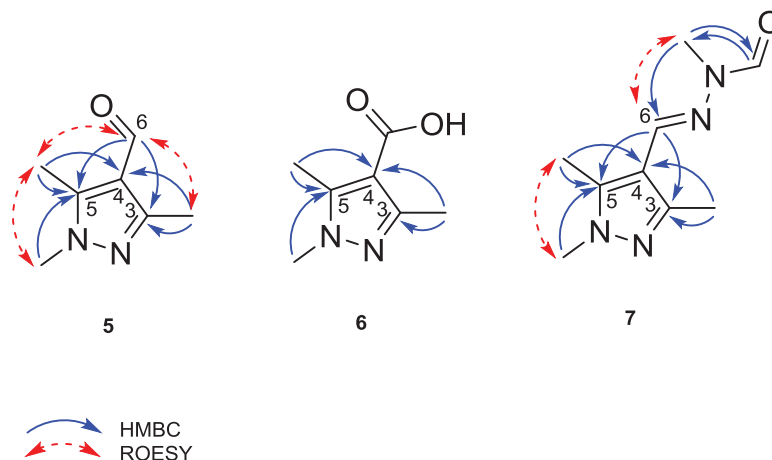


Figure 4. HMBC and ROESY correlations of 5 – 7

2.8. Proposed biosynthetic pathway for 5 - 7

A plausible biosynthetic pathway for the isolated pyrazole derivatives 5 – 7 is proposed, which includes the linkage of an acetoacetic acid and an *N*-acetyl-*N*-methylhydrazine unit via a Schiff base formation followed by cyclization and dehydration reactions to form 6. Subsequent reduction of the latter followed by a Schiff base formation with an *N*-formyl-*N*-methylhydrazine unit, a natural product originally isolated from the ascomycete fungus *Gyromitra esculenta*,¹¹⁴ would finally result in the formation of 5 and 7, respectively.

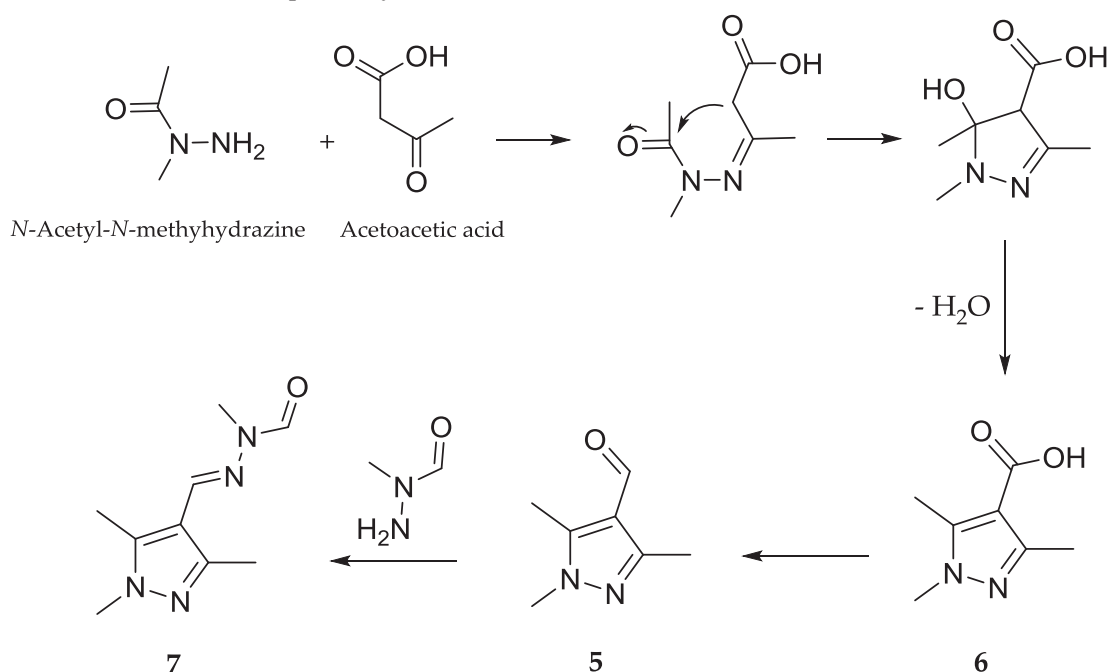


Figure 5. Proposed biosynthesis of 5 – 7

2.9. Bioactivity

All isolated compounds (**1** – **7**) were evaluated for their effects on the growth of the L5178Y mouse lymphoma cell line employing the MTT assay. Interestingly, the acetylenic acid derivatives **1** – **4** exhibited pronounced cytotoxicity with an IC₅₀ value of 0.3 μM compared to the positive control kahalalide F (IC₅₀ = 4.3 μM). The pyrazole derivatives (**5** – **7**) showed no cytotoxicity in the respective assay (IC₅₀ > 10 μM).

6.3 Discussion

Compounds **1** – **4** are acetylenic acid derivatives possessing a methoxy group at C-2 as well as an acetylene group at C-8/9; however, they differ at the number and/or position of double bonds at their aliphatic chain (Figure 1). Other examples of 2-methoxy acetylenic acids from marine sponges include corticatic acids A-E, isolated from sponge *Petrosia corticata* with antifungal activity,[14,15] taurospongins A from the sponge *Hippospongia* sp. with inhibitory activity against DNA polymerase β and HIV reverse transcriptase,¹¹⁵ as well as halicyonones A and B from the sponge *Haliclona* sp. with antitumor activity against the human colon tumor cell line (HCT-116),[16]. Compounds **5** – **7** possess an unusual 1,2,4-trimethylpyrazole core structure. It should be noted that **5** and **6** have been previously described as synthetic compounds and this is the first report of their isolation as natural products.¹¹⁶ Interestingly, compound **7** bears an additional hydrazone unit, which is rarely reported from marine invertebrates.¹¹⁷ To the best of our knowledge, in addition to **7**, the only examples so far of sponge-derived compounds bearing a hydrazone unit include cinachyramine, likewise from a marine sponge of the genus *Cinachyrella*,¹¹⁸ as well as psammaphin G, a potent inhibitor of DNA methyltransferase, from the sponge *Pseudoceratina purpurea*.¹¹⁹

6.4 Materials and Methods

4.1. General procedures

1D and 2D NMR spectra were recorded on a Bruker AVANCE III HD 600 NMR spectrometer and the chemical shifts were referenced to the solvent residual peaks. HRESIMS and EIMS were measured on a UHR-QTOF maxi 4G (Bruker Daltonics) or on a Thermo Finnigan TCQ 7000 mass spectrometer, respectively. ECD spectra were recorded with a J-810 spectropolarimeter. The HPLC analysis was carried out using a Dionex UltiMate-3400SD machine equipped with a LPG-3400SD pump and a DAD 300RS photodiode array detector. The analytical column was filled with Eurosphere-10 C18 (125 × 4 mm, L × i.d.) (Knauer, Germany), and the gradient consisted of 0 min (10% MeOH); 5 min (10% MeOH); 35 min (100% MeOH); 45 min (100% MeOH), with MeOH, 0.1% formic acid in H₂O solvent system. UV detection during HPLC was set at 235, 254, 280, and 340 nm. A Merck Hitachi HPLC System (UV detector L-7400; pump L-7100; Eurosphere-100 C18, 300 - 8 mm, Knauer, Germany), was used for semipreparative HPLC with a gradient system of MeOH/H₂O as mobile phase. Column chromatography was performed using Sephadex LH-20 (Sigma- Aldrich) and Merck MN silica gel 60 M (0.04 - 0.063 mm) as stationary phases. Thin-layer chromatography (TLC) was run using pre-coated silica gel 60 F254 plates (Merck) followed by UV detection at 254 nm or after spraying the plates with anisaldehyde reagent. Optical rotations were measured using a Jasco P-2000 polarimeter.

4.2. Sponge material

The sponge specimen was collected by SCUBA at Ambon, Indonesia and was identified as *Cinachyrella* sp. by Dr. Nicole de Voogd (Naturalis Biodiversity Center, Leiden, The Netherlands). A voucher specimen was deposited at the Naturalis Biodiversity Center under the reference number

RMNH POR. 10903. The sponge specimen was preserved in a mixture of EtOH and H₂O (70:30) and stored in a freezer (-20°C) prior to extraction.

4.3. Extraction and isolation

The sponge (wet weight 400 g) was cut into small pieces. The material was exhaustively extracted with methanol (3 x 1L) at room temperature and concentrated under vacuum to yield 1.4 g dry crude extract. The obtained extract was submitted to liquid-liquid partitioning to afford *n*-hexane, ethyl acetate and *n*-butanol fractions. The resulting fractions were further purified by column chromatography on Sephadex LH-20 (MeOH as mobile phase) and/or by vacuum liquid chromatography (VLC) using *n*-hexane/ethyl acetate and DCM/MeOH step gradient elution, followed by semipreparative HPLC, in a gradient system of H₂O/MeOH, to yield **1** (1 mg), **2** (1.3 mg), **3** (0.8 mg), and **4** (1 mg) from *n*-hexane, as well as **5** (2.5 mg), **6** (2.0 mg), and **7** (1.0 mg) from ethyl acetate fraction.

Cinachylenic acid B (**1**):

Yellow oil; $[\alpha]^{20}_{\text{D}} = -11.1$ (*c* 1.0, MeOH); UV (λ_{max} , MeOH) (log ϵ) 228.5 (4.1); ¹H NMR data (MeOH-*d*₄, 600 MHz) see Table 1; HRESIMS *m/z* 309.2420 [M + H]⁺ (calcd for C₁₉H₃₂O₃ 309.2424); EIMS *m/z* 178.0 [M - C₁₃H₂₂]⁺, 263.2 [M - C₁₈H₃₀O₂]⁺.

Cinachylenic acid C (**2**):

Yellow oil; $[\alpha]^{20}_{\text{D}} = -30.1$ (*c* 1.0, MeOH); UV (λ_{max} , MeOH) (log ϵ) 228.4 (4.0); ¹H NMR data (MeOH-*d*₄, 600 MHz) see Table 2; HRESIMS *m/z* 307.2266 [M + H]⁺ (calcd for C₁₉H₃₀O₃ 307.2268); EIMS *m/z* 175.0 [M - C₁₃H₁₉]⁺, 131.0 [M - C₆H₁₁O₃]⁺, 97.0 [M - C₇H₁₃]⁺.

Cinachylenic acid D (**3**):

Yellow oil; $[\alpha]^{20}_{\text{D}} = -19.56$ (*c* 1.0, MeOH); UV (λ_{max} , MeOH) (log ϵ) 228.1 (3.87); ¹H NMR data (MeOH-*d*₄, 600 MHz) see Table 3; HRESIMS *m/z* 307.2264 [M + H]⁺ (calcd for C₁₉H₃₀O₃ 307.2268); EIMS *m/z* 175.0 [M - C₁₃H₁₉]⁺, 131.0 [M - C₆H₁₁O₃]⁺, 278.1 [M - C₁₇H₂₅O₃]⁺.

Cinachyrazole A (**5**):

White, amorphous solid; UV (λ_{max} , MeOH) (log ϵ) 201.2 (3.29), 256.2 (3.77); ¹H NMR data (MeOH-*d*₄, 600 MHz) see Table 4; HRESIMS *m/z* 139.0865 [M + H]⁺ (calcd for C₇H₁₀N₂O 139.0866).

Cinachyrazole B (**6**):

White, amorphous solid; UV (λ_{max} , MeOH) (log ϵ) 229.1 (3.50); ¹H NMR data (MeOH-*d*₄, 600 MHz) see Table 5; HRESIMS *m/z* 155.0814 [M + H]⁺ (calcd for C₇H₁₀N₂O₂ 155.0815).

Cinachyrazole C (**7**):

White, amorphous solid; UV (λ_{max} , MeOH) (log ϵ) 265.6 (3.81), 288.2 (4.1); ¹H NMR data (MeOH-*d*₄, 600 MHz) see Table 5; HRESIMS *m/z* 195.1241 [M + H]⁺ (calcd for C₉H₁₄N₄O 195.1227).

6.5 Conclusions

In summary, chemical investigation of the marine sponge *Cinachyrella* sp. collected in Indonesia afforded three new acetylenic acid derivatives (**1** – **3**) and one known congener (**4**), in addition to three new pyrazole alkaloids (**5** – **7**). The unusual pyrazole ring of the latter is postulated to be derived via a Schiff base formation between an acetoacetic acid and an *N*-acetyl-*N*-methylhydrazine unit. Notably, the acetylenic acid derivatives **1** – **4** showed strong inhibitory effect on the growth of L5178Y mouse lymphoma cell line with IC₅₀ values of 0.3 μM. In this context, our report highlights the metabolic potential of marine sponges of the genus *Cinachyrella* as a rich source of novel bioactive secondary metabolites.

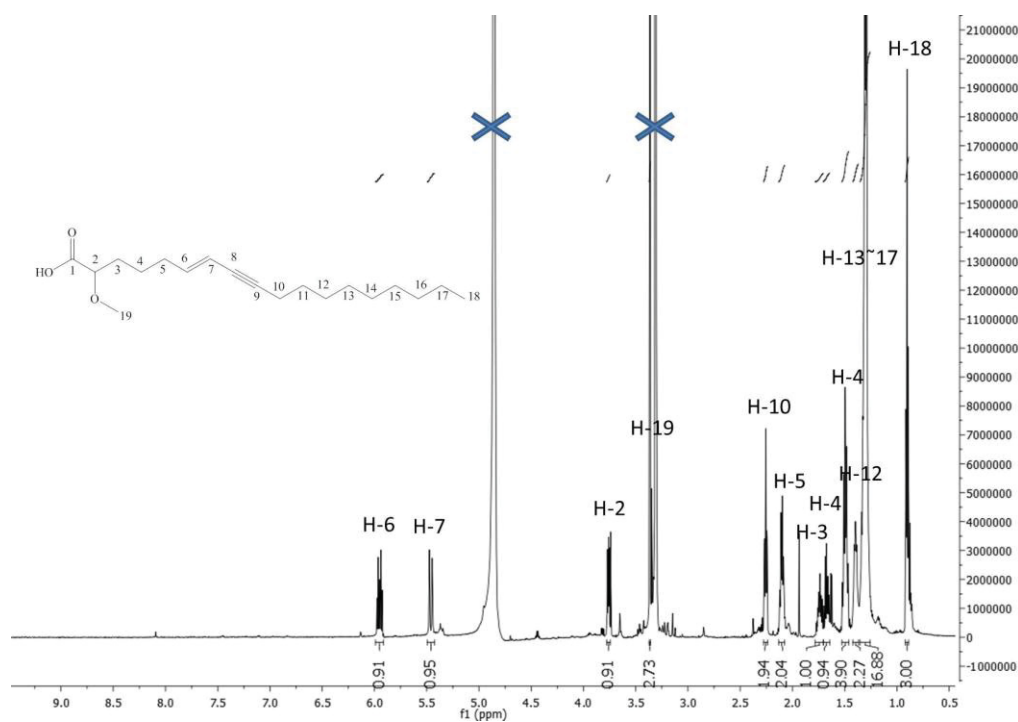
Supplementary Materials: The following are available online at www.mdpi.com/link, Supplementary Materials including HRESIMS, EIMS, 1D and 2D NMR spectra of **1 – 7**.

Acknowledgments: Financial support from BMBF (project BALIPEND) granted to P. P. and from Ministry of Science and Technology (MOST) to W. H. L. is gratefully acknowledged. A. M. gratefully acknowledges the Ministry of Science, Research and Technology (MSRT) of Iran for awarding him a scholarship. The authors acknowledge access to the Jülich-Düsseldorf Biomolecular NMR Center. T. K. thanks the National Research, Development and Innovation Office (NKFI K120181) for financial support. The authors are indebted to Dr. Nicole de Voogd (Leiden, Naturalis Biodiversity Center, Leiden, Netherlands) for identification of the sponge and acknowledge the support and help of Dr. Elizabeth Ferdinandus (University of Ambon, Indonesia) during sponge collection.

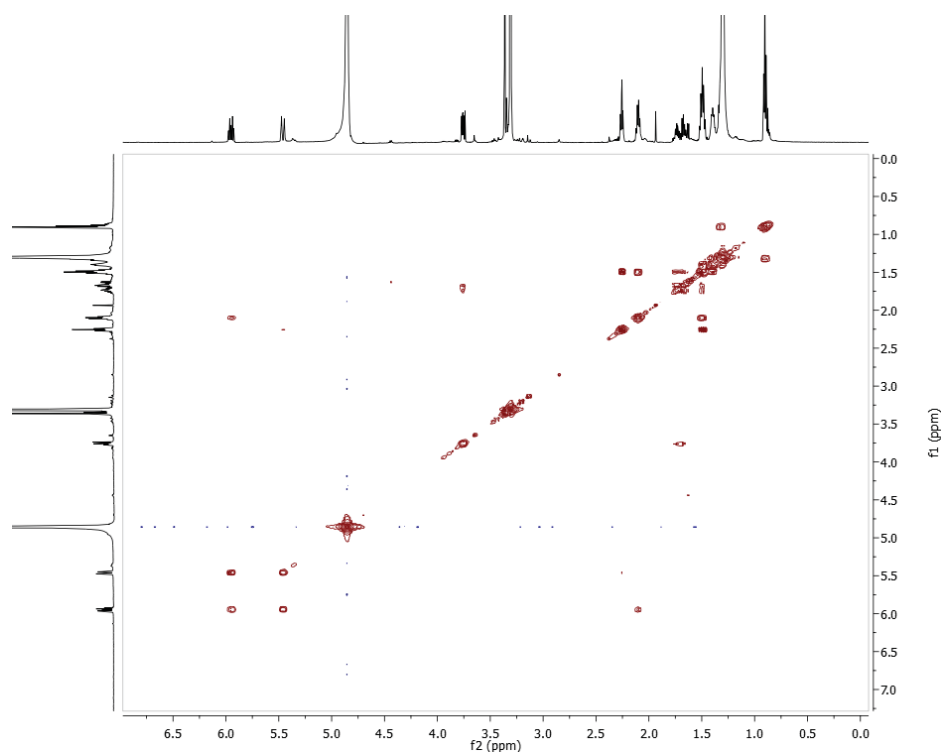
Conflicts of Interest: The authors declare no conflict of interest.

6.6 Supplementary material

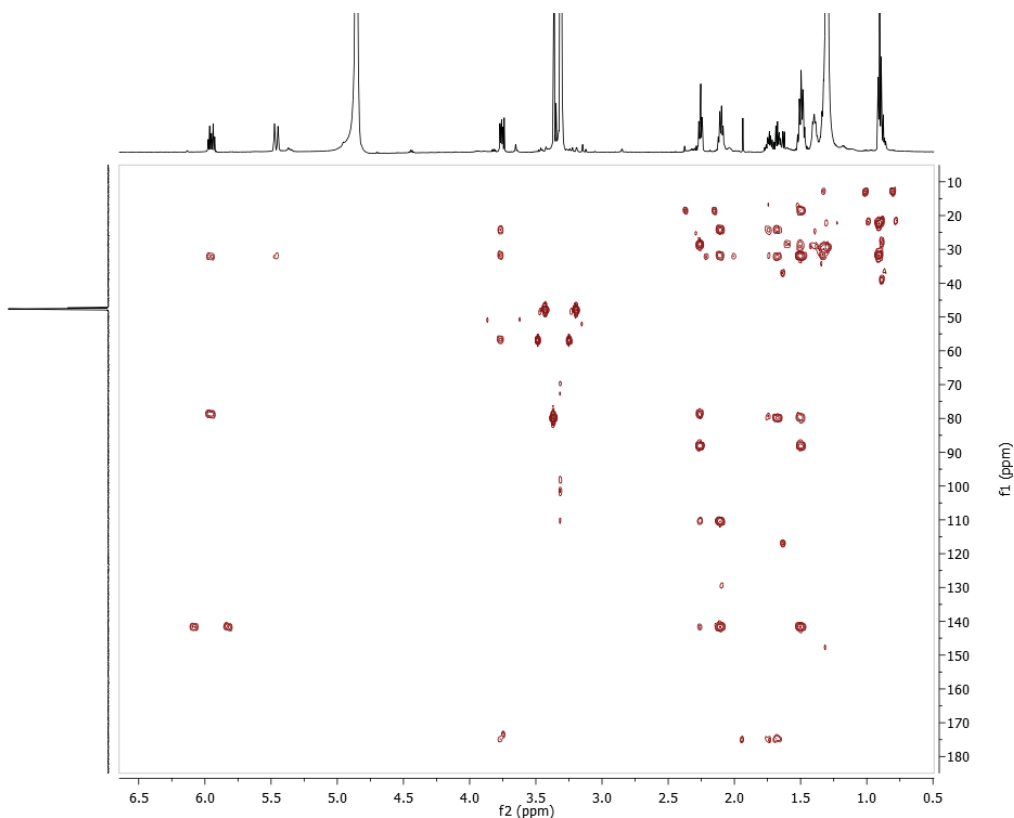
S1. Cinachylenic acid B (1)



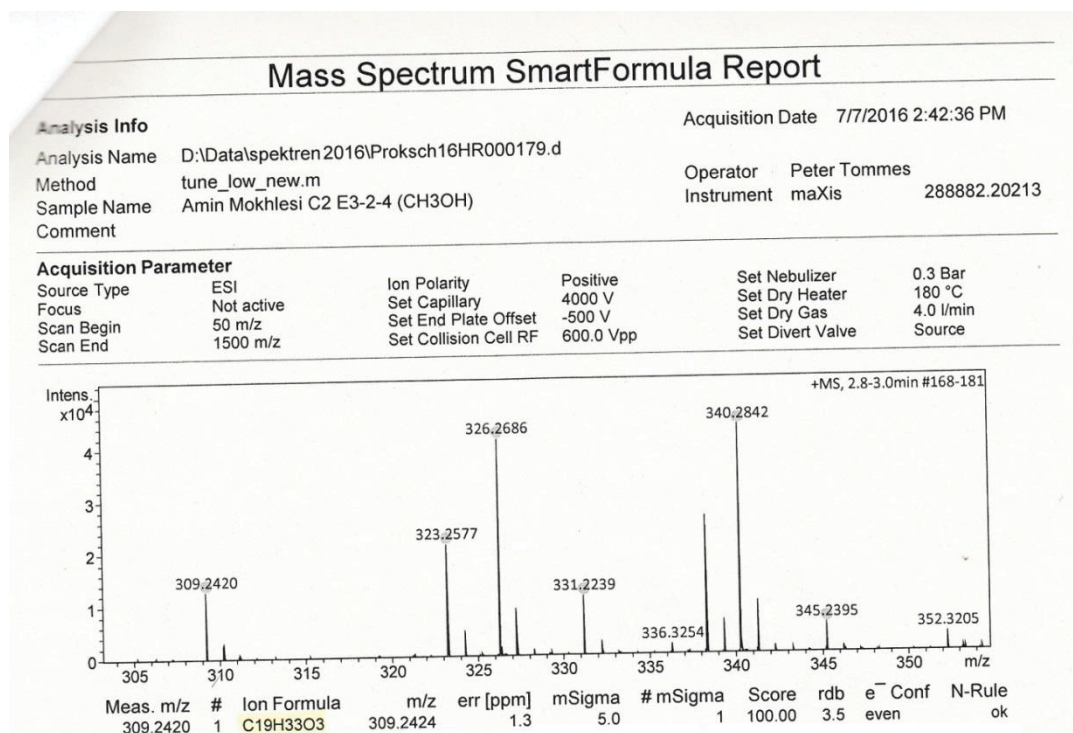
S1-1. ^1H NMR ($\text{MeOH-}d_4$, 600 MHz) spectrum of 1



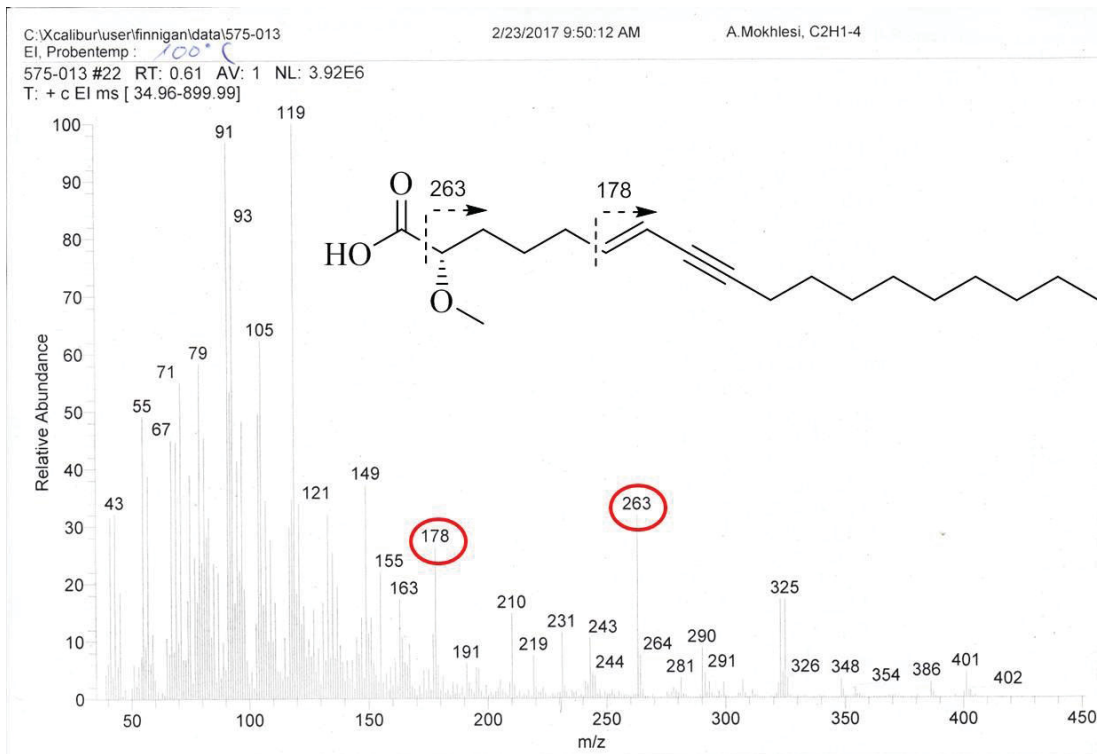
S1-2. COSY NMR ($\text{MeOH-}d_4$, 600 MHz) spectrum of 1



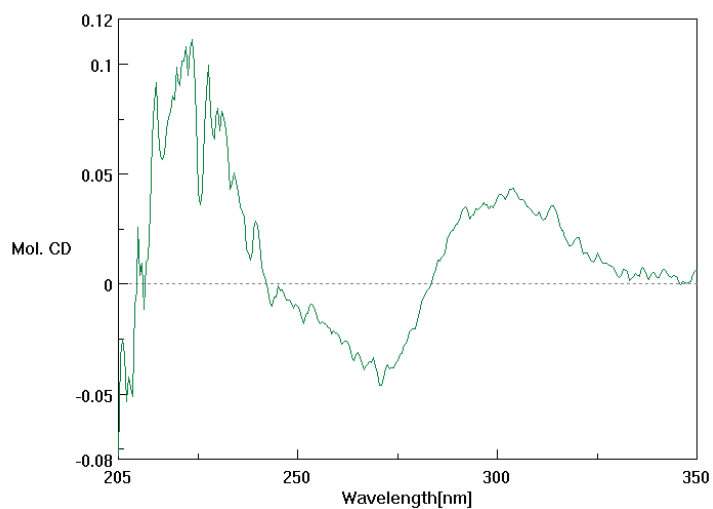
S1-3. HMBC NMR (MeOH-*d*₄, 600 MHz) spectrum of 1



S1-4. HRESIMS spectrum of 1



S1-5. EIMS spectrum of 1



S1-6. CD spectrum of 1

0.3 mg in 1.5 mL MeOH

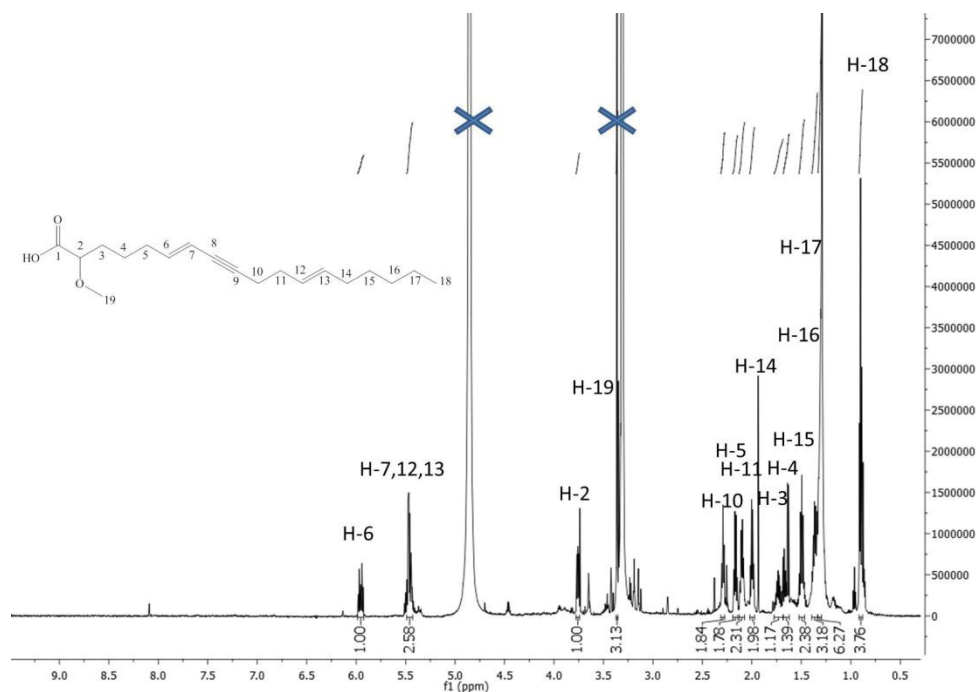
$c = 6.4838E-4$ M

cell length: 1 cm

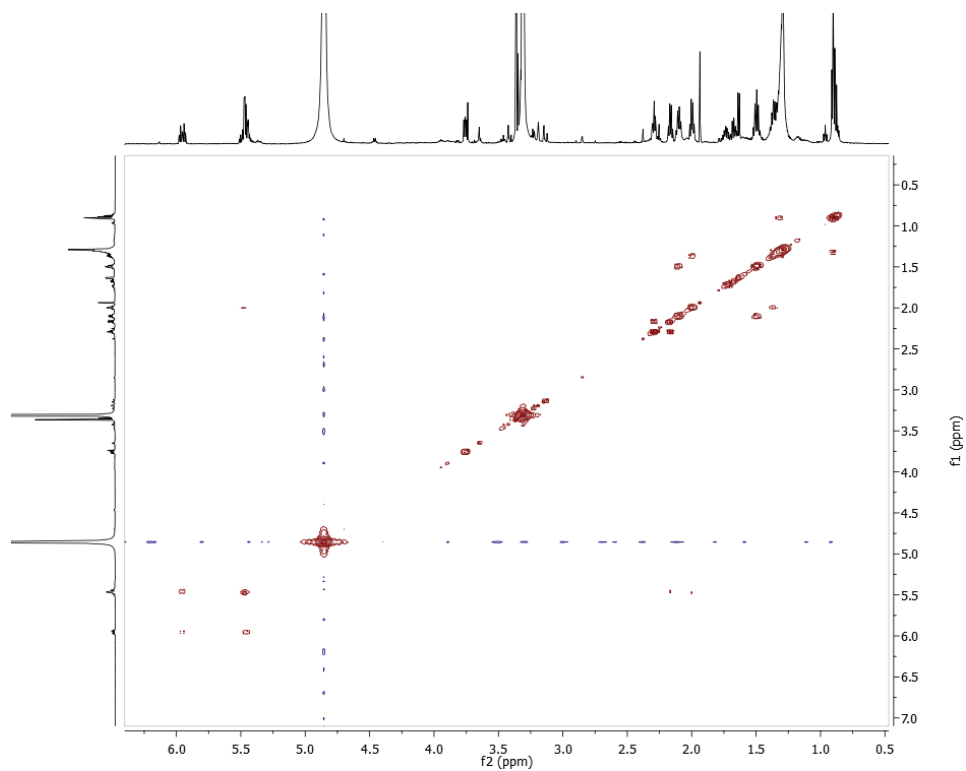
accumulation: 5

sensitivity: high (5 mdeg)

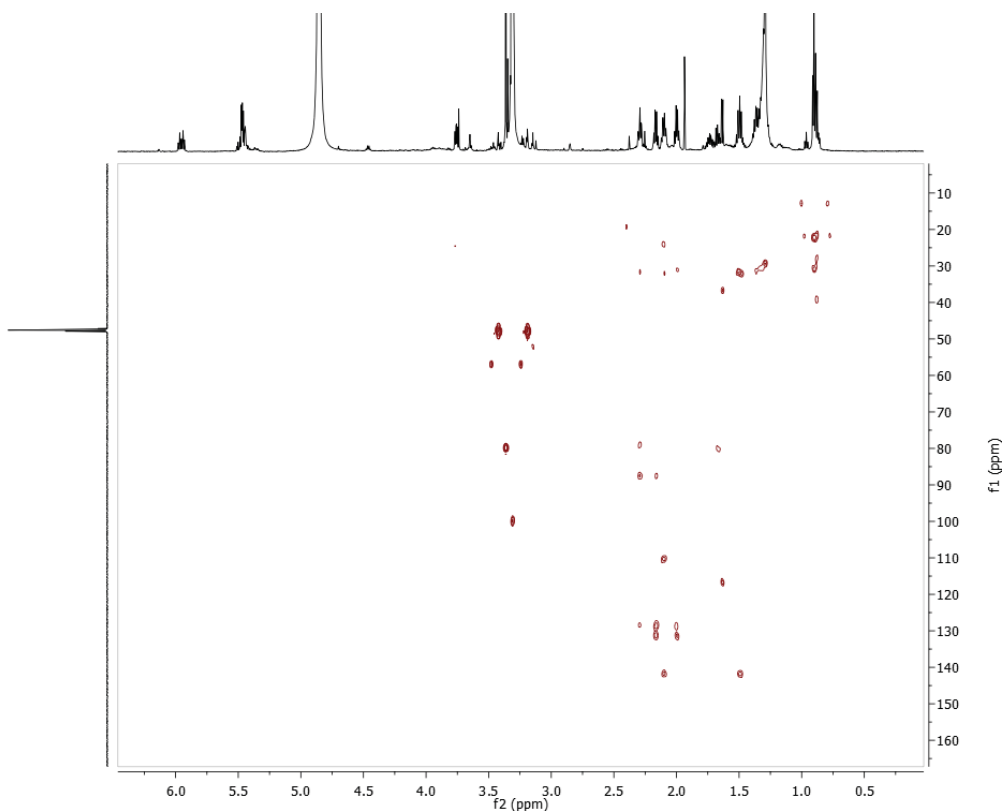
S2. Cinachylenic acid C (2)



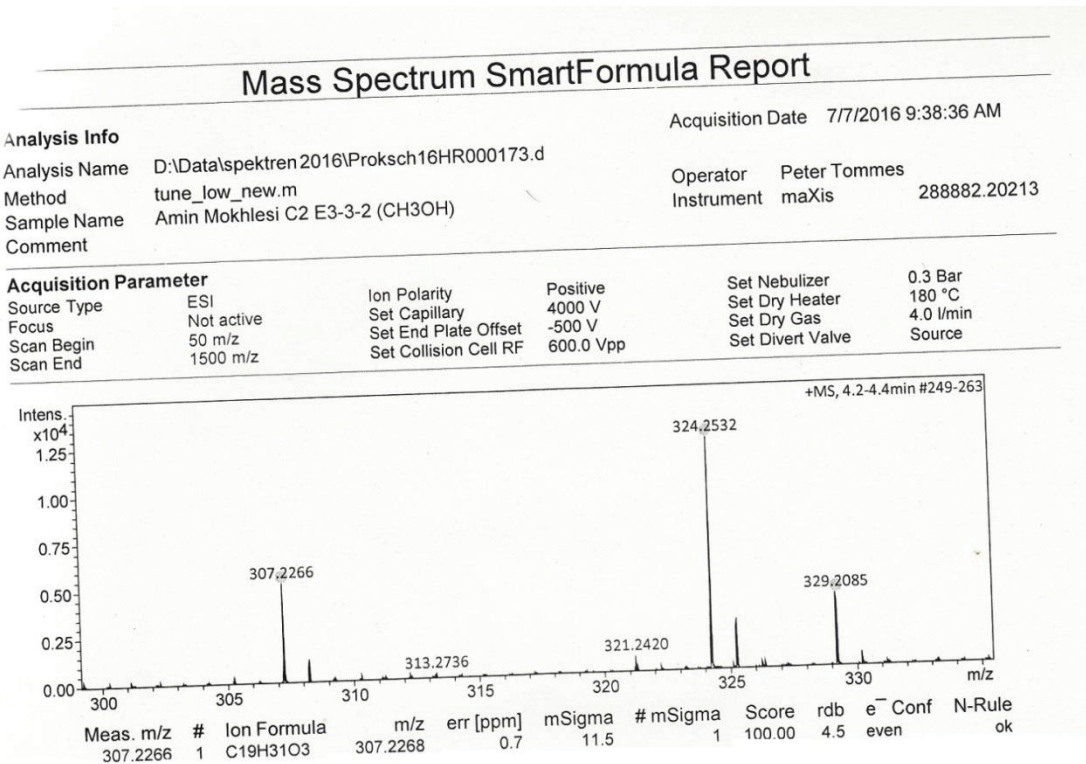
S2-1. ^1H NMR ($\text{MeOH-}d_4$, 600 MHz) spectrum of 2



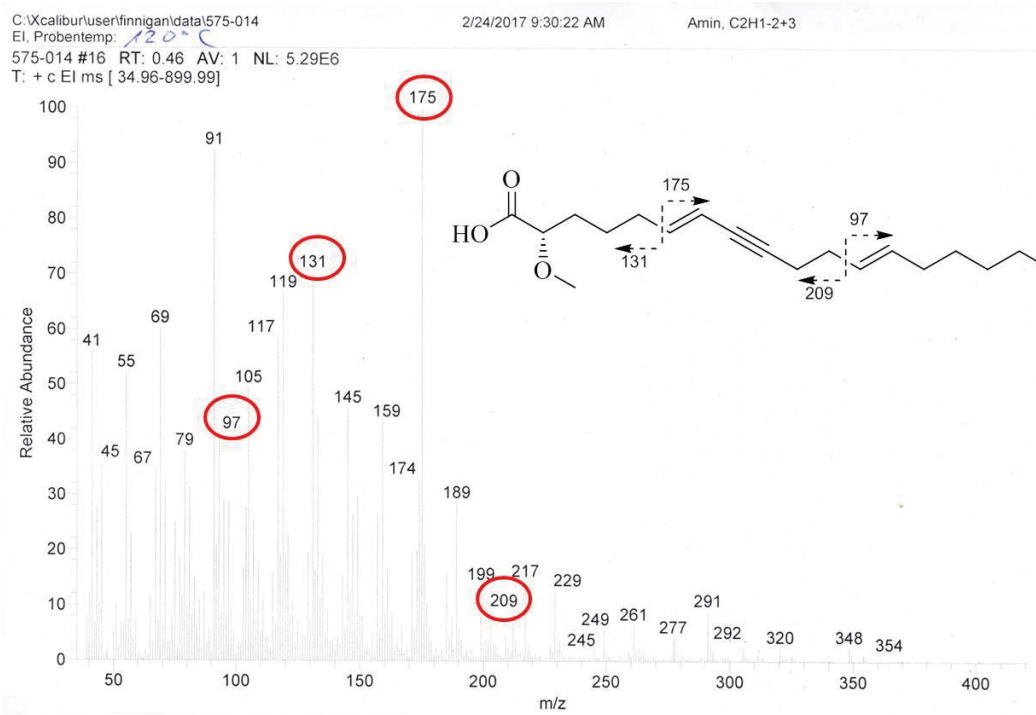
S2-2. COSY NMR ($\text{MeOH-}d_4$, 600 MHz) spectrum of 2



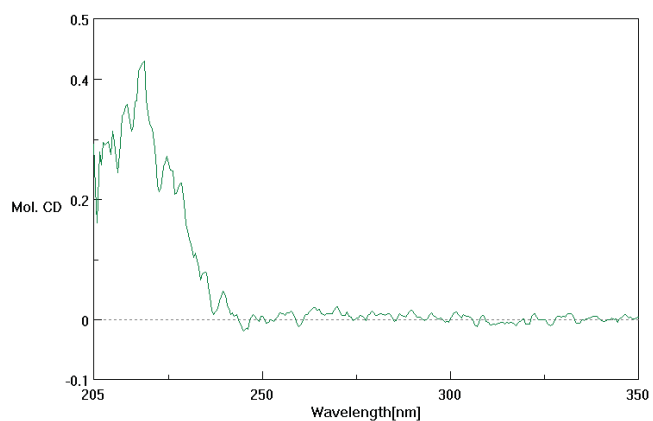
S2-3. HMBC NMR (MeOH-d₄, 600 MHz) spectrum of 2



S2-4. HRESIMS spectrum of 2



S2-5. EIMS spectrum of 2



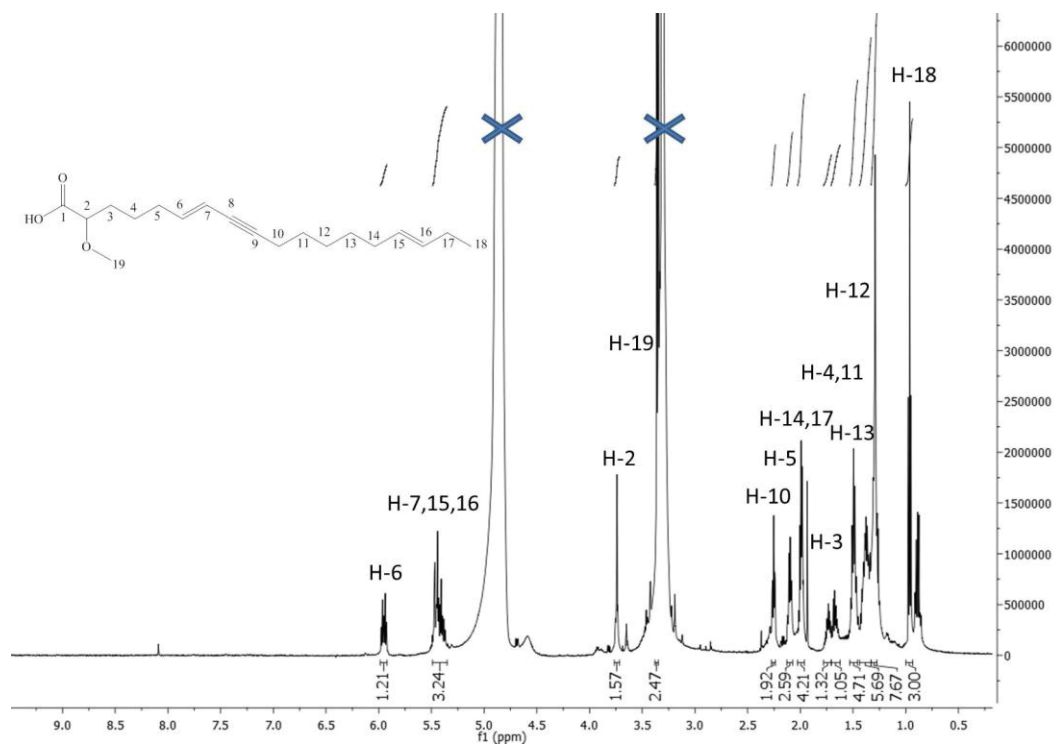
S2-6. CD spectrum of 2

0.3 mg in 2.5 mL MeOH

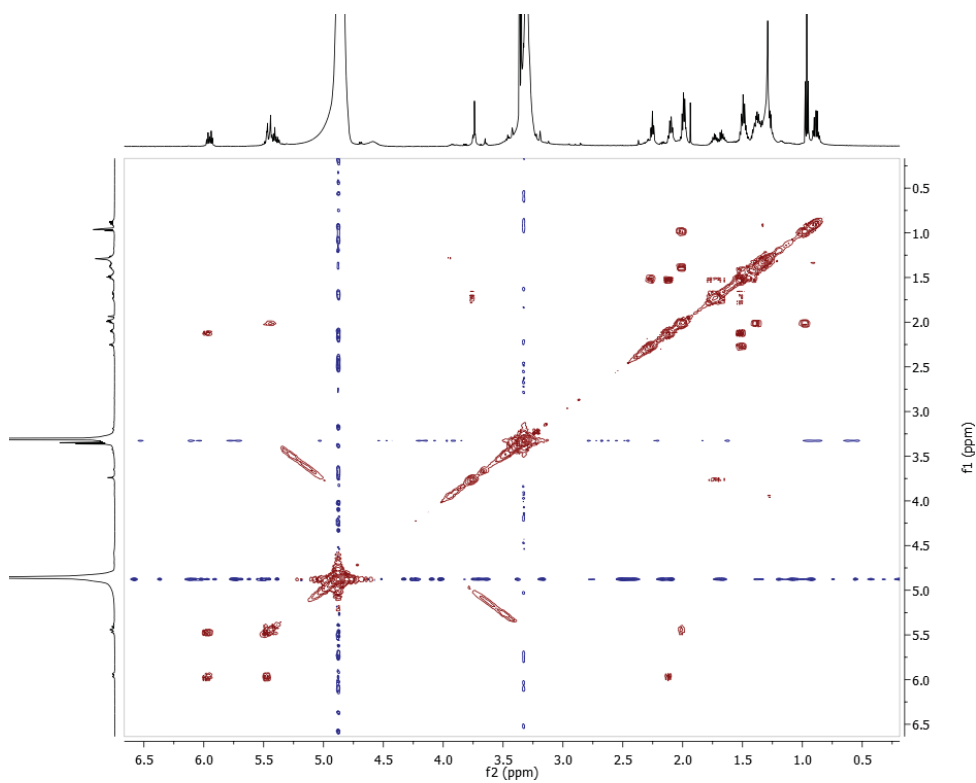
$c = 3.9159 \times 10^{-4}$ M

cell length: 1 cm

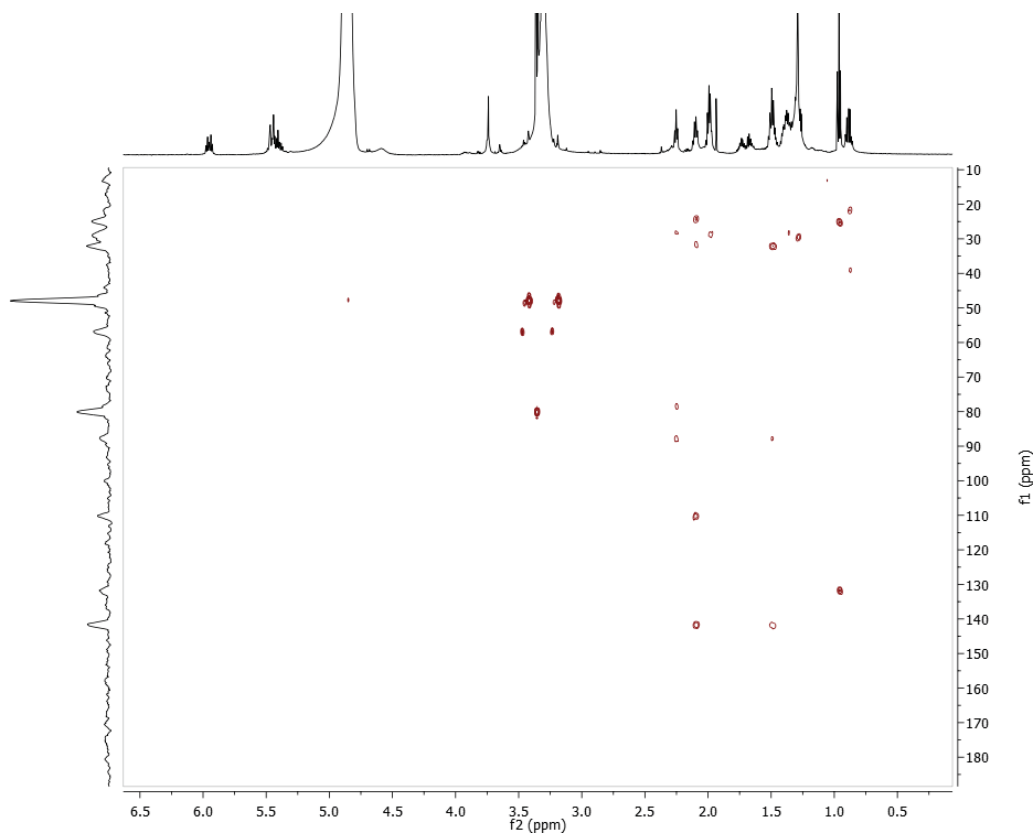
S3. Cinachylenic acid D (3)



S3-1. ^1H NMR (MeOH- d_4 , 600 MHz) spectrum of 3



S3-2. COSY NMR (MeOH- d_4 , 600 MHz) spectrum of 3



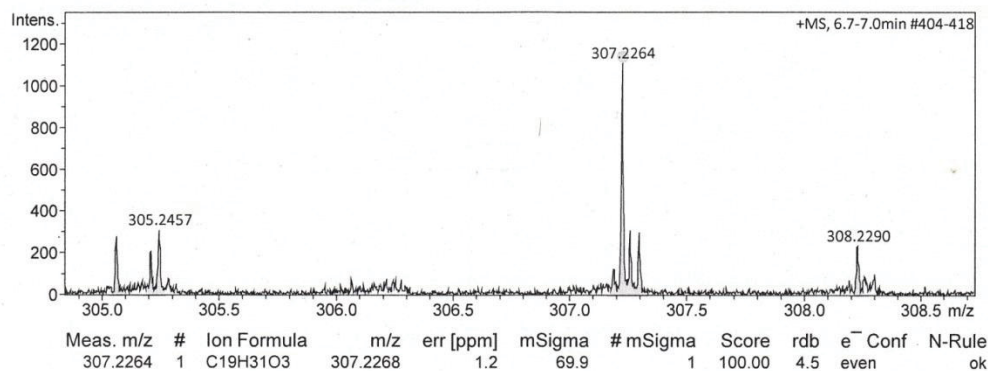
S3-3. HMBC NMR (MeOH- d_4 , 600 MHz) spectrum of 3

Mass Spectrum SmartFormula Report

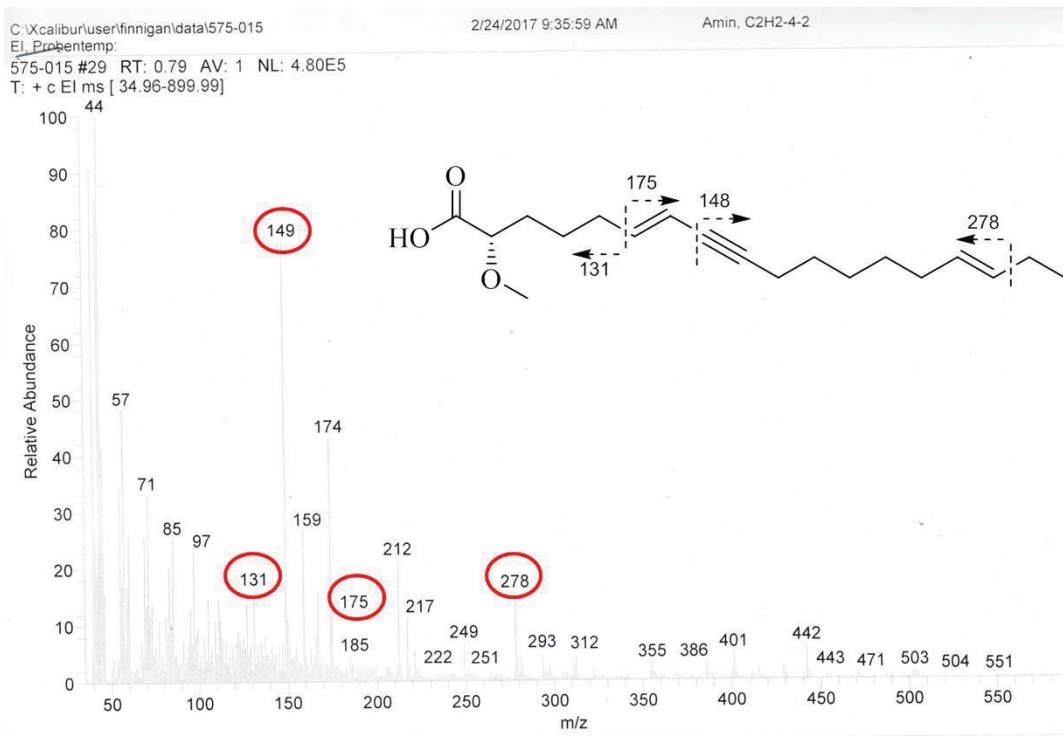
Analysis Info		Acquisition Date	3/17/2017 12:35:16 PM	
Analysis Name	D:\Data\spektren2017\Proksch17HR000112.d		Operator	Peter Tommes
Method	tune_low_new.m		Instrument	maXis 288882.20213
Sample Name	Amin C2E3-2-3 (CH3OH)			
Comment				

Acquisition Parameter

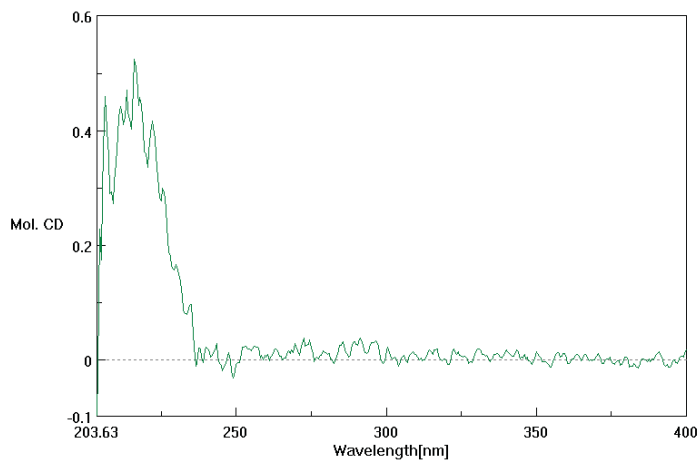
Source Type	ESI	Ion Polarity	Positive	Set Nebulizer	0.3 Bar
Focus	Not active	Set Capillary	4000 V	Set Dry Heater	180 °C
Scan Begin	50 m/z	Set End Plate Offset	-500 V	Set Dry Gas	4.0 l/min
Scan End	1500 m/z	Set Collision Cell RF	600.0 Vpp	Set Divert Valve	Source



S3-4. HRESIMS spectrum of 3



S3-5. EIMS spectrum of 3



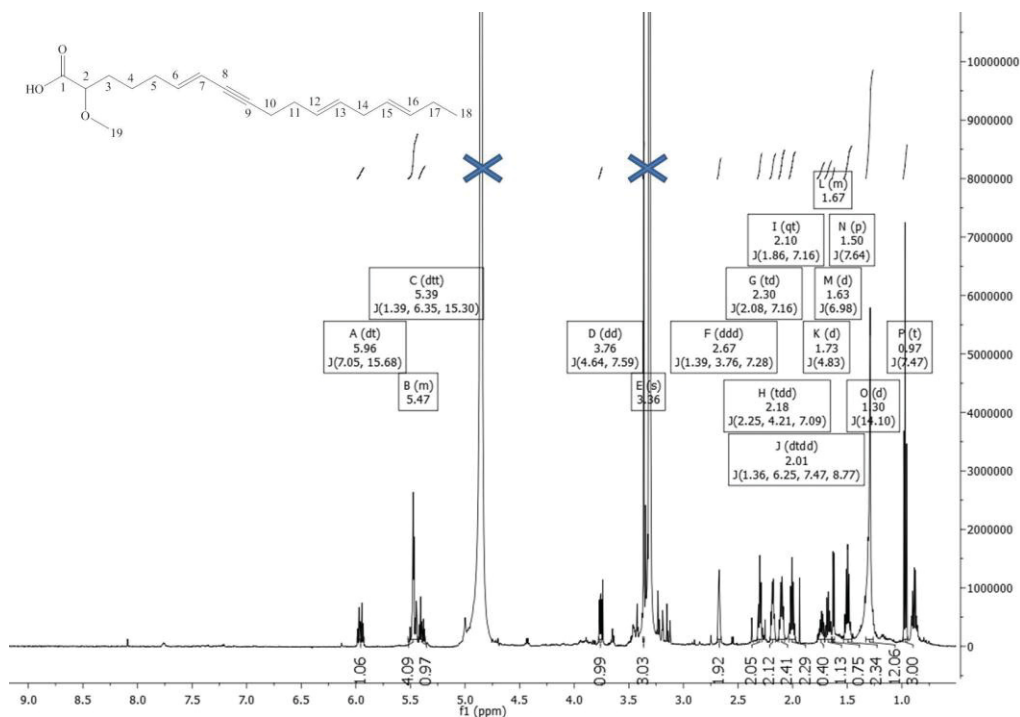
S3-6. CD spectrum of 3

0.3 mg in 4 mL MeOH

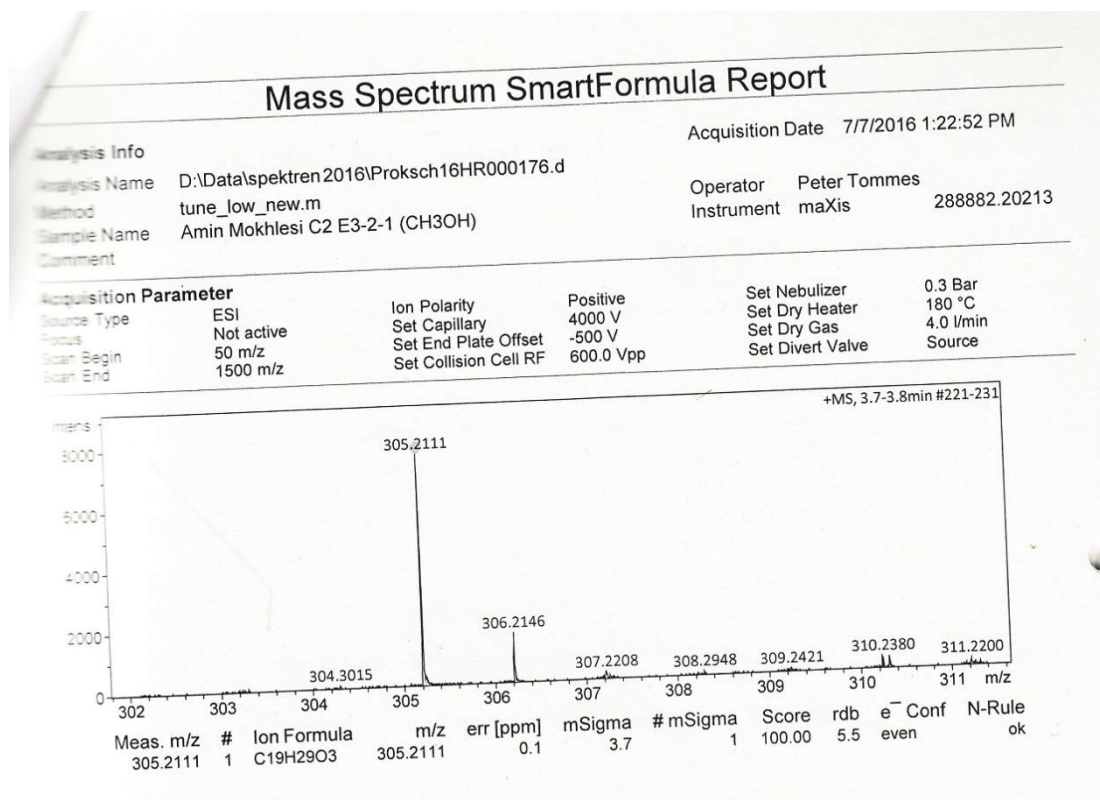
$c = 2.4475 \times 10^{-4}$ M

cell length: 1 cm

S4. Cinachylenic acid A (4)

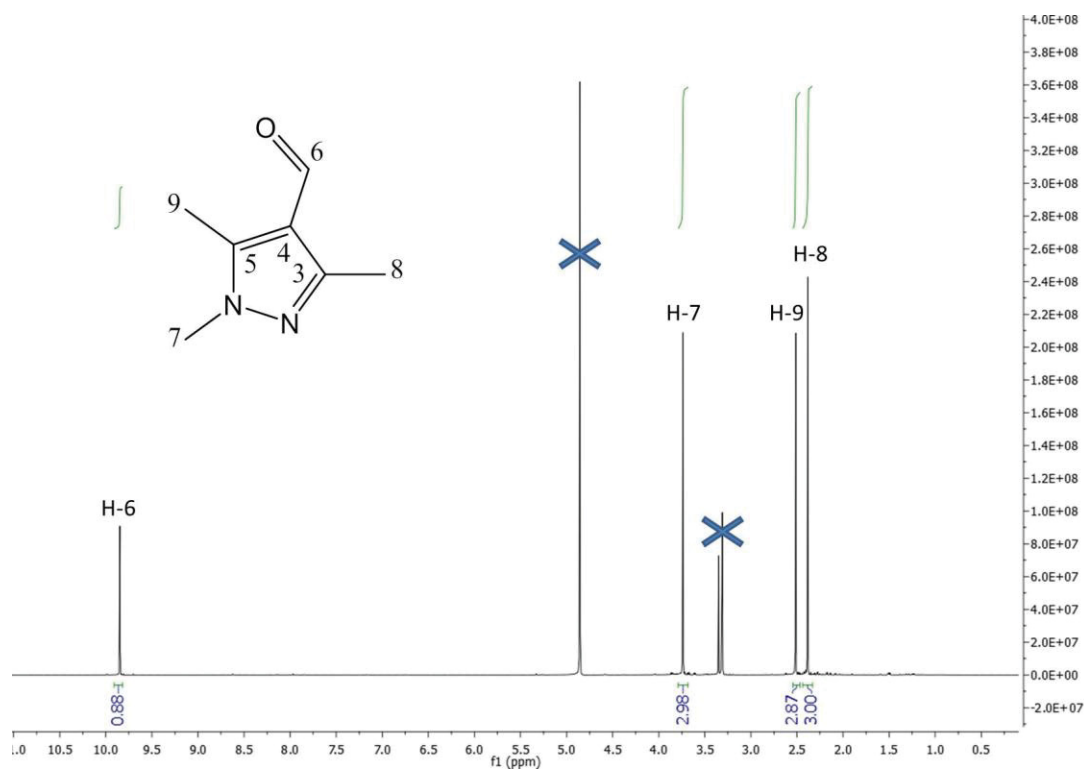


S4-1. ¹H NMR (MeOH-*d*₄, 600 MHz) spectrum of 4

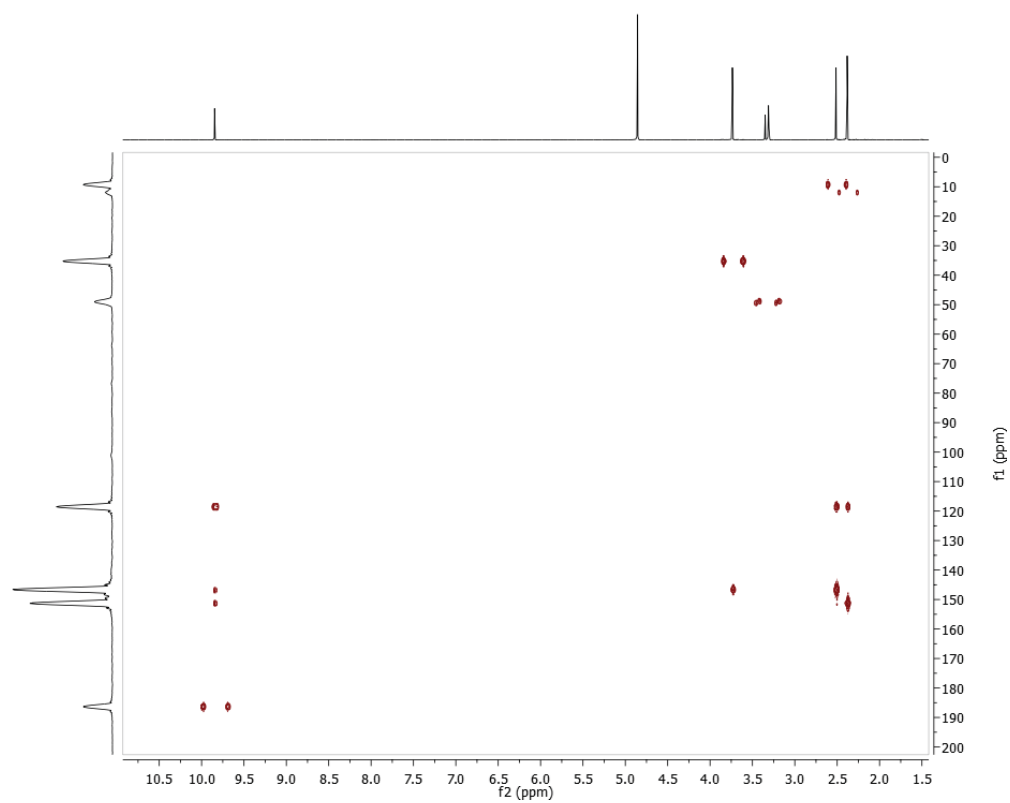


S4-2. HRESIMS spectrum of 4

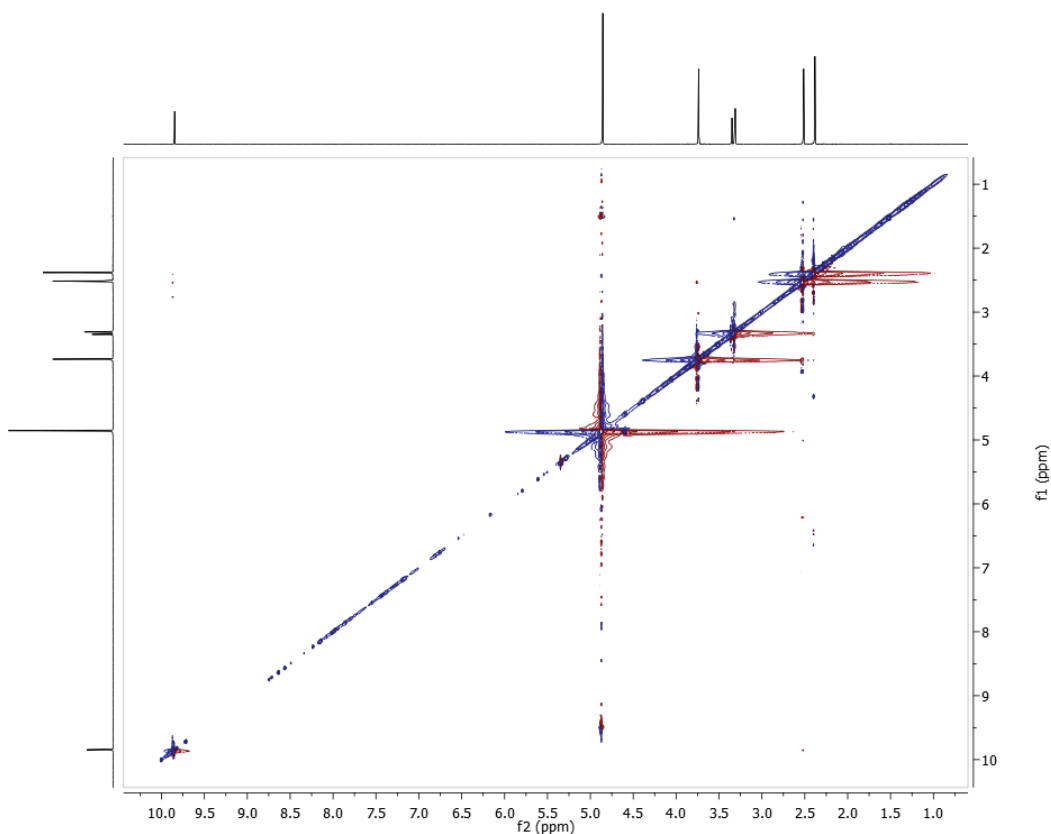
S5. Cinachyrazole A (5)



S5-1. ^1H NMR (MeOH- d_4 , 600 MHz) spectrum of 5



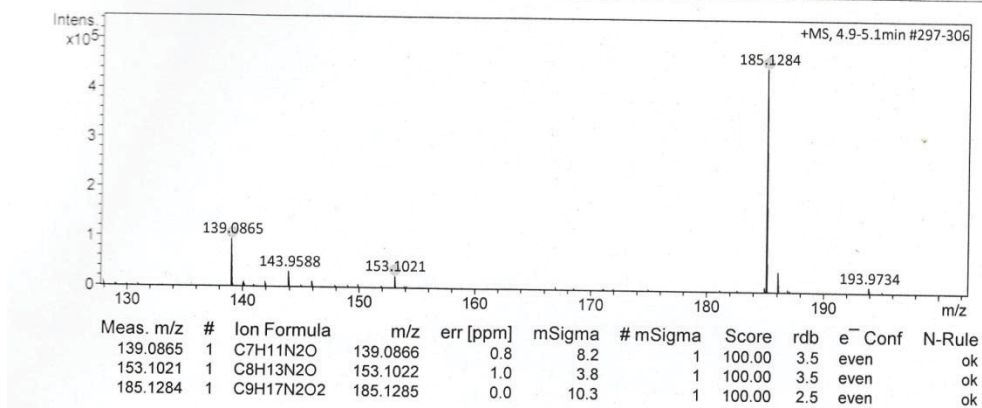
S5-2. HMBC NMR (MeOH- d_4 , 600 MHz) spectrum of 5



S5-3. ROESY NMR (MeOH- d_4 , 600 MHz) spectrum of 5

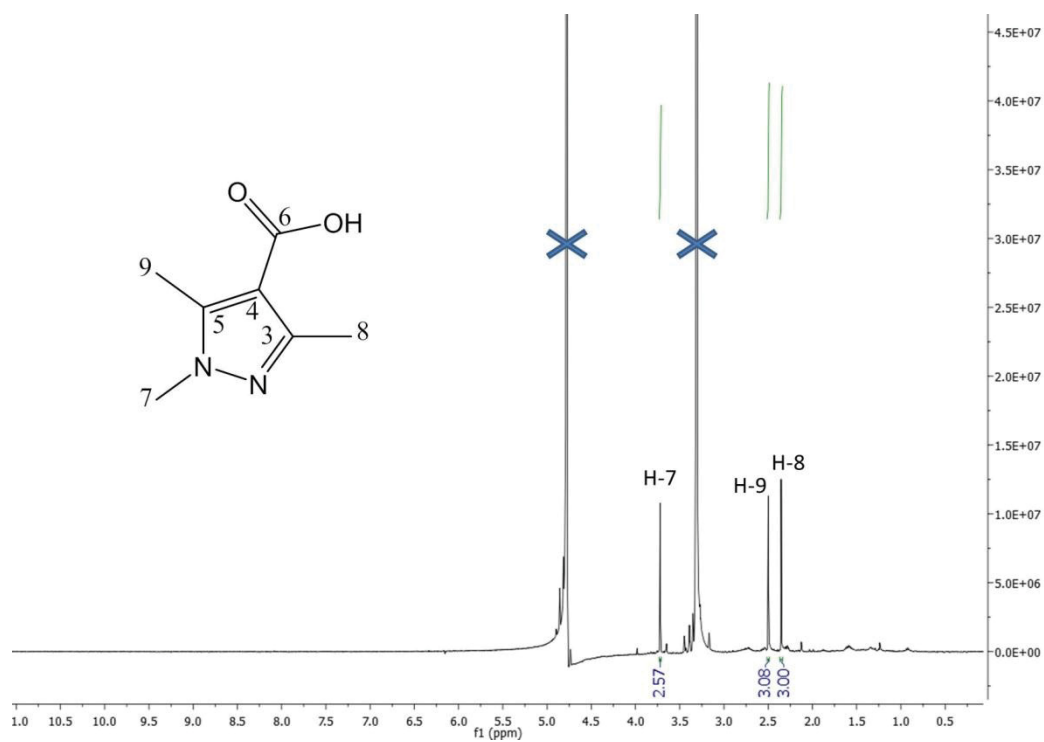
Mass Spectrum SmartFormula Report

Analysis Info		Acquisition Date	
Analysis Name	D:\Data\spektren2017\Proksch17HR000008.d	1/9/2017 3:42:53 PM	
Method	tune_low_new.m	Operator	Peter Tommes
Sample Name	Amin Mokhlesi C2E5-2 (CH3OH)	Instrument	maXis 288882.20213
Comment			
Acquisition Parameter			
Source Type	ESI	Ion Polarity	Positive
Focus	Not active	Set Capillary	4000 V
Scan Begin	50 m/z	Set End Plate Offset	-500 V
Scan End	1500 m/z	Set Collision Cell RF	600.0 Vpp
		Set Nebulizer	0.3 Bar
		Set Dry Heater	180 °C
		Set Dry Gas	4.0 l/min
		Set Divert Valve	Source

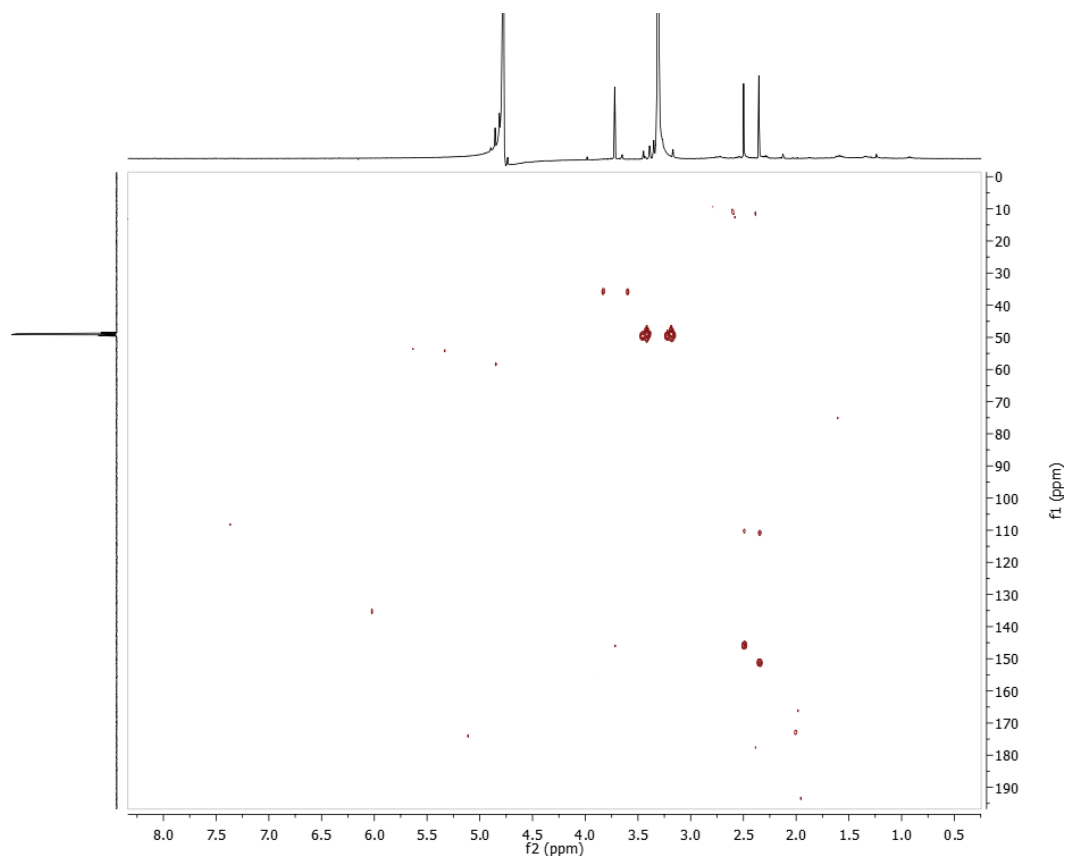


S5-4. HRESIMS spectrum of 5

S6. Cinachyrazole B (6)



S6-1. ^1H NMR (MeOH- d_4 , 600 MHz) spectrum of 6



S6-2. HMBC NMR (MeOH- d_4 , 600 MHz) spectrum of 6

Mass Spectrum SmartFormula Report

Analysis Info

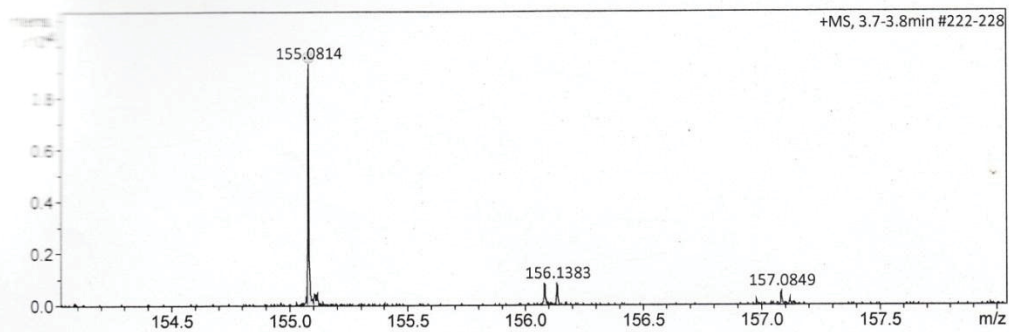
Analysis Name: D:\Data\Spektren\2017\Proksch17HR000025.d
 Method: tune_low_new.m
 Sample Name: Amin Wokhtlesi C2B5-2 (CH3OH)
 Comment:

Acquisition Date: 2/10/2017 9:29:17 AM

Operator: Peter Tommes
 Instrument: maXis 288882.20213

Acquisition Parameter

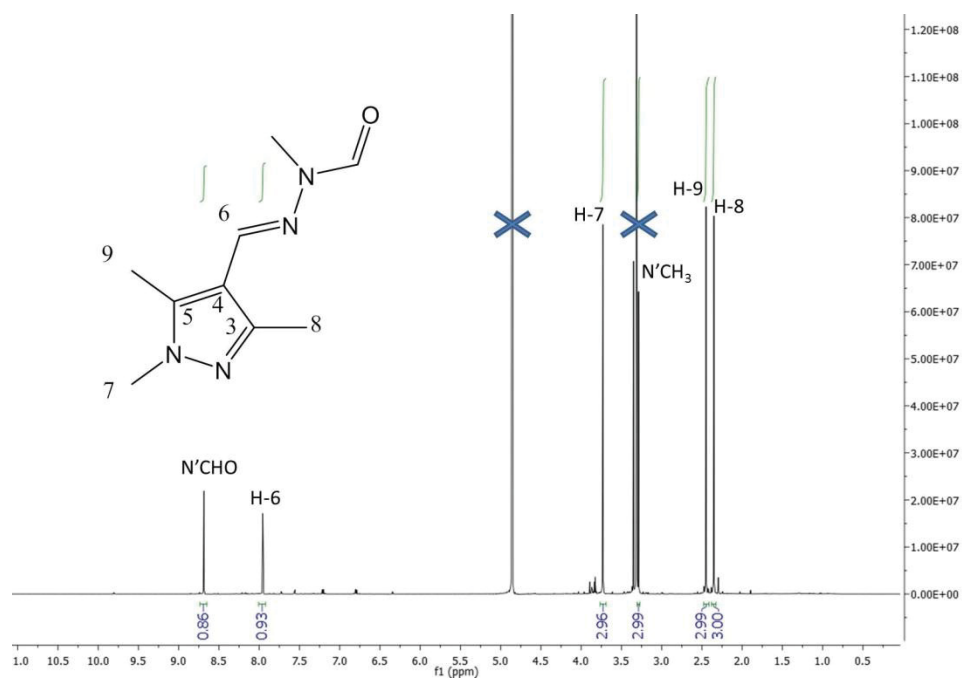
Source Type:	ESI	Ion Polarity:	Positive	Set Nebulizer:	0.3 Bar
Focals:	Not active	Set Capillary:	4000 V	Set Dry Heater:	180 °C
Scan Begin:	50 m/z	Set End Plate Offset:	-500 V	Set Dry Gas:	4.0 l/min
Scan End:	1500 m/z	Set Collision Cell RF:	600.0 Vpp	Set Divert Valve:	Source



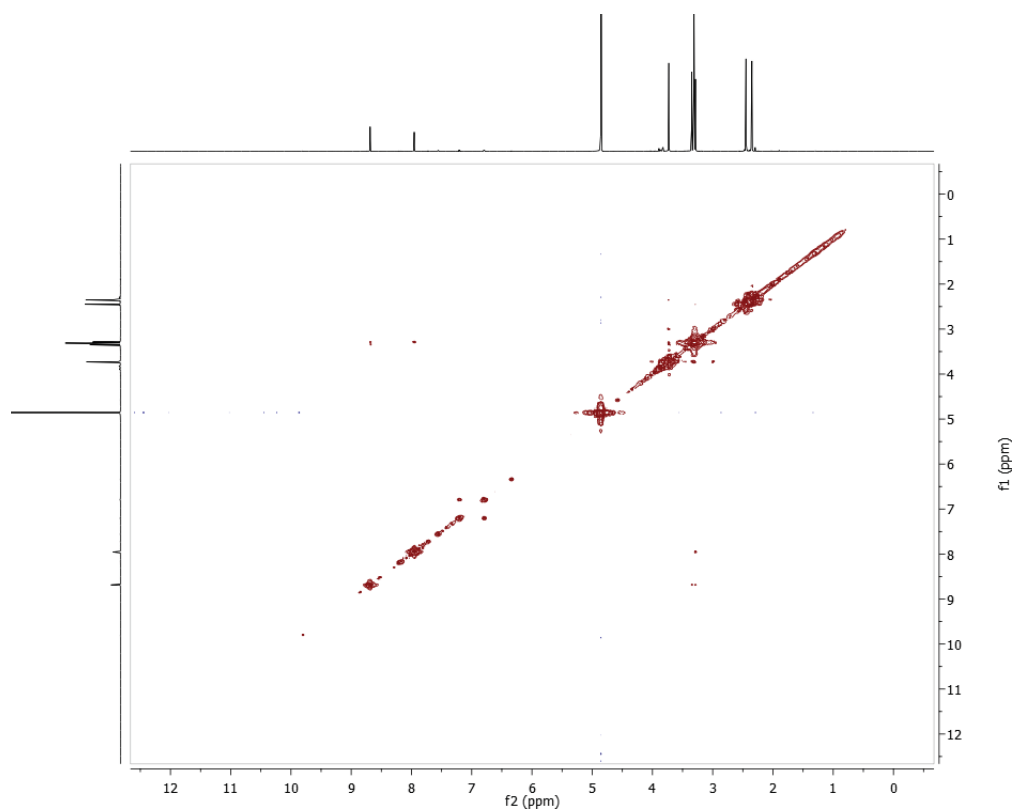
Meas. m/z	#	Ion Formula	m/z	err [ppm]	mSigma	# mSigma	Score	rdb	e ⁻ Conf	N-Rule
155.0814	1	C7H11N2O2	155.0815	0.6	27.8	1	100.00	3.5	even	ok

S6-3. HRESIMS spectrum of 6

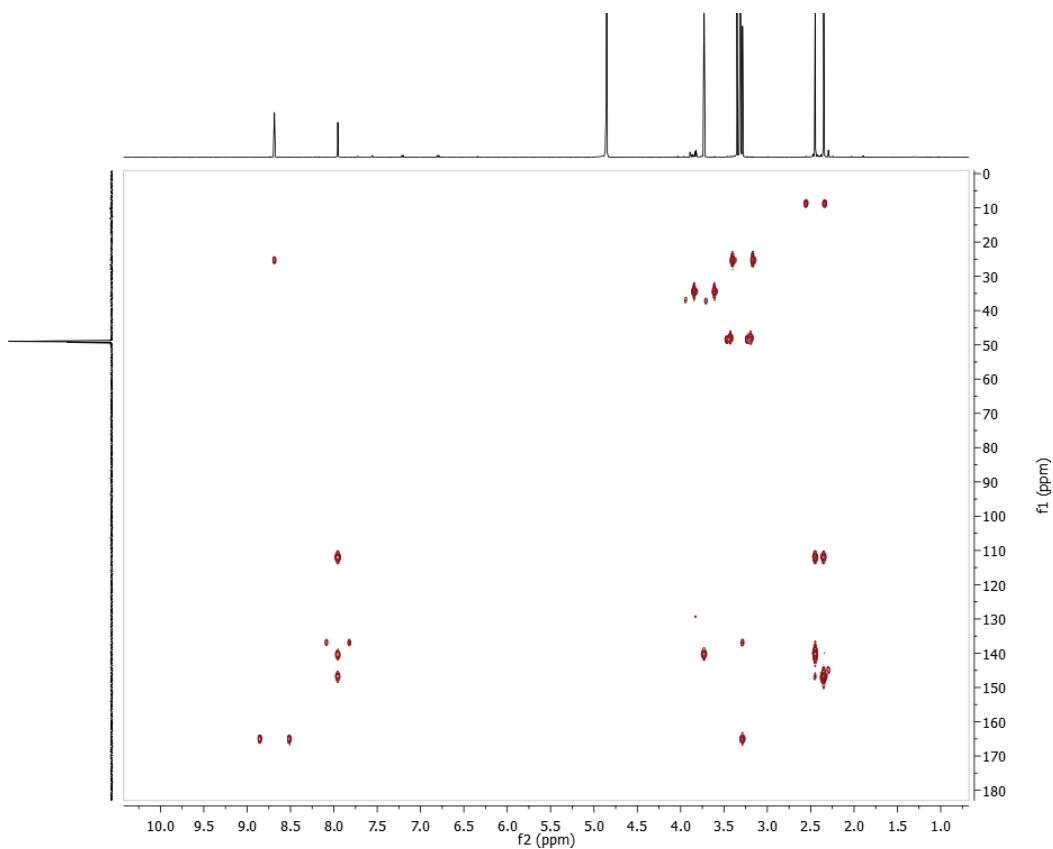
S7. Cinachyrazole C (7)



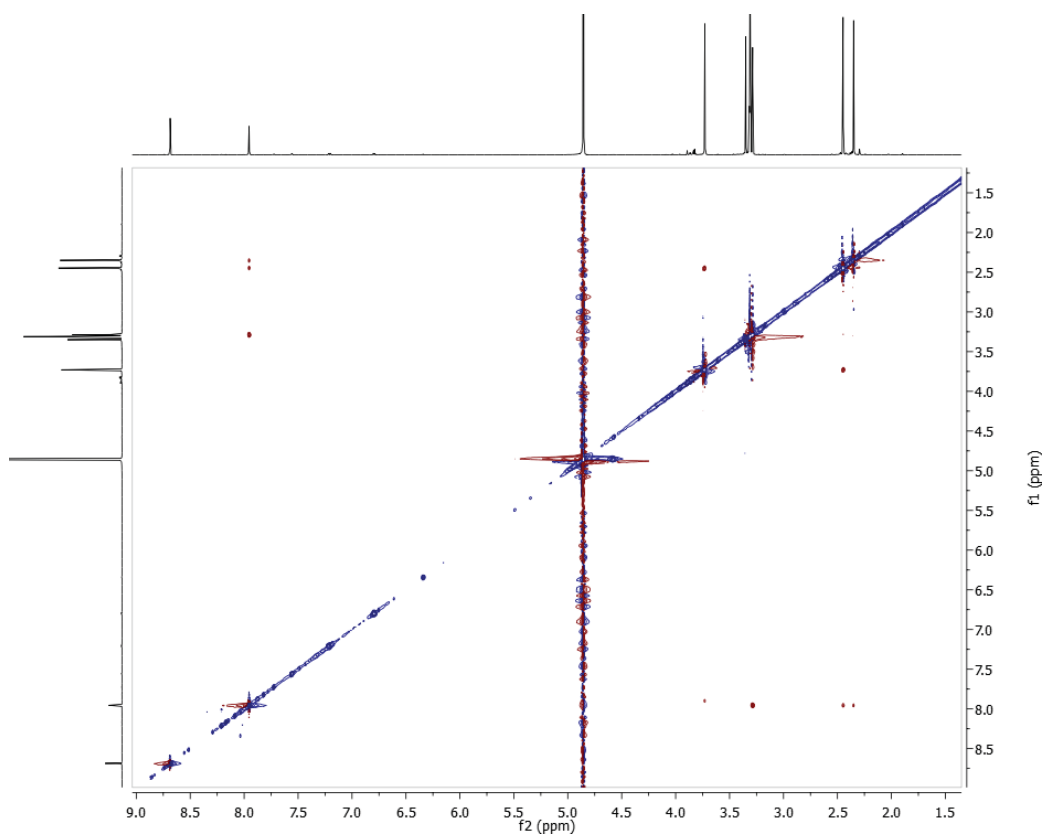
S7-1. ¹H NMR (MeOH-*d*₄, 600 MHz) spectrum of 7



S7-2. COSY NMR (MeOH-*d*₄, 600 MHz) spectrum of 7



S7-3. HMBC NMR (MeOH-*d*₄, 600 MHz) spectrum of 7



S7-4. ROESY NMR (MeOH-*d*₄, 600 MHz) spectrum of 7

Mass Spectrum SmartFormula Report

Analysis Info

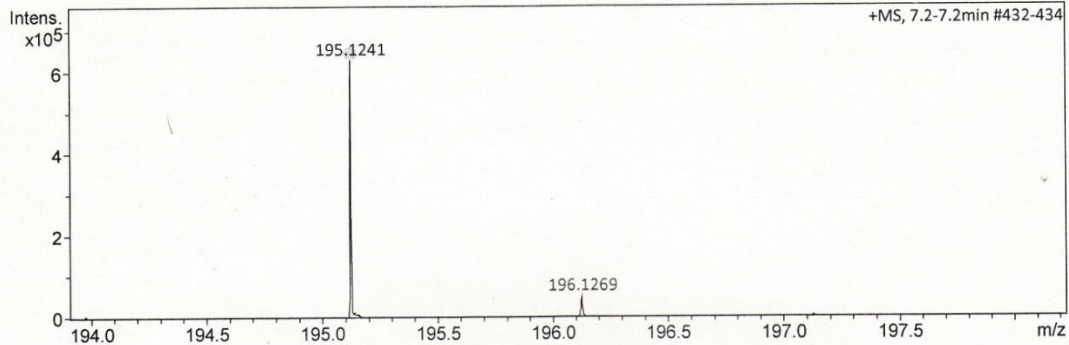
Analysis Name D:\Data\spektren 2017\Proksch17HR000006.d
Method tune_low_new.m
Sample Name Amin Mokhlesi C2E5-3 (CH3OH)
Comment

Acquisition Date 1/4/2017 3:09:42 PM

Operator Peter Tommes
Instrument maXis 288882.20213

Acquisition Parameter

Source Type	ESI	Ion Polarity	Positive	Set Nebulizer	0.3 Bar
Focus	Not active	Set Capillary	4000 V	Set Dry Heater	180 °C
Scan Begin	50 m/z	Set End Plate Offset	-500 V	Set Dry Gas	4.0 l/min
Scan End	1500 m/z	Set Collision Cell RF	600.0 Vpp	Set Divert Valve	Source



Meas. m/z	#	Ion Formula	m/z	err [ppm]	mSigma	# mSigma	Score	rdb	e ⁻ Conf	N-Rule
195.1241	1	C8H19O5	195.1227	-7.3	7.8	1	62.61	-0.5	even	ok

S7-5. HRESIMS spectrum of 7

7 Discussion

7.1 Natural products from *Lissodendoryx (Acanthodoryx) fibrosa*

Sponges of the genus *Lissodendoryx* are well known for the production of polyether macrolides, such as the halichondrins.¹²⁰ Several other types of secondary metabolites have been described from *Lissodendoryx (Acanthodoryx)* species, such as steroids,¹²¹ cembranes,¹²² and pyrrololactams.¹²³

7.1.1 *Lissodendrins A and B*

Two new alkaloids lissodendrins A and B were isolated from the EtOAc extract fraction of the Indonesian marine sponge *Lissodendoryx (Acanthodoryx) fibrosa*. Lissodendrins A and B were determined as 2-aminoimidazole alkaloids. Finding the chemical structures of lissodendrins, particularly for lissodendrin B, was challenging. The ¹H NMR spectrum of lissodendrin B showed two para-disubstituted benzene rings. The challenge faced was to determine the connection part between the two benzene rings, corresponding to the molecular formula C₄H₃N₃O. Further attempts to isolate these compounds led to 0.5 mg lissodendrin A and 3 mg lissodendrin B. In addition, attempts were made to change the solvent, temperature and/or pH parameters during the NMR measurements. The HRESIMS/MS fragmentation as well as long-range HMBC correlations were employed for further characterization of the structures.

In the ¹H NMR spectrum of lissodendrin B, changing of temperature indicated signals above 8 ppm, which were broad due to dynamic exchange processes, such as in the case of protons attached to heteroatoms. However, at 30°C the signals A and B appeared sharper in the ¹H NMR spectrum (Figure 7.1.1a). The integral of the signals in the proton spectrum showed that the signal C corresponds to two protons (NH₂) while the signals A and B correspond to one proton (NH) each.

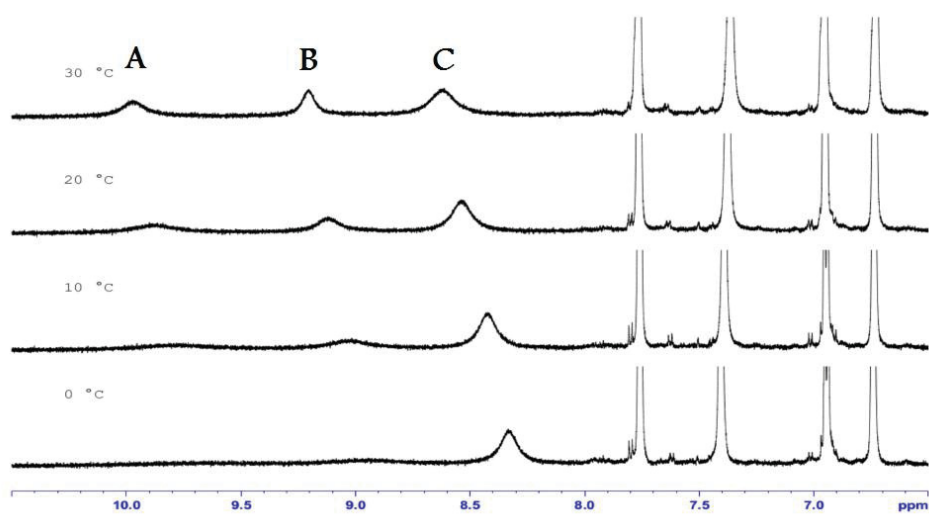


Figure 7.1.1a. Temperature dependence of the protons A, B and C in lissodendrin B (¹H NMR, 600MHz)

In addition, the one-dimensional ^1H , ^{15}N -HSQC spectrum of lissodendrin B confirmed the direct binding of a proton to nitrogen (Figure 7.1.1.b).

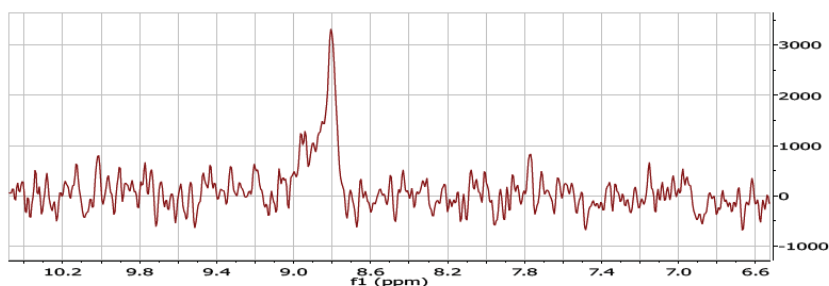


Figure 7.1.1b. 1D ^1H , ^{15}N -HSQC spectrum of lissodendrin B, 20 C, L = 600MHz

The results from the afore mentioned measurements indicated the presence of a guanidine moiety connected with two benzene rings. Finally, the structure of lissodendrin B was unambiguously elucidated based on long-chain HMBC correlations, as shown in Figure 7.1.1c.

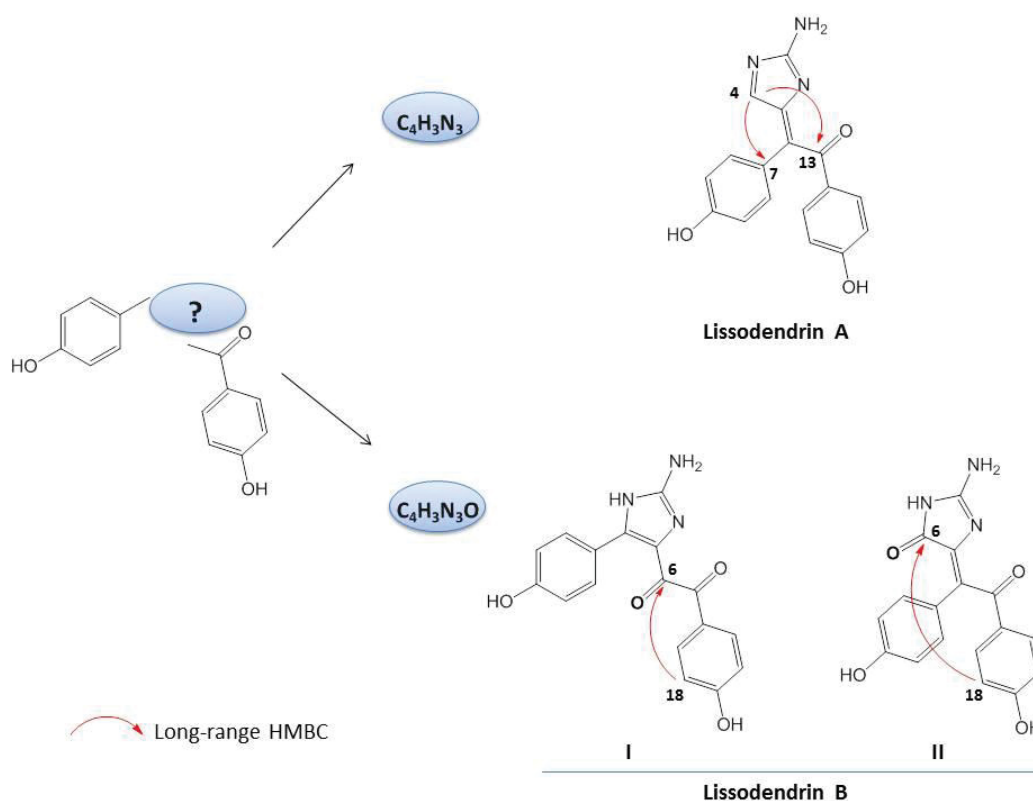


Figure 7.1.1c. Structure elucidation of lissodendrin A and B based on long-chain HMBC correlations. Lissodendrin B (I) is the only possible structure with 5J long-range HMBC

correlation from 18-H to C-6, while 7J long-range HMBC is not explainable for the proposed lissodendrin B (II).

The long-range HMBC measurement is a popular method for assembling different parts of a molecule into a complete structure.¹²⁴ There are several studies that use long-range HMBC correlations ($^n J_{C,H}$ $n>3$) for structure elucidation of heteroatom-rich compounds, such as ellagic acid derivatives, promothiocin B, distamycin A, and dichapetalin D (Figure 7.1.1d).¹²⁵ Likewise, lissodendrins A and B are good examples for using long-range HMBC correlations for structure determination.

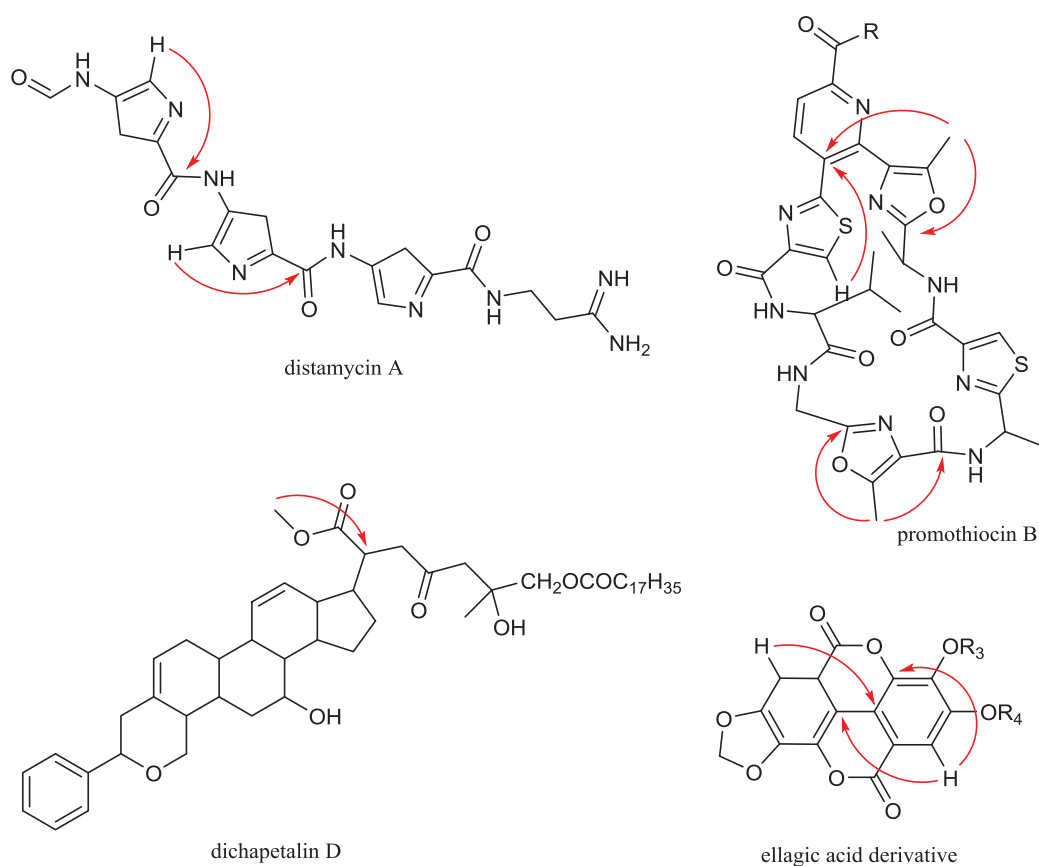


Figure 7.1.1d. Key $^4J(CH)$ and $^5J(CH)$ HMBC correlations of distamycin A, promothiocin B, dichapetalin D, and ellagic acid derivatives.

Although, lissodendrins showed no cytotoxicity toward mouse lymphoma cell line (L5178Y), the pharmaceutical role of 2-aminoimidazole derivatives has been proven in several reports.¹²⁶ The 2-aminoimidazole moiety plays an important role in the bioactivity of these compounds. Based on the donor-acceptor hydrogen bond and lower pKa value compared to that from guanidine, the 2-aminoimidazole moiety is a unique guanidine mimic for medicinal chemistry with high chances for cellular influence (Figure 7.1.1e).¹²⁶ Moreover, the 2-aminoimidazole is reported to potentially interact with aspartic acid in the catalytic site of enzymes, such as β -secretase involved in Alzheimer's disease.¹²⁷ Antioxidant

phorbatopsins isolated from the sponge *Phorbas topsenti*,¹²⁸ cytotoxic polyandrocarpamines from the ascidian *Polyandrocarpa* sp.,¹²⁹ antitumor naamines from the sponge *Leucetta chagosensis*, kinase inhibitor hymenialdisine from *Stylissa massa*,¹³⁰ and antimicrobial oroidin from the sponge *Agelas oroides*,¹³¹ are a few examples of bioactive 2-aminoimidazole natural products (Figure 7.1.1f).

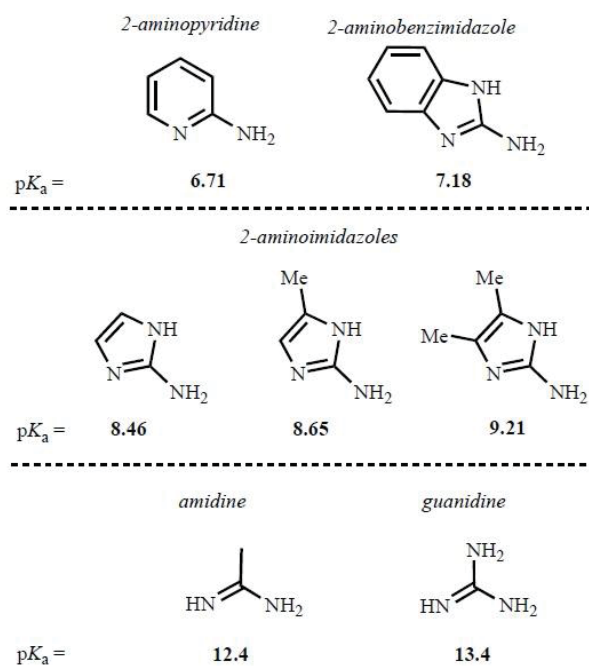


Figure 7.1.1e. pK_a values of common guanidine mimetics (equilibrium with the protonated species).¹²⁶

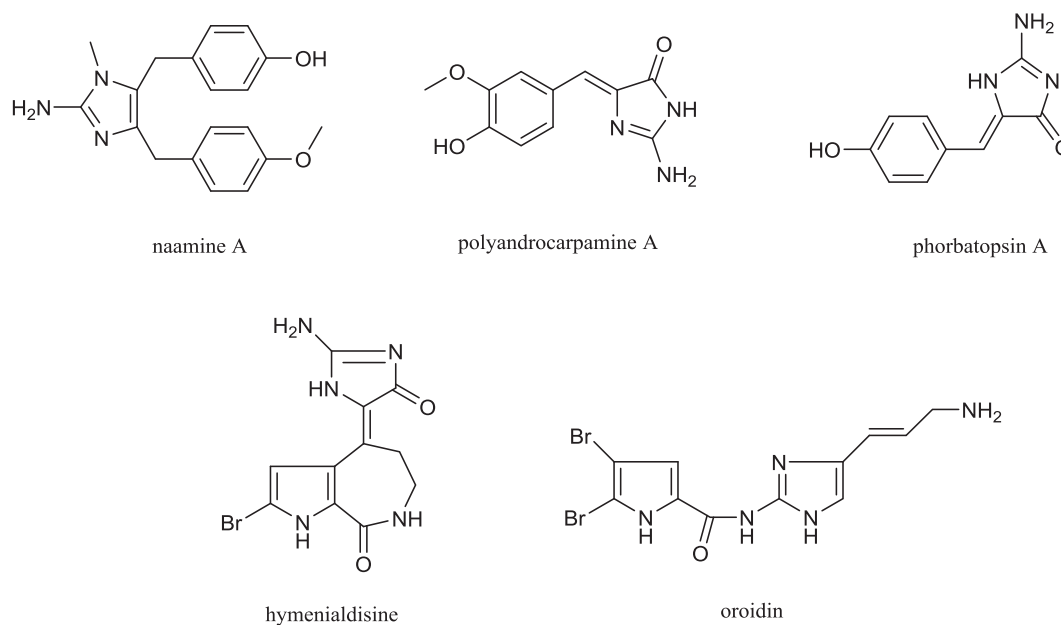


Figure 7.1.1f. Structures of bioactive 2-aminoimidazole natural products

In addition, lissodendrin B exhibited an unusual diketone moiety that is rarely reported in natural products, including hamigeranes B and G from the sponge *Hamigera tarangaensis*,¹³² hyrtiosin B from the sponge *Hyrtios* sp.¹³³, tryptethelone from marine fungi,¹³⁴ and elisabatins B from the sea whip *Pseudopterogorgia elisabethae*.¹³⁵ (Figure 7.1.1g).

In this study, a biosynthetic pathway, originating from tyrosine and arginine, was proposed for lissodendrins A and B (isolated in the current study), as in the case of phorbatopsins A and B (isolated from the Mediterranean marine sponge *Phorbas topsenti*),¹²⁸ and polyandrocarpamines A and B (isolated from the Fijian ascidian, *Polyandrocarpa* sp.).¹³⁶ The occurrence of 2-aminoimidazole compounds in various marine invertebrate species can possibly be attributed to the presence of associated microorganisms as the real producers.

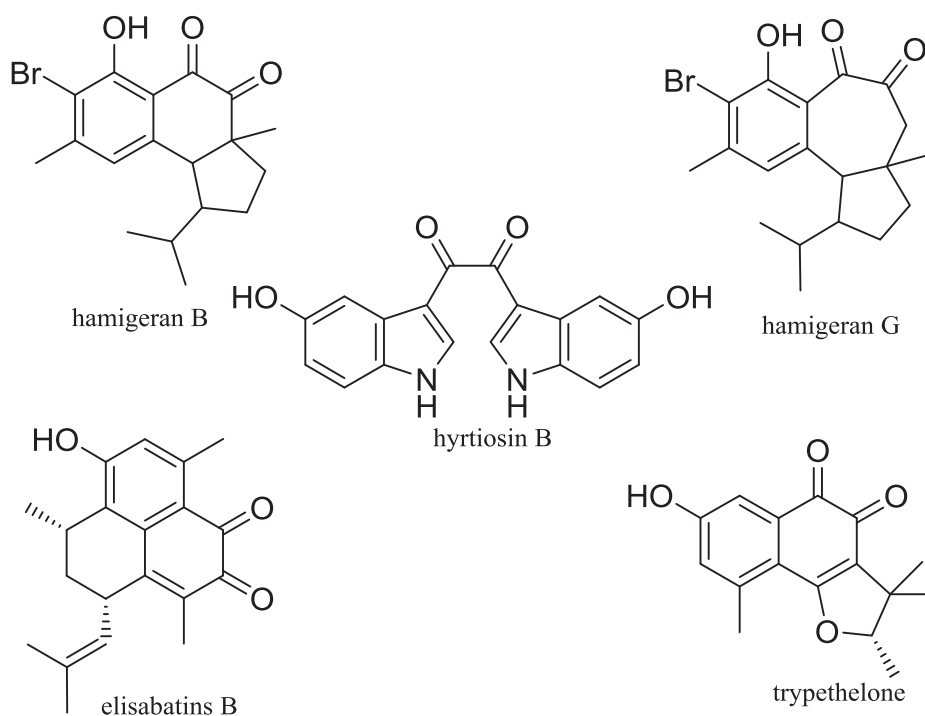


Figure 7.1.1g. Examples of diketone-containing natural products.

7.1.2 2-(4-hydroxyphenyl)-3-hydroxypyridine

Purification of the EtOAc extract of *Lissodendoryx (Acanthodoryx) fibrosa* led to a white, amorphous solid compound. The HRESIMS spectrum showed a prominent ion peak at m/z 188.0 $[M + H]^+$, indicating the molecular formula $C_{11}H_9NO_2$. The structure of the isolated compound was established based on 1H -NMR and HMBC correlations (Table 7.1.2 and Figure 7.1.2). The compound was determined as 2-(4-hydroxyphenyl)-3-hydroxypyridine.

Although, 2-(4-hydroxyphenyl)-3-hydroxypyridine has been previously reported as a synthetic compound, this is the first time that it has been isolated as a natural product.¹³⁷ It showed no cytotoxicity on mouse lymphoma cell line (L5178Y).

Table 7.1.2. ¹H (600 MHz), and HMBC NMR Data (MeOH-*d*₄, δ in ppm) of 2-(4-hydroxyphenyl)-3-hydroxypyridine.

Position	δ _c , type	δ _H (<i>J</i> in Hz)	HMBC
1	158.8, C		
2	115.6, CH	6.85, m	C-4, C-6
3	131.3, CH	7.71, m	C-1, C-5, C-7
4	129.6, C		
5	131.3, CH	7.71, m	C-1, C-3, C-7
6	115.6, CH	6.85, m	C-2, C-4
7	147.4, C		
8	OH		
9	153.0, C		
10	124.8, CH	7.29, dd (1.3, 8.1)	C-7, C-12
11	123.6, CH	7.16, dd (4.7, 8.2)	C-9
12	140.2, CH	8.04, dd (1.3, 4.7)	C-7, C10
13	N		
14	OH		

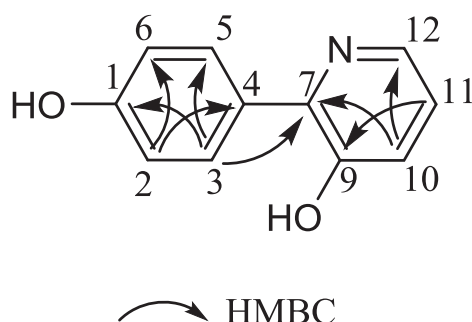


Figure 7.1.2. The HMBC correlation of 2-(4-hydroxyphenyl)-3-hydroxypyridine

7.1.3 Known compounds

7.1.3.1 Hymeniacidin

Further chromatographic separation of the *n*-butanol fraction of *Lissodendoryx (Acanthodoryx) fibrosa* led to the isolation of the known alkaloid hymeniacidin. The structure was confirmed by comparison of MS and ¹H-NMR data with those from the literature. Hymeniacidin has been already reported as a nematocidal natural product from the Great Australian Bight sponge *Hymeniacidon sp.*¹³⁸ Hymeniacidin was successfully synthesized

from initial methylation of caffeine, and it was suggested to be derived as a natural product from hydrolysis (enzyme mediated or otherwise) of a xanthine precursor (Figure 7.1.1h). Hymeniacidin showed no promising activity against mouse lymphoma L5178Y cell line in this study.

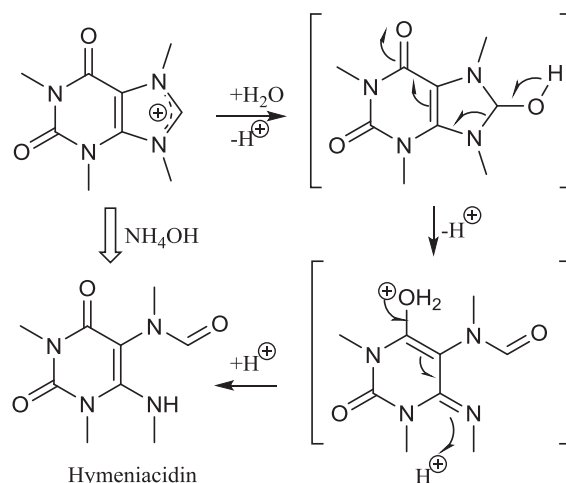


Figure 7.1.3.1. Proposed synthesis mechanism of hymeniacidin.¹³⁸

7.1.3.2 Miscellaneous derivatives

Three L5178Y inactive compounds were isolated from the EtOAc extract of *Lissodendoryx (Acanthodoryx) fibrosa*, including 1-(3-hydroxy-5-(hydroxymethyl)tetrahydrofuran-2-yl)pyrimidine-2,4(1H,3H)-dione as spongothymidine derivative,¹³⁹ 4-hydroxybenzaldehyde, and 4-hydroxybenzoic acid (Figure 7.1.3.2).

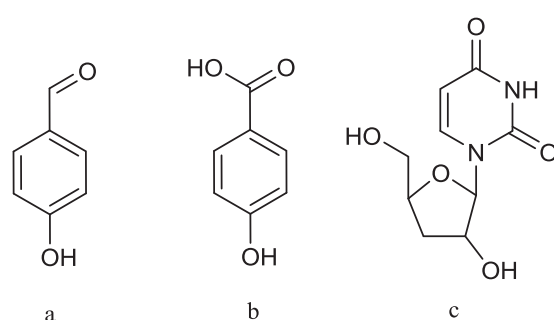


Figure 7.1.3.2. Miscellaneous derivatives isolated from *Lissodendoryx (Acanthodoryx) fibrosa*, a: 4-hydroxybenzaldehyde; b: 4-hydroxybenzoic acid; c: 1-(3-hydroxy-5-(hydroxymethyl)tetrahydrofuran-2-yl)pyrimidine-2,4(1H,3H)-dione

7.2 Natural products from *Clathria basilana*

The sponge genus *Clathria*, including more than 800 species, has been well investigated and yielded various types of natural products, including alkaloids (araiosamines,¹⁴⁰ pseudoanchynazines,¹⁴¹ mirabilin,¹⁴² clathryimine,^{79b} norbatzelladines and dinorbatzelladine¹⁴³); steroids (clathsterol,¹⁴⁴ and clathriol^{81b}); terpenoids (clathrimides,¹⁴⁵ and gombaspiroketal¹⁴⁶); and peptides (clathrynamides,¹⁴⁷ microcionamides,^{82a} and gombamide A,^{82b}). *Clathria basilana* has been rarely investigated and clathryimine A is the only secondary metabolite reported from the Indonesian sponge *Clathria basilana*.^{79b}

Herein, a sponge specimen of *Clathria basilana* collected from Ambon, Indonesia, was investigated for secondary metabolites. The results showed a high capability of *Clathria basilana* to produce a wide range of natural products, including cyclic and linear peptides, indole and lactam derivatives, brominated quinolinone, deoxythymidine, and nucleoside derivatives. In addition, the cyclic peptides microcionamides showed strong cytotoxicity via induction of apoptosis and inhibition of autophagy, in addition to Gram-positive bacterial growth inhibition via dissipation of the bacterial membrane potential, which suggests *Clathria basilana* as a rich source of marine bioactive metabolites.

7.2.1 Microcionamides and gombamides

Peptides from marine species display a broad range of bioactivities, such as anticancer, antimicrobial, antiviral, antioxidative, analgesic, cardioprotective, and immunomodulatory activities. This makes them attractive natural products for pharmaceutical development.⁷ Ziconotide (Prialt®), isolated from the marine cone snail *Conus magus*, was the first marine natural peptide approved by the FDA in 2004 and reached the pharmaceutical market as an analgesic.¹⁴⁸ The second FDA approved marine peptide is Brentuximab vedotin (Adcetris®), as a peptide derivative from a mollusk/cyanobacterium, used for cancer treatment.¹⁴⁹

Microcionamides A and B (with human breast antitumor activity on MCF-7 and SKBR-3 cells lines and inhibition of *Mycobacterium tuberculosis*), as well as gombamide A (with cytotoxicity against A549 and K562 cell lines and Na⁺/K⁺-ATPase inhibitory) are cyclic peptides that have been originally reported from the Phillipinian sponge *Clathria (Thalysias) abietina*, and the Korean sponge *Clathria gombawuiensis*, respectively.⁸²

A part of the current study was carried out on investigation of the secondary metabolites from the Indonesian sponge *Clathria basilana*, collected from Ambon Island. The results indicated *Clathria basilana* as a source of bioactive peptides, including the cyclic peptides, microcionamides A, C and D, gombamides B, C and D, as well as the linear amide (*E*)-2-amino-3-methyl-*N*-styrylbutanamide.

Microcionamides A, C and D were discovered as rare natural peptides with a 20-membered macrocycle, consisting of six amino acids that are cyclized via a disulfide bond. Moreover, the structures of microcionamides A, C and D contain an uncommon exocyclic 2-phenylethen-1-amine (PEA) residue. Two new cyclic peptides microcionamides C and D were identified as derivatives of the known microcionamides A and B, with the only difference of the substitution of the exocyclic valine by an isoleucine moiety. The *E*- or *Z*-


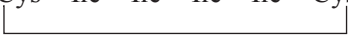

PEA isomeric residue is the only difference between microcionamides C and D, as in the case of microcionamides A and B, respectively. Moreover, microcionamide A was isolated for the first time from *Clathria basilana* in the current study (Table 7.2.1a).

In vitro assays showed potent cytotoxicity of microcionamides A, C and D against five human cancer cell lines (lymphoma, leukemia, and ovarian carcinoma cell lines, IC_{50} = from 0.45 to 5.92 μ M), as well as induction of apoptotic cell death in Jurkat J16 and Ramos cells. Moreover, the results confirmed that microcionamides C and D are capable of blocking autophagy upon starvation conditions.

Although all isolated microcionamides showed cytotoxicity against the tested cell lines, microcionamides C and D exhibited stronger activity compared to microcionamide A. Accordingly, microcionamides C and D showed IC_{50} values from 0.45 to 2.5 μ M, while microcionamide A exhibited IC_{50} values from 2.6 to 28.4 μ M (Table 5 of publication 2). Hence, it is suggested that the difference in toxicity could be due to the presence of an exocyclic Ile in microcionamides C and D, compared to the exocyclic Val in microcionamide A. Moreover, there is no significant difference in bioactivity based on *E*- or *Z*-*PEA* stereochemistry in microcionamides C and D, as observed in the case of microcionamides A and B. Microcionamides A and B displayed activity against MCF-7 and SKBR-3 cells with IC_{50} values from 98 to 125 nM. Furthermore, both compounds were reported to induce apoptosis within 24 h in MCF-7 cells at 5.7 μ M.^{82a}

In addition, microcionamides C and A showed growth inhibition against Gram-positive bacteria (*Staphylococcus aureus* and *Enterococcus faecium*) with minimal inhibitory concentrations (MIC) from 6.25 to 12.5 μ M via dissipation of the bacterial membrane. However, due to the insufficient isolated amount, microcionamide B was not measured in the respective antibacterial assays. According to the literature, microcionamides A and B displayed antituberculosis (H37Ra) activity with MIC values of 5.7 μ M.^{82a}

Table 7.2.1a. Structures or amino acid sequences of microcionamides

Peptide	Amino acid sequences
Microcionamide A ^{82a}	Val – Cys – Ile – Ile – Ile – Ile – Cys – <i>E</i> - <i>PEA</i> 
Microcionamide B ^{82a}	Val – Cys – Ile – Ile – Ile – Ile – Cys – <i>Z</i> - <i>PEA</i> 
Microcionamide C	Ile – Cys – Ile – Ile – Ile – Ile – Cys – <i>E</i> - <i>PEA</i> 

Microcionamide D

Ile – Cys – Ile – Ile – Ile – Ile – Cys – Z-PEA

Examples of cytotoxic peptides from marine sponges include jaspamides from *Jaspis sp.*¹⁵⁰, geodiamolides from *Geodia sp.*^{150a} and callyaerins from *Callyspongia aerizusa*¹⁰⁰. Similarly, neamphamides from *Neamphius huxleyi*¹⁵¹, reniochalistatins from *Reniochalina stalagmitis*¹⁵², and scleritodermin A from *Scleritoderma nodosum*¹⁵³, are further examples of cytotoxic cyclic peptides reported from marine sponges.

There are several examples of natural compounds reported from marine organisms as inducers of apoptosis. Heteronemin, a marine sesterterpene isolated from the sponges *Heteronema erecta* and *Hyrtios sp.*, showed biological effects on chronic myelogenous leukemia cells by inducing apoptosis;¹⁵⁴ jaspamide (jasplakinolide) is a cyclic depsipeptide isolated from sponges of the genus *Jaspis*. It exhibits insecticidal and antifungal activity, as well as cytotoxicity via caspase-3 activation against human promyelocytic leukemia and brain tumor T cells;^{150a, 155} Dolastatin 15 is an antimetabolic depsipeptide from the marine mollusc *Dolabella auricularia*, which has been reported to induce cell cycle at G2/M phase and apoptosis in different human myeloma cell lines via mitochondrial- and Fas (CD95)/Fas-L (CD95-L)- mediated pathways¹⁵⁶ the marine bacterial lipopeptide iturin A, derived from *Bacillus sp.* shows inhibition of human breast cancer cells through disrupting the protein kinase B (PKB) pathway and induction of apoptosis;¹⁵⁷ the disulfide dimer somocystinamide A, isolated from a Fijian cyanobacterium is another example of marine lipopeptides, capable of triggering apoptosis via caspase-8;¹⁵⁸ H-10 is a cyclic pentapeptide and derivative of sansalvamide A from a marine *Fusarium sp.*, which inhibits B16 cancer cell growth and induces cell apoptosis;¹⁵⁹ the lipopeptide jahanyne, from the marine cyanobacterium *Lyngbya sp.*, exhibits cytotoxicity on HeLa and HL60 cells via induction of caspase-dependent apoptosis¹⁶⁰ (Figure 7.2.1a).

Aplidine (also called plitidepsin) is a cyclic depsipeptide isolated from the tunicate *Aplidium albicans*. It has shown cytotoxicity against breast, melanoma and non-small-cell lung cancer cell lines. Its mechanism of action involves several pathways, including cell cycle arrest and protein synthesis inhibition. Moreover, aplidine induces apoptosis in MDA-MB-231 breast cancer cells and is currently in phase III clinical studies.¹⁶¹ Didemnin B, a cyclic depsipeptide isolated from the marine tunicate *Trididemnum sp.*, induces apoptosis and DNA fragmentation^{161c, 162} (Figure 7.2.1a).

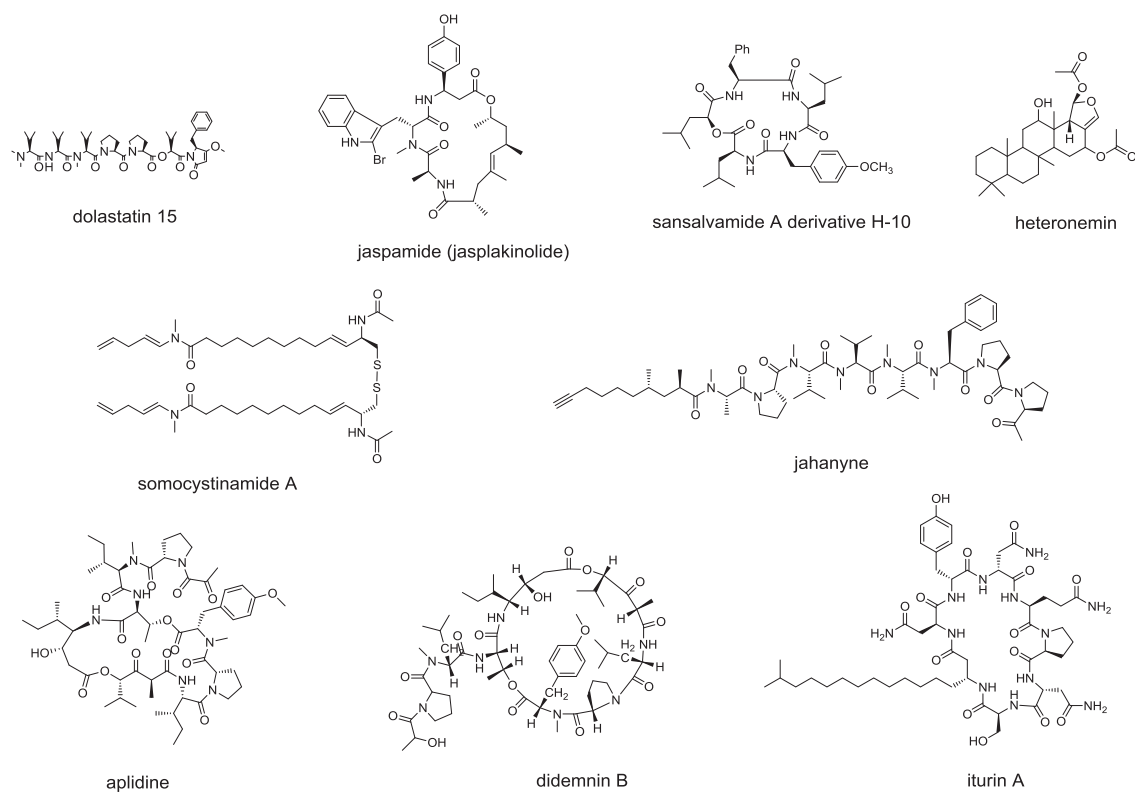


Figure 7.2.1a: Examples of cytotoxic marine peptides with apoptotic activity

Apart from peptides, other types of natural compounds have been identified from marine sponges with apoptosis-inducing anticancer properties, including alkaloids, lipids, macrolides, and terpenoids (Table 7.2.1b).^{154a}

Table 7.2.1b. Compounds isolated from marine sponges with pro-apoptotic activity^{154a}

Type	Compound	Sponge	Cell line
Alkaloid	2,3-dihydro-2,3-dioxoaaptamine	<i>Aaptos</i> sp.	THP-1
	3-(methylamino)demethyl (oxy)aaptamine	<i>Aaptos</i> sp.	THP-1
	6-(<i>N</i> -morpholinyl)-4,5-dihydro-5-oxo-demethyl (oxy)aaptamine	<i>Aaptos</i> sp.	THP-1
	kuanoniamine A	<i>Oceanapia sagittaria</i>	MCF-7
	kuanoniamine C	<i>Oceanapia sagittaria</i>	MCF-7
	Makaluvic acid C	<i>Strongyloidesma aliwaliensis</i>	WHC01 WHC06 KYSE30
	Monanchocidin	<i>Monanchora pulchra</i>	THP-1

			HeLa	
	<i>N</i> -1- β -D-ribofuranosyl damirone C	<i>Strongyloidesma aliwaliensis</i>	WHC01 WHC06 KYSE30	
	<i>N</i> -1- β -D-ribofuranosyl makalu-vamine I	<i>Strongyloidesma aliwaliensis</i>	WHC01 WHC06 KYSE30	
	<i>N</i> -1- β -D-ribofuranosyl makaluvic acid C	<i>Strongyloidesma aliwaliensis</i>	WHC01 WHC06 KYSE30	
	Naamidine A	<i>Leucetta chagosensis</i>	A-431	
	Psammaplysene A	<i>Psammaplysilla</i>	Ishikawa ECC1	
	Renieramycin M	<i>Xestospongia</i> sp.	NSCLC	
	Bastadin 6	<i>lanthella</i> sp.	HUVEC	
lipid	(<i>Z</i>)-stellettic acid C	<i>Stelletta</i> sp.	U937	
	5- α ,6- α -epoxy-petrosterol	<i>Lanthella</i> sp.	HL-60	
	Callyspongiolol	<i>Callyspongia</i> sp.	HL-60	
	Jaspine B	<i>Jaspis</i> sp.	SK-Mel28	
	Petrosterol	<i>Lanthella</i> sp.	HL-60	
	Petrosterol-3,6-dione	<i>Lanthella</i> sp.	HL-60	
	Rhizochalin	<i>Rhizochalina incrustata</i>	THP-1 HeLa SNU-C4	
	macrolide	Candidaspongiolide	<i>Candidaspongia</i> sp.	U251 HCT116
		Irciniastatin A	<i>Ircinia ramose</i>	Jurkat T
		Latrunculins A and B	<i>Negombata magnifica</i>	MKN45 NUGC-4
		Salarin C	<i>Fascaplysinopsis</i> sp.	K562
		Spongistatin 1	<i>Spongia</i>	Jurkat T
13 <i>E</i> ,17 <i>E</i> -globostellatic acid X methyl ester		<i>Rhabdastrella globostellata</i>	HUVEC	
3- <i>epi</i> -sodwanone K3-acetate		<i>Axinella</i> sp.	T47D HL-60	
Geoditin A		<i>Geodia japonica</i>	HT29	
Geoditin B		<i>Geodia japonica</i>	HL-60 K562	
Heteronemin		<i>Hyrtios</i> sp.	Jurkat T	
Ilimaquinone		<i>Hippospongia metachromia</i>	PC3	
terpenoid		Jaspolide B	<i>Jaspis</i> sp.	Bel-7402 HepG2
	Rhabdastrellic acid-A	<i>Rhabdastrella globostellata</i>	HL-60	

		KB-3-1
	<i>Callyspongia</i>	KB-C2
Sipholenol A	<i>siphonella</i>	KB-V1
	<i>Dactylospongia</i>	
Smenospongine	<i>elegans</i>	K56
Sodwanone V	<i>Axinella</i> sp.	MDA-MB-231
Stellettin A	<i>Geodia japonica</i>	HL-60
Stellettin B	<i>Geodia japonica</i>	HL-60

In addition to microcionamides, gombamides B, C and D were isolated from *Clathria basilana* as new cyclic derivatives of the thiopeptide gombamide A, reported from *Clathria gombawuiensis*.^{82b} The cyclic part of gombamides B, C and D, consisting of two cysteines, two prolines, and a phenylalanine, is formed through a disulfide bond between the two cysteine residues. In gombamide D phenylalanine is substituted by a leucine.

In addition, gombamide A contains an unusual exocyclic amino acid residue, namely parahydroxystyrylamide (pHSA), while gombamides B and C contain an uncommon exocyclic *E*- and *Z*-PEA moiety, respectively (Table 7.2.1c). Gombamide A was reported to show weak cytotoxicity against adenocarcinomic human alveolar basal epithelial (A549) and human leukemia (K562) cell lines, as well as moderate inhibition against Na⁺/K⁺-ATPase,^{82b} and it was successfully synthesised two years after its discovery.¹⁶³ However, gombamides B, C and D in the present study, exhibited no significant cytotoxic or antibacterial activity.

Table 7.2.1c. Structures or amino acid sequences of gombamides

Peptide	Amino acid sequences
Gombamide A ^{82b}	Glp – Cys – Pro – Pro – Phe – Cys – pHSA <div style="text-align: center;">└──────────────────┘</div>
Gombamide B	Glp – Ile – Leu – Cys – Pro – Pro – Phe – Cys – <i>E</i> -PEA <div style="text-align: center;">└──────────────────┘</div>
Gombamide C	Glp – Ile – Leu – Cys – Pro – Pro – Phe – Cys – <i>Z</i> -PEA <div style="text-align: center;">└──────────────────┘</div>
Gombamide D	Glp – Cys – Pro – Pro – Leu – Cys – Pro <div style="text-align: center;">└──────────────────┘</div>

Pyroglutamate (Glp) is a characteristic *N*-terminal residue in the linear peptide chain of gombamides. Eudistomides A and B are two cyclic thiopeptides, derivatives of gombamides, reported from a Fijian ascidian of the genus *Eudistoma*, in which the exocyclic Glp is substituted by an acyl group containing a lipid chain with fourteen carbon atoms (Table 7.2.1d).⁹⁴ Apart from microcionamides and gombamide A, the Glp residue has been rarely reported from marine peptides, including didemnins from the marine tunicate *Trididemnum* sp.⁹⁰ and callipeltin B from marine sponge *Callipelta* sp.¹⁶⁴ The existence of *N*-terminal blocked proteins is reported to be important for their hydrophobicity and proteolytic resistance.⁹² Accordingly, the presence of *N*-terminal blocked proteins is suggested to contribute to the chemical defence of sponges of the genus *Asteropus* preventing predation.⁹² In addition, the cyclization of protein *N*-terminal glutamine residues into pyroglutamate enables the peptides to adopt the right conformation for binding to their receptors and protects them from the action of exopeptidase enzymes.⁹³

Table 7.2.1d. Structures or amino acid sequences of eudistomides A and B⁹⁴

Peptide	Amino acid sequences
Eudistomides A	(C ₁₄ H ₂₆ O ₂) – Cys – Pro – Pro – Leu – Cys – (CO)
Eudistomides B	(C ₁₄ H ₂₈ O ₂) – Cys – Pro – Pro – Leu – Cys – (CO)

Microcionamides and gombamides are rare cyclic peptides with disulfide linkages from marine sponges. Other examples include neopetrosiamides from *Neopetrosia* sp. containing three disulfide bridges that inhibit amoeboid invasion by human tumor cells,¹⁶⁵ asteropsin A from the sponge *Asteropus* sp., which enhances neuronal Ca²⁺ influx,¹⁶⁶ and chujamides from *Suberites waedoensis* with weak cytotoxicity against A549 and K562 cell-lines.¹⁶⁷ Moreover, the presence of disulphide bonds has been reported to play an important role for the stability and structure of θ -defensins peptides.¹⁶⁸

Further examples of cyclic peptides from marine sponges include perthamides with a 25-membered macrocycle from the sponge *Theonella* sp. exhibiting anti-inflammatory activity,¹⁶⁹ geodiamolides, 18-membered cytotoxic depsipeptides from the sponge *Geodia* sp., which regulate actin cytoskeleton, migration and invasion of breast cancer cells;¹⁷⁰ the 25-membered cyclodepsipeptide homophymine, isolated from the marine sponge *Homophymia* sp. with antiproliferative activity against human prostate (PC3) and ovarian (OV3) carcinoma cell lines, as well as cytoprotective activity against HIV-1 infection;¹⁷¹ oriamide, a 22-membered cytotoxic cyclic peptide, containing an unusual 4-propenoyl-2-

tyrosylthiazole amino acid, from the marine sponge *Theonella* sp.,¹⁷² as well as the tetradecapeptides discodermins with a 19-membered microcyclic ring, isolated from the sponge *Discodermia kiiensis* with cytotoxic and antimicrobial activities¹⁷³ (Figure 7.2.1b).

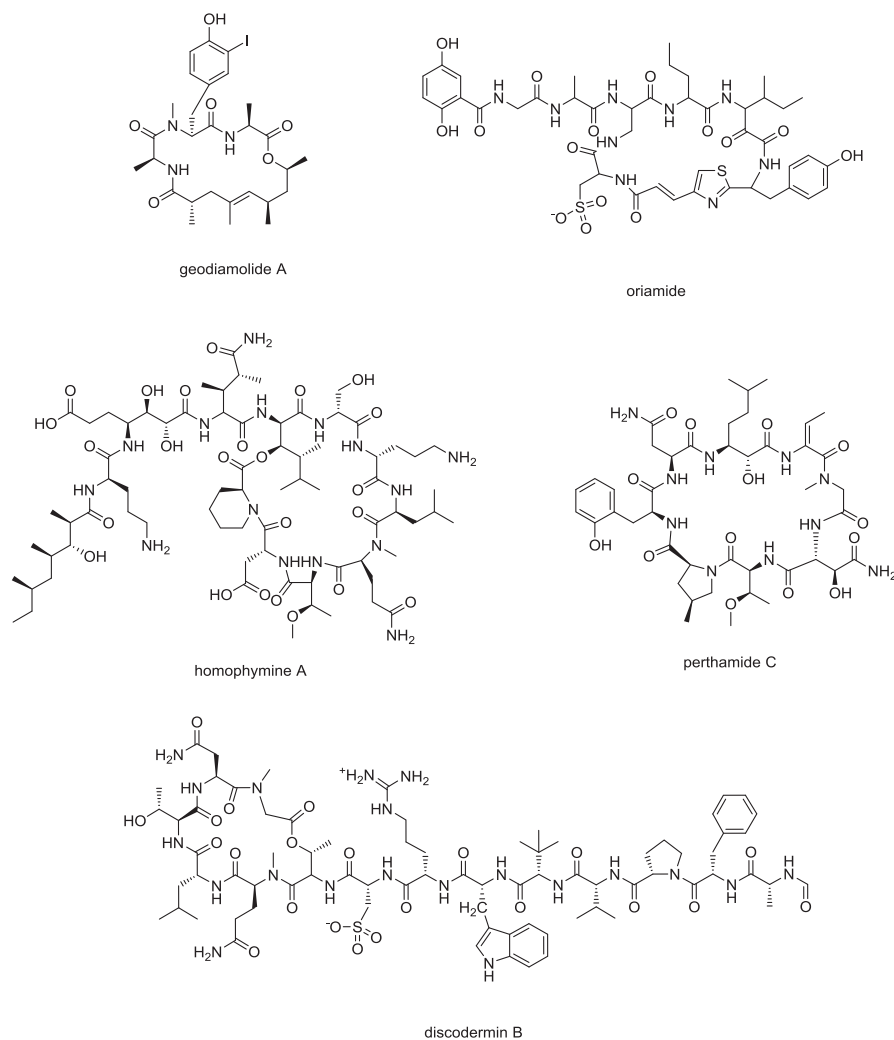
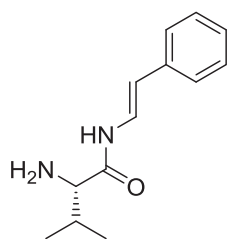


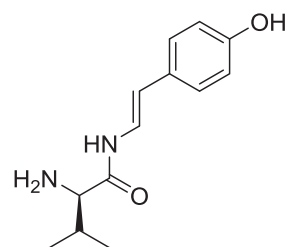
Figure 7.2.1b. Examples of cyclic peptides from marine sponges

7.2.2 (*E*)-2-amino-3-methyl-*N*-styrylbutanamide

(*E*)-2-amino-3-methyl-*N*-styrylbutanamide was isolated from the EtOAc fraction of *Clathria basilana* as a new amide containing a valine residue conjugated with a (*E*)-2-phenylethen-1-amine (*E*-PEA) moiety via a peptidic bond. Since in the isolated microcionamides and gombamides, the PEA residue is linked to a cysteine, the possibility of these derivatives being artefacts is rather low. The butanamide (*2S*)-2-amino-*N*-[2-(4-hydroxyphenyl)ethenyl]-3-methyl is the only related compound in the literature, which was reported as a synthetic intermediate from oxidation of di- and tripeptides of tyrosine and valine, mediated by oxygen, phosphate, and sulfate radicals.¹⁷⁴



(E)-2-amino-3-methyl-N-styrylbutanamide



(S)-2-amino-N-[2-(4-hydroxyphenyl)ethenyl]-3-methyl

Figure 7.2.2. Structures of the new amide and its synthetic derivative

7.2.3 Known compounds

Indole alkaloids are a wide group of marine secondary metabolites. The first indole compounds from marine sponges have been reported from the sponge *Dysidea etheria* promoting root growth in the lettuce seedling assay.^{83a} Bromo alkaloids are the most common natural compounds among halogenated alkaloids, which are usually found in marine eukaryotes and rarely in terrestrial organisms.¹⁷⁵ Herein, six known indole alkaloid derivatives were isolated from the EtOAc fraction of the sponge *Clathria basilana* with different substitutions at positions 3 and 6, including indole-3-carboxaldehyde, reported from the sponge *Dysidea etheria*;^{83a} indole-3-carboxylic acid, isolated from a fungal endophyte of *Solanum nigrum*;¹⁷⁶ as well as brominated indole alkaloids, namely 6-bromoindole-3-carbaldehyd and 6-bromoindole-3-carboxyrboxylic acid, isolated from *Pseudosukita hyalinus*;^{83b} 6-bromo-1H-indole-3-carboxylic acid methyl ester, reported from the sponge *Smenospongia* sp. with antimicrobial activity against *Staphylococcus epidermidis*;¹⁷⁷ and ethyl-6-bromo-3-indolcarboxylate, reported from the sponge *Pleroma menoui*¹⁷⁸ (Figure 7.2.3).

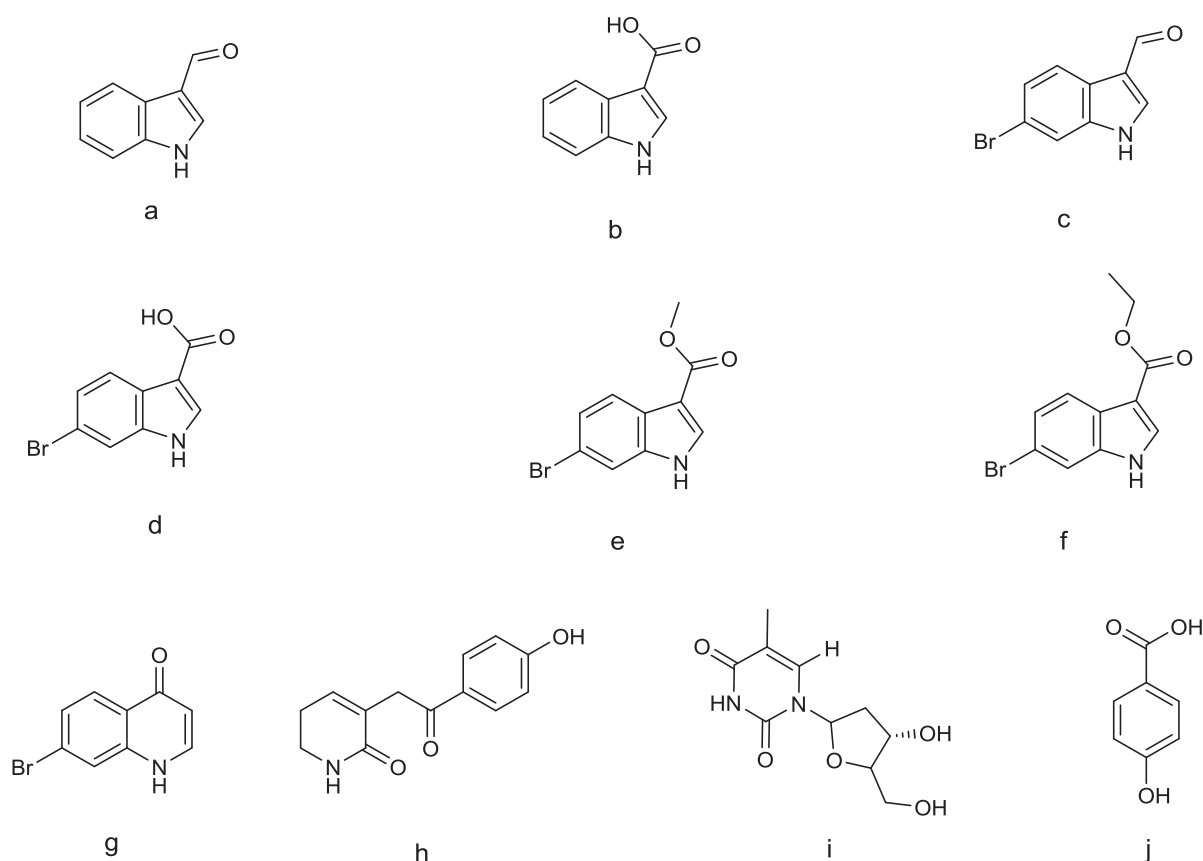


Figure 7.2.3. The known compounds isolated from *Clathria basilana*, a. indole-3-carboxaldehyde; b. indole-3-carboxylic acid; c. 6-bromoindole-3-carbaldehyde; d. 6-bromoindole-3-carboxylic acid; e. 6-bromo-1H-indole-3-carboxylic acid methyl ester; f. ethyl-6-bromo-3-indolcarboxylate; g. 7-bromoquinolin-4(1H)-one; h. (3-(2-(4-hydroxyphenyl)-2-oxoethyl)-5,6-dihydropyridin-2(1H)-one); i. 2-deoxythymidine; and j. 4-hydroxybenzoic acid.

7-Bromoquinolin-4(1H)-one is a derivative of the cytotoxic quinolinecarboxylic acid caelestine, reported from the Australian ascidian *Aplidium caelestism*,¹⁷⁹ that is isolated as another brominated natural compound from the EtOAc fraction of *Clathria basilana*, during our study. It was also reported from an unknown marine sponge collected in the Gulf of Aqaba.⁸⁴

Moreover, the δ -lactam derivative (3-(2-(4-hydroxyphenyl)-2-oxoethyl)-5,6-dihydropyridin-2(1H)-one), which was reported as a novel lactam from the marine sponge *Halichondria melanodocia*,⁸⁵ the nucleoside derivative 2-deoxythymidine, and 4-hydroxybenzoic acid were isolated from the EtOAc fraction of *Clathria basilana* (Figure 7.2.3).

7.3 Natural products from *Cinachyrella* sp.

Sponges of the genus *Cinachyrella* have been reported as a rich source of secondary metabolites, including fatty acids from *Cinachyrella* sp.¹⁰⁸ and *Cinachyrella alloclada*

Uliczka,¹⁸⁰ the alkaloid cinachyramine from *Cinachyrella* sp.,¹¹⁸ enigmazole A, a novel phosphate-containing macrolide isolated from *Cinachyrella enigmatica*,¹⁸¹ and sterols from *Cinachyrella cavernosa* (*Lamarck*).¹¹¹

7.3.1 *Cinachylenic acids A, B, C, and D*

Overall, three new (A, B, and C) 2-methoxy acetylenic acids, in addition to a known (D) derivative were isolated from the marine sponge *Cinachyrella* sp. However, the structural differences of cinachylenic acids were determined to be due to number and/or positions of the double bonds.

The similar cytotoxicity of cinachylenic acids suggests that the number and position of double bonds has no effect on the toxicity of compounds. In fact, the presence of a 2-methoxy moiety in chain fatty acids could be attributed to their toxicity. This idea is supported by further examples in the literature, including 2-methoxy-13 methyltetradecanoic acid from the sponge *Amphimedon complanata* with cytotoxic activity against leukemia (K-562, HL-60) and histiocytic lymphoma (U-937) cell lines,¹⁸² as well as long-chain 2-methoxylated $\Delta^{5,9}$ fatty acids from the sponge *Asteropus niger* with cytotoxic activity via inhibition of topoisomerase IB.¹⁸³ Moreover, the presence and position of acetylene groups may also have an effect on the toxicity of these compounds. Examples of cytotoxic 2-methoxylated 5-acetylenic acid compounds have been reported from the sponge *Stelletta* sp.^{113, 184}

Further examples of 2-methoxy acetylenic acids from marine sponges include corticatic acids A-E isolated from sponge *Petrosia corticata* with antifungal activity,¹⁸⁵ taurospongins A from the sponge *Hippospongia* sp. with inhibitory activity against DNA polymerase β and HIV reverse transcriptase, halicyonones A and B from the sponge *Haliclona* sp. with antitumor activity against the human colon tumour cell line (HCT-116),¹⁸⁶ and three cytotoxic acetylenic metabolites against human leukemia cell line (K562) reported from the sponge *Stelletta* sp.¹¹³ Mostly, fatty acids are frequently presented in the literature, which have been attributed to symbiotic bacteria.^{110b, 180, 187} The potential role of 2-methoxylated FA as antimicrobial lipids produced by marine sponges, as defense mechanism in a highly competitive environment was previously reported.¹⁸⁸

The presence of 2-methoxy acetylenic acid derivatives from different marine organisms, in particular from the sponge *Cinachyrella australiensis*,¹⁰⁹ suggests the possible origin of these metabolites from associated marine symbiotic bacteria.

7.3.2 *Cinachyrazole A, B, and C*

In addition to the cinachylenic acids, three new pyrazole derivatives (A, B, and C) were isolated from *Cinachyrella* sp. during this study. The structures of cinachyrazoles were determined similarly with a central pyrazole ring connected to three methyl moieties at C_{1,4} and N₂. The structural differences of cinachyrazoles were identified on the basis of different substituents at the pyrazole ring at C₅ (Figure 7.3.2). Accordingly, replacement of the

aldehyde of A with a carboxylic acid in B was the only structural difference between these two compounds. Rare examples of pyrazole derivatives from the marine environment include pyrazole-3(5)-carboxylic acid and 4-methylpyrazole-3(5)-carboxylic acid from the sponge *Tedania anhelans*,¹⁸⁹ as well as 4-acetoxypyrazole from the sea cucumber *Synapta muculata*.¹⁹⁰ Cinachyrazole C possess an additional hydrazone moiety at C₆, which is connected with a terminal methyl and an aldehyde group. Among heterocycle-containing secondary metabolites, pyrazoles are rarely found in nature probably due to the difficulty in the formation of an N-N bond.¹⁹¹ However, some examples have been reported from marine organisms, such as from the sponge *Tedania anhelans*¹⁸⁹ and the sea cucumber *Synapta muculata*.¹⁹⁰ Moreover, the presence of a novel hydrazone alkaloid cinachyramine has already been reported from *Cinachyrella* sp.¹¹⁸

The same plausible biosynthetic pathway was suggested for the isolated pyrazole derivatives A, B and C, originating from acetoacetic acid and an *N*-acetyl-*N*-methylhydrazine. Formation of cinachyrazole C from cinachyrazole B was performed by adding the intermediate *N*-formyl-*N*-methylhydrazine, which is synthesized from the toxic natural product gyromitrin, reported from the ascomycete fungus *Gyromitra esculenta* (Figure 7.3.3).¹¹⁴

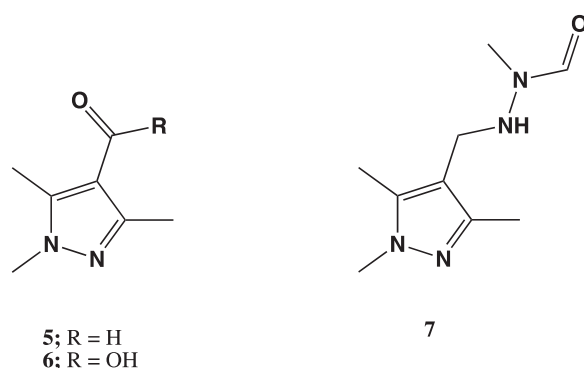


Figure 7.3.2. Structures of cinachyrazoles A, B, and C (5 – 7)

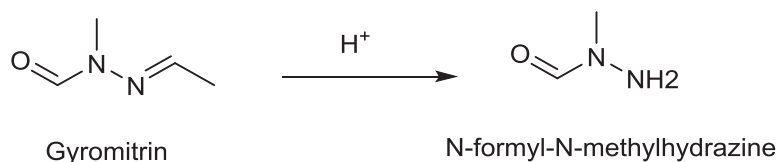


Figure 7.3.3. Synthesis of *N*-formyl-*N*-methylhydrazine from gyromitrin.

8 Abbreviations

ara	Arabinoside
AIDS	Acquired ImmunoDeficiency Syndrome
ATP	Adenosine Triphosphate
Atg	Autophagy-related
BAC	Bacitracin
BAX	<i>BCL2 Associated X, Apoptosis</i> Regulator
BCL2	B-cell lymphoma 2
BuOH	Butanol
br	Broad signal
CD	Circular Dichroism
CDCI3	Deuterated Chloroform
CH2Cl2	Dichloromethane
CHCl3	Chloroform
CHL	Chloramphenicol
CIP	Ciprofloxacin
CLSI	Clinical and Laboratory Standards Institute
cm	Centimeter
Cys	Cysteine
CVS	Crystal violet Staining
COSY	Correlation Spectroscopy
CoA	Coenzyme A
COOH	Carboxyl group
d	Doublet
DBD	DNA-Binding Domai
DR5	<i>Death</i> Receptor 5
DCM	Dichloromethane
dd	Doublet of Doublet
DMSO	Dimethyl Sulfoxide
DNA	Deoxyribonucleic Acid
ED	Effective Dose
EGF	Epidermal Growth Factor
EI	Electron Impact Ionization
ESI	Electrospray Ionization
et al.	et altera (and others)
EtOAc	Ethyl acetate
FAs	Fatty Acids
FDA	1-Fluoro-2-4-Dinitrophenyl-5-L-Alanine Amide
FDA	Food and Drug Administration of US
g	gram
GLP	Pyroglutamic Acid
HeLa	Human Cervical Carcinoma
HIV	<i>Human Immunodeficiency Virus</i>

HMBC	Heteronuclear Multiple Bond Connectivity
HSQC	Heteronuclear Multiple Quantum Coherence
HPLC	High Performance Liquid Chromatography
HRMS	High Resolution Mass Spectrometry
Hz	Herz
HL	Human Promyelocytic Leukemia Cells
IC50	The half maximal inhibitory concentration
Ile	Isoleucine
L	Liter
LB	Lysogeny Broth
LC	Liquid Chromatography
LC3	Microtubule-associated protein 1A/1B-Light Chain 3
LC/MS	Liquid Chromatography-Mass Spectrometry
LTB4	Potent Leukotriene B4
Leu	Leucine
m	Multiplet
M	Molar
MALDI	Matrix Assistierte Laser Desorption Ionisierung
MeOD	Deuterated Methanol
MeOH	Methanol
MEF	Murine Embryonic Fibroblast
mg	Milligram
MHz	Mega Herz
min	minute
mL	milliliter
mRNA	messenger RNA
MIC	<i>Minimum Inhibitory Concentration</i>
MS	Mass Spectrometry
MTT	Microculture Tetrazolium assay
MUFAs	Monounsaturated Fatty Acids
m/z	mass per charge
NMR	Nuclear Magnetic Resonance
NOESY	Nuclear Overhauser and Exchange Spectroscopy
n.d.	not detected
PARP	the enzyme Poly ADP Ribose Polymerase
PEA	2-phenylethen-1-amine
PKB	Protein Kinase B
PGME	Phenylglycine Methyl esters
Phe	Phenylalanine
pH	potential of Hydrogen
Pro	Proline
PUFAs	Polyunsaturated Fatty Acids
ppm	parts per million

RIF	Rifampicin
ROESY	Rotating Frame overhauser Enhancement Spectroscopy
RP18	Reversed Phase C 18
RNA	Ribonucleic acid
s	singlet
Sp.	Species (singular)
SD	Standard Definition
t	triplet
TFA	Trifluoroacetic Acid
TLC	Thin Layer Chromatography
TOCSY	Total Correlation Spectroscopy
UV	Ultra Violet
VAN	Vancomycin
Val	Valine
VLC	Vacuum Liquid Chromatography
WPD	World Porifera Database
μg	microgram
μL	microliter
μM	micromol
$[\alpha]^{20}_D$	specific rotation at the sodium D-line

9 Research contributions

Publications

9.1. A. Mokhlesi, R. Hartmann, E. Achten, Chaidir, T. Hartmann, W. Lin, G. Daletos and P. Proksch (2016) Lissodendrins A and B: 2-Aminoimidazole Alkaloids from the Marine Sponge *Lissodendoryx (Acanthodoryx) fibrosa*. *European Journal of Organic Chemistry*, 4: 639-643.

The first author performed the experiments and laboratory works included of compound isolation and structure elucidation, as well as the manuscript preparation.

9.2. A. Mokhlesi, F. Stuhldreier, K. W. Wex, A. Berscheid, R. Hartmann, N. Rehberg, P. Sureechatchaiyan, C. Chaidir, M. U. Kassack, R. Kalscheuer, H. B.-Oesterhelt, S. Wesselborg, B. Stork, G. Daletos and P. Proksch (2017) Cyclic cystine-bridged peptides from the marine sponge *Clathria basilana* induce apoptosis in tumor cells and depolarize the bacterial cytoplasmic membrane. *Journal of Natural Products*, Nov 2.

The first author performed the experiments and laboratory works included of compound isolation, structure elucidation and marfey analysis, as well as the manuscript preparation.

9.3. A. Mokhlesi, R. Hartmann, T. Kurtán, H. Weber, W. Lin, C. Chaidir, W. E. G. Müller, G. Daletos and P. Proksch (2017) New 2-methoxy acetylenic acids and pyrazole alkaloids from the marine sponge *Cinachyrella* sp., *Marine Drugs*, 15, 356.

The first author performed the experiments and laboratory works included of compound isolation and structure elucidation, as well as the manuscript preparation.

10 Acknowledgements

The following people and organizations were direct or indirect involved in my PhD project. Foremost, I would like to express my heartfelt appreciation and gratitude to Prof. h.c. Dr. Dr. rer. nat. Peter Proksch for giving me the opportunity to take part in his scientific research group at the Institute Pharmaceutical Biology and Biotechnology, Heinrich-Heine University, Duesseldorf. I wholeheartedly appreciated his patient guidance, critical insights and fully support of my work. I never be able to convey my full appreciate, but I owe him my eternal gratefulness.

Moreover, I would like to express my sincere gratitude to Dr. Georgios Daletos for sharing his knowledge and ideas throughout my PhD, and as well helping to improve my manuscripts, recheck of NMR data and the nice suggestions for the experiments.

I take this opportunity to express my thanks to Prof. Dr. rer. nat. Rainer Kalscheuer (Institute of Pharmaceutical Biology and Biotechnology, Henrich-Heine University Duesseldorf) for evaluating my doctorate research as the second referee, and as well collaboration on antimicrobial assays.

My appreciation goes to Prof. Dr. Wenhan Lin (National Research Laboratories of Natural and Biomimetic Drugs, Peking University, Health Science Center) for structure elucidation help and confirmed structure of the isolated compounds.

I wish to thanks of my lab partners, Dr. Cong-Dat Pham, Dr. Huiqin Chen, and Mr. Hao Wang for their help, guidance, suggestions and warm atmosphere during working together in the laboratory.

My sincere thanks to Dr. Rudolf Hartmann (Institute of Complex Systems: Strukturbiochemie, Forschungszentrum Jülich GmbH, ICS-6, 52425 Jülich, Germany) for NMR measurements, and suggestion with regards to the structure elucidation of my substances.

I gratefully acknowledges to Prof. Dr. Tibor Kurtán (Department of Organic Chemistry, University of Debrecen, Hungary) for helping in CD measurement, Prof. Sebastian Wesselborg and Mr. Fabian Stuhldreier, Prof. Dr. rer. nat. Werner E. G. Müller (Institute of Physiological Chemistry and Pathobiochemistry, University of Mainz) and Prof. Dr. Matthias U. Kassack (Institut für Pharmazeutische und Medizinische Chemie, Heinrich Heine University Duesseldorf) for their collaboration on cytotoxicity assays, and as well to Prof. Dr. Heike Brötz-Oesterhelt (Interfakultäres Institut für Mikrobiologie und Infektionsmedizin, Mikrobielle Wirkstoffe, Tübingen, Germany) for antibiotic assays.

I also wish to thanks of Mrs. Claudia Eckelskemper and all the technicians Mrs.

Waltraud Schlag, Mrs. Simone Miljanovic, Mrs. Katja Friedrich, Mrs Eva Müller, Ms. Linda Wiegand, Mrs. Simone Monninghoff-Putzer and Mr. Dieter Jansen for their nice and kindness help.

I would like to appreciate of the Ministry of Science, Research and Technology (MSRT) of Iran for awarding a full term PhD scholarship.

Thanks of my friendes, Marian Frank and Nam Michael Tran-Cong for translated the summery of this thesis to German.

I wish to thanks all of my group members for making a warm and friendly atmosphere and for the time to time help and supporting me during my PhD study, thanks to my dear friends

Dr. Yang Liu, Dr. Catalina Pérez Hemphill, Dr. Antonius Ola, Dr. Shuai Liu, Dr. Sergi Akone, Dr. Andreas Marmann, Dr. Hendrick Niemann, Dr. Sherif Elsayed, Dr. Weaam Ebrahim, Dr. Ramsay Kamdem, Dr. Zhen Liu, Dr. Han Xiao, Dr. Lena Hammerschmidt and Dr. Mousa. Al Tarabeen, Dr. Rudi Rudiyanasyah, Dr. Mohamed Elnaggar, Dr. Rini Muharini, Dr. Elena Ancheeva Dr. Yanbo Zeng, Dr. Fang Lv, Ferhat Oezkaya, Imke Form, Mi-Yong Chung, Mariam Moussa, Haiqian Yu, Xiaoqin Yu, Dr. Linghong Meng, Dr. Xin Li, Feng Pan, Arta Kuci, Blessing Umeokoli, Peter Eze, Tino Seidemann, Julia Werner, Pamela Nangmo Kemda, Dr. Festus Okoye, Lisa Kuppers, Catherine Bogner, Ni Putu Ariantari, Harwoko, Nada Mohamed, Miada Fouad, Dina El-Kashef, and Ying Gao.

I am deeply and forever indebted to my parents for their love, support and encouragement throughout my entire life.

Finally, I wish to gratefully thanks to my wife, Nasrin, who always supported me during my Phd period, and special thanks to her for the patient care of our newborn baby, Elin, when I was busy with my doctorant procedure.

11 References

1. Li, K.; Chung-Davidson, Y.-W.; Bussy, U.; Li, W., Recent advances and applications of experimental technologies in marine natural product research. *Marine Drugs* **2015**, *13* (5), 2694-2713.
2. Haefner, B., Drugs from the deep: marine natural products as drug candidates. *Drug Discovery Today* **2003**, *8* (12), 536-544.
3. Mehbub, M. F.; Lei, J.; Franco, C.; Zhang, W., Marine sponge derived natural products between 2001 and 2010: trends and opportunities for discovery of bioactives. *Marine Drugs* **2014**, *12* (8), 4539-4577.
4. Van Soest, R. W. M.; Boury-Esnault, N.; Vacelet, J.; Dohrmann, M.; Erpenbeck, D.; De Voogd, N. J.; Santodomingo, N.; Vanhoorne, B.; Kelly, M.; Hooper, J. N. A., Global diversity of sponges (Porifera). *Plos One* **2012**, *7* (4), e35105.
5. Perdicaris, S.; Vlachogianni, T.; Valavanidis, A., Bioactive natural substances from marine sponges: new developments and prospects for future pharmaceuticals. *Natural Products Chemistry & Research* **2013**.
6. Chasanah, E., Marine biodiversity research in Indonesia: challenges and rewards. *Journal of Coastal Development* **2011**, *12* (1), 12.
7. Cheung, R. C. F.; Ng, T. B.; Wong, J. H., Marine peptides: Bioactivities and applications. *Marine drugs* **2015**, *13* (7), 4006-4043.
8. Jha, R. K.; Zi-rong, X., Biomedical Compounds from Marine organisms. *Marine Drugs* **2004**, *2* (3), 123-146.
9. Manivasagan, P.; Venkatesan, J.; Sivakumar, K.; Kim, S.-K., Marine actinobacterial metabolites: Current status and future perspectives. *Microbiological Research* **2013**, *168* (6), 311-332.
10. (a) Thakur, N. L.; Thakur, A. N.; Müller, W. E., Marine natural products in drug discovery. **2005**; (b) Abdelmohsen, U. R.; Bayer, K.; Hentschel, U., Diversity, abundance and natural products of marine sponge-associated actinomycetes. *Natural Product Reports* **2014**, *31* (3), 381-399.
11. Ananthan, G.; Karthikeyan, M. M.; Selva, P. A.; Raghunathan, C., Studies on the seasonal variations in the proximate composition of ascidians from the Palk Bay, Southeast coast of India. *Asian Pacific Journal of Tropical Biomedicine* **2012**, *2* (10), 793-797.
12. Gerd, L.; Yves, L. G.; Roland, U., Aquaculture of "non-food organisms" for natural substance production. *Advances in biochemical engineering, biotechnology* **2005**, *97*, 1-28.
13. (a) Detmer, S.; Ronald, O.; Wolfgang, S.; Dominick, M.; Johannes, T.; H, W. R., Large-scale production of pharmaceuticals by Marine sponges : Sea, cell, or synthesis? *Biotechnology and bioengineering* **2005**, *90* (2), 201-222; (b) Laport, M. S.; Santos, O. C. S.; Muricy, G., Marine Sponges: Potential Sources of New Antimicrobial Drugs. *Current Pharmaceutical Biotechnology* **2009**, *10* (1), 86-105.
14. Peter Castro, P. D.; Michael E. Huber, P. D., *Marine Biology*. Janice Roerig-Blong: 2008; p 484.
15. Hooper, J. N.; Van Soest, R. W.; Debrenne, F., Phylum Porifera Grant, 1836. In *Systema Porifera*, Springer: 2002; pp 9-13.

16. (<https://en.wikipedia.org/wiki/Sponge> - cite_note-Cavalcanti2012-62).
17. Ute, H.; Jörn, H.; Matthias, H.; B, F. A.; Michael, W.; Jörg, H.; S, M. B., Molecular evidence for a uniform microbial community in sponges from different oceans. *Applied and environmental microbiology (Print)* **2002**, 68 (9), 4431-4440.
18. Belarbi, E. H.; Contreras Gómez, A.; Chisti, Y.; Garcı; amp; x; a Camacho, F.; Molina Grima, E., Producing drugs from marine sponges. *Biotechnology Advances* **2003**, 21 (7), 585-598.
19. Kim, S.-K., *Introduction to Anticancer Drugs from Marine Origin*. 2015.
20. Thoms, C.; Schupp, P., Biotechnological potential of marine sponges and their associated bacteria as producers of new pharmaceuticals (Part II). In *Journal of International Biotechnology Law*, 2005; Vol. 2, p 257.
21. Vogel, S., Current-induced flow through living sponges in nature. *Proceedings of the National Academy of Sciences of the United States of America* **1977**, 74 (5), 2069-2071.
22. Proksch, P., Defensive roles for secondary metabolites from marine sponges and sponge-feeding nudibranchs. *Toxicon* **1994**, 32 (6), 639-655.
23. Bhakuni, D. S.; Rawat, D. S., *Bioactive Marine Natural Products*. Springer 233 Spring Street, New York 10013, USA. Anamaya Publishers, New Delhi, India, 2005; p 396.
24. Kamalakkannan, P., Marine sponges a good source of bioactive compounds in anticancer agents. *International Journal of Pharmaceutical Sciences Review and Research* **2015**, 31 (2), 132-135.
25. Villa, F. A.; Gerwick, L., Marine natural product drug discovery: Leads for treatment of inflammation, cancer, infections, and neurological disorders. *Immunopharmacology and Immunotoxicology* **2010**, 32 (2), 228-237.
26. Bergmann, W.; Feeney, R. J., the isolation of a new thymine pentoside from Sponges. *Journal of the American Chemical Society* **1950**, 72 (6), 2809-2810.
27. Proksch, P.; Edrada, R.; Ebel, R., Drugs from the seas current status and microbiological implications. *Applied Microbiology and Biotechnology* **2002**, 59 (2), 125-134.
28. Faulkner, D. J., Marine natural products. *Natural Product Reports* **2001**, 18 (1), 1R-49R.
29. Pallela, R.; Ehrlich, H., *Marine Sponges: Chemicobiological and Biomedical Applications*. Springer: 2016.
30. Torres, Y. R.; Berlinck, R. G.; Nascimento, G. G.; Fortier, S. C.; Pessoa, C.; de Moraes, M. O., Antibacterial activity against resistant bacteria and cytotoxicity of four alkaloid toxins isolated from the marine sponge *Arenosclera brasiliensis*. *Toxicon* **2002**, 40 (7), 885-891.
31. Perry, N. B.; Blunt, J. W.; Munro, M. H.; Higa, T.; Sakai, R., Discorhabdin D, an antitumor alkaloid from the sponges *Latrunculia brevis* and *Prianos* sp. *The Journal of Organic Chemistry* **1988**, 53 (17), 4127-4128.
32. Nakamura, H.; Ohizumi, Y.; Kobayashi, J. i.; Hirata, Y., Keramadine, a novel antagonist of serotonergic receptors isolated from the Okinawan sea sponge *Agelas* sp. *Tetrahedron letters* **1984**, 25 (23), 2475-2478.

33. Fattorusso, E.; Tagliatela-Scafati, O., Two novel pyrrole-imidazole alkaloids from the Mediterranean sponge *Agelas oroides*. *Tetrahedron Letters* **2000**, *41* (50), 9917-9922.
34. Cutignano, A.; Bifulco, G.; Bruno, I.; Casapullo, A.; Gomez-Paloma, L.; Riccio, R., Dragmacidin F: A new antiviral bromoindole alkaloid from the Mediterranean sponge *Halicortex* sp. *Tetrahedron* **2000**, *56* (23), 3743-3748.
35. Phife, D. W.; Ramos, R. A.; Feng, M.; King, I.; Gunasekera, S. P.; Wright, A.; Patel, M.; Pachter, J. A.; Coval, S. J., Marine sponge bis (indole) alkaloids that displace ligand binding to $\alpha 1$ adrenergic receptors. *Bioorganic & Medicinal Chemistry Letters* **1996**, *6* (17), 2103-2106.
36. de Guzman, F. S.; Carte, B.; Troupe, N.; Faulkner, D. J.; Harper, M. K.; Concepcion, G. P.; Mangalindan, G. C.; Matsumoto, S. S.; Barrows, L. R.; Ireland, C. M., Neoamphimedine: a new pyridoacridine topoisomerase II inhibitor which catenates DNA. *The Journal of Organic Chemistry* **1999**, *64* (4), 1400-1402.
37. Dunbar, D. C.; Rimoldi, J. M.; Clark, A. M.; Kelly, M.; Hamann, M. T., Anti-cryptococcal and nitric oxide synthase inhibitory imidazole alkaloids from the calcareous sponge *Leucetta cf chagosensis*. *Tetrahedron* **2000**, *56* (45), 8795-8798.
38. De Smet, P.; Parys, J. B.; Callewaert, G.; Weidema, A. F.; Hill, E.; De Smedt, H.; Erneux, C.; Sorrentino, V.; Missiaen, L., Xestospongine C is an equally potent inhibitor of the inositol 1, 4, 5-trisphosphate receptor and the endoplasmic-reticulum Ca^{2+} pumps. *Cell calcium* **1999**, *26* (1-2), 9-13.
39. Perry, N. B.; Ettouati, L.; Litaudon, M.; Blunt, J. W.; Munro, M. H.; Parkin, S.; Hope, H., Alkaloids from the antarctic sponge *Kirkpatrickia variolosa*: Part 1: Variolin b, a new antitumour and antiviral compound. *Tetrahedron* **1994**, *50* (13), 3987-3992.
40. Ang, K. K.; Holmes, M. J.; Higa, T.; Hamann, M. T.; Kara, U. A., *In vivo* antimalarial activity of the beta-carboline alkaloid manzamine A. *Antimicrobial agents and Chemotherapy* **2000**, *44* (6), 1645-1649.
41. Urban, S.; de Almeida Leone, P.; Carroll, A. R.; Fechner, G. A.; Smith, J.; Hooper, J. N.; Quinn, R. J., Axinellamines A–D, novel imidazo azolo imidazole alkaloids from the Australian Marine Sponge *Axinella* sp. *The Journal of organic chemistry* **1999**, *64* (3), 731-735.
42. Matsunaga, S.; Fusetani, N.; Konosu, S., Bioactive marine metabolites, IV. Isolation and the amino acid composition of discodermin A, an antimicrobial peptide, from the marine sponge *Discodermia kiiensis*. *Journal of natural products* **1985**, *48* (2), 236-241.
43. Sable, R.; Parajuli, P.; Jois, S., Peptides, Peptidomimetics, and Polypeptides from Marine Sources: A Wealth of Natural Sources for Pharmaceutical Applications. *Marine drugs* **2017**, *15* (4), 124.
44. (a) Lu, Z.; Van Wagoner, R. M.; Harper, M. K.; Baker, H. L.; Hooper, J. N.; Bewley, C. A.; Ireland, C. M., Mirabamides E–H, HIV-inhibitory depsipeptides from the sponge *Stelletta clavosa*. *Journal of natural products* **2011**, *74* (2), 185-193; (b) Plaza, A.; Gustchina, E.; Baker, H. L.; Kelly, M.; Bewley, C. A., Mirabamides A–D, depsipeptides from the sponge *Siliquariaspongia mirabilis* that inhibit HIV-1 fusion. *Journal of natural products* **2007**, *70* (11), 1753-1760.
45. (a) Ford, P. W.; Gustafson, K. R.; McKee, T. C.; Shigematsu, N.; Maurizi, L. K.; Pannell, L. K.; Williams, D. E.; Dilip de Silva, E.; Lassota, P.; Allen, T. M., Papuamides A–D, HIV-Inhibitory and Cytotoxic Depsipeptides from the Sponges *Theonella mirabilis* and

- Theonella swinhoei* Collected in Papua New Guinea. *Journal of the American Chemical Society* **1999**, *121* (25), 5899-5909; (b) Prasad, P.; Aalbersberg, W.; Feussner, K. D.; Van Wagoner, R. M., Papuamides E and F, cytotoxic depsipeptides from the marine sponge *Melophlus* sp. *Tetrahedron* **2011**, *67* (44), 8529-8531.
46. Plaza, A.; Bifulco, G.; Keffer, J. L.; Lloyd, J. R.; Baker, H. L.; Bewley, C. A., Celebesides A–C and theopapuamides B–D, depsipeptides from an Indonesian sponge that inhibit HIV-1 entry. *The Journal of organic chemistry* **2008**, *74* (2), 504-512.
47. (a) Espiritu, R. A.; Cornelio, K.; Kinoshita, M.; Matsumori, N.; Murata, M.; Nishimura, S.; Kakeya, H.; Yoshida, M.; Matsunaga, S., Marine sponge cyclic peptide theonellamide A disrupts lipid bilayer integrity without forming distinct membrane pores. *Biochimica et Biophysica Acta (BBA)-Biomembranes* **2016**, *1858* (6), 1373-1379; (b) Youssef, D. T.; Shaala, L. A.; Mohamed, G. A.; Badr, J. M.; Bamanie, F. H.; Ibrahim, S. R., Theonellamide G, a potent antifungal and cytotoxic bicyclic glycopeptide from the Red Sea marine sponge *Theonella swinhoei*. *Marine drugs* **2014**, *12* (4), 1911-1923.
48. Tran, T. D.; Pham, N. B.; Fechner, G. A.; Hooper, J. N.; Quinn, R. J., Potent cytotoxic peptides from the Australian marine sponge *Pipestela candelabra*. *Marine drugs* **2014**, *12* (6), 3399-3415.
49. Kim, S. K., *Springer handbook of marine biotechnology*. Springer: 2015.
50. Rod'kina, S., Fatty acids and other lipids of marine sponges. *Russian Journal of Marine Biology* **2005**, *31* (1), S49-S60.
51. Ichiba, T.; J Scheuer, P.; Kelly Borges, M., Two Cytotoxic 3,6-Epidioxy Fatty Acids from an Indonesian Sponge, *Plakortis* sp. 1. *Tetrahedron* **1995**, *51* (45), 12195-12202.
52. (a) Keffer, J. L.; Plaza, A.; Bewley, C. A., Motualevic acids A–F, antimicrobial acids from the sponge *Siliquariaspongia* sp. *Organic Letters* **2009**, *11* (5), 1087-1090; (b) Youssef, D. T. A.; Badr, J. M.; Shaala, L. A.; Mohamed, G. A.; Bamanie, F. H., Ehrenasterol and biemnic acid; new bioactive compounds from the Red Sea sponge *Biemna ehrenbergi*. *Phytochemistry Letters* **2015**, *12*, 296-301.
53. Sata, N. U.; Matsunaga, S.; Fusetani, N.; van Soest, R. W. M., Aurantosides D, E, and F: New antifungal tetramic acid glycosides from the marine sponge *Siliquariaspongia japonica*. *Journal of Natural Products* **1999**, *62* (7), 969-971.
54. Makarieva, T. N.; Santalova, E. A.; Gorshkova, I. A.; Dmitrenok, A. S.; Guzii, A. G.; Gorbach, V. I.; Svetashev, V. I.; Stonik, V. A., A new cytotoxic fatty acid (5Z, 9Z)-22-methyl-5, 9-tetracosadienoic acid and the sterols from the far eastern sponge *Geodinella robusta*. *Lipids* **2002**, *37* (1), 75-80.
55. (a) Hu, Y.; Chen, J.; Hu, G.; Yu, J.; Zhu, X.; Lin, Y.; Chen, S.; Yuan, J., Statistical research on the bioactivity of new marine natural products discovered during the 28 years from 1985 to 2012. *Marine drugs* **2015**, *13* (1), 202-221; (b) Blunt, J. W.; Copp, B. R.; Munro, M. H.; Northcote, P. T.; Prinsep, M. R., *Marine natural products*. **2006**.
56. Dyshlovoy, S. A.; Honecker, F., *Marine compounds and cancer: Where Do We Stand? Multidisciplinary Digital Publishing Institute*: 2015.
57. Śliwka, L.; Wiktorska, K.; Suchocki, P.; Milczarek, M.; Mielczarek, S.; Lubelska, K.; Cierpień, T.; Łyżwa, P.; Kielbasiński, P.; Jaromin, A.; Flis, A.; Chilmonczyk, Z., The comparison of MTT and CVS assays for the assessment of anticancer agent interactions. *Plos One* **2016**, *11* (5), e0155772.

58. (a) Arandjelovic, S.; Ravichandran, K. S., Phagocytosis of apoptotic cells in homeostasis. *Nature immunology* **2015**, *16* (9), 907-917; (b) https://en.wikipedia.org/wiki/Apoptosis#cite_note-4.
59. Elmore, S. A.; Dixon, D.; Hailey, J. R.; Harada, T.; Herbert, R. A.; Maronpot, R. R.; Nolte, T.; Rehg, J. E.; Rittinghausen, S.; Rosol, T. J.; Satoh, H.; Vidal, J. D.; Willard-Mack, C. L.; Creasy, D. M., Recommendations from the INHAND apoptosis/necrosis working group. *Toxicologic pathology* **2016**, *44* (2), 173-188.
60. (a) Elmore, S., Apoptosis: A Review of Programmed Cell Death. *Toxicologic pathology* **2007**, *35* (4), 495-516; (b) Tsujimoto, Y., apoptosis and necrosis: intracellular ATP level as a determinant for cell death modes. *Cell Death & Differentiation* **1997**, *4* (6).
61. Mizushima, N., Autophagy: process and function. *Genes and Development* **2007**, *21* (22), 2861-73.
62. Boya, P.; Reggiori, F.; Codogno, P., Emerging regulation and functions of autophagy. *Nature cell biology* **2013**, *15* (7), 713.
63. Warnes, G., Measurement of autophagy by flow cytometry. *Current protocols in cytometry* **2014**, 9.45. 1-9.45. 10.
64. Taylor, R. C.; Cullen, S. P.; Martin, S. J., Apoptosis: controlled demolition at the cellular level. *Nature reviews Molecular cell biology* **2008**, *9* (3), 231-241.
65. (a) Daniel, P. T.; Koert, U.; Schuppan, J., Apoptolidin: induction of apoptosis by a natural product. *Angewandte Chemie International Edition* **2006**, *45* (6), 872-893; (b) Thornberry, N. A.; Lazebnik, Y., Caspases: Enemies Within. *Science* **1998**, *281* (5381), 1312-1316.
66. Jin, Z.; El Deiry, W. S., Overview of cell death signaling pathways. *Cancer biology & therapy* **2005**, *4* (2), 147-171.
67. Firoozinia, M.; Moghadamtousi, S. Z.; Sadeghilar, A.; Karimian, H.; Noordin, M. I. B., Golden natural plant compounds activate apoptosis via both mitochondrial and death receptor pathways: A Review. *Electronic Journal of Biology* **2015**.
68. Martinez, M. M.; Reif, R. D.; Pappas, D., Detection of apoptosis: A review of conventional and novel techniques. *Analytical methods* **2010**, *2* (8), 996-1004.
69. Chaitanya, G. V.; Alexander, J. S.; Babu, P. P., PARP-1 cleavage fragments: signatures of cell-death proteases in neurodegeneration. *Cell Communication and Signaling : CCS* **2010**, *8*, 31-31.
70. Ruggieri, G., Drugs from the sea. *Science* **1976**, *194* (4264), 491-497.
71. Molinski, T. F.; Dalisay, D. S.; Lievens, S. L.; Saludes, J. P., Drug development from marine natural products. *Nat Rev Drug Discov* **2009**, *8* (1), 69-85.
72. Rangel, M.; Falkenberg, M., An overview of the marine natural products in clinical trials and on the market. *J. Coast. Life Med* **2015**, *3*, 421-428.
73. Mayer, A.; Rodríguez, A. D.; Taglialatela-Scafati, O.; Fusetani, N., Marine pharmacology in 2009–2011: Marine compounds with antibacterial, antidiabetic, antifungal, anti-inflammatory, antiprotozoal, antituberculosis, and antiviral activities; affecting the immune and nervous systems, and other miscellaneous mechanisms of action. *Marine drugs* **2013**, *11* (7), 2510-2573.

74. Toshiyuki, W.; Karen, C. T.; Hiroki, T.; Ikuro, A., Cytotoxic cyclic peptides from the marine sponges. In *Handbook of Anticancer Drugs from Marine Origin*, Springer International Publishing Switzerland: 2015; pp 113-144.
75. Fusetani, N.; Warabi, K.; Nogata, Y.; Nakao, Y.; Matsunaga, S.; Van Soest, R. R. M., Koshikamide A1, a new cytotoxic linear peptide isolated from a marine sponge, *Theonella* sp. *Tetrahedron Letters* **1999**, *40* (25), 4687-4690.
76. Kimura, M.; Wakimoto, T.; Egami, Y.; Tan, K. C.; Ise, Y.; Abe, I., Calyxamides A and B, cytotoxic cyclic peptides from the marine sponge *Discodermia calyx*. *Journal of Natural Products* **2012**, *75* (2), 290-294.
77. Daletos, G.; Kalscheuer, R.; Koliwer-Brandl, H.; Hartmann, R.; de Voogd, N. J.; Wray, V.; Lin, W.; Proksch, P., Callyaerins from the marine sponge *Callyspongia aerizusa*: Cyclic peptides with antitubercular activity. *Journal of Natural Products* **2015**, *78* (8), 1910-1925.
78. Kim, H. J.; Sim, C. J., Two new marine sponges of genus *Clathria* (*Clathria*) (Poecilosclerida: Microcionidae) from Korea. *Korean Journal of Systematic Zoology* **2005a**, *21* (1), 111-122.
79. (a) El-Naggar, M.; Conte, M.; Capon, R. J., Mirabilins revisited: polyketide alkaloids from a southern Australian marine sponge, *Clathria* sp. *Organic & Biomolecular Chemistry* **2010**, *8* (2), 407-412; (b) Sperry, S.; Crews, P., A novel alkaloid from the Indo-Pacific sponge *Clathria basilana*. *Tetrahedron Letters* **1996**, *37* (14), 2389-2390.
80. Tanaka, Y.; Katayama, T., Biochemical Studies on The Carotenoids in Porifera. The Structure of Clathriaxanthin in Sea Sponge, *Clathria frondifera* (Bowerbank). *Nippon Suisan Gakkaishi* **1976**, *42* (7), 801-805.
81. (a) Aiello, A.; Ciminiello, P.; Fattorusso, E.; Magno, S., Three new 7-keto sterols from the Mediterranean sponge *Clathrina clathrus*. *Steroids* **1988**, *52* (5-6), 533-542; (b) Keyzers, R. A.; Northcote, P. T.; Webb, V., Clathriol, a Novel Polyoxygenated 14 β Steroid Isolated from the New Zealand Marine Sponge *Clathria lissosclera*. *Journal of Natural Products* **2002**, *65* (4), 598-600.
82. (a) Davis, R. A.; Mangalindan, G. C.; Bojo, Z. P.; Antemano, R. R.; Rodriguez, N. O.; Concepcion, G. P.; Samson, S. C.; de Guzman, D.; Cruz, L. J.; Tasmimir, D.; Harper, M. K.; Feng, X.; Carter, G. T.; Ireland, C. M., Microcionamides A and B, bioactive peptides from the Philippine sponge *Clathria (Thalysias) abietina*. *The Journal of Organic Chemistry* **2004**, *69* (12), 4170-4176; (b) Woo, J. K.; Jeon, J. e.; Kim, C. K.; Sim, C. J.; Oh, D. C.; Oh, K. B.; Shin, J., Gombamide A, a cyclic thiopeptide from the sponge *Clathria gombawuiensis*. *Journal of Natural Products* **2013**, *76* (7), 1380-1383.
83. (a) Cardellina, J. H.; Nigh, D.; VanWagenen, B. C., Plant growth regulatory indoles from the sponges *Dysidea etheria* and *Ulosa ruetzleri*. *Journal of Natural Products* **1986**, *49* (6), 1065-1067; (b) Rasmussen, T.; Jensen, J.; Anthoni, U.; Christophersen, C.; Nielsen, P. H., Structure and synthesis of bromoindoles from the marine sponge *Pseudosuberites hyalinus*. *Journal of Natural Products* **1993**, *56* (9), 1553-1558.
84. AlTarabeen, M.; Hassan Aly, A.; Perez Hemphill Catalina, F.; Rasheed, M.; Wray, V.; Proksch, P., New nitrogenous compounds from a Red Sea sponge from the Gulf of Aqaba. In *Zeitschrift für Naturforschung C*, 2015; Vol. 70, p 75.
85. Gopichand, Y.; Schmitz, F. J., Two novel lactams from the marine sponge *Halichondria melanodocia*. *The Journal of Organic Chemistry* **1979**, *44* (26), 4995-4997.

86. Lidgren, G.; Bohlin, L.; Christophersen, C., Studies of Swedish marine organisms, Part X. Biologically active compounds from the marine sponge *Geodia baretii*. *Journal of Natural Products* **1988**, *51* (6), 1277-1280.
87. Marfey, P., Determination of D-amino acids. II. Use of a bifunctional reagent, 1,5-difluoro-2,4-dinitrobenzene. *Carlsberg Research Communications* **1984**, *49* (6), 591.
88. Vijayasathy, S.; Prasad, P.; Fremlin, L. J.; Ratnayake, R.; Salim, A. A.; Khalil, Z.; Capon, R. J., C3 and 2D C3 Marfey's methods for amino acid analysis in natural products. *Journal of Natural Products* **2016**, *79* (2), 421-427.
89. Siemion, I. Z.; Wieland, T.; Pook, K. H., Influence of the distance of the proline carbonyl from the β and γ carbon on the ^{13}C chemical shifts. *Angewandte Chemie International Edition in English* **1975**, *14* (10), 702-703.
90. Rinehart, K. L.; Kishore, V.; Bible, K. C.; Sakai, R.; Sullins, D. W.; Li, K. M., Didemmins and tunichlorin: novel natural products from the marine tunicate *Trididemnum solidum*. *Journal of Natural Products* **1988**, *51* (1), 1-21.
91. Li, H.; Bowling, J. J.; Fronczek, F. R.; Hong, J.; Jabba, S. V.; Murray, T. F.; Ha, N. C.; Hamann, M. T.; Jung, J. H., Asteropsin A: an unusual cystine-crosslinked peptide from porifera enhances neuronal Ca^{2+} influx. *Biochimica et Biophysica Acta (BBA) - General Subjects* **2013**, *1830* (3), 2591-2599.
92. Li, H.; Dang, H. T.; Li, J.; Sim, C. J.; Hong, J.; Kim, D. K.; Jung, J. H., Pyroglutamyl dipeptides and tetrahydro- β -carboline alkaloids from a marine sponge *Asteropus* sp. *Biochemical Systematics and Ecology* **2010**, *38* (5), 1049-1051.
93. Calvaresi, M.; Garavelli, M.; Bottoni, A., Computational evidence for the catalytic mechanism of glutaminyl cyclase. A DFT investigation. *Proteins: Structure, Function, and Bioinformatics* **2008**, *73* (3), 527-538.
94. Whitson, E. L.; Ratnayake, A. S.; Bugni, T. S.; Harper, M. K.; Ireland, C. M., Isolation, structure elucidation, and synthesis of eudistomides A and B, lipopeptides from a Fijian ascidian *Eudistoma* sp. *The Journal of Organic Chemistry* **2009**, *74* (3), 1156-1162.
95. (a) Guo, J. Y.; Chen, H.-Y.; Mathew, R.; Fan, J.; Strohecker, A. M.; Karsli-Uzunbas, G.; Kamphorst, J. J.; Chen, G.; Lemons, J. M. S.; Karantza, V.; Coller, H. A.; DiPaola, R. S.; Gelinias, C.; Rabinowitz, J. D.; White, E., Activated Ras requires autophagy to maintain oxidative metabolism and tumorigenesis. *Genes & Development* **2011**, *25* (5), 460-470; (b) Degenhardt, K.; Mathew, R.; Beaudoin, B.; Bray, K.; Anderson, D.; Chen, G.; Mukherjee, C.; Shi, Y.; Gelinias, C.; Fan, Y.; Nelson, D. A.; Jin, S.; White, E., Autophagy promotes tumor cell survival and restricts necrosis, inflammation, and tumorigenesis. *Cancer cell* **2006**, *10* (1), 51-64.
96. Klionsky, D. J.; Abdelmohsen, K.; Abe, A.; Abedin, M. J.; Abeliovich, H.; Acevedo Arozena, A.; Adachi, H.; Adams, C. M.; Adams, P. D.; Adeli, K., Guidelines for the use and interpretation of assays for monitoring autophagy. *Autophagy* **2016**, *12* (1), 1-222.
97. Urban, A.; Eckermann, S.; Fast, B.; Metzger, S.; Gehling, M.; Ziegelbauer, K.; RübSamen-Waigmann, H.; Freiberg, C., Novel whole cell antibiotic biosensors for compound discovery. *Applied and Environmental Microbiology* **2007**, *73* (20), 6436-6443.
98. Mascher, T.; Zimmer, S. L.; Smith, T.-A.; Helmann, J. D., Antibiotic inducible promoter regulated by the cell envelope stress sensing two component system LiaRS of *Bacillus subtilis*. *Antimicrobial Agents and Chemotherapy* **2004**, *48* (8), 2888-2896.

99. Brötz, H.; Josten, M.; Wiedemann, I.; Schneider, U.; Götz, F.; Bierbaum, G.; Sahl, H. G., Role of lipid-bound peptidoglycan precursors in the formation of pores by nisin, epidermin and other lantibiotics. *Molecular Microbiology* **1998**, *30* (2), 317-327.
100. Ibrahim, S. R. M.; Min, C. C.; Teuscher, F.; Ebel, R.; Kakoschke, C.; Lin, W.; Wray, V.; Edrada-Ebel, R.; Proksch, P., Callyaerins A–F and H, new cytotoxic cyclic peptides from the Indonesian marine sponge *Callyspongia aerizusa*. *Bioorganic & Medicinal Chemistry* **2010**, *18* (14), 4947-4956.
101. Shang, L.; Chen, S.; Du, F.; Li, S.; Zhao, L.; Wang, X., Nutrient starvation elicits an acute autophagic response mediated by Ulk1 dephosphorylation and its subsequent dissociation from AMPK. *Proceedings of the National Academy of Sciences of the United States of America* **2011**, *108* (12), 4788-4793.
102. Patel, J. B.; Cockerill, F. R.; Bradford, P. A.; Eliopoulos, G. M.; Hindler, J. A.; Jenkins, S. G.; Lewis, J. S.; Limbago, B.; Miller, L. A.; Nicolau, D. P.; Powell, M.; Swenson, J. M.; Turnidge, J. D.; Weinstein, M. P.; Zimmer, B. L., *Methods for dilution antimicrobial susceptibility tests for bacteria that grow aerobically. Approved Standard - Tenth Edition*. Clinical and Laboratory Standards Institute: USA, 2015; Vol. 35.
103. Woodford, N.; Adebisi, A.-M. A.; Paleou, M.-F. I.; Cookson, B. D., Diversity of VanA glycopeptide resistance elements in enterococci from humans and nonhuman Sources. *Antimicrobial Agents and Chemotherapy* **1998**, *42* (3), 502-508.
104. Czugala, M.; Mykhaylyk, O.; Böhrer, P.; Onderka, J.; Stork, B.; Wesselborg, S.; Kruse, F. E.; Plank, C.; Singer, B. B.; Fuchsluger, T. A., Efficient and safe gene delivery to human corneal endothelium using magnetic nanoparticles. *Nanomedicine* **2016**, *11* (14), 1787-1800.
105. Shvets, E.; Fass, E.; Elazar, Z., Utilizing flow cytometry to monitor autophagy in living mammalian cells. *Autophagy* **2008**, *4* (5), 621-628.
106. Stülke, J.; Hanschke, R.; Hecker, M., Temporal activation of β -glucanase synthesis in *Bacillus subtilis* is mediated by the GTP pool. *Microbiology* **1993**, *139* (9), 2041-2045.
107. Simmons, T. L.; Andrianasolo, E.; McPhail, K.; Flatt, P.; Gerwick, W. H., Marine natural products as anticancer drugs. *Molecular Cancer Therapeutics* **2005**, *4* (2), 333-342.
108. Barnathan, G.; Miralles, J.; Njinkoue, J.-M.; Mangoni, A.; Fattorusso, E.; Debitus, C.; Boury Esnault, N.; Kornprobst, J. M., Sterol composition of three marine sponge species from the genus *Cinachyrella*. *Comparative Biochemistry and Physiology Part B: Comparative Biochemistry* **1992**, *103* (4), 1043-1047.
109. LY, L.; ZW, D.; J, L.; HZ, F.; WH, L., Chemical constituents from Chinese marine sponge *Cinachyrella australiensis*. *Beijing Da Xue Xue Bao* **2004**, *36* (1), 7-12.
110. (a) Barnathan, G.; Miralles, J.; Kornprobst, J.M., Sponge fatty acids. Co-occurrence of two isoprenoid fatty acids (4,8,12-Trimethyltridecanoic and 5,9,13-Trimethyltetradecanoic) in phospholipids of marine sponges from the genus *Cinachyrella*. *Natural Product Letters* **1993**, *3* (2), 113-118; (b) Barnathan, G.; Doumenq, P.; Njinkoué, J.-M.; Mirallès, J.; Debitus, C.; Lévi, C.; Kornprobst, J. M., Sponge fatty acids. 3. Occurrence of series of n-7 monoenoic and iso-5,9 dienoic long-chain fatty acids in the phospholipids of the marine sponge *Cinachyrella aff. schulzei* keller. *Lipids* **1994**, *29* (4), 297.
111. Wahidullah, S.; Naik, B. G.; Al-Fadhli, A. A., Chemotaxonomic study of the demosponge *Cinachyrella cavernosa* (Lamarck). *Biochemical Systematics and Ecology* **2015**, *58*, 91-96.

112. Oku, N.; Takada, K.; Fuller, R. W.; Wilson, J. A.; Peach, M. L.; Pannell, L. K.; McMahon, J. B.; Gustafson, K. R., Isolation, structural elucidation, and absolute stereochemistry of enigmazole A, a cytotoxic phosphomacrolide from the papua new guinea marine sponge *Cinachyrella enigmatica*. *Journal of the American Chemical Society* **2010**, *132* (30), 10278-10285.
113. Zhao, Q.; Lee, S.Y.; Hong, J.; Lee, C.O.; Im, K. S.; Sim, C. J.; Lee, D. S.; Jung, J. H., New acetylenic acids from the marine sponge *Stelletta* species. *Journal of Natural Products* **2003**, *66* (3), 408-411.
114. Patocka, J.; Pita, R.; Kuca, K., Gyromitrin, mushroom toxin of *Gyromitra* spp. *Mil. Med. Sci. Lett. (Voj. Zdrav. Listy)* **2012**, *81* (2), 61.
115. Ishiyama, H.; Ishibashi, M.; Ogawa, A.; Yoshida, S.; Kobayashi, J. i., Taurospongins A, a novel acetylenic fatty acid derivative inhibiting DNA polymerase β and HIV reverse transcriptase from sponge *Hippospongia* sp. *The Journal of Organic Chemistry* **1997**, *62* (12), 3831-3836.
116. (a) Saakyan, A., Esterification of pyrazole-3-and 4-carboxylic acids. *Russian Journal of General Chemistry* **2011**, *81* (8), 1745-1746; (b) Gevorkyan, Q. A.; Arutyunyan, A. D.; Arutyunyan, G. L.; Gasparyan, S. P.; Danagulyan, G. G., Synthesis of novel pyrazolyl derivatives of 1, 3-diazaadamantane. *Chemistry of Heterocyclic Compounds* **2017**, *53* (2), 192-195.
117. Le Goff, G.; Ouazzani, J., Natural hydrazine-containing compounds: Biosynthesis, isolation, biological activities and synthesis. *Bioorganic & medicinal chemistry* **2014**, *22* (23), 6529-6544.
118. Shimogawa, H.; Kuribayashi, S.; Teruya, T.; Suenaga, K.; Kigoshi, H., Cinachyramine, the novel alkaloid possessing a hydrazone and two aminals from *Cinachyrella* sp. *Tetrahedron Letters* **2006**, *47* (9), 1409-1411.
119. Piña, I. C.; Gautschi, J. T.; Wang, G.-Y.-S.; Sanders, M. L.; Schmitz, F. J.; France, D.; Cornell-Kennon, S.; Sambucetti, L. C.; Remiszewski, S. W.; Perez, L. B., Psammaplins from the Sponge *Pseudoceratina purpurea*: Inhibition of both histone deacetylase and DNA methyltransferase. *The Journal of organic chemistry* **2003**, *68* (10), 3866-3873.
120. Hickford, S. J. H.; Blunt, J. W.; Munro, M. H. G., Antitumour polyether macrolides: Four new halichondrins from the New Zealand deep-water marine sponge *Lissodendoryx* sp. *Bioorganic & Medicinal Chemistry* **2009**, *17* (6), 2199-2203.
121. Whitson, E. L.; Bugni, T. S.; Chockalingam, P. S.; Concepcion, G. P.; Feng, X.; Jin, G.; Harper, M. K.; Mangalindan, G. C.; McDonald, L. A.; Ireland, C. M., Fibrosterol sulfates from the Philippine sponge *Lissodendoryx (Acanthodoryx) fibrosa*: sterol dimers that inhibit PKC ζ . *The Journal of Organic Chemistry* **2009**, *74* (16), 5902-5908.
122. Fontana, A.; Ciavatta, M. L.; Amodeo, P.; Cimino, G., Single solution phase conformation of new antiproliferative cembranes. *Tetrahedron* **1999**, *55* (4), 1143-1152.
123. Bingham, B. L.; Young, C. M., Influence of sponges on invertebrate recruitment: A field test of allelopathy. *Mar. Biol.* **1991**, *109* (1), 19-26.
124. Araya-Maturana, R.; Pessoa-Mahana, H.; Weiss-Lopez, B., Very long-range correlations (n_{JC} , $H_{n>3}$) in HMBC spectra. *Nat. Prod. Commun* **2008**, *3*, 445-450.

125. Araya-Maturana, R.; Cardona, W.; Weiss-Lopez, B., Use of Long-Range CH heteronuclear multiple bond connectivity in the assignment of the ^{13}C NMR spectra of complex organic molecules. *Current Organic Chemistry* **2001**, *5* (3), 253-263.
126. Sullivan, J.; Giles, R.; Looper, R., 2-Aminoimidazoles from *Leucetta* sponges: synthesis and biology of an important pharmacophore. *Current Bioactive Compounds* **2009**, *5* (1), 39-78.
127. Chiriano, G.; De Simone, A.; Mancini, F.; Perez, D. I.; Cavalli, A.; Bolognesi, M. L.; Legname, G.; Martinez, A.; Andrisano, V.; Carloni, P., A small chemical library of 2-aminoimidazole derivatives as BACE-1 inhibitors: Structure-based design, synthesis, and biological evaluation. *European journal of medicinal chemistry* **2012**, *48*, 206-213.
128. Nguyen, T. D.; Nguyen, X. C.; Longeon, A.; Keryhuel, A.; Le, M. H.; Kim, Y. H.; Chau, V. M.; Bourguet-Kondracki, M.-L., Antioxidant benzylidene 2-aminoimidazolones from the Mediterranean sponge *Phorbas topsenti*. *Tetrahedron* **2012**, *68* (45), 9256-9259.
129. Davis, R. A.; Baron, P. S.; Neve, J. E.; Cullinane, C., A microwave-assisted stereoselective synthesis of polyandrocarpamines A and B. *Tetrahedron Letters* **2009**, *50* (8), 880-882.
130. Tasdemir, D.; Mallon, R.; Greenstein, M.; Feldberg, L. R.; Kim, S. C.; Collins, K.; Wojciechowicz, D.; Mangalindan, G. C.; Concepción, G. P.; Harper, M. K.; Ireland, C. M., aldisine alkaloids from the Philippine sponge *Stylissa massaare* potent inhibitors of mitogen-activated protein kinase kinase-1 (MEK-1). *Journal of Medicinal Chemistry* **2002**, *45* (2), 529-532.
131. (a) Forenza, S.; Minale, L.; Riccio, R.; Fattorusso, E., New bromo-pyrrole derivatives from the sponge *Agelas oroides*. *Journal of the Chemical Society D: Chemical Communications* **1971**, (18), 1129-1130; (b) Zidar, N.; Montalvão, S.; Hodnik, Ž.; Nawrot, D. A.; Žula, A.; Ilaš, J.; Kikelj, D.; Tammela, P.; Mašič, L. P., Antimicrobial activity of the marine alkaloids, clathrodin and oroidin, and their synthetic analogues. *Marine drugs* **2014**, *12* (2), 940-963.
132. Singh, A. J.; Dattelbaum, J. D.; Field, J. J.; Smart, Z.; Woolly, E. F.; Barber, J. M.; Heathcott, R.; Miller, J. H.; Northcote, P. T., Structurally diverse hamigerans from the New Zealand marine sponge *Hamigera tarangaensis*: NMR-directed isolation, structure elucidation and antifungal activity. *Organic & Biomolecular Chemistry* **2013**, *11* (46), 8041-8051.
133. Kobayashi, J. i.; Murayama, T.; Ishibashi, M.; Kosuge, S.; Takamatsu, M.; Ohizumi, Y.; Kobayashi, H.; Ohta, T.; Nozoe, S.; Takuma, S., Hyrtiosins A and B, new indole alkaloids from the Okinawan marine sponge *Hyrtios erecta*. *Tetrahedron* **1990**, *46* (23), 7699-7702.
134. Elsebai, M. F.; Natesan, L.; Kehraus, S.; Mohamed, I. E.; Schnakenburg, G.; Sasse, F.; Shaaban, S.; Gütschow, M.; König, G. M., HLE inhibitory alkaloids with a polyketide skeleton from the marine derived fungus *Coniothyrium cereale*. *Journal of Natural Products* **2011**, *74* (10), 2282-2285.
135. Rodríguez, A. D.; Ramírez, C.; Rodríguez, I. I., Elisabatins A and B: New amphilectane-type diterpenes from the west Indian Sea whip *Pseudopterogorgia elisabethae*. *Journal of Natural Products* **1999**, *62* (7), 997-999.

136. Davis, R. A.; Aalbersberg, W.; Meo, S.; Rocha, R. M. d.; Ireland, C. M., The isolation and synthesis of polyandrocarpamines A and B. Two new 2-aminoimidazolone compounds from the Fijian ascidian, *Polyandrocarpa* sp. *Tetrahedron* **2002**, *58* (16), 3263-3269.
137. Smirnov, L.; Kuz'min, V.; Lezina, V.; Dyumaev, K., Nitration of 2-phenyl-3-hydroxypyridine. *Russian Chemical Bulletin* **1970**, *19* (8), 1791-1793.
138. Capon, R. J.; Skene, C.; Vuong, D.; Lacey, E.; Heiland, K.; Friedel, T., Equilibrating isomers: bromoindoles and a seco-xanthine encountered during a study of nematocides from the southern Australian marine sponge *Hymeniacidon* sp. *Journal of Natural Products* **2002**, *65* (3), 368-370.
139. Bergmann, W.; Feeney, R. J., Contribution to the study of marine products. XXXII. The nucleosides of sponges. I.1. *The Journal of Organic Chemistry* **1951**, *16* (6), 981-987.
140. Araisamines, A., tris-bromoindole cyclic guanidine alkaloids from the marine sponge *Clathria (Thalysias) araiosa* Wei, Xiaomei; Henriksen, Niel M.; Skalicky, Jack J. Harper, Mary Kay.
141. Zuleta, I. A.; Vitelli, M. a. L.; Baggio, R.; Garland, M. a. T.; Seldes, A. M.; Palermo, J. A., Novel pteridine alkaloids from the sponge *Clathria* sp. *Tetrahedron* **2002**, *58* (22), 4481-4486.
142. Conte, M.; J Capon, R.; El-Naggar, M., Mirabilins revisited: polyketide alkaloids from a southern Australian marine sponge, *Clathria* sp. **2010**.
143. Laville, R. m.; Thomas, O. P.; Berru e, F.; Marquez, D.; Vacelet, J.; Amade, P., Bioactive guanidine alkaloids from two Caribbean marine sponges. *Journal of natural products* **2009**, *72* (9), 1589-1594.
144. Rudi, A.; Yosief, T.; Loya, S.; Hizi, A.; Schleyer, M.; Kashman, Y., Clathsterol, a novel anti-HIV-1 RT sulfated sterol from the sponge *Clathria* species. *Journal of natural products* **2001**, *64* (11), 1451-1453.
145. Gupta, P.; Sharma, U.; Schulz, T. C.; McLean, A. B.; Robins, A. J.; West, L. M., Bicyclic C21 terpenoids from the marine sponge *Clathria compressa*. *Journal of natural products* **2012**, *75* (6), 1223-1227.
146. Woo, J. K.; Kim, C. K.; Kim, S. H.; Kim, H.; Oh, D. C.; Oh, K. B.; Shin, J., Gombaspiroketal A–C, Sesterterpenes from the sponge *Clathria gombawuiensis*. *Organic letters* **2014**, *16* (11), 2826-2829.
147. Ohta, S.; Okada, H.; Kobayashi, H.; Oclarit, J. M.; Ikegami, S., Clathrynamides A, B, and C: novel amides from a marine sponge *Clathria* sp. that inhibit cell division of fertilized starfish eggs. *Tetrahedron letters* **1993**, *34* (37), 5935-5938.
148. Olivera, B. M., Conus peptides: biodiversity-based discovery and exogenomics. *Journal of Biological Chemistry* **2006**, *281* (42), 31173-31177.
149. Bradley, A. M.; Devine, M.; DeRemer, D., Brentuximab vedotin: An anti-CD30 antibody drug conjugate. *American Journal of Health-System Pharmacy* **2013**, *70* (7).
150. (a) Zabriskie, T. M.; Klocke, J. A.; Ireland, C. M.; Marcus, A. H.; Molinski, T. F.; Faulkner, D. J.; Xu, C.; Clardy, J., Jaspamide, a modified peptide from a Jaspis sponge, with insecticidal and antifungal activity. *Journal of the American Chemical Society* **1986**, *108* (11), 3123-3124; (b) Ebada, S. S.; Wray, V.; de Voogd, N. J.; Deng, Z.; Lin, W.; Proksch, P., Two new jaspamide derivatives from the marine sponge *Jaspis splendens*. *Marine Drugs* **2009**, *7* (3), 434-444.

151. Tran, T. D.; Pham, N. B.; Fechner, G.; Zencak, D.; Vu, H. T.; Hooper, J. N. A.; Quinn, R. J., Cytotoxic cyclic depsipeptides from the Australian marine sponge *Neamphius huxleyi*. *Journal of Natural Products* **2012**, *75* (12), 2200-2208.
152. Zhan, K. X.; Jiao, W. H.; Yang, F.; Li, J.; Wang, S.-P.; Li, Y. S.; Han, B. N.; Lin, H. W., Reniochalistatins A–E, cyclic peptides from the marine sponge *Reniochalina stalagmitis*. *Journal of Natural Products* **2014**, *77* (12), 2678-2684.
153. Schmidt, E. W.; Raventos-Suarez, C.; Bifano, M.; Menendez, A. T.; Fairchild, C. R.; Faulkner, D. J., Scleritodermin A, a cytotoxic cyclic peptide from the Lithistid sponge *Scleritoderma nodosum*. *Journal of Natural Products* **2004**, *67* (3), 475-478.
154. (a) Essack, M.; Bajic, V. B.; Archer, J. A. C., Recently Confirmed apoptosis inducing lead compounds isolated from marine sponge of potential relevance in cancer treatment. *Marine Drugs* **2011**, *9* (9), 1580-1606; (b) Kazlauskas, R.; Murphy, P. T.; Quinn, R. J.; Wells, R. J., Heteronemin, a new scalarin type sesterterpene from the sponge *Heteronema erecta*. *Tetrahedron Letters* **1976**, *17* (30), 2631-2634.
155. (a) Braekman, J. C.; Daloze, D.; Moussiaux, B.; Riccio, R., Jaspamide from the marine sponge *Jaspis johnstoni*. *Journal of natural products* **1987**, *50* (5), 994-995; (b) Cioca, D.; Kitano, K., Induction of apoptosis and CD10/neutral endopeptidase expression by jaspamide in HL-60 line cells. *Cellular and molecular life sciences* **2002**, *59* (8), 1377-1387.
156. Sato, M.; Sagawa, M.; Nakazato, T.; Ikeda, Y.; Kizaki, M., A natural peptide, dolastatin 15, induces G2/M cell cycle arrest and apoptosis of human multiple myeloma cells. *International journal of oncology* **2007**, *30* (6), 1453-1459.
157. (a) Son, S.; Ko, S. K.; Jang, M.; Kim, J. W.; Kim, G. S.; Lee, J. K.; Jeon, E. S.; Futamura, Y.; Ryoo, I. J.; Lee, J. S., New cyclic lipopeptides of the iturin class produced by saltern-derived *Bacillus* sp. KCB14S006. *Marine drugs* **2016**, *14* (4), 72; (b) Dey, G.; Bharti, R.; Dhanarajan, G.; Das, S.; Dey, K. K.; Kumar, B. P.; Sen, R.; Mandal, M., Marine lipopeptide Iturin A inhibits Akt mediated GSK3 β and FoxO3a signaling and triggers apoptosis in breast cancer. *Scientific reports* **2015**, *5*, 10316.
158. (a) Wrasidlo, W.; Mielgo, A.; Torres, V. A.; Barbero, S.; Stoletov, K.; Suyama, T. L.; Klemke, R. L.; Gerwick, W. H.; Carson, D. A.; Stupack, D. G., The marine lipopeptide somocystinamide A triggers apoptosis via caspase 8. *Proceedings of the National Academy of Sciences* **2008**, *105* (7), 2313-2318; (b) Nogle, L. M.; Gerwick, W. H., Somocystinamide A, a novel cytotoxic disulfide dimer from a Fijian marine cyanobacterial mixed assemblage. *Organic letters* **2002**, *4* (7), 1095-1098.
159. Belofsky, G. N.; Jensen, P. R.; Fenical, W., Sansalvamide: A new cytotoxic cyclic depsipeptide produced by a marine fungus of the genus *Fusarium*. *Tetrahedron Letters* **1999**, *40* (15), 2913-2916.
160. Iwasaki, A.; Ohno, O.; Sumimoto, S.; Ogawa, H.; Nguyen, K. A.; Suenaga, K., Jahanyne, an apoptosis-inducing lipopeptide from the marine cyanobacterium *Lyngbya* sp. *Organic letters* **2015**, *17* (3), 652-655.
161. (a) Maroun, J.; Belanger, K.; Seymour, L.; Matthews, S.; Roach, J.; Dionne, J.; Soulieres, D.; Stewart, D.; Goel, R.; Charpentier, D., Phase I study of Aplidine in a daily \times 5 one-hour infusion every 3 weeks in patients with solid tumors refractory to standard therapy. A National Cancer Institute of Canada Clinical Trials Group study: NCIC CTG IND 115. *Annals of oncology* **2006**, *17* (9), 1371-1378; (b) Zak, M.; Yuen, P.-w.; Liu, X.; Patel, S.; Sampath, D.; Oeh, J.; Liederer, B. M.; Wang, W.; O'Brien, T.; Xiao, Y.; Skelton, N.; Hua,

- R.; Sodhi, J.; Wang, Y.; Zhang, L.; Zhao, G.; Zheng, X.; Ho, Y.-C.; Bair, K. W.; Dragovich, P. S., Minimizing CYP2C9 Inhibition of exposed-pyridine NAMPT (Nicotinamide Phosphoribosyltransferase) inhibitors. *Journal of Medicinal Chemistry* **2016**, *59* (18), 8345-8368; (c) Zheng, L.-H.; Wang, Y.-J.; Sheng, J.; Wang, F.; Zheng, Y.; Lin, X.-K.; Sun, M., Antitumor peptides from marine organisms. *Marine drugs* **2011**, *9* (10), 1840-1859.
162. Grubb, D. R.; Wolvetang, E. J.; Lawen, A., Didemnin B induces cell death by apoptosis: the fastest induction of apoptosis ever described. *Biochemical and biophysical research communications* **1995**, *215* (3), 1130-1136.
163. Garcia-Barrantes, P. M.; Lindsley, C. W., Total synthesis of gombamide A. *Organic Letters* **2016**, *18* (15), 3810-3813.
164. Valeria D'Auria, M.; Zampella, A.; Paloma, L. G.; Minale, L.; Debitus, C.; Roussakis, C.; Le Bert, V., Callipeltins B and C; bioactive peptides from a marine Lithistida sponge *Callipelta* sp. *Tetrahedron* **1996**, *52* (28), 9589-9596.
165. Williams, D. E.; Austin, P.; Diaz-Marrero, A. R.; Soest, R. V.; Matainaho, T.; Roskelley, C. D.; Roberge, M.; Andersen, R. J., Neopetrosiamides, peptides from the marine sponge *Neopetrosia* sp. that inhibit amoeboid invasion by human tumor cells. *Organic Letters* **2005**, *7* (19), 4173-4176.
166. Li, H.; Bowling, J. J.; Fronczek, F. R.; Hong, J.; Jabba, S. V.; Murray, T. F.; Ha, N.-C.; Hamann, M. T.; Jung, J. H., Asteropsin A: an unusual cystine-crosslinked peptide from porifera enhances neuronal Ca²⁺ influx. *Biochimica et biophysica acta* **2013**, *1830* (3), 2591-2599.
167. Song, J.; Jeon, J. e.; Won, T. H.; Sim, C.; Oh, D. C.; Oh, K. B.; Shin, J., New cyclic cystine bridged peptides from the sponge *Suberites waedoensis*. *Marine Drugs* **2014**, *12* (5), 2760-2770.
168. Conibear, A. C.; Bochen, A.; Rosengren, K. J.; Stupar, P.; Wang, C.; Kessler, H.; Craik, D. J., The cyclic cystine ladder of theta defensins as a stable, bifunctional scaffold: A proof-of-concept study using the integrin binding RGD Motif. *ChemBioChem* **2014**, *15* (3), 451-459.
169. (a) Festa, C.; De Marino, S.; D'Auria, M. V.; Monti, M. C.; Bucci, M.; Vellecco, V.; Debitus, C.; Zampella, A., Anti-inflammatory cyclopeptides from the marine sponge *Theonella swinhoei*. *Tetrahedron* **2012**, *68* (13), 2851-2857; (b) Gulavita, N. K.; Pomponi, S. A.; Wright, A. E.; Yarwood, D.; Sills, M. A., Isolation and structure elucidation of perthamide B, a novel peptide from the sponge *Theonella* sp. *Tetrahedron letters* **1994**, *35* (37), 6815-6818; (c) Festa, C.; De Marino, S.; Sepe, V.; Monti, M. C.; Luciano, P.; D'Auria, M. V.; Debitus, C.; Bucci, M.; Vellecco, V.; Zampella, A., Perthamides C and D, two new potent anti-inflammatory cyclopeptides from a Solomon Lithistid sponge *Theonella swinhoei*. *Tetrahedron* **2009**, *65* (50), 10424-10429.
170. (a) Freitas, V. M.; Rangel, M.; Bisson, L. F.; Jaeger, R. G.; Machado-Santelli, G. M., The geodiamolide H, derived from brazilian sponge *Geodia corticostylifera*, regulates actin cytoskeleton, migration and invasion of breast cancer cells cultured in three-dimensional environment. *Journal of cellular physiology* **2008**, *216* (3), 583-594; (b) Chan, W. R.; Tinto, W. F.; Manchand, P. S.; Todaro, L. J., Stereostructures of geodiamolides A and B, novel cyclodepsipeptides from the marine sponge *Geodia* sp. *The Journal of Organic Chemistry* **1987**, *52* (14), 3091-3093.

171. (a) Zampella, A.; Sepe, V.; Luciano, P.; Bellotta, F.; Monti, M. C.; D'Auria, M. V.; Jepsen, T.; Petek, S.; Adeline, M. T. r. s.; Laprévôte, O., Homophymine A, an anti-HIV cyclodepsipeptide from the sponge *Homophymia* sp. *The Journal of organic chemistry* **2008**, *73* (14), 5319-5327; (b) Zampella, A.; Sepe, V.; Bellotta, F.; Luciano, P.; D'Auria, M. V.; Cresteil, T.; Debitus, C.; Petek, S.; Poupat, C.; Ahond, A., Homophymines B-E and A1-E1, a family of bioactive cyclodepsipeptides from the sponge *Homophymia* sp. *Organic & biomolecular chemistry* **2009**, *7* (19), 4037-4044.
172. Chill, L.; Kashman, Y.; Schleyer, M., Oriamide, a new cytotoxic cyclic peptide containing a novel amino acid from the marine sponge *Theonella* sp. *Tetrahedron* **1997**, *53* (47), 16147-16152.
173. (a) Matsunaga, S.; Fusetani, N.; Konosu, S., Bioactive marine metabolites VI. Structure elucidation of discodermin a, an antimicrobial peptide from the marine sponge *Discodermia kiiensis*. *Tetrahedron Letters* **1984**, *25* (45), 5165-5168; (b) Ryu, G.; Matsunaga, S.; Fusetani, N., Discodermins F-H, cytotoxic and antimicrobial tetradecapeptides from the marine sponge *Discodermia kiiensis*: Structure revision of discodermins A-D. *Tetrahedron* **1994**, *50* (47), 13409-13416.
174. Criado, S.; Marioli, J. M.; Allegretti, P. E.; Furlong, J.; Nieto, F. J. R. g.; Mártire, D. O.; García, N. A., Oxidation of di- and tripeptides of tyrosine and valine mediated by singlet molecular oxygen, phosphate radicals and sulfate radicals. *Journal of Photochemistry and Photobiology B: Biology* **2001**, *65* (1), 74-84.
175. Dembitsky, V., Bromo- and iodo-containing alkaloids from marine microorganisms and sponges. *Russian Journal of Bioorganic Chemistry* **2002**, *28* (3), 170-182.
176. El-Hawary, S. S.; Sayed, A. M.; Rateb, M. E.; Bakeer, W.; AbouZid, S. F.; Mohammed, R., Secondary metabolites from fungal endophytes of *Solanum nigrum*. *Natural Product Research* **2017**, 1-4.
177. Segraves, N. L.; Crews, P., Investigation of brominated tryptophan alkaloids from two Thorectidae sponges: *Thorectandra* and *Smenospongia*. *Journal of natural products* **2005**, *68* (10), 1484-1488.
178. Guella, G.; Mancini, I.; Duhet, D.; Richer de Forges, B.; Pietra, F., Ethyl 6-bromo-3-indolcarboxylate and 3-hydroxyacetal-6-bromoindole, novel bromoindoles from the sponge *Pleroma menoui* of the coral sea. *Zeitschrift für Naturforschung C* **1989**, *44* (11-12), 914-916.
179. Yin, S.; Boyle, G. M.; Carroll, A. R.; Kotiw, M.; Dearnaley, J.; Quinn, R. J.; Davis, R. A., Caelestines A-D, brominated quinolinecarboxylic acids from the Australian ascidian *Aplidium caelestis*. *Journal of natural products* **2010**, *73* (9), 1586-1589.
180. Barnathan, G.; Mirallès, J.; Gaydou, E. M.; Boury-Esnault, N.; Kornprobst, J.-M., New phospholipid fatty acids from the marine sponge *Cinachyrella alloclada uliczka*. *Lipids* **1992**, *27* (10), 779-784.
181. Skepper, C. K.; Quach, T.; Molinski, T. F., Total Synthesis of enigmazole A from *Cinachyrella enigmatica*. Bidirectional bond constructions with an ambident 2,4-disubstituted oxazole synthon. *Journal of the American Chemical Society* **2010**, *132* (30), 10286-10292.
182. Carballeira, N. M.; Cruz, H.; Orellano, E. A.; González, F. A., The first total synthesis of the marine fatty acid (±)-2-methoxy-13-methyltetradecanoic acid: a cytotoxic fatty acid to leukemia cells. *Chemistry and Physics of Lipids* **2003**, *126* (2), 149-153.
183. Carballeira, N. M.; Montano, N.; Amador, L. A.; Rodríguez, A. D.; Golovko, M. Y.; Golovko, S. A.; Reguera, R. M.; Álvarez-Velilla, R.; Balaña-Fouce, R., Novel very long

chain α -methoxylated $\Delta_{5,9}$ fatty acids from the sponge *Asteropus niger* are effective inhibitors of topoisomerases IB. *Lipids* **2016**, *51* (2), 245-256.

184. Lee, H.-S.; Rho, J.-R.; Sim, C. J.; Shin, J., New acetylenic acids from a sponge of the genus *Stelletta*. *Journal of Natural Products* **2003**, *66* (4), 566-568.

185. (a) HY, L.; S, M.; N, F., Corticatic acids A-C, antifungal acetylenic acids from the marine sponge, *Petrosia corticata*. *Journal of Natural Products* **1994**, *57* (10), 1464-1467; (b) Nishimura, S.; Matsunaga, S.; Shibazaki, M.; Suzuki, K.; Harada, N.; Naoki, H.; Fusetani, N., Corticatic acids D and E, polyacetylenic geranylgeranyltransferase type I inhibitors, from the marine sponge *Petrosia corticata*. *Journal of Natural Products* **2002**, *65* (9), 1353-1356.

186. Zhou, G. X.; Molinski, T., Long chain acetylenic ketones from the micronesian sponge *Haliclona* sp. Importance of the 1-yn-3-ol group for antitumor activity. *Marine Drugs* **2003**, *1* (1), 46.

187. Carballeira, N. M.; Pagán, M., New methoxylated fatty acids from the caribbean sponge *Callyspongia fallax*. *Journal of Natural Products* **2001**, *64* (5), 620-623.

188. Carballeira, N. M.; Cruz, H.; Kwong, C. D.; Wan, B.; Franzblau, S., 2-Methoxylated fatty acids in marine sponges: Defense mechanism against mycobacteria. *Lipids* **2004**, *39* (7), 675-680.

189. Parameswaran, P. S.; Naik, C. G.; Hegde, V. R., Secondary metabolites from the sponge *Tedania anhelans*: Isolation and characterization of two novel pyrazole acids and other metabolites. *Journal of Natural Products* **1997**, *60* (8), 802-803.

190. V. A. S. Pradeep Kumar, S.; Dhananjaya, N.; B. S. Reddy, G., Two new hydroxy sterol xylosides from the sea cucumber *Synapta muculata*. *Journal of Chemical Research, Synopses* **1998**, (7), 404-405.

191. Kumar, V.; Kaur, K.; Gupta, G. K.; Sharma, A. K., Pyrazole containing natural products: Synthetic preview and biological significance. *European Journal of Medicinal Chemistry* **2013**, *69*, 735-753.